VOT 74164

STATIC AND DYNAMIC IMPACTS OF THREE TO SIX-PHASE CONVERSION OF SELECTED TRANSMISSION LINE IN AN ELECTRIC ENERGY SYSTEM

(KESAN STATIK DAN DINAMIK TERHADAP PENUKARAN TALIAN PENGHANTARAN TERPILIH DARIPADA TIGA KE ENAM-FASA DALAM SISTEM TENAGA ELEKTRIK)

MOHD WAZIR BIN MUSTAFA

RESEARCH VOTE NO:

74164

Jabatan Kuasa

Fakulti Kejuruteraan Elektrik

Universiti Teknologi Malaysia

2006

ACKNOWLEDGEMENTS

I would like to take this opportunity to express my deepest gratitude to Ministry of Science, Technology and Innovation (MOSTI) and Malaysia government for their financial support in all the stages of this research. I also like to thank to Universiti Teknologi Malaysia for their supports especially to Faculty of Electrical Engineering which provided the facilities and help in this research.

I would also like to acknowledge the valuable help of Professor K.L. Lo, external advisor from Department of Electronic and Electrical Engineering of University of Strathclyde in improving the quality of this works.

The author also would like to express greatest thankfulness to Tenaga Nasional Berhad, System Planning and Operation Department, Transmission Division especially the General Manager, Dr. Baharum Hamzah and Planning Engineer, Mr. Ahmad Khairulnizam Khairuddin for their valuable help in providing the 19-Bus TNB Kelantan network's data.

Finally, the author wishes to express his warmest gratitude to his beloved parents, family members and who forever have given their unfailing support and patience to the author.

ABSTRACT

Electricity is considered as the driving force for a country, which is undergoing rapid industrialization. Constrains on the availability of land and planning permission for overhead transmission lines have renewed interest in techniques to increase the power carrying capacity of existing right-of-ways (ROW). Six-phase transmission appears to be the most promising solution to the need to increase the capability of existing transmission lines and at the same time, respond to the concerns related to electromagnetic fields. One of the main advantages of six-phase transmission is that a six-phase line can carry up to 73% more electric power than a three-phase double-circuit line on the same transmission right-of-way. However, this conversion will have impacts on the power system operations. In this project, the digital load flow, short circuit, and transient stability cases of the IEEE Test Systems and 19-Bus TNB Kelantan System is investigated in time domain considering conversion of three-phase double-circuit to six-phase single-circuit transmission system by using *Power System Computer Aided Design/Electromagnetic Transient and Direct Current* PSCAD/EMTDC program. These studies were performed in sufficient detail to determine how the six-phase conversion will affect steady state operation, fault current duties, and system stability. A laboratory prototype of Kuala Krai to Gua Musang TNB Kelantan Thevenin equivalent systems is developed to validate the simulation results. From the simulation results, it has been shown that the IEEE Test Systems and 19-Bus TNB Kelantan System with six-phase single-circuit transmission has a better stability limits compare to the three-phase double-circuit transmission. Besides, load flow results shown the voltage level at all buses are remains in the acceptable limits. Furthermore, fault current for the same type of fault on the mid point of selected transmission line is reduced while six-phase transmission is used compare to three-phase double-circuit.

ABSTRAK

Tenaga elektrik merupakan pemacu kepada kepesatan sektor perindustrian negara. Kesukaran mendapatkan kebenaran dan tanah untuk membina talian penghantaran atas yang baru telah menarik minat terhadap teknik meningkatkan keupayaan pemindahan kuasa menggunakan talian sedia ada. Sistem penghantaran kuasa enam-fasa muncul sebagai satu penyelesaian bagi meningkatkan keupayaan talian sedia dan pada masa yang sama, ianya menitikberatkan kesan medan elektromagnet. Kebaikan utama sistem penghantaran enam-fasa ialah dapat membawa 73% lebih kuasa berbanding dengan sistem penghantaran talian-berkembar tiga-fasa walaupun ruang talian atas yang sama digunakan. Walaubagaimanapun, penukaran ini mempunyai kesan terhadap operasi sistem kuasa. Projek ini mengkaji aliran beban, litar pintas, dan kestabilan fana bagi beberapa sistem ujian termasuk Sistem Ujian IEEE dan juga Sistem TNB Kelantan 19-Bas dalam domain masa dengan mengambil kira penukaran sistem talian-berkembar tiga-fasa kepada sistem enam-fasa menggunakan program PSCAD/EMTDC. Kajian ini dilakukan dengan teliti untuk melihat kesan bagaimana penukaran kepada sistem enam-fasa mempengaruhi keadaan mantap, sambutan arus kerosakan, dan kestabilan sistem. Prototaip makmal bagi litar setara Thevenin Kuala Krai ke Gua Musang, Sistem TNB Kelantan telah dibina. Daripada hasil simulasi, ia telah menunjukkan Sistem Ujian IEEE dan Sistem TNB Kelantan 19-Bas dengan talian penghantaran enam-fasa mempunyai had kestabillan yang lebih baik berbanding dengan sistem penghantaran tiga-fasa berkembar. Keputusan analisa aliran beban menunjukkan paras voltan semua bas tetap berada pada had yang dibenarkan. Selain daripada itu, untuk jenis kerosakan yang sama pada bahagian tengah talian penghantran terpilih, arus kerosakan yang mengalir untuk sistem enam-fasa adalah lebih rendah berbanding sistem tiga-fasa.

TABLE OF CONTENTS

LIST OF TABLES

LIST OF FIGURES

LIST OF SYMBOLS AND ACRONYMS

α	-	Angular acceleration, radians/second²
δ	-	Angle difference between the voltages, degree
θ	-	Angular displacement, radians
π	-	3.1416 radians or 180°
ω	-	Angular velocity, radians/second
a	-	Transformer turn ratio or $1 \angle 120°$ in polar number
AC	-	Asynchronous current
APS	-	Allegheny Power Services Corporation
C	-	Capacitance, μF
DC	-	Direct current
DOE	-	Department of Energy
E	-	Excitation voltage
EHV	-	Extra-high voltage
EPRI	-	Electric Power Research Institute
ESEERCO	-	Empire State Electric Energy Research Corporation
f	-	Frequency, Hz
G	-	Machine rating in, MVA
GSU	-	Generator step-up
H	-	Inertia constant or Height, m
HPO	-	High phase order
HVDC	-	High-voltage DC
I	-	Current
L	-	Inductance, mH
M	-	Angular momentum, joule-sec/radian

MATLAB	-	Matrix laboratory software
MATPOWER	-	A MATLAB^{TM} Power System Simulation Package
N	-	Number (of phases/phase conductors, turns, etc) or Neutral
n	-	Speed
NYSEG	-	New York State Electric and Gas Corporation
NYSERDA	-	New York State Energy Research and Development Authority
P	-	Real power
P_a	-	Accelerating power
P_e	-	Electrical output of machine
P_m	-	Mechanical power input of machine
PSCAD/ EMTDC	-	Power System Computer Aided Design/ Electromagnetic Transient for Direct Current
PTI	-	Power Technologies Incorporated
S_{KVA}	-	Three-phase apparent power, kVA
SIL	-	Surge Impedance Loading
T_a	-	Torque, Nm
TNB	-	Tenaga National Berhad
UHV	-	Ultra-high voltages
V	-	Voltage
V_P	-	Phase-to-neutral voltage
V_L	-	Phase-to-phase voltage
V_{LP}	-	Phase-to-phase voltage at primary side
V_{LS}	-	Phase-to-phase voltage at secondary side
V_{PP}	-	Phase-to-neutral voltage at primary side
V_{PS}	-	Phase-to-neutral voltage at secondary side
W	-	Wide, m
x	-	Positive-sequence impedance, Ω
x_e	-	System reactance, Ω
x_s	-	Generator synchronous reactance, Ω
X_L	-	Leakage Reactance as seen from winding 1, Ω
y	-	Admittance, mho
Y-Y	-	Wye-Wye connection of the transformer winding

Y-Δ	-	Wye-Delta connection of the transformer winding
Δ-Y	-	Delta-Wye connection of the transformer winding
Δ-Δ	-	Delta-Delta connection of the transformer winding
z	-	Impedance, Ω
Z_c	-	Positive-sequence surge impedance of the line, Ω

LIST OF APPENDICES

CHAPTER I

INTRODUCTION

1.1 Research Background

Electricity is considered as the driving force for a country, which is undergoing rapid industrialization. Traditionally, the need for increasing power transmission capability and more efficient use of ROW space has been accomplished by the use of successively higher system voltages. Constrains on the availability of land and planning permission for overhead transmission lines have renewed interest in techniques to increase the power carrying capacity of existing ROWs. High phase order (HPO) transmission is the use of more phase than the conventional three-phase transmission system. The increased interest in HPO electric power transmission over past thirty years can be traced on a CIRGE paper published by L. D. Barthold and H. C. Barnes. Since then, the concept of HPO transmission has been described in the literature in several papers and reports [1].

Among the HPO, six-phase transmission appears to be the most promising solution to the need to increase the capability of existing transmission lines and at the same time, respond to the concerns related to electromagnetic fields. One of the main advantages of six-phase transmission is that a six-phase line can carry up to

73% more electric power than a three-phase double-circuit line on the same transmission ROW [6]. For this reason, the current research has been carried out to have a better picture and clearer understanding of the six-phase power transmission system. This research studies the static and dynamic impacts during normal and abnormal operating conditions for electric power system considering three to six-phase conversions of selected transmission lines in an electric energy system.

The steady state analysis, fault analysis, and transient stability analysis were performed on all test systems including IEEE test systems and 19-Bus TNB Kelantan system in sufficient detail using the graphical electromagnetic transient simulation program, PSCAD/EMTDC in time domain basis to determine how six-phase conversion will affect steady state operation, fault current duties, and system stability. The study includes 5 cases which are names as Test System I through Test System IV and also 19-Bus TNB Kelantan System.

All the selected test systems, included IEEE Test Systems and 19-Bus TNB Kelantan System has been considered to have a conversion of one of its existing three-phase double-circuit lines into six-phase ones. The simulation model consists of a static AC equivalent circuit, generators, exciters, hydro governors, converter transformer, transmission lines and loads. The parameters of equivalent AC networks, generators, exciters, and etc. are modelled through the PSCAD/EMTDC program.

1.2 Literature Reviews

Electric power transmission was originally developed with direct current (DC). In 1878, Thomas A. Edison began work on the electric light and formulated the concept of centrally located power station with distributed lighting serving a

surround area. He perfected his light by October 1879, and the opening of his historic Pearl Street Station in New York City on September 4, 1882, marked the beginning of the electric utility industry. At Pearl Street, DC generators, then called dynamos, were driven by steam engines to supply an initial load of 30 kW for 110 V incandescent lighting to 59 customers in a one-squre-mile area. From this beginning in 1882 through 1972, the electric utility industry grew at a remarkable pace. A growth based on continuous reductions in the price of electricity due primarily to technological accomplishment and creative engineering. The introduction of the practical DC motor by Sprague Electric, as well as the growth of incandescent lighting, promoted the expansion of Edison's DC system. The development of three-wire 220 V DC systems allowed load to increase somewhat, but as transmission distances and loads continued increase, voltage problems were encountered. These limitations of maximum distance and load were overcome in 1885 by William Stanley's development of a commercial practical transformer. With the transformer, the ability to transmit power at high voltage with corresponding lower current and lower line-voltage drops made AC more attractive than DC.

The first single-phase AC line in the United States operated in 1889 in Oregon, between Oregon City and Portland (21 km at 4 kV). The growth of AC systems was further encourage in 1888 when Nikola Tesla presented a paper at a meeting of America Institute of Electrical Engineers describing two-phase induction and synchronous motors, which made evident the advantages of polyphase versus single-phase system. The first three-phase line in Germany became operational in 1891, transmitting power 179 km at 12 kV. The first three-phase line in United States is in California become operational in 1893, transmitting power 12 km at 2.3 kV. The three-phase induction motor conceive by Tesla went on to become the workhorse of the industry. There have been increases in three-phase transmission voltage in USA. From Edison's 220 V three-wire DC grids to 4 kV single-phase and 2.3 kV three-phase transmissions, AC transmission voltage in United States have risen progressively to 150, 230, 345, 500, and now 765 kV. And ultra-high voltages (UHV) above 1000 kV are now being studied. The Incentives for increasing transmission voltages have been: (1) increases in transmission distance and transmission capacity, (2) smaller line-voltage drops, (3) reduced line losses, (4)

reduced ROW requirements per MW transfer, and (5) lower capital and operating costs of transmission.

For transmitting power over very long distances it may be economical to convert the EHV AC to EHV DC, transmit the power over two lines, and invert it back to AC at the other end. In 1954, the first modern high-voltage DC (HVDC) transmission line was put into operation in Sweden between Vastervik and the island of Gotland in the Baltic Sea. It was operated at 100 kV for a distance of 100 km. The first HVDC line in the United States was the ±400 kV, 1360 km Pacific Intertie line installed between Oregon and California in 1970. As of 2000, four other HVDC lines up to 400 kV and five back-to-back AC-DC links had been installed in the United States, and a total of 30 HVDC lines up to 533 kV had been installed worldwide. For an HVDC line embedded in an AC system, solid-state converters at both ends of the DC line operate as rectifiers and inverters. Since the cost of an HVDC transmission line is less than that of an AC line with the same capacity, the additional cost of converters for DC transmission is offset when the line is long enough. Studies show that it is advantageous to consider overhead HVDC transmission lines when the transmission distance is longer than 600 km [3]. HVDC lines have no reactance and are capable of transferring more power for the same conductor size than AC lines. DC transmission is especially advantageous when two remotely located large systems are to be connected. The DC transmission tie line acts as an asynchronous link between the two rigid systems eliminating the instability problem inherent in the AC links. The main disadvantage of the DC is the production of harmonics which requires filtering, and a large amount of reactive power compensation required at both ends of the line [3].

The HPO electric power transmission introduced in [1] sparked the industry curiosity by suggesting that with a concern over the aesthetic impact of transmission lines, it seem timely to review some fundamental principals of overhead transmission and examine the space efficiency of overhead conductors. One variable which relates to that efficiency is the number of phases. The paper had focused the industry on the practical aspect of concepts that were first explained by Fostesque [2] in 1918

and E. Clark [5] in 1943. Since this corner stone work, much has been added to the available knowledge base on HPO transmission primarily in the areas of feasibility considerations, analysis of system characteristics and system protection. In the late 1970s, W. C. Guyker et al. extended the transmission concept by describing fault analysis methodologies and symmetrical component theory [5]. They also assessed the feasibility of upgrading an existing 138 kV line to six-phase [6] to increase the power transmission capability by 73 % while reducing conductor field gradients and improving system stability which potentially could obtain public acceptance since the nominal voltage of the line would remain unchanged. These authors also lain ground work for EPRI Research in 1984 on fault protection for HPO transmission line [7-8].

Allegheny Power Services Corporation (APS) in cooperation with West Virginia University began seriously investigating the details of a HPO designing in 1976. Their studies, funded in part by the National Science Foundation, showed the HPO transmission should be considered as a viable alternative to conventional, three-phase transmission system. They completed detailed analysis of HPO designs and protection philosophies, but stopped short of actually demonstrating the technologies on an operating line. Load projections for their service territory were reduced, thus eliminating the incentive to pursue increased power transfer capabilities. The project was abandoned; however, through their initiative, APS paved the way for future research [9].

A feasibility analysis of HPO transmission was conducted by J. Steward and D. Wilson for the U.S. Department of Energy 1976/1977. This initial study addressed the definition of system voltage, developed fundamental frequency system parameters (symmetrical components, transmission line impedances and unbalanced operation), considered transient over voltage performance (switching surges, rate-of-rise of recovery voltage on circuit breakers and lightning), evaluated electrical environmental parameters (electric fields, radio and audio noise) and gave initial consideration to hardware and equipment, mechanical considerations and economics. The results of this feasibility analysis were sufficient favourable that the U.S.

Department of Energy (DOE) and New York State Energy Research and Development Authority (NYSERDA) sponsored construction of six-phase and twelve-phase test line at Malta, New York. Contacts were issued to Power Technologies Incorporated (PTI) to develop design calculations for corona effects and electric field effects of the first six-phase transmission test line. The line was build at NYSERDA's Malta, New York testing facility. A final report issued in September 1983 concluded that six-phase transmission "can provided the same power transfer capacity as three-phase with significantly less ROW for the same electric field and audible noise criteria, smaller transmission structures, and reduced overall cost". Based upon these results, it was recommended that the research continue into twelve-phase designs [9-11].

In 1985, PTI was awarded to study 12-phase transmission and to construct a 12-phase line. The project was cofunded by DOE, NYSERDA and Empire State Electric Energy Research Corporation (ESEERCO). It was through this project that NYSEG (New York State Electric and Gas Corporation) became more involved. The final report for this project was released and shown that 12-phase also appears to offer significant benefits over three-phase options depending upon power transfer capacities required and given the fact that the 12-phase line can be designed for optimum 12-phase operation. In any event, the PTI project has confirmed the technology in a test situation and all that remain was to implement high-phase transmission into an existing transmission network. NYSEG expressed an interest to become involved in this project demonstration. Because of this reason, the demonstration project was developed [9].

For a demonstration project, a six-phase system was selected since it presents an optimum between the proportional increased in loading and the proportional increased in surge impedance obtained by increasing the number of phases with the increase in power transfer capability. The project which was conceived in 1988 had as its primary objective, the demonstration of commercial feasibility of HPO transmission by electrically reconfiguring the existing 115 kV owned and operated by NYSEG into a six-phase single-circuit line operated at 93 kV. The needs for this

demonstration project stems from the industry's need for high reliability demanded by the public coupled with a conservative approach to new technology. To fill the void, the ESEERCO has undertaken the HPO project, and in a collaboration with NYSEG have selected the Goudey-Oakdale line as the most likely candidate for the demonstration project after an exhaustive search of all three-phase double-circuit lines within New York State with due to length of line, outage potential, extent of modifications required and accessibility to conduct tests [12].

Reference [13] presents the feasibility of six-phase transmission system in term of insulation performance, corona and field effects, and load flow and system stability for this project. Based on detailed insulation coordination analysis, the study shown that Goudey-Oakdale line capable of operation at 97.6 kV six-phase and existing clearances are adequate for power frequency and switching surge considerations. This paper also concluded that lightning performance is essentially unchanged, radio and audible noise are within acceptable limits and steady state and contingency cases will not adversely affect or degrade the NYSEG system by the conversion of Goudey-Oakdale line.

Referring to reference [14], the potential advantages of NYSEG HPO as a means of field mitigation are discussed. It conclude that, it is possible to develop HPO alternative to three-phase lines with comparable power handling capacity, significantly smaller size and at the same or reduced ground level fields. The performances of the protection system that used for the Goudey-Oakdale test line are discussed in reference [15]. The protection system for the first commercially Goudey-Oakdale operated six-phase transmission line consist of state of the art microprocessor based relays designed for protection of conventional three-phase systems. The study done from this paper shown that, the six-phase protection is capable of operating according to the trip and reclose requirements for any fault combination. Furthermore, this study also reviewed the comparison between calculated and measured fault currents at both ends of the six-phase line proves that a HPO transmission line can be modelled accurately for any type of faults in a conventional short circuit program.

Reference [16] gives the experimental results of the NYSEG demonstration project in term of corona and field effects on an operating six-phase transmission line. This study has gives verification to available methods for calculation of electric and magnetic fields, radio noise and audio noise from six-phase overhead lines. From references [13-16], it has been shown that the six-phase transmission system can provide the same power transfer capability with lower ROW or can transfer 73% more power for the same ROW compared to the three-phase double-circuit system. Some of the advantages by using the six-phase transmission system are increased transmission capability, increased utilization of ROW, lower corona effects, lower insulation requirement and better voltage regulation. These benefits are among the reasons why power system engineers are enticed to consistently pursue knowledge on the power system.

In 1998, Landers et al. done some research works about the comparison of installation costs for constructing a standard 115 kV three-phase double-circuit transmission line to constructing 66 kV six-phase transmission line to illustrate that the use of six-phase transmission can be a cost effective solution. As results from their research, they made a conclusion that, the cost penalty for constructing a new six-phase line versus a three-phase line of the same voltage level is not excessive, particularly if physical constraints exist. Therefore they concluded that six-phase should be considered when developing the optimum line that will meet the physical, environmental and regulatory constraints of a specific project. After 1998 till recently, various papers about six-phase fault analysis and reliability studies have been published and discussed [18-21].

Reference [17] demonstrates the various experiences with the use of the PSCAD/EMTDC software. This paper describes the development of suites of simulation examples or “laboratory experiments” for use in undergraduate and graduate power engineering courses. The examples used in three separate courses are presented: Power Electronics, HVDC Transmission and Power System Relaying.

In addition, the use of PSCAD/EMTDC in various projects is also presented. Experiences with the use of the PSCAD/EMTDC software have been positive and have enhanced the quality of research and teaching. Besides, the simulation based approaches proved to be very effective.

1.3 Research Objectives

The major objective of this research is to analyse the static and dynamic impacts of power system with a six-phase converted transmission lines. The analysis includes steady state stability analysis, fault analysis and transient stability analysis. Its measurable objectives are as below:

a) To conduct a load flow analysis of test systems and 19-Bus TNB Kelantan System considering conversion of its existing three-phase double-circuit lines into six-phase single-circuit line.

b) To carry out a fault analysis of the same system as in (a). This will determine the adequacy of existing switchgear's short circuit capacity for permitting three to six-phase conversions.

c) To make a transient stability analysis of the same system as in (a). This will determine the impacts of conversion on the security of the system following outage of a converted line.

d) To verify the computer simulation results (a to c) by developing a laboratory prototype of the Kuala Krai to Gua Musang TNB Kelantan Thevenin equivalent system's and then conducting tests on that prototype.

The main contributions of this research are the completed analysis of static and the dynamic impacts of three to six-phase converted transmission lines of test

systems including IEEE Test Systems and 19-Bus TNB Kelantan System and developed a prototype of the six-phase power transmission system that can be used for the demonstration purposes. Modeling of the 19-Bus TNB Kelantan system into the PSCAD/EMTDC V4.1 simulation package is also a part of the research contribution.

1.4 Thesis Structure

This thesis is primarily concerned with the understanding, modeling, and analysing of static and dynamic impacts of three to six-phase conversion of selected transmission line in electric power systems. All the work done in this research is presented systematically in 7 chapters. An introductory chapter describes the objectives and background of the research. The overview of the thesis structure is also included in this chapter.

The following Chapter II and Chapter III provide the literature reviews of this research. Chapter II presents a thorough basic theory of six-phase power transmission system. The advantages of six-phase transmission system over three-phase transmission systems are also described in this chapter. Introduction to the static and dynamic impacts of power system with six-phase converted transmission line is covered in Chapter III. The aims of this chapter are to provide the basic theory of steady state analysis, fault analysis, and transient stability analysis of power system considering conversion of three-phase double-circuit to six-phase single-circuit transmission.

Chapter IV is devoted to the modelling of six-phase transmission systems using the PSCAD/EMTDC as derived in Chapter II. To illustrate all the analysis in a clearer view, the algorithm and basic concept of PSCAD/EMTDC is described in this

chapter. Chapter V described about development of the laboratory prototype. All the analysis and simulation results along with the discussions are shown in the Chapter VI. The results are presented in the form of graphs and charts for all types of analyses which are steady state analysis, fault analysis, and transient stability analysis. Chapter VII is devoted to conclusions of the research and suggestions of the future work.

CHAPTER II

SIX-PHASE TRANSMISSION SYSTEM

2.1 Introduction

Electric engineers are concerned with every step in the process of generation, transmission, distribution, and utilization of electrical energy. The electric utility industry is probably the largest and most complex industry in the world. The electrical engineer who works in that industry will encounter challenging problems in designing future power systems to deliver increasing amounts of electrical energy in safe, clean, and economical manner. The future growth of power systems will rely more on increasing capability of already existing transmission systems, rather than on building new transmission lines and power stations, for economical and environmental reasons. The external pressure have mounted on the power transmission to find the best solutions about the need to transmit greater amounts of power through long distances with fewer aesthetic and electrical impacts on the environment. The pressures have led to re-examination of basics of the three-phase system.

In the past, increase in the transmission capacity has been accomplished by increasing maximum system voltages. As technology advances for higher voltages,

increasingly data and analysis techniques have advanced in the insulator design and clearance requirements paving the way to less phase spacing. However, increasing the transmission voltage on the conventional three-phase lines as a way of transmitting more power is associated with several problems such as increase in the ground level electric field and the electric surface field on phase conductors. While the electric field on the conductor surface characterizes the undesirable consequences of corona such as audible noise, radio interference and corona power loss, the electric field on the ground determines the ROW. In some applications, for transmitting power over very long distances it may be more economical to convert the EHV AC to EHV DC, transmit the power over two lines, and invert it back to AC at the other end. But the main disadvantage of the DC link is the production of harmonics which requires filtering, and a large amount of reactive power compensation required at both ends of the line [3].

For other applications, it has seemed advantageous to optimize some form of AC. These have renewed interest in techniques to increase the power carrying capacity of existing ROW by using the higher order transmission system. Six-phase transmission appears to be the best solution to the need to increase the capability of an existing transmission line and at the same time, responds to the concerns relating to economical and environmental effects [5-16]. This chapter will provide the basic principles of power transmission system including surge impedance and surge impedance loading. Another important issue discussed here is line loadability. Three major line loading limit are the thermal limit, voltage-drop limit, and steady-state stability limit.

2.2 Electric Power Transmission

The purpose of an overhead transmission network is to transfer electric energy from generating units at various locations to the distribution system which

ultimately supplies the load. Transmission lines also interconnect neighbouring utilities which permits not only economic dispatch of power within regions during normal conditions, but also the transfer of power between regions during emergencies. The operating frequency is 60 Hz in the U.S. and 50 Hz in Europe, Australia, and part of Asia. Malaysia is one of the East Asia countries that used 50 Hz as the operating frequency. The three-phase system has three phase conductors while six-phase system has six phase conductors. The overhead transmission lines are used in open areas such as interconnections between cities or along wide roads within the city. In congested areas within cities, underground cables are used for electric energy transmission. The underground transmission system is environmentally preferable but has a significantly higher cost. The cost per mile of overhead transmission lines is 6% to 10% less than underground cables [3]. Standard transmission voltages are established in the United States by the American National Standards Institute (ANSI). Transmission voltage lines operating at more than 60 kV are standardized at 69 kV, 115 kV, 138 kV, 161 kV, 230 kV, 345 kV, 500 kV, and 765 kV line-to-line. TNB Malaysia used different standards for the transmission voltages. Transmission voltage lines operating for TNB system are standardized at 11 kV, 13 kV, 33 kV, 66 kV, 132 kV, 230 kV, 275 kV, 400 kV and 500 kV line-to-line. Transmission voltages above 230 kV are usually referred to as extra-high voltage (EHV).

A three-phase double-circuit AC system is used for most transmission lines. This will make the idea of transmitting power using six-phase transmission system much easier because six conductors of three-phase double-circuit transmission line can be converted to six-phase transmission line. Conversion of an existing three-phase double-circuit overhead transmission line to a six-phase operation needed phase conversion transformers to obtain the 60° phase shift between adjacent phases. A three-phase double-circuit transmission line can be easily converted to a six-phase transmission line by using three-to-six-phase conversion transformer. There are several combinations of identical three-phase transformers that can be used to form three-to-six-phase and six-to-three-phase conversion transformers. However, the most suitable one is by using two pairs of identical delta-wye three-phase transformers. One of each pair of transformers has reverse polarity to obtain the

required 60° phase shift. This combination were selected as appropriate for determining short circuit currents because the delta open circuits the zero sequence network and simplifies the fault analysis [31]. For the reason of this fact, three-to-six-phase and six-to-three-phase conversion transformers that forms by using this combination has been used throughout this study.

This section will discuss the concepts of surge impedance and surge impedance loading for lossless lines. When line losses are neglected, simpler expression for the line parameters are obtained and above concepts are more easily understood. Since transmission and distribution lines for power transfer generally are designed to have low losses, the equations and concepts shows here can be used for quick and reasonably accurate hand calculations leading to initial designs. More accurate calculations can then be made with computer programs for follow-up analysis and design.

2.2.1 Surge Impedance

System limitations on power flow include among other considerations voltage drop and stability. A rule of thumb estimate of power-handling capacity of a transmission line is given by line-surge-impedance loading. For a lossless line, R = G = 0. Moreover, these will give the impedance and admittance as follows [3]:

$$z = j\omega L \ \Omega/\text{m} \tag{2.1}$$

$$y = j\omega C \ \Omega/\text{m} \tag{2.2}$$

Characteristic impedance Z_c is given by [3]:

$$Z_c = \sqrt{\frac{z}{y}} = \sqrt{\frac{j\omega L}{j\omega C}} = \sqrt{\frac{L}{C}} \ \ \Omega \tag{2.3}$$

The characteristic impedance $Z_c = \sqrt{L/C}$ is commonly called surge impedance for a lossless line, is pure real-that is, resistive.

2.2.2 Surge Impedance Loading

Surge Impedance Loading (SIL) is the power delivered by a lossless line to load resistance equal to the surge impedance $Z_c = \sqrt{L/C}$. SIL is that loading at which VArs generated in the line capacitance cancel the VArs absorbed in the line inductance and is equivalent to the case of an impedance-matched line. Figure 2.1 shows a lossless line terminated by a resistance equal to its surge impedance. This line represents either a single-phase line or one phase-to-neutral of balanced three-phase or six-phase line.

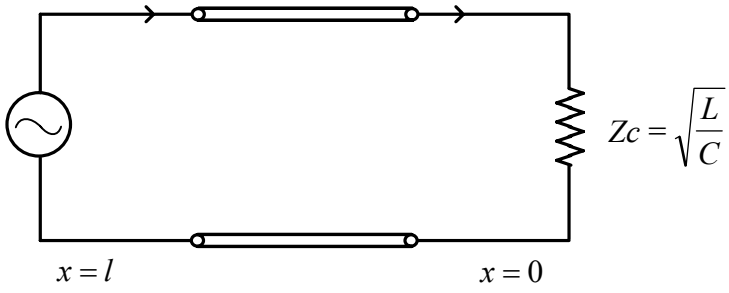

Figure 2.1: Lossless line terminated by its surge impedance

The real power along the lossless line at SIL remains constant from the sending end to the receiving end. The reactive power flow is zero. At rated line voltage, the real power delivered (SIL) is given by [23]:

$$\text{SIL} = \frac{NV^2}{Z_c} \tag{2.4}$$

2.2.3 Line Loadability

In practice, power line are not operated to deliver their theoretical maximum power, which is based on rated terminal voltages and an angular displacement $\delta = 90°$ across the line. The relation of line loadability to SIL as a function of line length is given in Figure 2.2. While a transmission system would not be constructed according to the curve in Figure 2.2, it is a useful way of visualizing the impact of a conversion which allows an increase of line voltage with small change in surge impedance. Because SIL is a function of square of the phase-to-neutral voltage, an increase in voltage can have a significant impact on the line SIL. When developing three- and six-phase transmission line alternatives, it is possible to develop six-phase lines with comparable thermal or surge-impedance loading characteristics to the three-phase alternative. The appropriate comparison to use is related to the specific application, especially whether the line limits the system or the system limits the line.

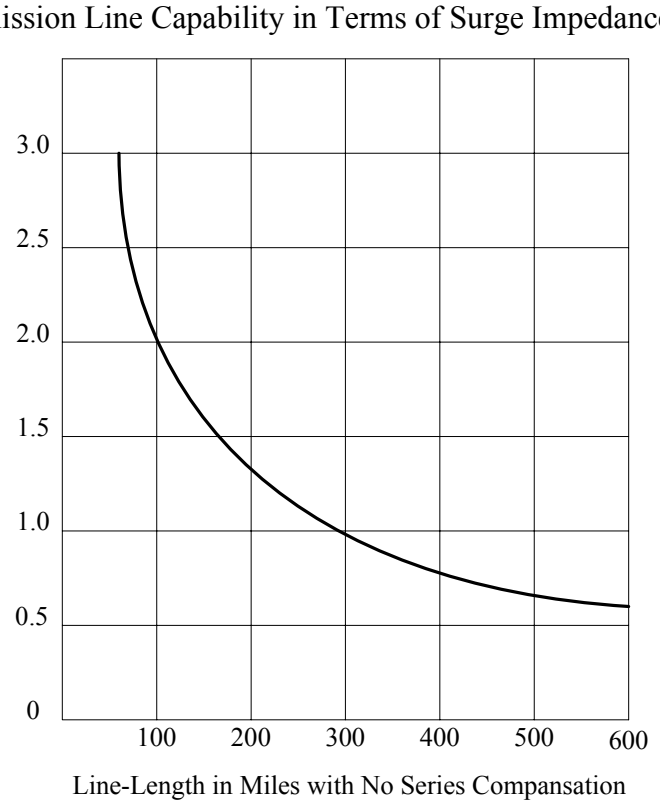

Figure 2.2: Surge impedance loading characteristic curve

2.2.4 Stability Performance

The power flow through any transmission line, neglecting the effect of line resistance is given by [23]:

$$P = \frac{NV_1V_2 \sin\delta}{x} \tag{2.5}$$

The power flow is maximum when $\delta = 90°$. If the angle δ exceeds 90°, the power decreases with increasing angle, a condition of voltage instability. System changes which reduce δ for the same power enhanced the system stability, because there is additional margin for the system to swing without exceeding the 90° limit. Increasing phase-to-neutral voltage by a six-phase conversion increases the per-unit positive-sequence impedance, thus generally enhancing system stability in the same manner as system stability is enhanced by any conversion that results in a higher line operating voltage [23]. Of course, this statement is somewhat of an over simplification, because a higher-voltage line generally carries a greater load, which results in a greater system disturbance in the even of a line trip. The basic effect of a six-phase line on system stability is similar to the effect of a higher-voltage three-phase line and must be evaluated by the same type of stability analysis.

2.3 Power Transformer

A transformer has been defined by ANSI/IEEE as a static electrical device, involving no continuously moving parts, used in electric power systems to transfer power between circuits through the use of electromagnetic induction. The term power transformer is used to refer to those transformers used between the generator and the distribution circuits and are usually rated at 500 kVA and above. The power transformer is a major power system component that permits economical power

transmission with high efficiency and low series-voltage drops. Since electric power is proportional to the product of voltage and current, low current levels (and therefore low I^2R losses and low IZ voltage drops) can be maintained for given power levels via high voltages.

Power systems typically consist of a large number of generation locations, distribution points, and interconnections within the system or with nearby systems, such as a neighbouring utility. The complexity of the system leads to a variety of transmission and distribution voltages. Power transformers must be used at each of these points where there is a transition between voltage levels. Power transformers are selected based on the application, with the emphasis towards custom design being more apparent the larger the unit. Power transformers are available for step-up operation, primarily used at the generator and referred to as generator step-up (GSU) transformers, and for step-down operation, mainly used to feed distribution circuits. Power transformers are available as a single-phase or three-phase apparatus. The construction of a transformer depends upon the application, with transformers intended for indoor use primarily dry-type but also as liquid immersed and for outdoor use usually liquid immersed. The example of outdoor liquid-immersed transformers has been shown in Figure. 2.3.

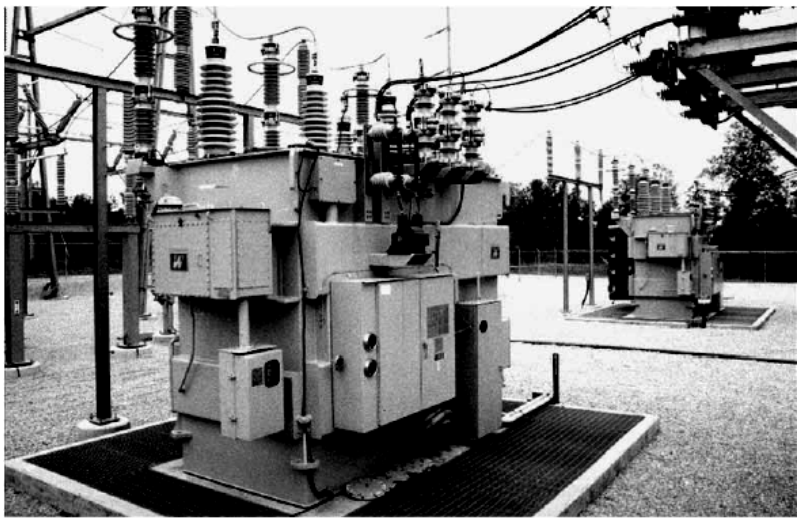

Figure 2.3: 20 MVA three-phase transformers.

Power transformers transform AC voltage and current to optimum levels for generation, transmission, distribution, and utilization of electric power. The development in 1885 by William Stanley of a commercially practical was what made AC power systems more attractive than DC power systems. The AC system with a transformer overcome voltage problems encountered in DC systems as load levels and transmission distances increased. Today's modern power transformers have nearly 100% efficiency, with ratings up to and beyond 1300 MVA.

A transformer is two sets of coils coupled together through a magnetic field. In an ideal transformer, the voltages on the input and the output are related by the turn's ratio of the transformer and given as below:

$$V_1 = \frac{N_1}{N_2} V_2 \tag{2.6}$$

In a real transformer, not all of the flux couples between windings. This leakage flux creates a voltage drop between windings, so the voltage is more accurately described by

$$V_1 = \frac{N_1}{N_2} V_2 - X_L I_1 \tag{2.7}$$

The current also transforms by the turns ratio, opposite of the voltage as

$$I_1 = \frac{N_2}{N_1} I_2 \text{ or } N_1 I_1 = N_2 I_2 \tag{2.8}$$

The vast majority of distribution transformers used are single phase, usually serving a single residence or as many as 14 to 16, depending on the characteristics of the residential load. Single-phase transformers can be connected into banks of two or three separate units. Each unit in a bank should have the same voltage ratings but need not supply the same kVA load. The primary winding of a single-phase

transformer can be connected between a phase conductor and ground or between two phase conductors of the primary system.

2.4 Three-Phase Transformer Connections

Three-phase transformers have one coaxial coil for each phase encircling a vertical leg of the core structure. Stacked cores have three or possibly four vertical legs, while wound cores have a total of four loops creating five legs or vertical paths: three down through the centre of the three coils and one on the end of each outside coil. The use of three versus four or five legs in the core structure has a bearing on which electrical connections and loads can be used by a particular transformer. The advantage of three-phase electrical systems in general is the economy gained by having the phases share common conductors and other components. This is especially true of three-phase transformers using common core structures. Three-phase overhead transformer services are normally constructed from three single-phase units. Three-phase transformers for underground service (either pad mounted, direct buried, or in a vault or building or manhole) are normally single units, usually on a three- or five-legged core. The kVA rating for a three-phase bank is the total of all three phases. The full-load current in amps in each phase of a three-phase unit or bank is

$$I = \frac{S_{kVA}}{3V_{P,kV}} = \frac{S_{kVA}}{\sqrt{3}V_{L,kV}} \tag{2.9}$$

There are two ways that can be used to construct a three-phase transformer. First, three identical single-phase two-winding transformers may be connected to form three-phase bank. Secondly, a three-phase transformer can be constructed by winding three single-phase transformers on a single core. Voltage and current magnitude depends on the windings connection used at the primary and the

secondary sides of that three-phase transformer. The primary or secondary sides of the three-phase transformer may be connected by using either Wye (Y) or Delta (Δ) connections. There are four common combinations used in three-phase transformer which is, Y-Y, Y-Δ, Δ-Y, Δ-Δ.

i. Wye-Wye, (Y-Y)
ii. Wye-Delta (Y-Δ)
iii. Delta-Wye (Δ-Y)
iv. Delta-Delta (Δ-Δ)

2.4.1 Y-Y Connection

The three transformer windings in Figure 2.4 have been labelled as A, B and C respectively. One end of each primary lead has been labelled as H_1 and the other end has been labelled as H_2. Furthermore, one end of each secondary lead has been labelled as X_1 and the other end has been labelled as X_2. The three transformer windings have been connected to form a three-phase transformer with Y-Y connection as shown in Figure 2.4. The schematic diagram for Y-Y connected three-phase transformer is shown in Figure 2.5. For a three-phase transformer with Y-Y connection, voltage relation on primary winding for all phase is given by $V_{PP} = V_{LP}/\sqrt{3}$. Primary phase-to-neutral voltage relates to secondary phase-to-neutral voltage by number of winding turns. The relation of phase-to-neutral voltage and phase-to-phase voltage on secondary side is given by $V_{LS} = \sqrt{3}V_{PS}$ [3].

$$\frac{V_{LP}}{V_{LS}} = \frac{\sqrt{3}V_{PP}}{\sqrt{3}V_{PS}} = a \tag{2.10}$$

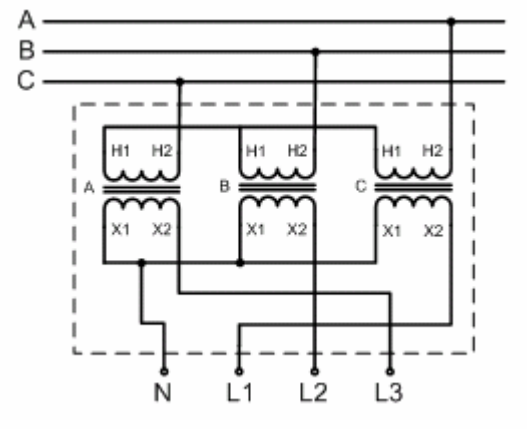

Figure 2.4: Y-Y connected three-phase transformer

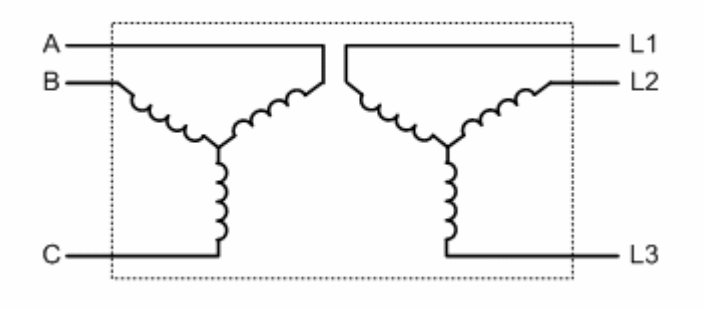

Figure 2.5: Schematic diagram of Y-Y connected three-phase transformer

2.4.2 Y-Δ Connection

Figure 2.6 shows the three-phase transformer with Y-Δ connection. The schematic diagram for Y-Δ connected three-phase transformer is shown in Figure 2.7. The relation between phase-to-neutral voltage and phase-to-phase voltage for primary and secondary side is given by [3]:

$$V_{LP} = \sqrt{3} V_{PP} \;\&\; V_{LS} = V_{PS}$$

$$\frac{V_{PP}}{V_{PS}} = a$$

$$\frac{V_{LP}}{V_{LS}} = \frac{\sqrt{3}V_{PP}}{V_{PS}}$$

$$\frac{V_{LP}}{V_{LS}} = \sqrt{3}a \tag{2.11}$$

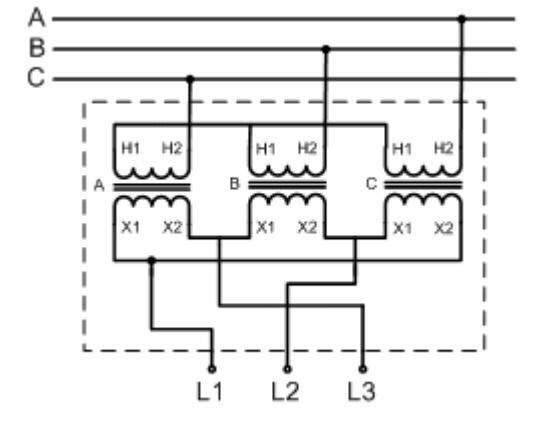

Figure 2.6: Y-Δ connected three-phase transformer

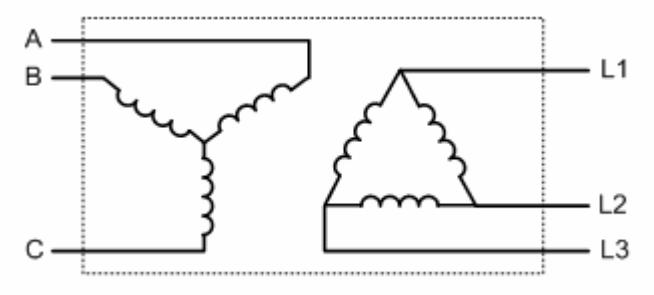

Figure 2.7: Schematic diagram of Y-Δ connected three-phase transformer

2.4.3 Δ-Y Connection

Figure 2.8 shows the three-phase transformer with Δ-Y connection. The schematic diagram for Δ-Y connected three-phase transformer is shown in Figure 2.9. The relation between phase-to-neutral voltage and phase-to-phase voltage for primary and secondary side is given by [3]:

$$V_{LP} = V_{PP} \;\&\; V_{LS} = \sqrt{3} V_{PS}$$
$$\frac{V_{LP}}{V_{LS}} = \frac{V_{PP}}{\sqrt{3} V_{PS}} \qquad (2.12)$$
$$\frac{V_{LP}}{V_{LS}} = \frac{a}{\sqrt{3}}$$

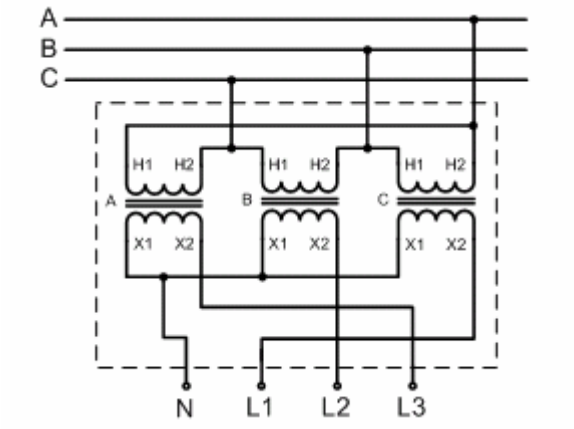

Figure 2.8: Δ-Y connected three-phase transformer

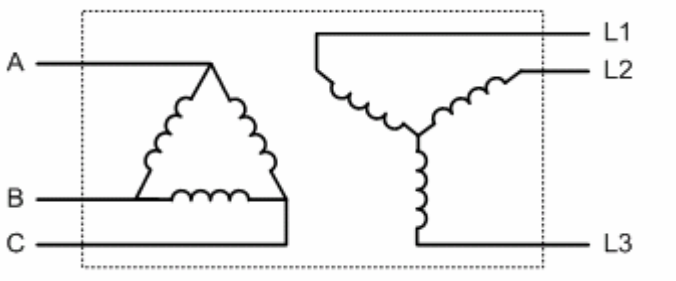

Figure 2.9: Schematic diagram of Δ-Y connected three-phase transformer

2.4.4 Δ-Δ Connection

Figure 2.10 shows the three-phase transformer with Δ-Δ connection. The schematic diagram for Δ-Δ connected three-phase transformer is shown in Figure 2.11. The relation between phase-to-neutral voltage and phase-to-phase voltage for primary and secondary side is given by [3]:

$$V_{LP} = V_{PP}$$
$$V_{LS} = V_{PS}$$
$$\frac{V_{LP}}{V_{LS}} = \frac{V_{PP}}{V_{PS}} = a \qquad (2.13)$$

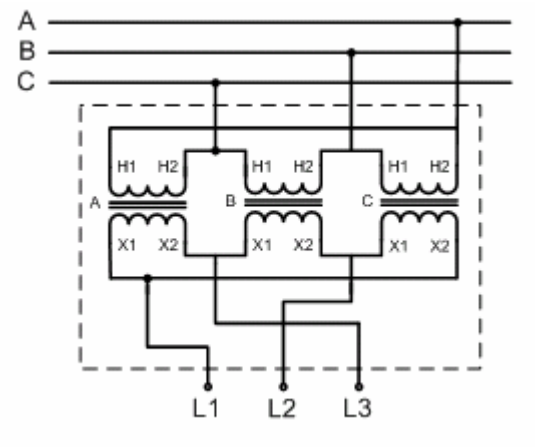

Figure 2.10: Δ-Δ connected three-phase transformer

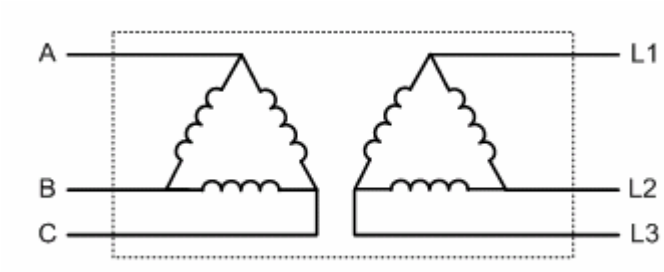

Figure 2.11: Schematic diagram of Δ-Δ connected three-phase transformer

2.5 Six-Phase Transformer Connections

There are two types of single-phase transformers can be used to build a three-to-six-phase conversion transformer. First, six identical single-phase two-winding transformers may be connected to form three-to-six-phase bank. Secondly, three identical single-phase three-winding transformers may be connected together to form three-to-six-phase bank. Voltage and current magnitude depends on the windings connection used on the primary and the secondary sides of the three-to-six-phase conversion transformer. The primary or secondary side of the three-to-six-phase conversion transformer may be connected by using any combinations of either Wye (Y) or Delta (Δ) connections. There are five common connections and combinations that can be used to form a three-to-six-phase conversion transformer which is Y-Y and Y-Inverted Y, Δ-Y & Δ-Inverted Y, Diametrical, Double-Delta and Double-Wye.

2.5.1 Y-Y and Y-Inverted Y

The six transformer windings in Figure 2.12 have been labelled as A, B, C, D, E and F respectively. One end of each primary lead has been labelled as H_1 and the other end has been labelled as H_2. Furthermore, one end of each secondary lead has been labelled as X_1 and the other end has been labelled as X_2. Figure 2.12 shows the Y-Y and Y-Inverted Y connected three-to-six-phase conversion transformer. The schematic diagram for Y-Y and Y-Inverted Y connected three-to-six-phase conversion transformer is shown in Figure 2.13.

From Figure 2.12 and Figure 2.13, we can see that the first three-phase transformer is used Y-Y connection and produced three phase line on the secondary side name as lines L1, L3 and L5. At the other hand, the second three-phase

transformer is used Y-Inverted Y connection and produced another three phase line on the secondary side name as lines L2, L4 and L6. Combination of all these line will produce six-phase line name as L1, L2, L3, L4, L5 and L6. Neutral line name as *N* is the common for all neutral lines of transformers.

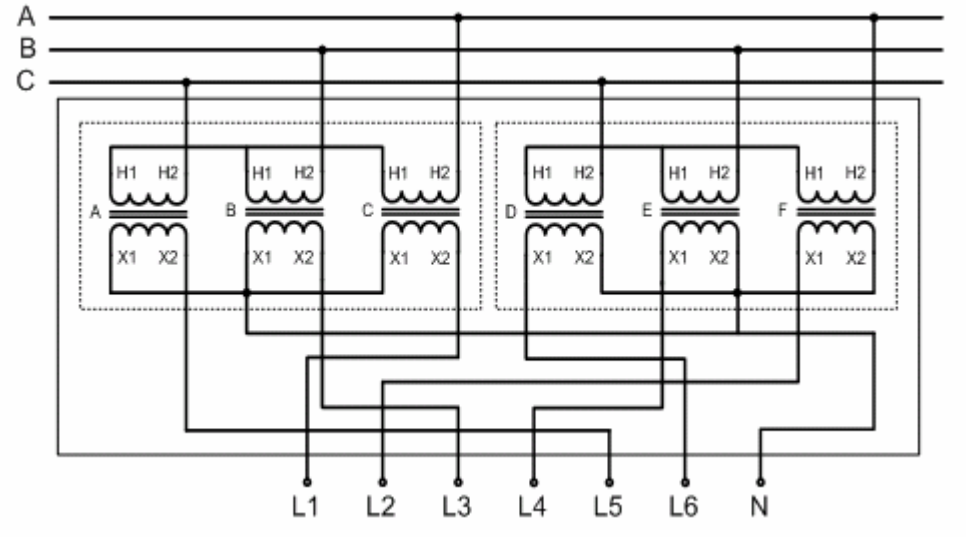

Figure 2.12: Y-Y and Y-Inverted Y connected three-to-six-phase conversion transformer

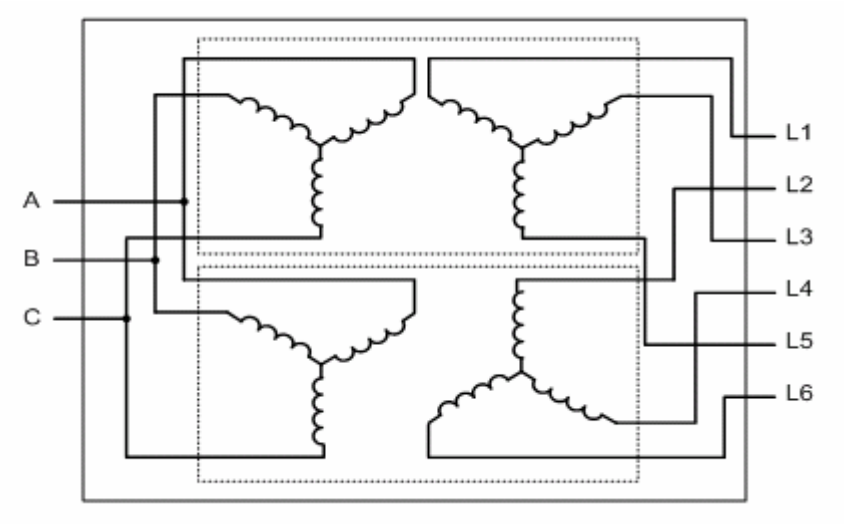

Figure 2.13: Schematic diagram of Y-Y and Y-Inverted Y connected three-to-six-phase conversion transformer

2.5.2 Δ-Y and Δ-Inverted Y

Figure 2.14 shows the Δ-Y and Δ-Inverted Y connected three-to-six-phase conversion transformer. The schematic diagram for Δ-Y and Δ-Inverted Y connected three-to-six-phase conversion transformer is shown in Figure 2.15.

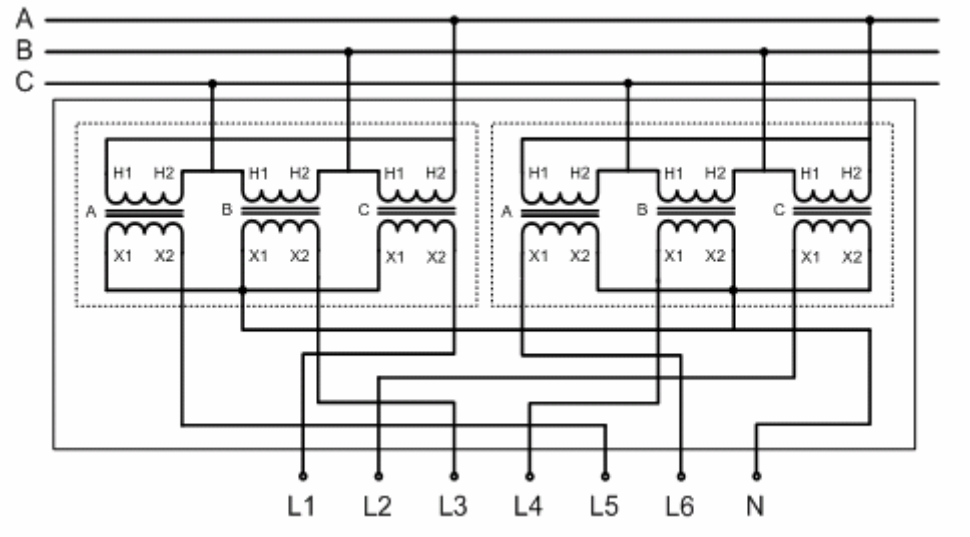

Figure 2.14: Δ-Y and Δ-Inverted Y connected three-to-six-phase conversion transformer

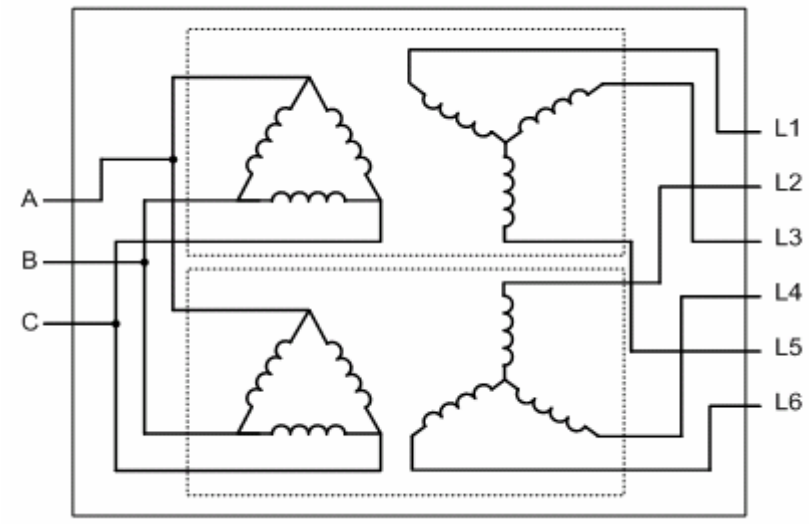

Figure 2.15: Schematic diagram of Δ-Y and Δ-Inverted Y connected three-to-six-phase conversion transformer

2.5.3 Diametrical

Figure 2.16 shows the Diametrical connected three-to-six-phase conversion transformer. The schematic diagram for Diametrical connected three-to-six-phase conversion transformer is shown in Figure 2.17.

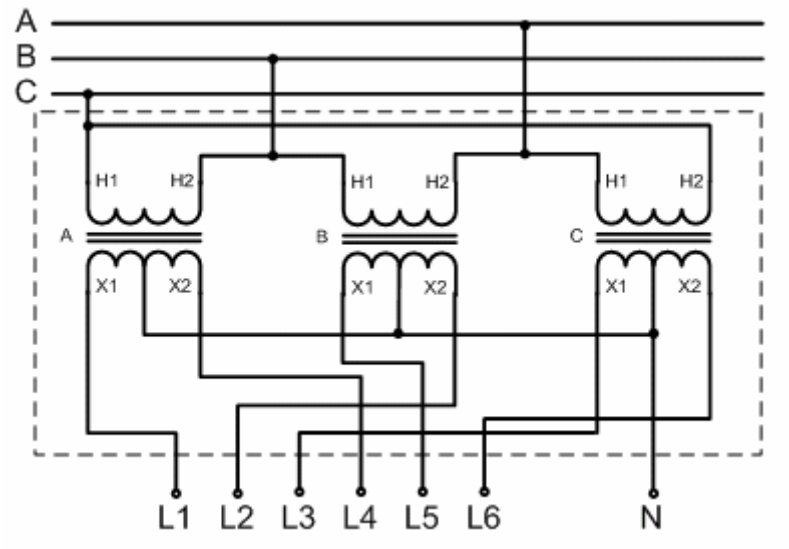

Figure 2.16: Diametrical connected three-to-six-phase conversion transformer

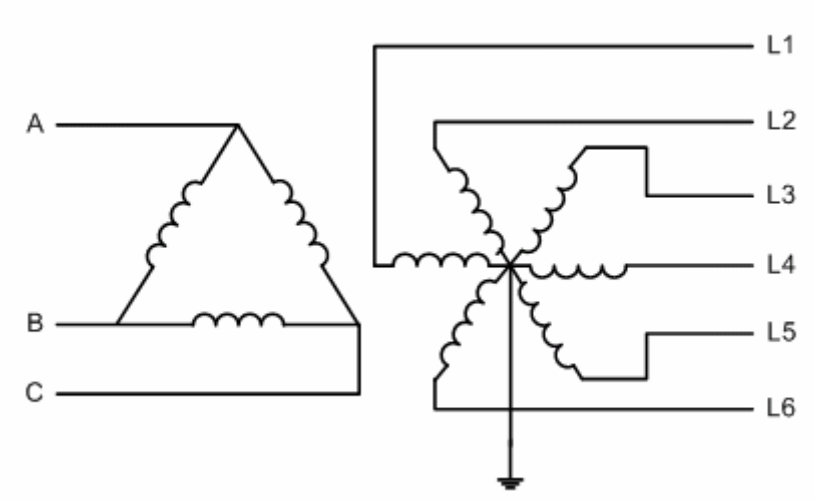

Figure 2.17: Schematic diagram of Diametrical connected three-to-six-phase conversion transformer

2.5.4 Double-Delta

Figure 2.18 shows the Double-Delta connected three-to-six-phase conversion transformer. The schematic diagram for Double-Delta connected three-to-six-phase conversion transformer is shown in Figure 2.19.

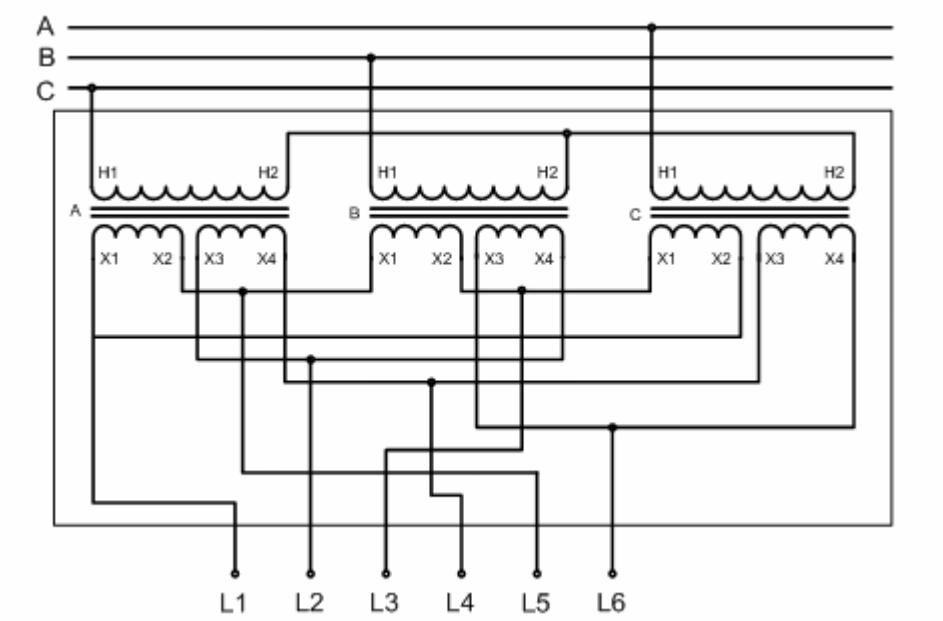

Figure 2.18: Double-Delta connected three-to-six-phase conversion transformer

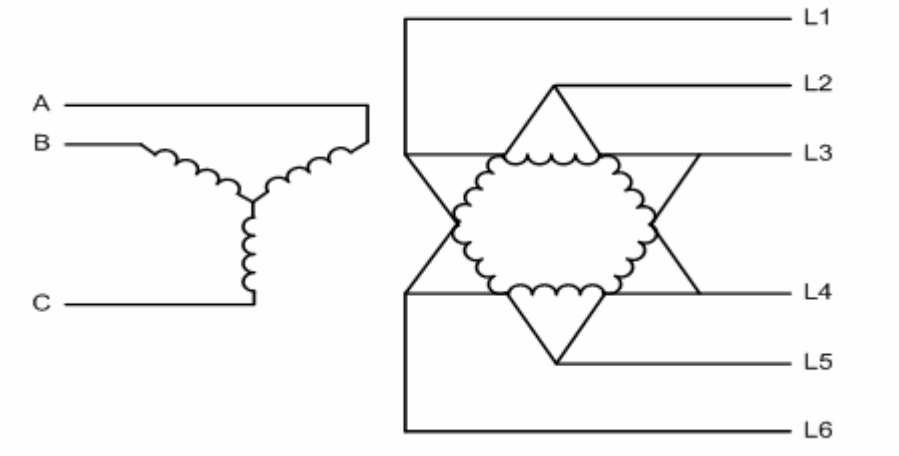

Figure 2.19: Schematic diagram of Double-Delta connected three-to-six-phase conversion transformer

2.5.5 Double-Wye

Figure 2.20 shows the Double-Wye connected three-to-six-phase conversion transformer. The schematic diagram for Double-Wye connected three-to-six-phase conversion transformer is shown in Figure 2.21.

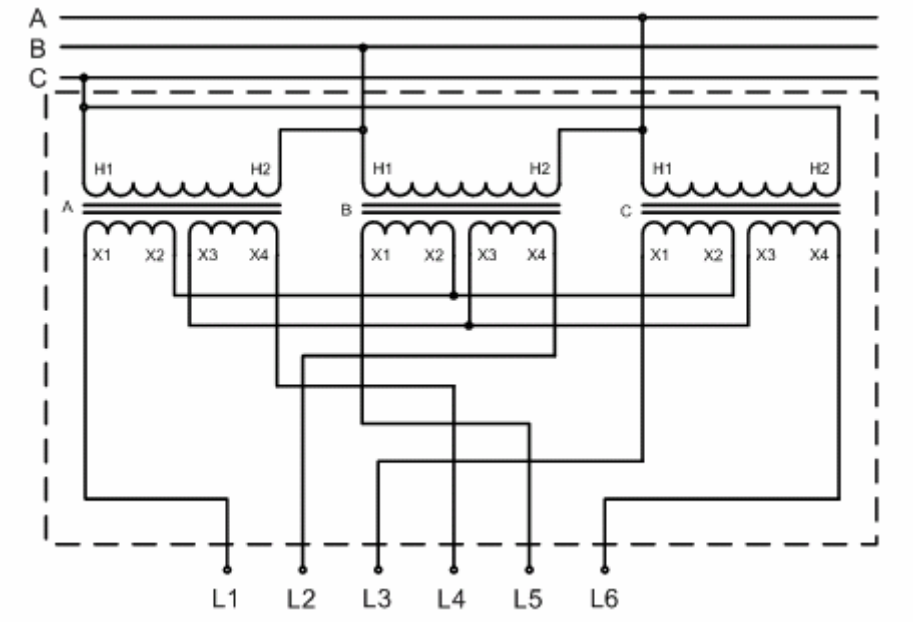

Figure 2.20: Double-Wye connected three-to-six-phase conversion transformer

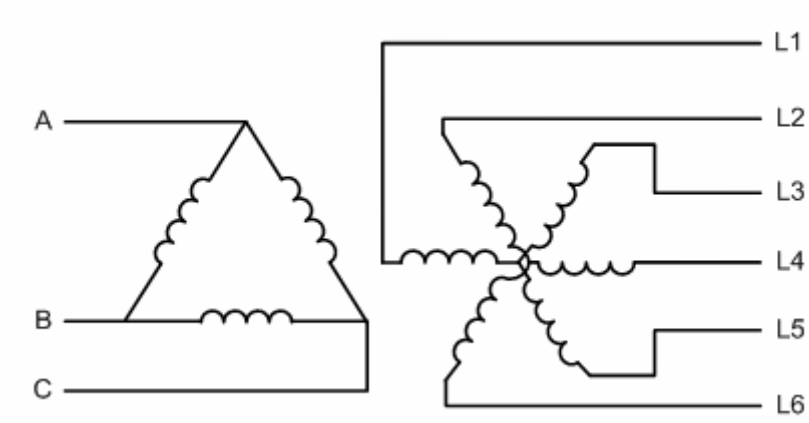

Figure 2.21: Schematic diagram of Double-Wye connected three-to-six-phase conversion transformer

2.6 Phasor Concept

Basic knowledge of phasor relationship is necessary in order to further understand the feasibility of six-phase transmission. For the purpose of comparison, the phasor relationship of three-phase and six-phase system will be described in details to make this subject understandable.

2.6.1 Phasor Relationship in Three-Phase System

A typical balanced three-phase system has 120^{o} electrical degrees between each phase as shown in Figure 2.22. From Figure 2.22, we can obtain the relation of phase-to-phase voltage and phase-to-neutral voltage. The phase-to-phase voltage is $\sqrt{3}$ of the phase-to-neutral voltage. Generally phase-to-neutral voltage, V_{AN} is assumed as reference.

$$V_{AN} = V_{AN} \angle 0°$$
$$V_{BN} = V_{BN} \angle -120°$$
$$V_{CN} = V_{CN} \angle 120°$$

Assuming the $V_{AN} = V_{BN} = V_{CN} = V_P$,

$$\begin{aligned} V_{AB} &= V_{AN} \angle 0° - V_{BN} \angle -120° \\ &= V_P (1 \angle 0° - 1 \angle -120°) \\ &= V_P (1+j0 - (-0.5 - j0.866)) \\ &= V_P (1.5 + j0.866) \\ &= \sqrt{3}\, V_P \angle 30° \end{aligned} \tag{2.14}$$

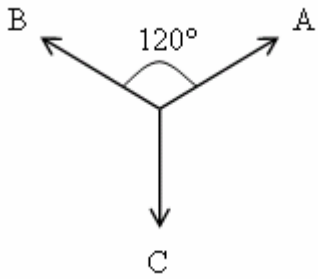

Figure 2.22: Phasors of a three-phase system

The same correlation is applies for phase-to-phase voltage V_{BC} and V_{CA}. In general, the relationship between phase-to-phase voltage and phase-to-neutral voltage is given as follow:

$$V_L = \sqrt{3}\, V_P \angle 30° \qquad (2.15)$$

A three-phase system, with 120° between phases has a phase-to-phase voltage equal to $\sqrt{3}$ phase-to-neutral voltage and always leading phase-to-neutral voltage by 30°. If the phase-to-phase voltage is 132 kV, then the phase-to-neutral voltage is 76.2 kV.

2.6.2 Phasor Relationship In Six-Phase System

A balanced six-phase system has 60^o electrical degrees between each phase as shown in Figure 2.23. From Figure 2.23, we can obtain the relation of phase-to-phase voltage and phase-to-neutral voltage for a six-phase system.

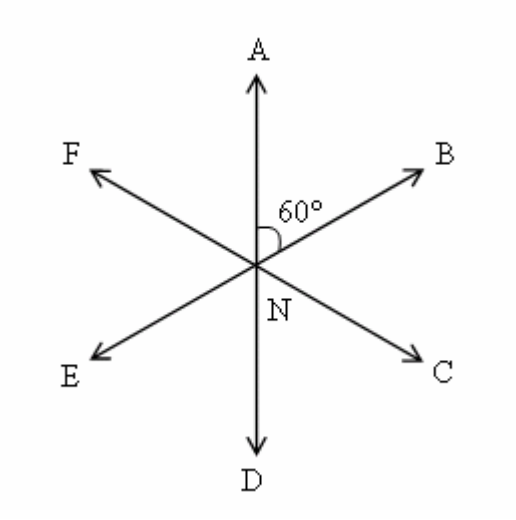

Figure 2.23: Phasors of a six-phase system

Generally, the relation of phase-to-phase voltage to phase-to-neutral voltage for a six-phase system is referring to the relation between adjacent phase-voltage to phase-to-neutral voltage. For six-phase system, the phase-to-phase voltage is equal to phase-to-neutral voltage. The types of voltages relationship for a six-phase system can be divided as follow [5]:

a) Phase-to-phase voltage, V_L : V_{AB}, V_{BC}, V_{CD}, V_{DE}, V_{EF}, V_{FA}.
b) Phase-to-group voltage, $V_{L\text{-}Group}$: V_{AC}, V_{BD}, V_{CE}, V_{DF}, V_{EA}, V_{FB}.
c) Phase-to-crossphase voltage, $V_{L\text{-}Crossphase}$: V_{AD}, V_{BE}, V_{CF}.

The voltage relationship for the phases in a six-phase system can be divided into three groups as refer to the phase shift between all six lines. First group has 60°, second group has 120° and last group has 180° phase shift between phases. Generally phase-to-neutral voltage, V_{AN} is assumed as reference.

$$V_{AN} = V_{AN} \angle 0°$$
$$V_{BN} = V_{BN} \angle -60°$$
$$V_{CN} = V_{CN} \angle -120°$$
$$V_{DN} = V_{DN} \angle -180°$$
$$V_{EN} = V_{EN} \angle -240°$$
$$V_{FN} = V_{FN} \angle -300°$$

2.6.3 Phase-to-Phase Voltage

Phase-to-phase voltage is a potential between adjacent phases where their phase difference is 60°. Figure 2.24 shows the potential between phase A and phase B. Assuming the $V_{AN} = V_{BN} = V_{CN} = V_{DN} = V_{EN} = V_{FN} = V_P$,

$$\begin{aligned} V_{AB} &= V_{AN} \angle 0° - V_{BN} \angle -60° \\ &= V_P (1 \angle 0° - 1 \angle -60°) \\ &= V_P (1+j0 - (0.5 - j0.866)) \\ &= V_P (0.5 + j0.866) \\ &= V_P \angle 60° \end{aligned} \tag{2.16}$$

The same correlation is applies for phase-to-phase voltages V_{AB}, V_{BC}, V_{CD}, V_{DE}, V_{EF} and V_{FA}. For a six-phase system, the magnitude of phase-to-phase voltage is equal to the magnitude of the phase-to-neutral voltage and phase-to-phase voltage always leading the phase-to-neutral voltage by 60°. In general, the relationship between phase-to-phase voltage and phase-to-neutral voltage is given as follow:

$$V_L = V_P \angle 60° \tag{2.17}$$

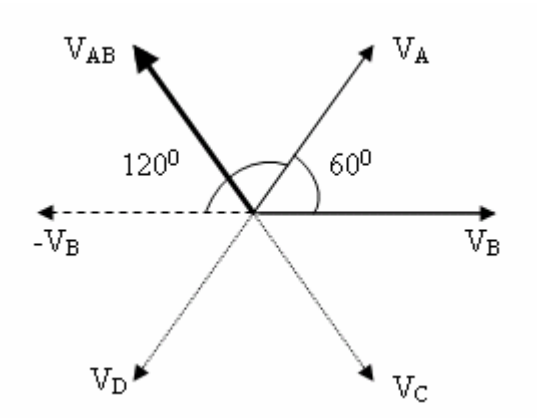

Figure 2.24: Potential between phase A and phase B

2.6.4 Phase-to-Group Voltage

Phase-to-group voltage is a potential between phases where the phase difference is 120°. Figure 2.25 shows the potential between phase A and phase C.

$$\begin{aligned} V_{AC} &= V_{AN} \angle 0° - V_{CN} \angle -120° \\ &= V_P (1 \angle 0° - 1 \angle -120°) \\ &= V_P (1+j0 - (-0.5 - j0.866)) \\ &= V_P (1.5 + j0.866) \\ &= \sqrt{3}\, V_P \angle 30° \end{aligned} \tag{2.18}$$

The same correlation is applies for phase-to-phase voltages V_{AC}, V_{BD}, V_{CE}, V_{DF}, V_{EA} and V_{FB}. The magnitude of phase-to-group voltage is $\sqrt{3}$ times the magnitude of the phase-to-neutral voltage and phase-to-phase voltage always leading the phase-to-neutral voltage by 30°. In general, the relationship between phase-to-group voltage and phase-to-neutral voltage is given as follow:

$$V_{L\text{-}Group} = \sqrt{3}\, V_P \angle 30° \tag{2.19}$$

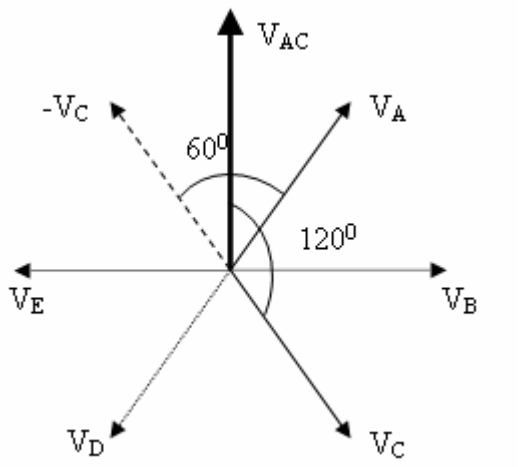

Figure 2.25: Potential between phase A and phase C

2.6.5 Phase-to-Crossphase Voltage

Phase-to-crossphase voltage is a potential between phases where the phase difference is 180°. Figure 2.26 shows the potential between phase A and phase D.

$$\begin{aligned} V_{AD} &= V_{AN} \angle 0° - V_{DN} \angle -180° \\ &= V_P (1 \angle 0° - 1 \angle -180°) \\ &= V_P (1+j0 - (-1.0 + j0)) \\ &= V_P (2) \\ &= 2V_P \angle 0° \end{aligned} \tag{2.20}$$

The same correlation is applies for phase-to-phase voltages V_{AD}, V_{BE} and V_{CF}. The magnitude of phase-to-crossphase voltage is two times the magnitude of the phase-to-neutral voltage. In general, the relationship between phase-to-crossphase voltage and phase-to-neutral voltage is given as follow:

$$V_{L\text{-}Crossphase} = 2V_P \angle 0° \tag{2.21}$$

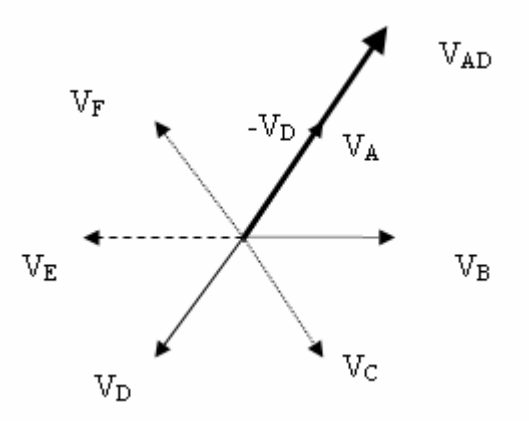

Figure 2.26: Potential between phase A and phase D

2.7 Advantages

With the growing concern over the environmental effects of power system, six-phase transmission offers several advantages over conventional three-phase double-circuit networks. The following subtitles show the advantages of six-phase transmission line. These benefits are among the reasons why power system engineers are consistently pursues knowledge on the power system technology.

2.7.1 Higher Power Transfer Capability

Traditionally, the need for increased power transmission capability and more efficient use of ROW space has been accomplished by the use of successively higher system voltages. Recently, environmental and land use constraints have demanded increased design sophistication including the investigation of alternate technologies including HVDC and HPO transmission. One of the main advantages of six-phase technology is that the six-phase line can carry up to 73% more electric power than a conventional three-phase double-circuit line on the same transmission conductor, tower size and ROW [18].

Taking for example, a conventional three-phase 138 kV double-circuit line can transmit $2(\sqrt{3} \times 138 \times I_{line} \cos\theta) = 478\ I_{line} \cos\theta$ MW of power, assuming I_{line} is in kA. If this particular line is converted to a six-phase line, it will allow transmission of $6 \times 138 \times I_{line} \cos\theta = 828\ I_{line} \cos\theta$ MW of power, (Note that in six-phase, the $V_P = V_L = 138$ kV) [18].

Power transmission capability is directly proportional to phase-to-phase voltage. As seen by the phasor relationship, for the same phase-to-phase voltage in the three-phase system, a six-phase system has a 73% increase in phase-to-neutral voltage. Therefore, it can be observed that, when a three-phase double-circuit line is converted to six-phase line, the power capability is increased by 73%.

2.7.2 Increased Utilization of Right-of-Way

Six-phase transmission increases power density. Power density refers to the amount of power that can be transmitted down a given window of ROW assuming there are environmental and technical constraints that limits size of ROW. Thus, these lines can transfer more power over a given ROW than equivalently loaded three-phase lines [9].

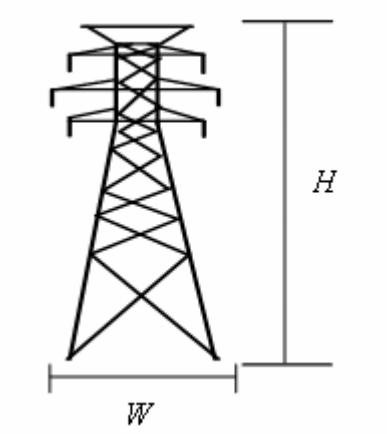

Figure 2.27: Determining power density

Refers to Figure 2.27, the correlation between power density and ROW is given as follow:

$$\text{AREA} = H \text{ x } W\, ft^2$$

$$\text{Power Density} = \frac{Power \quad transmitted(KW)}{Area(ft^2)} \tag{2.22}$$

2.7.3 Smaller Structure

The phase-to-phase voltages between adjacent phases in a six-phase system are lower than the phase-to-phase voltages for a three-phase system for a given phase-to-neutral voltage. This advantage permits smaller towers for the same power rating. As a result, the minimum spacing between conductors on the six-phase transmission tower is reduced. The smaller structures provide increased power transfer for a given ROW. This is especially important since ROW is becoming more difficult to obtain and increasingly expensive.

The six-phase lines intrinsically have a lower likelihood of incident lightning strikes because of the smaller structure. Besides the troubles caused by the wind induced movements and visual impact can be reduced. These two troubles increase the caused of maintenance for the structures of the transmission line and which, sometimes may caused the danger of life [9].

2.7.4 Lower Insulation Requirement

For a six-phase system, the insulation required to support one phase from an adjacent phase is equal to that required to support a phase from the zero potential point. Thus, utilities can save on various insulating materials for various components of transmission system [13].

2.7.5 Better Stability Margin

A six-phase line can be operated at a smaller power angle than a three-phase line. This means that the six-phase line offers better stability margin than its three-phase counterpart [18].

2.7.6 Lower Corona and Field Effects

Conversion from three-phase double-circuit to six-phase single-circuit has the effect of reducing electric field at the conductor surface for the same phase-to-neutral voltage. Conductor gradients decrease as the number of phases increases for a given conductor size and tower configuration. Thus, radio and audio noise can be reduced which in turn leads to lesser television and radio interference. The reduction in electric field can be utilized in either of two ways [18]:

a) Increase the phase-to-neutral voltage until the conductor surface electric field is a maximum for corona thus increasing the power handling capacity of the line.

b) Maintain the same phase-to-neutral voltage and decrease the conductor spacing until the conductor surface electric field is a maximum for corona, thus making the line more compact.

2.7.7 Lightning Performance

When the line is converted to six-phase operation, there is an increase in the shielding failure rate and a reduction in the backflash rate, resulting in a net reduction in the trip out of rate. However, the total flashovers are so close before and after conversion that there will not be any noticeable difference in lightning performance at the line. Table 2.1 presents the results of the lightning calculation in flashovers per year referred to a line length of 2.4 km [18].

Table 2.1: Goudey-Oakdale lightning performance flashovers per year for 2.4 km of line

Configuration	Shielding Failures	Backflashes	Total
115 kV three-phase	0.029	0.126	0.155
93 kV six-phase	0.049	0.077	0.127

2.8 Feasibility

The aim of improving efficiency of transmission network is indeed the driving factor for electrical utility engineers to consider the six-phase transmission. Six-phase transmission system offers the opportunity to meet the increasing demands for power yet at the same time meet the environmental and regulatory constraints.

However, the economy factors have to be considered. Terminal expenses can be quite high for six-phase lines. A six-phase line would require conversion transformers that would cause the terminals to be more costly. The high cost of terminals is offset by reduced tower and lower foundation costs, ROW cost and losses.

2.9 Summary

This chapter deals with the principles of the six-phase transmission system. Some theoretical aspects of electric power transmission are described. Hence, more clearly view about the idea of six-phase transmission system is also discussed. Moreover, the phasors relationship for both three-phase and six-phase system is discussed in details. For a three-phase system, phase-to-phase voltage is equal to $\sqrt{3}$ phase-to-neutral voltage. The phase-to-phase voltages always lead the phase-to-neutral voltage by 30°. In a six-phase system, the phasors relationship can be divided into three categories. They are categorized depends to the phase difference between phases which is 60°, 120° and 180°. These categories are phase-to-phase voltages, phase-to-group voltages and phase-to-crossphase voltages. As proves that discussed in this chapter, six-phase have a great deal of advantages over three-phase transmission system.

CHAPTER III

STATIC AND DYNAMIC IMPACT OF SIX-PHASE TRANSMISSION SYSTEM

3.1 Introduction

Power system planning, design and operations require careful studies in order to evaluate the system performance, safety, efficiency, reliability and economics. Such studies help to identify the potential deficiencies of the proposed system. In the existing system, the cause of the equipment failure and malfunction can be determined through a system study. Preliminary research effort applied elsewhere in the world e.g. at New York State Electric and Gas (NYSEG) Corporation, has prove the economic and technical viability of an alternative option of three to six-phase conversion of an existing double-circuit line permitting about 73% more energy transmission without any change of the existing line tower and conductors.

However, this conversion will have impact among others on static (steady state voltage profile, line flow, fault level) and dynamic (transient stability) performance of the power system. These impacts can be studied independently of the other impacts.

The modern interconnected power systems are complex, with several thousand buses and components. The manual calculation of the performance indices is time consuming. The computational efforts are very much simplified in the present day calculations due to the availability of efficient program and powerful microcomputers. The main focus in this chapter is the literature reviews of static and dynamic impacts of three to six-phase conversion of selected transmission line in an electric energy system. The basic concepts of load flow analysis, fault analysis and transient stability analysis will be described in more details.

3.2 Load Flow Analysis

The bulk power is generated by three main methods which is hydro sources, coal fired stations and nuclear generating stations. Isolated power supplies are obtained from diesel engine driven generators, wind electric generators, solar panels and batteries. The bulk power is commonly generated at 4.16 kV, 13.8 kV, 18 kV or 22 kV and is stepped up to high voltages for transmission. In Malaysia country, TNB normally generate power at their voltage standard which is 11 kV, 13.8 kV, 16 kV and 22 kV. The load centres are usually located away from generating stations. Therefore, the power is transmitted to the load centres by using higher transmission system voltages and is stepped down to distribution levels.

The load is supplied at various voltage levels. The load may be residential, industrial or commercial. Depending on the requirement the loads are switch on and off. Therefore, there are peak load hours and off peak load hours. When there is a need, power is transmitted from one area to the other area through the tie lines. The control of generation, transmission, distribution and area exchange are performed from a centralized location. In order to perform the control functions satisfactory, the steady state load flow must be known. Therefore, the entire system is modelled

as electric networks and a solution is simulated using s digital program. Such a problem solution practice is called load flow analysis.

Load flow analysis is the steady state analysis of an interconnected power system during normal operation. The system is assumed to be operating under balanced condition and is represented by a single-phase network. The network contains hundreds of nodes and branches with impedances specified in per unit on a command MVA base. Network equations can be formulated systematically in a variety of forms. However, the node-voltage method, which is the most suitable form for many power system analyses, is commonly used.

Load flow studies are used to determined the bus voltage, branch current, active and reactive load flow for a specified generation and load conditions in a given power system. A number of operating conditions can be analyzed including contingencies such as loss of generator, loss of transmission line, loss of a transformer or a load. These conditions may cause equipment overloads or unacceptable voltage levels. The study results can be used to determine the optimum size and location of the capacitors for power factor improvement. Further, the results of the load flow analysis are the starting point for the stability analysis. Digital computers are used extensively in load flow study because of large-scale nature of the problem and the complexities involved. For the load flow analysis, the acceptable voltage levels are derived from the industry standards. The line and transformers loadings are evaluated according to the normal, short-term emergency and long-term emergency ratings.

Nowadays, numerous software's and developed programs are available to solve load flow for a large-scale power system. In this research, a MATPOWER (MATLAB^{TM} Power System Simulation Package) is used to get load flow solutions of the test systems. MATPOWER is a package of Matlab m-files for solving load flow and optimal load flow problems. It is intended as a simulation tool for researchers and educators that are easy to use and modify. MATPOWER has been

designed to give the best performance possible while keeping the code simple to understand and modify. MATPOWER is used to solve load flow of all test systems with three-phase double-circuit transmission system. The important of running load flow by using MATPOWER is to get the steady state values that will be used in modelling of power system by using PSCAD/EMTDC.

The results from load flow analysis by using MATPOWER are used to model the test systems in PSCAD. The completed model in PSCAD then has been studied. It is done by making comparisons of load flow results from MATPOWER and PSCAD. The results from PSCAD should be the same or close as the results from MATPOWER to make sure that the model developed in PSCAD is accurate. Once the load flow results from PSCAD has been validated, the model of the test systems in PSCAD are ready to be used to other types of analysis such as fault analysis and transient stability analysis.

3.3 Fault Analysis

In power system, faults occur once in a while due to lightning, flashover due to polluted insulation, falling of three branches on the overhead system, animal intrusion and erroneous operations. When the fault current magnitudes are significant, it can cause damage to equipment and explosion if the fault is not cleared for prolonged time. Also, electrical fire hazards to people are possible in a faulted power system. Therefore, it is important to design the power system such as the fault is isolated quickly to minimize the equipment damage and improve personal safety.

Fault analyses are performed to determine the magnitude of the current flowing throughout the power system at various time intervals after a fault. The magnitude of the current through the power system after a fault varies with time until

it reaches a steady state condition. During the fault, the power system is called on to detect, interrupt and isolate these faults. The duty impressed on the equipment is dependent on the magnitude of the current, which is a function of the time of fault initiation. Such calculations are performed for various types of fault such as six-phase-to-ground, three-phase-to-ground, three-phase, two-phase-to-ground, two-phase, single-phase-to-ground and at different location of the system. The calculated fault currents are used to select fuses, circuit breakers, and surge protective relays. The symmetrical component model is used in the analysis of the unsymmetrical faults.

3.3.1 Power System Fault

One of the most important items in applying six-phase alternative in transmission planning is the design of an adequate protective scheme. This requires a detailed and realistic fault analysis which is the main theme of this section. General definition for fault is “any failure that interferes with the normal flow of current”. The fault current that occurs in power system is usually large and dangerous. Faults can occur because of short circuits or partial short circuits, open circuits, unbalanced conditions or any other reasons. Short circuit faults are the most common and most damaging, as the excessive current can cause thermal and mechanical damage to the plant carrying it.

The complexity of fault analysis in a six-phase system is greater than in a three-phase system. Six-phase faults are the least common while single-line-to-ground faults are the most common. In addition, faults involving two and three phases with several distinct possibilities could be more frequent in six-phase systems compared to three-phase system.

3.3.2 Faults on Six-Phase Power System

The faults that can occur on six-phase power systems are of symmetrical or unsymmetrical types, which may consist of short circuits, faults through impedances, or open conductors. The fault analysis in six-phase power systems are more complicated than in the conventional three-phase power systems. This is due to the fact that there are six-phases, each subjected to a different voltage, and the presence of a neutral makes the number of fault types much greater. The total number of possible faults in three-phase system is 11 while that in six-phase is 120. The number of possible significant faults in three-phase and six-phase systems is 5 and 23 respectively. Consider phase-to-phase faults that do not involve ground in six-phase system. Therefore, current magnitude and circuit asymmetry for a fault on phases A and B is the same as that on B and C, and so on. Therefore, the 15 two-phase fault combinations are reducing to three significant combinations. There are [19]:

a) Faults between phases 60^o apart (e.g.: phase *a* to phase *b*)

b) Faults between phases 120^o apart (e.g.: phase *a* to phase *c*)

c) Faults between phases 180^o apart (e.g.: phase *a* to phase *d*)

In a similar manner, analysis for all faults can be confined to 23 significant combinations as mentioned. For the purpose of comparisons, the types of faults for both three-phase transmission and six-phase transmission system are shown in Table 3.1 and Table 3.2 respectively.

Table 3.1: Types of faults on three-phase system and the combinations

Fault Type	Total Number of Combinations	Significant Number of Combinations	Faulted Phases for Significant Combinations
Three-phase	1	1	a-b-c
Three-phase-to-ground	1	1	a-b-c-g
Two-phase	3	1	b-c
Two-phase-to-ground	3	1	b-c-g
Single-phase-to-ground	3	1	a-g
Total	11	5	

Table 3.2: Types of faults on six-phase system and the combinations

Fault Type	Total Number of Combinations	Significant number of Combinations	Faulted Phases for Significant Combinations
Six-phase	1	1	a-b-c-d-e-f
Six-phase-to-ground	1	1	a-b-c-d-e-f-g
Five-phase	6	1	b-c-d-e-f
Five-phase-to-ground	6	1	b-c-d-e-f-g
Four-phase	15	3	b-c-e-f, a-b-c-d, a-b-d-f
Four-phase-to-ground	15	3	b-c-e-f-g, a-b-c-d-g, a-b-d-f-g
Three-phase	20	3	b-d-f, a-b-d, a-b-f
Three-phase-to-ground	20	3	b-d-f-g, a-b-d-g, a-b-f-g
Two-phase	15	3	a-d, b-f, b-c
Two-phase-to-ground	15	3	a-d-g, b-f-g, b-c-g
Single-phase to ground	6	1	a-g
Total	120	23	

3.3.3 Symmetrical Components

The method of symmetrical components is the most powerful tool for dealing with unbalanced polyphase systems. Fostescue's work has proved that an unbalanced system of *N* related phasors can be resolved into *N* systems of balanced phasors called the symmetrical components of the original phasors. This method is

commonly used in the case of unsymmetrical faults. The method is applicable to analytical solution or simulating to calculating boards [3].

To understand the concept of symmetrical components that used for fault analysis in a six-phase system, it is important to know the definition of symmetrical components in three-phase systems. Assume that a set of three-phase voltages designated as V_a, V_b, V_c is given. In accordance with Fostescue, these phase voltages are resolves into the following three sets of sequence components [3]:

a) *Zero-sequence* components, consisting of three phasors with equal magnitudes and with zero phase displacement as shown in Figure 3.1 (a).

b) *Positive-sequence* components, consisting of three phasors with equal magnitudes, $\pm 120^o$ phase displacement, and positive sequence as in Figure 3.1 (b).

b) *Negative-sequence* components, consisting of three phasors with equal magnitudes, $\pm 120^o$ phase displacement, and negative sequence as in Figure 3.1 (c).

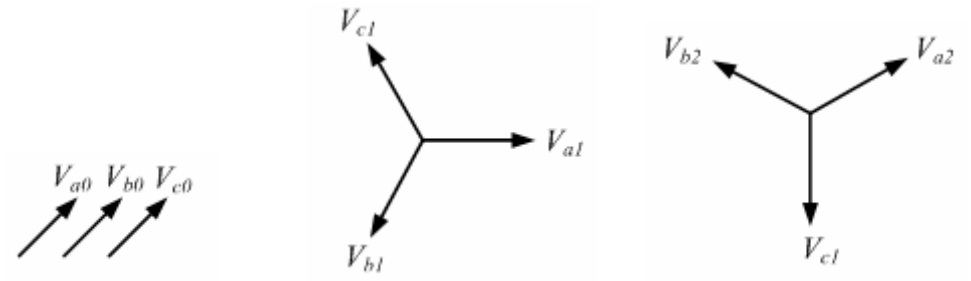

(a) Zero-sequence components

(b) Positive-sequence components

(c) Negative- sequence components

Figure 3.1: Resolving phase voltages into three sets of sequence components

Based only on phase A of the three-phase system, the sequence components for phase A can be written as V_{a0}, V_{a1}, and V_{a2} respectively. With a sequence transformation matrix, V_a, V_b and V_c can be obtained [21].

$$\begin{bmatrix} V_a \\ V_b \\ V_c \end{bmatrix} = \begin{bmatrix} 1 & 1 & 1 \\ 1 & a^2 & a \\ 1 & a & a^2 \end{bmatrix} \begin{bmatrix} V_{a0} \\ V_{a1} \\ V_{a2} \end{bmatrix} \tag{3.1}$$

This theorem has proved that an unbalanced system of N related phasors could be resolved into N systems of balanced phasors called the symmetrical components of the original phasors [21]. The symmetrical component method also applicable in six-phase power systems based on splitting the six-phase system into two systems of phasor arrangements (a, b, c) and (a', b', c') as shown in Figure 3.2.

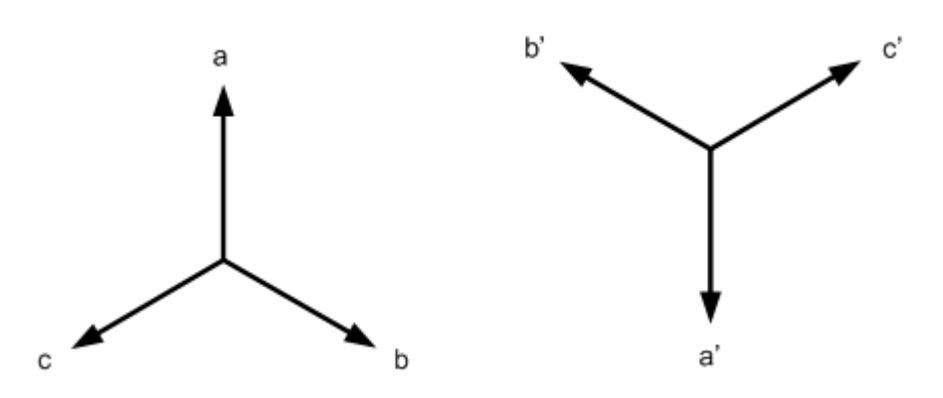

Figure 3.2: Six-phase system split to 2 three-phase system

The three sets of the first system (a, b, c) are termed the first zero, first positive and first negative-sequence components. Meanwhile, the three sets of the second system (a', b', c') are termed as the second zero, second positive and second negative-sequence components. Each of the first positive, first negative, second positive, and second negative-sequence component consists of three phasors equal in magnitude, displaced from each other by 120^o in phase. The first positive and

second positive sequences have the same phase sequence as the original phasors while the first negative and second negative-sequences have the phase sequence opposite to the original phasors [21].

In three-phase unsymmetrical fault, the operator a = $1\angle 120^{o}$ = (-0.5 + j0.866) is introduce to relate between the sequence components. Some modification is made resulting in a symmetrical component transformation matrix, *S* that accommodates the operator *a*. The matrix *S* is given by [21]:

$$S = \begin{bmatrix} 1 & 1 & 1 & 0 & 0 & 0 \\ 1 & a^2 & a & 0 & 0 & 0 \\ 1 & a & a^2 & 0 & 0 & 0 \\ 0 & 0 & 0 & 1 & 1 & 1 \\ 0 & 0 & 0 & 1 & a^2 & a \\ 0 & 0 & 0 & 1 & a & a^2 \end{bmatrix} \tag{3.2}$$

The inverse matrix of S^{-1} is

$$S^{-1} = \frac{1}{3}\begin{bmatrix} 1 & 1 & 1 & 0 & 0 & 0 \\ 1 & a & a^2 & 0 & 0 & 0 \\ 1 & a^2 & a & 0 & 0 & 0 \\ 0 & 0 & 0 & 1 & 1 & 1 \\ 0 & 0 & 0 & 1 & a & a^2 \\ 0 & 0 & 0 & 1 & a^2 & a \end{bmatrix} \tag{3.3}$$

Supposing,

The original phase voltages are denoted as, $V_P = \begin{bmatrix} V_a \\ V_c \\ V_e \\ V_d \\ V_f \\ V_b \end{bmatrix}$ (3.4)

Sequence component voltages, $V_S = \begin{bmatrix} V_{a0} \\ V_{a1} \\ V_{a2} \\ V_{a'0} \\ V_{a'1} \\ V_{a'2} \end{bmatrix}$ (3.5)

The phase voltage can be related to the sequential components of voltage by the relation [21]:

$$[V_P] = [S][V_S] \tag{3.6}$$

$$[V_S] = [S^{-1}][V_P] \tag{3.7}$$

V_{a0}, V_{a1}, and V_{a2} represents the first zero, first positive and first negative voltage coming from the three-phase line without phase shift while $V_{a'0}$, $V_{a'1}$, and $V_{a'2}$ represents the second zero, second positive and second negative voltage coming from the three-phase line with 60^o phase shift [21]. The current can also similarly be shown to be:

$$[I_P] = [S][I_S] \tag{3.8}$$

$$[I_S] = [S^{-1}][I_P] \tag{3.9}$$

Where phase current, $I_P = \begin{bmatrix} I_a \\ I_c \\ I_e \\ I_d \\ I_f \\ I_b \end{bmatrix}$ (3.10)

$$\text{Sequential components of currents, } I_S = \begin{bmatrix} I_{a0} \\ I_{a1} \\ I_{a2} \\ I_{a'0} \\ I_{a'1} \\ I_{a'2} \end{bmatrix} \tag{3.11}$$

The sequence voltages can be related to the current sequences by the following equation [21]:

$$\begin{bmatrix} V_{a0} \\ V_{a1} \\ V_{a2} \\ V_{a'0} \\ V_{a'1} \\ V_{a'2} \end{bmatrix} = \begin{bmatrix} 0 \\ E_{a1} \\ 0 \\ 0 \\ E_{a'1} \\ 0 \end{bmatrix} - \begin{bmatrix} Z_0 & 0 & 0 & 0 & 0 & 0 \\ 0 & Z_1 & 0 & 0 & 0 & 0 \\ 0 & 0 & Z_2 & 0 & 0 & 0 \\ 0 & 0 & 0 & Z'_0 & 0 & 0 \\ 0 & 0 & 0 & 0 & Z'_1 & 0 \\ 0 & 0 & 0 & 0 & 0 & Z'_2 \end{bmatrix} \begin{bmatrix} I_{a0} \\ I_{a1} \\ I_{a2} \\ I_{a'0} \\ I_{a'1} \\ I_{a'2} \end{bmatrix} \tag{3.12}$$

Where E_{a1} and $E_{a'1}$ are the first positive and second positive sequence component of the voltage source Z_0, Z_0', Z_1, Z_1', Z_2 and Z_2' are the first zero, second zero, first positive, second positive, first negative and second negative-sequence impedance. The six sets of balanced phasors of a six-phase system are as shown in Figure 3.3(a) - (f).

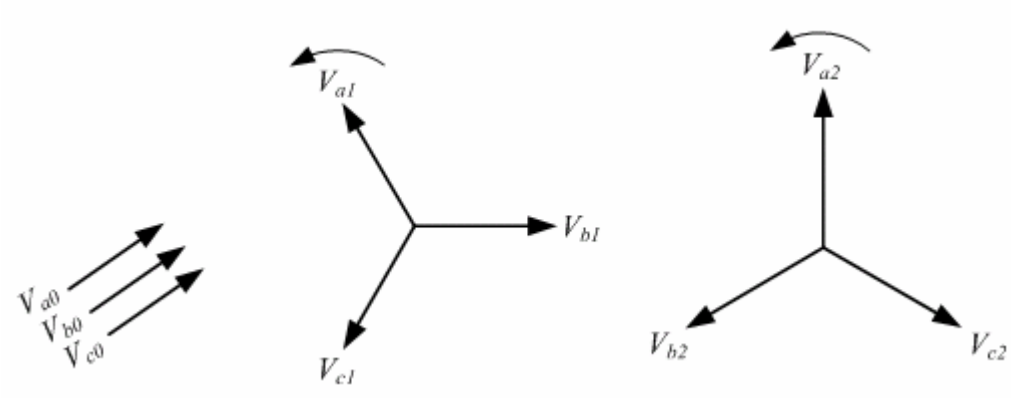

(a) First zero-sequence components

(b) First positive-sequence components

(c) First negative-sequence components

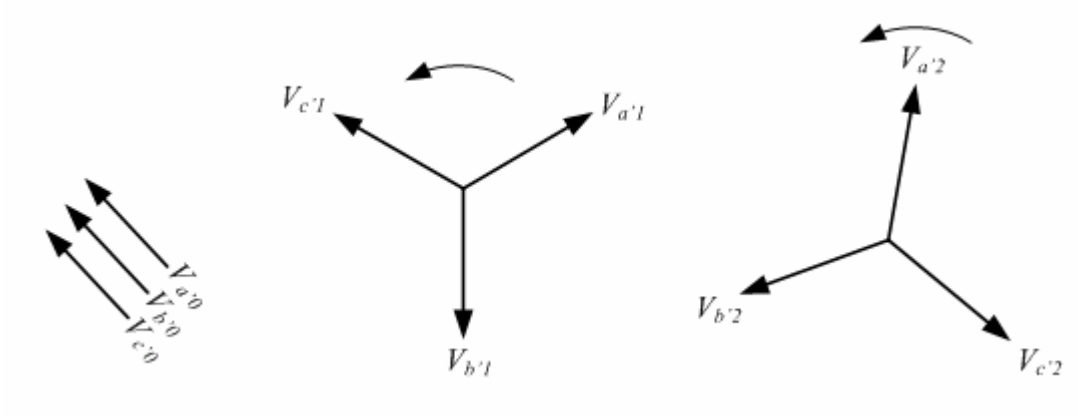

(d) Second zero sequence-components

(e) Second positive-sequence components

(f) Second negative-sequence components

Figure 3.3: Six sets of balanced phasors which are the symmetrical components of six unbalanced phasors

3.3.4 Sequential Component Relation for Faults

Consequentially, with the step taken by substituting the appropriate fault conditions into equations namely, 3.1, 3.2, 3.10 and 3.12, the sequence component relations can be presented as in Table 3.3 to Table 3.9 [21].

Table 3.3: Sequential component relation for single-line-to-ground fault

Faulted Phase	Conditions at the Fault	Sequence Component Relations
a-g	$V_a = 0$ $I_b = I_c = I_{a'} = I_{b'} = I_{c'} = 0$	$V_{a0} + V_{a1} + V_{a2} = 0$ $I_{a0} = I_{a1} = I_{a2}$ $I_{a'0} = I_{a'1} = I_{a'2} = 0$

Table 3.4: Sequential component relations for line-to-line and two line-to-ground faults

Faulted Phase	Conditions at the Fault	Sequence Component Relations
b-c	$V_b = V_c$ $I_c = I_{a'} = I_{b'} = I_{c'} = 0$ $I_b = -I_c$	$V_{a1} = V_{a2}$ $I_{a1} = -I_{a2}$ $I_{a0} = I_{a'0} = I_{a'1} = I_{a'2} = 0$
a-c’	$V_c = V_{c'}$ $I_b = I_c = I_{a'} = I_{b'} = 0$ $I_a = -I_c$	$V_{a0} + V_{a1} + V_{a2} = V_{a'0} + aV_{a'1} + a^2V_{a'2}$ $I_{a0} = I_{a1} = I_{a2}$ $I_{a'0} = aI_{a'1} = a^2I_{a'2} = -I_{a0}$
a-a’	$V_a = V_{a'}$ $I_b = I_c = I_{b'} = I_{c'} = 0$ $I_a = -I_{a'}$	$V_{a0} + V_{a1} + V_{a2} = V_{a'0} + V_{a'1} + V_{a'2}$ $I_{a0} = I_{a1} = I_{a2} = -I_{a'0} = -I_{a'1} = -I_{a'2}$
b-c-g	$V_b = V_c = 0$ $I_a = I_{c'} = I_{a'} = I_{b'} = 0$	$V_{a0} = V_{a1} = V_{a2}$ $I_{a0} + I_{a1} + I_{a2} = I_{a'0} = I_{a'1} = I_{a'2} = 0$
a-c’-g	$V_a = V_{c'} = 0$ $I_{a'} = I_b = I_c = I_{b'} = 0$	$V_{a0} + V_{a1} + V_{a2} = 0$ $V_{a'0} + aV_{a'1} + a^2V_{a'2} = 0$ $I_{a0} = I_{a1} = I_{a2}$ $I_{a'0} = aI_{a'1} = a^2I_{a'2}$
a-a’-g	$V_a = V_{a'} = 0$ $I_b = I_c = I_{b'} = I_{c'} = 0$	$V_{a0} + V_{a1} + V_{a2} = V_{a'0} + V_{a'1} + V_{a'2} = 0$ $I_{a0} = I_{a1} = I_{a2}$ $I_{a'0} = I_{a'1} = I_{a'2}$

Table 3.5: Sequential component relations for three line and three line-to-ground faults

Faulted Phase	Conditions at the Fault	Sequence Component Relations
a-b’-c’	$V_a = V_{b'} = V_{c'}$ $I_b = I_c = I_{a'} = 0$ $I_a + I_{b'} + I_{c'} = 0$	$V_{a0} + V_{a1} + V_{a2} = V_{a'0} - V_{a'1}$ $V_{a'1} = V_{a'2}$ $I_{a0} = I_{a1} = I_{a2} = -I_{a'0}$ $I_{a'0} + I_{a'1} + I_{a'2} = 0$

a-b-c	$V_a = V_b = V_c$ $I_{a'} = I_{b'} = I_{c'} = 0$ $I_a + I_b + I_c = 0$	$V_{a1} = V_{a2} = 0$ $I_{a0} = I_{a'0} = I_{a'1} = I_{a'2} = 0$
a-a'-b'	$V_a = V_{a'} = V_{b'}$ $I_b = I_c = I_{c'} = 0$ $I_a + I_{a'} + I_{b'} = 0$	$V_{a0} + V_{a1} + V_{a2} = V_{a'0} - aV_{a'1}$ $aV_{a'1} = a^2V_{a'2}$ $I_{a0} = I_{a1} = I_{a2} = -I_{a'0}$ $I_{a'0} + aI_{a'1} + a^2I_{a'2} = 0$
a-b'-c'-g	$V_a = V_{b'} = V_{c'} = 0$ $I_b = I_c = I_{a'} = 0$	$V_{a0} + V_{a1} + V_{a2} = 0$ $V_{a'0} = V_{a'1} = V_{a'2}$ $I_{a0} = I_{a1} = I_{a2}$ $I_{a'0} + I_{a'1} + I_{a'2} = 0$
a-b-c-g	$V_a = V_b = V_c = 0$ $I_{a'} = I_{b'} = I_{c'} = 0$	$V_{a0} = V_{a1} = V_{a2} = 0$ $I_{a'0} = I_{a'1} = I_{a'2} = 0$
a-a'-b'-g	$V_a = V_{a'} = V_{b'} = 0$ $I_b = I_c = I_{c'} = 0$	$V_{a0} + V_{a1} + V_{a2} = 0$ $V_{a'0} = aV_{a'1} = a^2V_{a'2}$ $I_{a0} = I_{a1} = I_{a2}$ $I_{a'0} + aI_{a'1} + a^2I_{a'2} = 0$

Table 3.6: Sequential component relations for four line and four line-to-ground faults

Faulted Phase	Conditions at the Fault	Sequence Component Relations
b-c-a'-b'	$V_b = V_c = V_{a'} = V_{b'}$ $I_a = I_{c'} = 0$ $I_b + I_c + I_{a'} + I_{b'} = 0$	$V_{a0} - V_{a1} = V_{a'0} - aV_{a'1}$ $V_{a1} = V_{a2}$ $aV_{a'1} = a^2V_{a'2}$ $I_{a0} + I_{a1} + I_{a2} = I_{a'0} + aI_{a'1} + a^2I_{a'2} = 0$ $I_{a'0} = -I_{a0}$
b-c-b'-c'	$V_b = V_c = V_{b'} = V_{c'}$ $I_a = I_{a'} = 0$ $I_b + I_c + I_{b'} + I_{c'} = 0$	$V_{a1} = V_{a2}$ $V_{a'1} = V_{a'2}$ $V_{a0} - V_{a'0} = V_{a1} - V_{a'1} = V_{a2} - V_{a'2}$ $I_{a0} + I_{a1} + I_{a2} = I_{a'0} + I_{a'1} + I_{a'2} = 0$ $I_{a'0} = -I_{a0}$

a-a'-b'-c'	$V_a = V_{a'} = V_{b'} = V_{c'}$ $I_b = I_c = 0$ $I_a + I_{a'} + I_{b'} + I_{c'} = 0$	$V_{a0} + V_{a1} + V_{a2} = V_{a'0}$ $V_{a'1} = V_{a'2} = 0$ $I_{a0} = I_{a1} = I_{a2}$ $I_{a'0} = -I_{a0}$
b-c-a'-b'-g	$V_b = V_c = V_{a'} = V_{b'} = 0$ $I_a = I_{c'} = 0$	$V_{a0} = V_{a1} = V_{a2}$ $V_{a'0} = aV_{a'1} = a^2V_{a'2}$ $I_{a0} + I_{a1} + I_{a2} = I_{b0} + aI_{b1} + a^2I_{b2} = 0$
b-c-b'-c'-g	$V_b = V_{b'} = V_c = V_{c'} = 0$ $I_a = I_{a'} = 0$	$V_{a0} = V_{a1} = V_{a2}$ $V_{a'0} = V_{a'1} = V_{a'2}$ $I_{a0} + I_{a1} + I_{a2} = I_{a'0} + I_{a'1} + I_{a'2} = 0$
a-a'-b'-c'-g	$V_a = V_{a'} = V_{b'} = V_{c'} = 0$ $I_b = I_c = 0$	$V_{a0} + V_{a1} + V_{a2} = V_{b0} + V_{b1} + V_{b2} = 0$ $I_{a0} = I_{a1} = I_{a2}$

Table 3.7: Sequential component relations for five line and five line-to-ground faults

Faulted Phase	Conditions at the Fault	Sequence Component Relations
b-c-a'-b'-c'	$V_b = V_c = V_{a'} = V_{b'} = V_{c'}$ $I_a = 0$ $I_b + I_c + I_{a'} + I_{b'} + I_{c'} = 0$	$V_{a0} - V_{a'0} = V_{a1} = V_{a2}$ $V_{a'1} = V_{a'2} = 0$ $I_{a0} + I_{a1} + I_{a2} = 0$ $I_{a'0} = -I_{a0}$
b-c-a'-b'-c'-g	$V_b = V_c = V_{a'} = V_{b'} = V_{c'} = 0$ $I_a = 0$	$V_{a0} = V_{a1} = V_{a2}$ $V_{a'0} = V_{a'1} = V_{a'2} = 0$ $I_{a0} + I_{a1} + I_{a2} = 0$

Table 3.8: Sequential component relations for six line and six line-to-ground faults

Faulted Phase	Conditions at the Fault	Sequence Component Relations
a-b-c-a'-b'-c'	$V_a = V_{a'} = V_b = V_{b'} = V_c$ $= V_{c'}$ $I_a + I_b + I_c + I_{a'} + I_{b'} + I_{c'} = 0$	$V_{a1} = V_{a2} = V_{a'1} = V_{a'2} = 0$ $V_{a0} = V_{a'0}$ $I_{a0} = -I_{a'0}$
a-b-c-d-e-f-g	$V_a = V_{a'} = V_b = V_{b'} = V_c$ $= V_{c'} = 0$	$V_{a0} = V_{a1} = V_{a2} = 0$ $V_{a'0} = V_{a'1} = V_{a'2} = 0$

3.4 Transient Stability Analysis

Transient stability studies are related to the effects of transmission line faults on generator synchronism. During the fault, the electrical power from the nearby generators is reduced and the power from remote generators remains relatively unchanged. The resultant differences in acceleration produce speed differences over the time interval of the fault and it is important to clear the fault as quickly as possible. The fault clearing removes one of the transmission line elements and weakens the system. The change in the transmission system produces change in the generator rotor angles. If the changes are such that the accelerated machines pick up additional load, they slow down and a new equilibrium position is reached. Commonly, the loss of synchronism will be evident within one second of the initial disturbance.

Faults on heavily loaded lines are more likely to cause instability than the faults on the lightly loaded lines because they tend to produce more acceleration during the faults. For the six-phase transmission system, six-phase fault will produce greater acceleration than other types of fault. Faults not cleared by primary faults produce more angle deviations in the nearby generators. Also, the backup fault clearing is performed after a time delay and hence produces severe oscillations. The loss of major load or a major generating station produces significant disturbance in the system. In the power system, the various electrical phenomena occur in different time frames as shown in Figure 3.4. These include:

- Switching surges, below one cycle operation.
- Power swings, a few cycles.
- Frequency changes, a few minutes to one hour.
- Operation and planning issues, several days to years.

The transient stability studies are performed as a part of the planning to the additional of new generators, transmission lines and power factor correction equipment. The system response is usually nonlinear and hence the transient

stability simulations performed for one condition cannot apply to a similar condition in another part of the network. Therefore, various operating conditions are studied during the transient analysis. In transient stability studies, the study period of interest is usually limited to 3 to 5 seconds following the disturbance, although it may be extend to about 10 seconds for very large systems with dominant inter-area modes of oscillation.

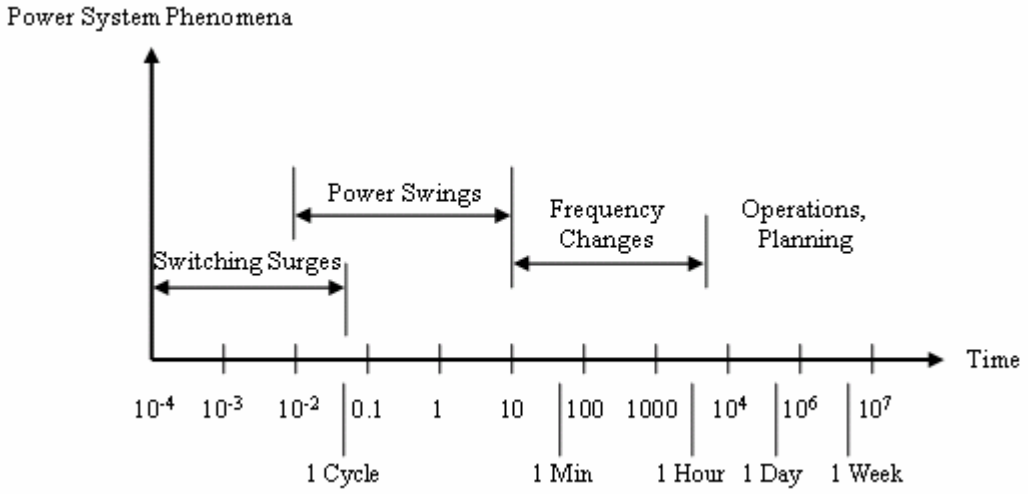

Figure 3.4: Power system transients

Transient stability is the ability of a power system to remain in synchronism when subjected to a severe transient disturbance [24]. The resulting system response involves large excursions of generator rotor angles and is influenced by the nonlinear power-angle relationship. Stability depends on both the initial operating state of the system and the severity of the disturbance. Usually, the system altered so that the post–disturbance steady-state operation is differs from that prior to the disturbance. Disturbances of widely varying degrees of severity and probability of occurrence can occur on the system. The system is, however designed and operated so as to be stable for a selected set of contingencies. The contingencies usually considered are short-circuits of different types such as phase-to-ground, phase-to-phase, phase-to-phase-to-ground, three phase faults etc. They are usually assumed to occur on

transmission lines, but occasionally bus or transformer faults are also considered. The fault is assumed to be cleared by opening of appropriate breakers to isolate the faulted element. In some cases, high-speed reclosure may be assumed.

Figure 3.5 illustrates the behaviour of a synchronous machine for stable and unstable situations. In (stable case) Case 1, the rotor angle increases to a maximum, then decreases and oscillates with decreasing amplitude until reaches a steady-state. In Case 2, the rotor angle continues to increase steadily until synchronism is lost. This form of instability is referred to as first-swing instability and is caused by insufficient synchronizing torque. In Case 3, the system is stable in the first-swing but becomes unstable as a results of growing oscillations as the end state is approached. This form of instability generally occurs when the post-fault steady-state condition itself is "small-signal" unstable, and not necessarily as a result of the transient disturbance. In a large power system, transient stability may not always occur as first-swing instability. It could be the result of the superposition of several modes of oscillation causing large excursions of rotor angle beyond the first swing.

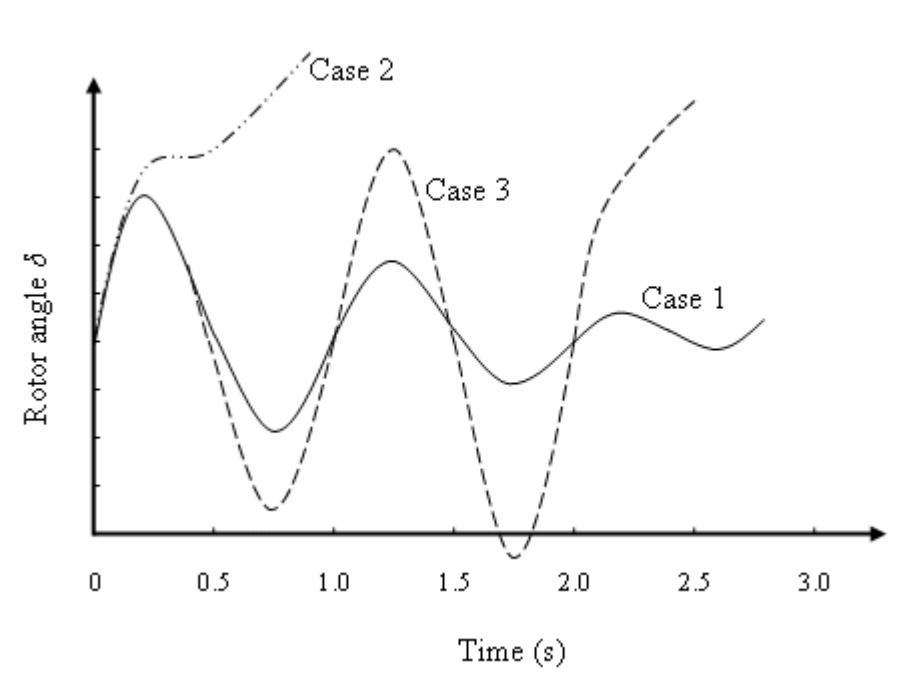

Figure 3.5: Rotor angle response to a transient disturbance

A system operating at a constant frequency must be in a state of power balanced. The total system generated real power must be equal to the system real power loads, losses, and tie flows out of the system. When this balance is upset, the system frequency will begin to change. If sudden load changes are occurred, the power generated may be greater or lesser than the demands. Too much generation will increase the system frequency while too little generation will cause the system frequency to drops. Remember that the frequency of the generators generated voltage is determined by the speed of its rotor. Thus, controlling the frequency is equivalent to controlling generator-turbine speed.

Since the system frequency is essentially the same everywhere, the generators must be running at the same speed or synchronized. Fortunately, synchronized generators operating in parallel are inherently stable. If this were not the case, multigenerator systems would be impossible. The stable mean that the machines can normally recover from small random perturbing forces and still remain synchronized. Consider an isolated multigenerator power system operating at constant frequency in a state of perfect power balance. By isolated, it means that there are no ties to external systems. Now, consider that a consumer suddenly switches in a load at an arbitrary point in the system. This modifies the network topology instantly, changing the voltage magnitude and phase at the terminals of each generator. The real power requirements of the system load plus losses are instantly met by the generators. However, the generator powers are produced through an electromagnetic torque on the generator-turbine rotor in opposition to rotation. The sudden increase in load causes the generator torques to increase suddenly. The turbine-generator torques is now out of balance, with the net balance opposing rotation. The rotors thus begin to decelerate.

Several different effects come into play that arrests this accumulating reduction in speed. First, steam and hydraulic turbines inherently develop more torque at slower speeds and would even if unregulated eventually reduce the torque unbalance to zero. Furthermore, turbines have speed control systems such that if a low-speed condition is detected, control valves open to increase the flow and thus the

torque. Furthermore, it is an almost universal characteristic of motor mechanical loads that they increase with motor speed. Since motor speed typically varies directly with system frequency, if the frequency drops, total system load will typically also drop, balancing out the original load increase. In additional to these effects, there is a frequency control designed to hold the integral of frequency error (i.e., deviation from a reference level) to within certain tolerances. Thus, the average frequency is adjusted precisely to the reference value. This control action is again implemented by adjusting the turbine control valves.

There are major disturbances that can cause the dynamic response of a system to become so violent that the generators cannot remain synchronized. The most severe disturbances include applying faults, clearing faults, and inadvertently tripping lines and generators. This problem is referred to as transient stability. From a mathematical viewpoint, we shall see that the problem is that of solving a system of nonlinear differential equations and therefore will require numerical analysis techniques. It is important to appreciate that the question of stability will be affected by the initial conditions, that is, the loaded condition of the system before switching.

As far as transient stability is concerned, the most severe switching action is the balanced three-phase or balanced six-phase fault. This is fortunate from an analytical viewpoint, since it simplifies the complexity of our system model, requiring only the positive-sequence network. Another basic simplification is that the time constants of relevance are of such values that AC circuit techniques may still be used; that is, transient AC methods, are applicable. We shall also assume that all the machines are lossless. This simplification is defensible for two reasons: (1) Practical machines, while not lossless are highly efficient (~95%); and (2) our results based on this assumption will be conservative (the system will be somewhat more stable than our results predict).

For more clarification, let’s refer to Figure 3.6, when synchronous machines are electrically tied in parallel, and they are working at the same average frequency.

Synchronous machine speed is directly related to the line frequency and given by [25]:

$$n = \frac{120\,f}{number\ of\ \ poles} \tag{3.13}$$

As we can see from the formula, speed n and frequency f is proportional, however, we can expect minor speed fluctuations to occur because of small changes in the circuit at any time and the same average frequency must exist through the system.

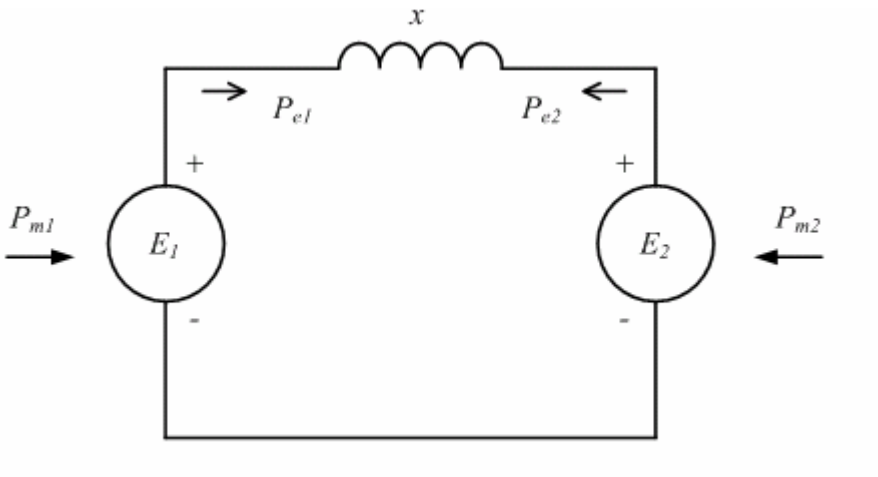

Figure 3.6: Schematic diagram for stability studies

Transient reactance's associated with E_1 and E_2 are included in the transmission line. P_{e1} and P_{e2} are the electrical power output of machines 1 and 2. P_{m1} and P_{m2} are the shaft or mechanical power input of machine 1 and 2. Based on Figure 3.6, machine number one is parallel to machine number two through a total reactance x. Any sudden disturbance like fault, load change and line opening would suddenly change the electrical output of the machines before the mechanical inputs have time to react. Neglecting losses, if $P_{m1} > P_{e1}$, the extra input would appear as accelerating power, attempting to increase the speed and power angles of then generator. A system that is able to develop restoring forces sufficient to overcome the disturbing forces and restore equilibrium is said to remain stable. For example,

any sudden advance in speed and rotor position of machine one would increase the generated output P_{e1} with a corresponding slowing effect. At the time the additional electrical power transferred to machine two tends to speed up the rotor of machine two, thus bringing the machine angle (and frequency) back toward on another.

3.4.1 Power Transfer Equation

Consider the generator of Figure 3.7 which is tied to a very large system (infinite bus). Resistance has been neglected and x will represent all of the reactance from source to infinite bus, including generator synchronous reactance x_s plus equivalent system reactance x_e to the infinite bus. It is clearly seen in Figure 3.8 that the power angle δ is the angle between the excitation voltage E and voltage V. In general, as seen from the vector diagram, lagging current oppose the main field flux (in establish E_t) while leading current adds to the main field flux.

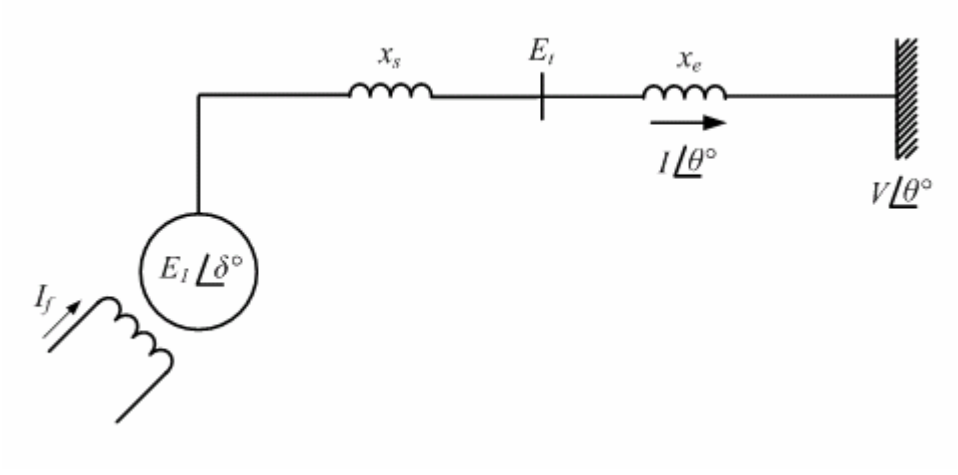

Figure 3.7: One generator connected to infinite bus

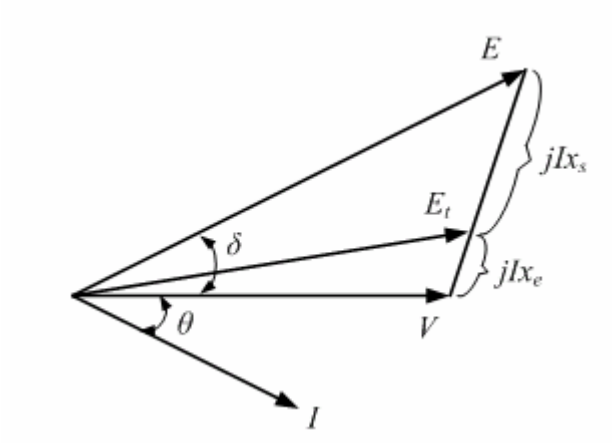

Figure 3.8: Phasor diagram of a synchronous machine for stability studies

The amount of power transferred from a machine from a large system was given by:

$$P = \frac{|E||V|}{x_s + x_e} Sin\delta \tag{3.14}$$

The infinite bus is considered as connected to the machine through an equivalent system reactance (x_e). By referring to the Figure 3.7, derivation of the power transfer equation for a cylindrical rotor machine is given as follows [24]:

$$P_e = |E||I|\cos(\delta - \theta) \tag{3.15}$$

The current is expressed as

$$I = \frac{E - V}{jx} = \frac{E}{jx} - \frac{V}{jx}$$
$$= \underbrace{\frac{|E| \angle(\delta - 90°)}{x}}_{I_1} + \underbrace{\frac{|V| \angle(+90°)}{x}}_{I_2} \tag{3.16}$$

The two components of current will be treated separately and substituted into Equation (3.15).

$$P_e = |E||I_1|\cos(\delta - \theta_1) + |E||I_2|\cos(\delta - \theta_2)$$

$$= |E|\frac{|E|}{x}\cos[\delta - (\delta - 90°)] + |E|\frac{|V|}{x}\cos(\delta - 90°)$$

$$P_e = \frac{|E||V|}{x_s + x_e}\sin\delta \tag{3.17}$$

The relationship of transferred electrical power P_e versus δ from Equation (3.17) is plotted in Figure 3.9. This plot assumes $|E|$ and $|V|$ constant. The positive power angle corresponds to generator action and a rotor advanced in the direction of rotation.

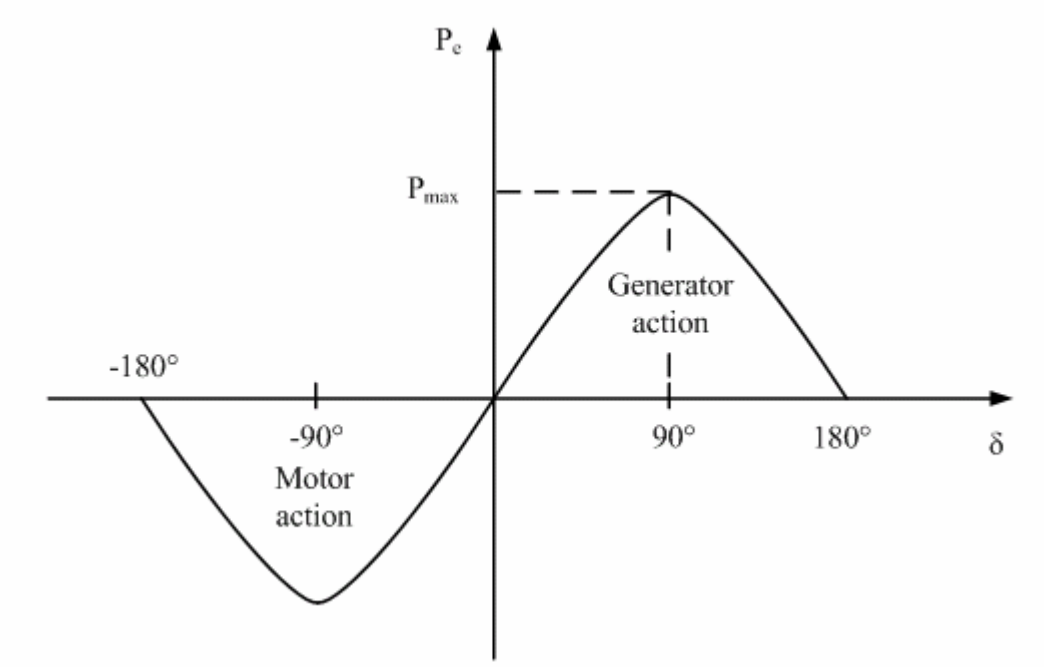

Figure 3.9: Power transfer curve

3.4.2 Steady State Stability Limit

In treating the subject of steady state stability, we are concerned with the maximum power transfer permissible from a synchronous machine while maintaining stability during a gradual power increase. Again, refer to the Figures 3.7 and Figure 3.9 will notice the maximum power that can be delivered from the machine occurs when δ has been advanced to the 90° point or given by:

$$P_{\max} = \frac{|E||V|}{x} \tag{3.18}$$

Obviously, if an attempt were made to advance δ further by further increasing the shaft input, the electrical power output will decrease from the $P_{\max}$ point. Therefore, the angle δ of excitation voltage E increases further as the machine accelerates, thus driving the machine and system apart electrically. The value of $P_{\max}$ is often referred to as the pull-out power. Another term given this value is the “steady state stability limit”.

3.4.3 Swing Curve Equation

As indicated previously, the subject of transient stability is concerned with sudden disturbances that might occur in the system (fault, line switching, sudden application or removal of loads). Since the coverage must necessarily be limited, certain assumptions and simplifications have been made. System resistances could be considered negligible with respect to reactance’s which is conservative in the stability viewpoint. One of the assumptions often made for the first seconds following a disturbance is that the shaft input power to the machine remains constant. This is often done, considering that the mechanical system of governors, steam

valves, and the like is relatively slow with respect to the rapidly changing electrical quantities.

One of the stability problems of stability revolves around the determination of whether or not the machine power angle δ (or torque angle) will stabilize after sudden disturbance. This torque angle is the angle between the generator excitation voltage and the system voltage as explained in previous section. If a study reveals that δ continues to increase (or decreases) after the disturbance, the machine will certainly go out of step with the system. On the other hand, if provision can be made to alleviate the extreme condition (such as faster relaying for isolation of a faulted line, or perhaps a more rapid field excitation response) the unstable situation may be avoided without loss of the machine. The rotor and angle of excitation voltage accelerates (or decelerates) in a manner proportional to the accelerating torque. Neglecting losses, this accelerating and decelerating torque T_a is always the difference between the mechanical or shaft input torque T_s and the electromagnetic output torque T_e or given by [3]:

$$T_a = T_s - T_e \tag{3.19}$$

For a generator, when the shaft torque $T_s > T_e$, then T_a is positive, tending to accelerate the rotor.

A number of symbols are useful at this point in reviewing the necessary equations of rotational mechanics, as well as in arriving at the so-called “swing” equation for the synchronous machine [24].

$$H = \frac{\text{kinetic energy stored in megajoules}}{\text{Machine MVA rating}} \tag{3.20}$$

Accelerating power is related to torque by the familiar equation of rotational mechanics, where

$$P_a = T_a \omega \tag{3.21}$$

A power expression can be written which is similar to the torque Equation (3.20):

$$P_a = T_a \omega = P_s - P_e \tag{3.22}$$

Two additional equations of rotational mechanics are given below as:

$$T_a = I\alpha \tag{3.23}$$

and

$$M = I \omega \tag{3.24}$$

Substituting Equations (3-23) and (3-24) into Equation (3-21) yields

$$P_a = (I\alpha)\, \omega = M\alpha = P_s - P_e \tag{3-25}$$

Up to this point, the angular quantities ω and α in Equations (3-20) through (3-24) have been in terms of mechanical radians of the rotor. However, at this point we will change from mechanical radians to electrical radians, remembering that the number of electrical radians equal to the number of mechanical radians times the number of poles/2. For example, the unit on α in Equation (4-24) changes from mechanical radians/sec² to electrical radians/sec². This is easily accomplished by being consistent with the unit on M, changing M from megajoule-sec per mechanical radian to megajoule-sec per electrical radian.

The angular acceleration (α) is written as

$$\alpha = \frac{d^2\theta}{dt^2} \text{ electrical radians/sec}^2 \tag{3.26}$$

However, θ can be expresses as the sum of the time varying angle (ωt) on the rotating reference axis plus torque angle δ of the rotor with respect to the rotating reference axis. In other words,

$$\theta = \omega t + \delta \text{ electrical radians} \tag{3.27}$$

Substituting into Equation (3.26),

$$\alpha = \frac{d^2(\omega t + \delta)}{dt^2} \tag{3.28}$$

$$\alpha = \frac{d^2\delta}{dt^2} \text{ electrical radians/sec}^2 \tag{3.29}$$

Now substituting Equation (3.29) back into Equation (3.25) results in the "swing" equation for the machine:

$$P_a = M\frac{d^2\delta}{dt^2} = P_s - P_e \tag{3.30}$$

Solving this differential equation and plotting δ as a function of t would result in the "swing curve" for a machine. In general, the swing curve will reveal any tendency of the torque angle to oscillate or increase beyond the point of return. The trend in large machine designs today is toward smaller H constants. This factor, if taken by it self, makes the transient stability problem more critical as the rotor will accelerate or decelerate faster. When only one particular machine (and system) is under study for transient stability, a simpler model applies and a conventional method of dealing with this problem utilizes the equal-area criterion as cover in this section. However, for multi-machine studies, the conventional solution has used-step-by step, incremental solution to determine the movement of the individual machine angle. Nowadays, various power system programs have features to studies the contingencies of power system including transient stability. Such program is PSCAD/EMTDC which is used to study the transient stability of power system with six-phase transmission line.

3.5 Summary

This chapter deals with the principles of the static and dynamic impacts of three to six-phase conversions in power system. The theoretical of the load flow analysis, fault analysis and transient stability analysis have been described. This will clarify the idea regarding the impacts of three to six-phase conversion of selected transmission line in an electric power system.

CHAPTER IV

MODELING OF SIX-PHASE TRANSMISSION SYSTEM

4.1 Introduction

Power system planning, design and operations require careful studies in order to evaluate the performance, safety, efficiency, reliability and economics. Such studies help to identify the potential deficiencies of the proposed system. In the existing system, the cause of the equipment failure and malfunction can be determined through a system study. The modern interconnected power systems are complex, with several thousand buses and components. The manual calculation of the performance indices is time consuming. The computational efforts are very much simplified in the present day calculations due to the availability of efficient programs and powerful microcomputers. The well-developed graphic facilities available in an industry standard power system package, namely PSCAD/EMTDC, are used as tools to conduct the analysis of the six-phase transmission system and its operation. It also used to carry out extensive simulation studies.

Simplicity of use is one of the outstanding futures of PSCAD/EMTDC. It's great many modelling capabilities and highly complex algorithms and methods are transparent to the user. This will help users to concentrate their efforts on the

analysis of results rather than on mathematical modelling. For the purpose of system assembling, the user can either use the large base of build-in components available in PSCAD/EMTDC or to its own user-defined models. PSCAD is a powerful and flexible graphical user interface to the world-renowned, EMTDC solution engine. PSCAD enables the user to schematically construct a circuit, run a simulation, analyze the results, and manage the data in a completely integrated, graphical environment. Online plotting functions, controls and meters are also included, so that the user can alter system parameters during a simulation run, and view the results directly. PSCAD comes complete with a library of pre-programmed and tested models, ranging from simple passive elements and control functions, to more complex models, such as electric machines, FACTS devices, transmission lines and cables. If a particular model does not exist, PSCAD provides the flexibility of building custom models, either by assembling those graphically using existing models, or by utilizing an intuitively designed Design Editor.

One of the ways to understand the behaviours of complicated systems is to study the response when subjected to disturbances or parametric variations. Computer simulation is one way of producing these responses, which can be studied by observing time domain instantaneous values, time domain RMS values, or the frequency components of the response. EMTDC is most suitable for simulating the time domain instantaneous responses (also popularly known as electromagnetic transients) of electrical systems. The power of EMTDC is greatly enhanced by its state-of-the-art Graphical User Interface called PSCAD. EMTDC represents and solves differential equations for both electromagnetic and electromechanical systems in the time domain. Solutions are calculated based on a fixed time step, and its program structure allows for the representation of control systems, either with or without electromagnetic or electromechanical systems present.

The general concept for the modelling is to represent each individual main component in the graphical electromagnetic simulation scheme as well as control software function by a separate “module”. Representation of the entire system is therefore achieved by dragging and dropping the appropriate model block on the

drawing canvas and connecting it by drag and stretch wires. The basic EMTDC flow chart is as shown in Appendix A. The further descriptions of the PSCAD/EMTDC software, EMTP method and EMTDC structure are given in Appendix B. This chapter presents a straightforward use of such building blocks to model power system networks with a six-phase transmission using the graphical digital electro-magnetic transients program (PSCAD/EMTDC) [22].

4.2 Modeling Using PSCAD/EMTDC

The ideal approach to study the transient phenomena in a power system is to capture and record the transients using wide bandwidth transducers and recording equipment and then analyze these waveforms. However, capturing transient signal this way representing all possible scenarios is not realistic. An alternative technique is to simulate the power system using a suitable PSCAD/EMTDC program. The PSCAD/EMTDC programs available in the market today represent the power system components with realistic models. These models usually match the main characteristics of the components while keeping the complexity of the models to a minimum. The power system simulation programs not only present a convenient way to generate the signals required to analyze a certain feature (example, the six-phase transmission in this case), but also allow the user to study the worst case scenarios that are unlikely to be generated in real world.

In order to investigate the concept of static and dynamic impacts of six-phase transmission system discussed in the previous chapter, simulation studies were carried out on the test systems including the IEEE Test Systems and 19-Bus TNB Kelantan System using PSCAD/EMTDC program. The main objectives here are to investigate the static and dynamic impacts of three to six-phase conversion of selected transmission line in an electric energy system. Modelling of the six-phase transmission in power system can be performed by using PSCAD/EMTDC software.

Basic knowledge relates to vector groups of the three-phase transformers are significant in such applications. This knowledge was used to determine a suitable combination of three-phase transformer with specific vector group to form the three-to-six-phase conversion transformer. As described in chapter II, conversion of an existing three-phase double-circuit overhead transmission line to a six-phase single-circuit operation is needed phase conversion transformers to obtain the 60° phase shift between adjacent phases.

Three-phase double-circuit transmission line can be easily converted to a six-phase single-circuit transmission line by using two pairs of identical delta-wye three-phase transformers connected at each end of the line as shown in Figure 4.1. One of each pair of transformer has reverse polarity to obtain the required 60° phase shift. This arrangement were selected as appropriate for determining short circuit currents because the delta open circuits the zero sequence network and simplifies the fault analysis [31].

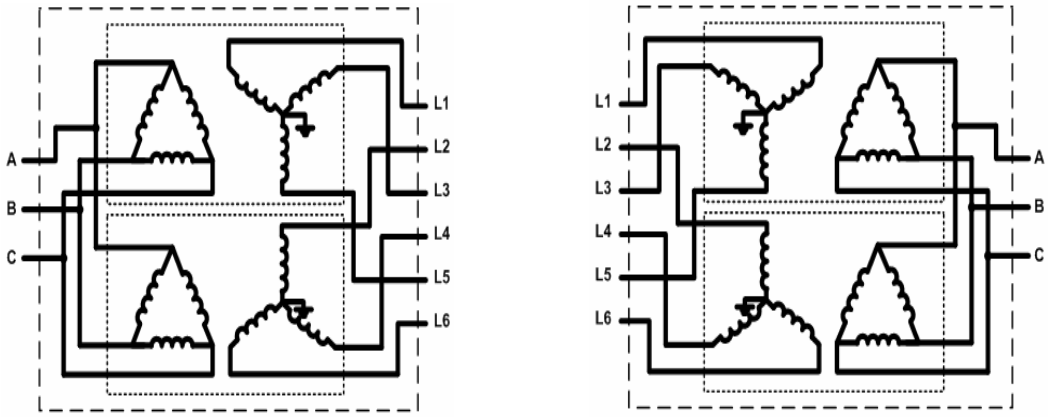

(a) (b)

Figure 4.1: Phase conversion transformer. (a) Three-to-six-phase conversion transformer and (b) Six-to-three phase conversion transformer

To make descriptions about the six-phase transmission model used in this studies become understandable, six-phase model for Test System I by using

PSCAD/EMTDC is shown in Figure 4.2. As can be seen, there have several sub-modules used to model the generators, conversion transformers and transmission line.

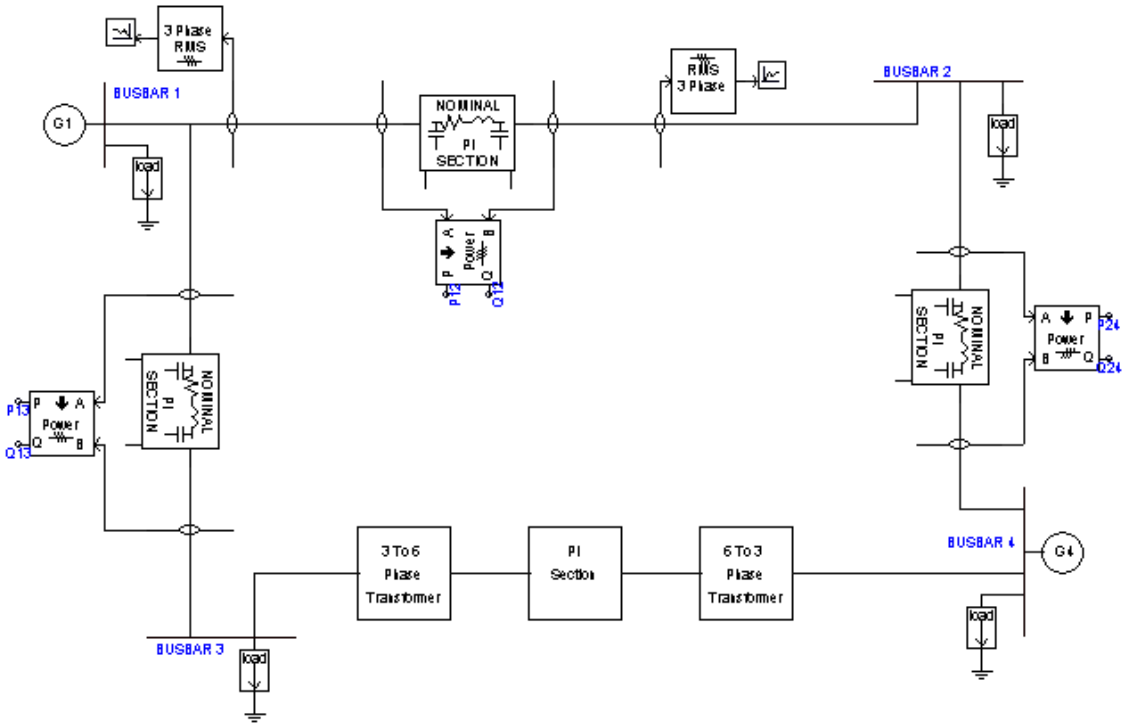

Figure 4.2: Model of six-phase transmission for Test System I in PSCAD.

Test System I used here to show how the six-phase transmission system was developed in these studies. All the data used to model Test System I is attached in Appendix D.2. Sub-modules named as G1 and G2 in Figure 4.3 is used to model the generators at bus 1 and bus 4. These sub-modules contain the synchronous machine, exciter and several continuous system model functions with digital and analog control blocks. Figure 4.3 shows the connection of all the components used inside sub-modules G1 and G2 to form generators at bus 1 and bus 4. The synchronous machines used are the same as described in the next section. The only different thing here is the graphic display because it used a single line view.

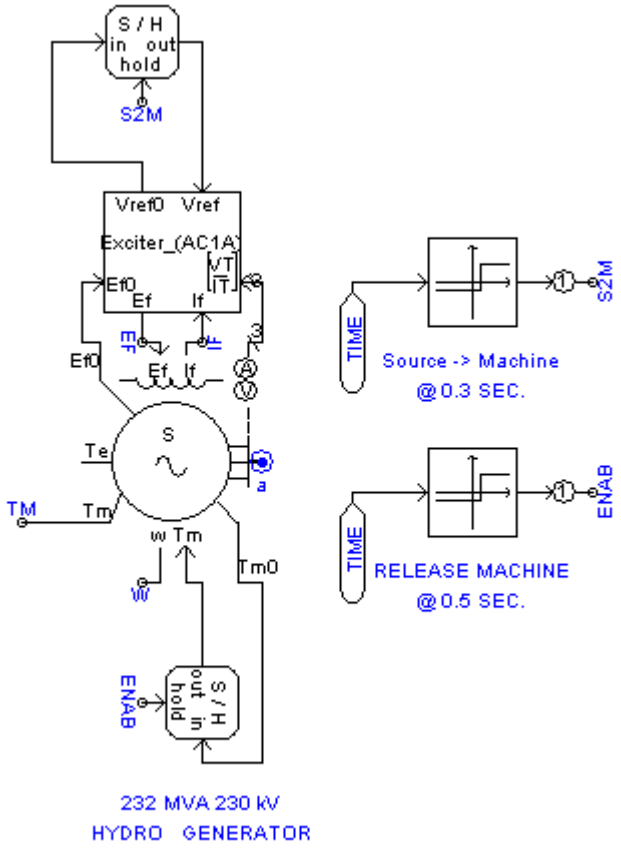

Figure 4.3: Model of generator inside sub-modules G1 and G2

The conversion transformers are modelled by using the sub-modules name as 3-to-6 Phase Transformer and 6-to-3 Phase Transformer. Inside these sub-modules, there have a pair of three-phase UMEC transformers. One of them has a vector group DY1 and another has vector group DY11. Three-phase transformer with vector group DY1 mean the Delta connection will lag Wye connection by 30°. Meanwhile, DY11 mean the Delta connection will lead Wye connection by 30°. Figure 4.4 shows a combination of two three-phase transformers to convert three-phase double-circuit to six-phase single-circuit transmission. Although both of the three-phase transformers is looks similar from their outlooks, the configuration were set inside each transformers are different. This is to make sure the representation of vector groups is accurate with DY1 and DY11 respectively.

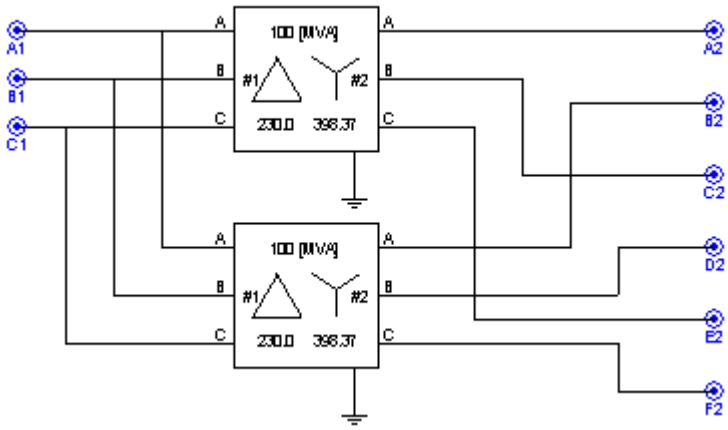

Figure 4.4: 2 Three-phase transformers inside the sub-module of 3-to-6 Phase Transformer

Similar to a three-to-six-phase conversion transformer, same technique is applied to form a six-to-three-phase conversion transformer. It is used the same combination of three-phase transformer. Delta connection is always use on the three-phase side while Wye connection use on the six-phase side. The connection of the six-to-three-phase conversion transformer is as shown in Figure 4.5.

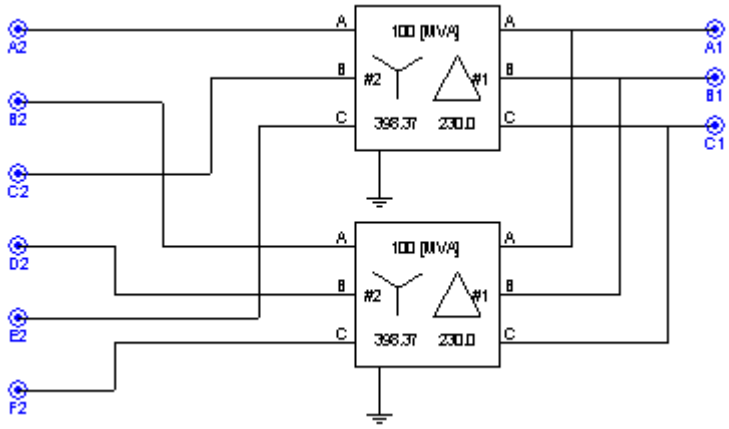

Figure 4.5: 2 Three-phase transformers inside the sub-module of 6-to-3 Phase Transformer

4.3 System Configuration

In AC system studies involving electromagnetic transient analysis, only a limited part of a transmission system can be modelled in detail. The remaining parts of the system have to be reduced to an equivalent circuit to represent the total AC system of interest. This is because detailed representation of large systems of AC network is restricted in digital simulation program such as PSCAD/EMTDC. The factors that are taken into consideration during transient simulations include time consumption, initial modelling preparatory work and the CPU run time of the computer [26].

The three-phase networks for simulation studies are based on the test systems including IEEE Test Systems and 19-Bus TNB Kelantan System. However for the instance purposes, only the 19-Bus TNB Kelantan System is shown and discussed in details here. This is in view of the fact that the laboratory prototype was developed by using Kuala Krai to Gua Musang TNB Kelantan Thevenin equivalent system's (taken from 19-Bus TNB Kelantan System). The detailed diagram of the 19-Bus TNB Kelantan System with its main components is shown in Figure 4.6. This system has 19 busbars, 8 generators and 29 lines. Transmission system voltage is operated at 132 kV and 275 kV as stated at every busbars and can be seen in Figure 4.6. Generation voltages at busbars 1 to 4 are 16 kV and 13.8 kV at busbars 5 to 8. The system data is taken from Transmission Division, TNB Wilayah Persekutuan Kuala Lumpur. This system was chosen as appropriated to implement a conversion from three-phase double-circuit to six-phase single-circuit considering to the facts that the only transmission line which supplied electric power to the ever increasing Gua Musang loads area. This line is the longest transmission line with sufficient voltage level, 132 kV to apply the six-phase transmission.

The 113 km long Kuala Krai to Gua Musang transmission line (line from bus 18 to 19) is selected and converted to the six-phase single-circuit transmission. The voltage level is significant because such conversion will increase the phase-to-neutral

voltage. This line is operated at 132 kV phase-to-phase voltages (equal to 76.2 kV phase-to-neutral voltage) for the three-phase double-circuit operation. For the six-phase single-circuit operation, the phase-to-neutral voltage will increase to 132 kV and equal to the phase-to-phase voltage. Thus, the insulation strength required by the towers is also increase. The selection of the longest transmission line is significant to analyse the transient effect of the conversion to the electric power system and also to compensate the extra cost requires for additional phase conversion transformers. Load flow data provided by TNB Wilayah Persekutuan Kuala Lumpur are used to model the system in PSCAD/EMTDC. All data are tabulated and can be seen in Appendix D.6.

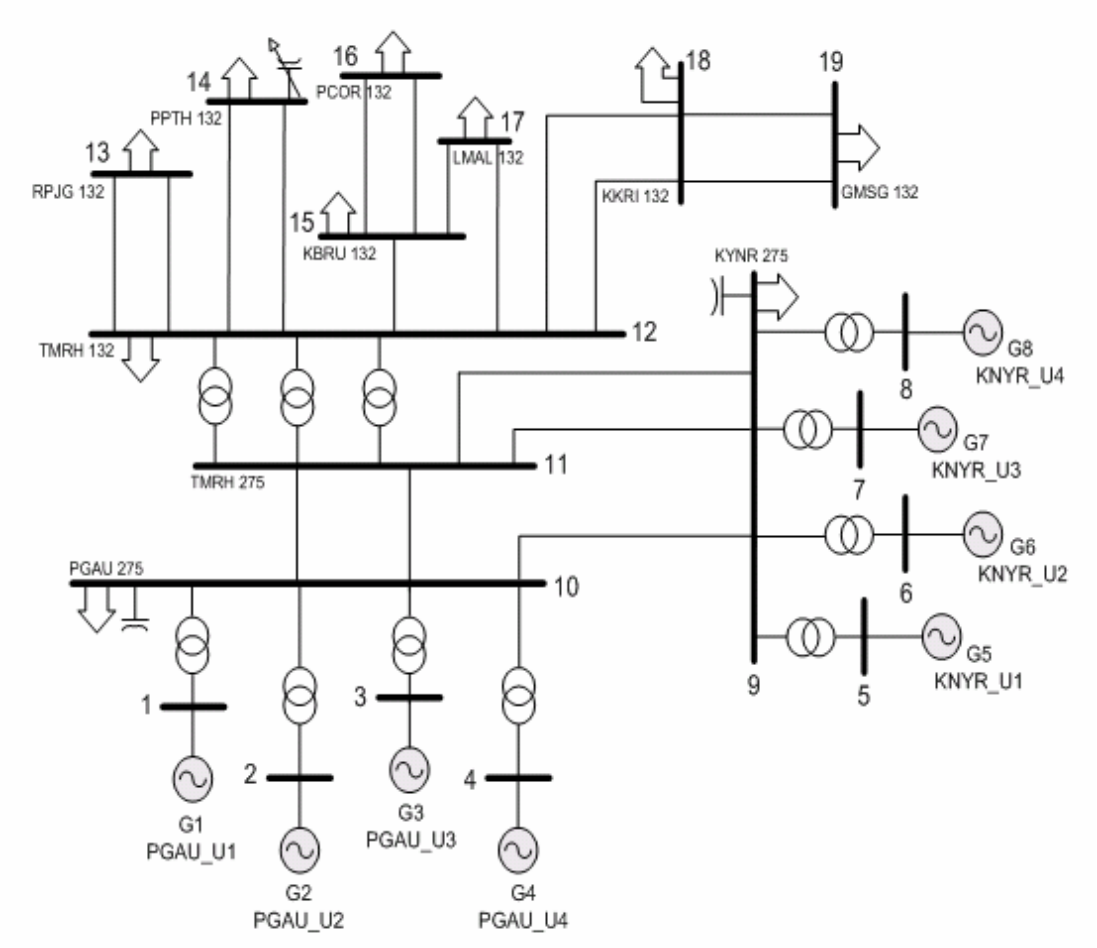

Figure 4.6: Single line diagram of 19-Bus TNB Kelantan System

4.4 PSCAD Components Used

The following subsections show the components of PSCAD/EMTDC library components that are used in this project. For the purposes of an illustration, the typical and the TNB data are set into the basic parameters for every single component discussed here.

4.4.1 Three-Phase Voltage Source Model 1

The three-phase voltage source model 1 is as shown in Figure 4.7. This component models a three-phase AC voltage source, with specified source and/or zero-sequence impedance. A zero-sequence impedance branch may be added directly within the component. Also, this component allows the user to regulate the bus voltage on a remote location on the network, or the internal phase angle can be regulated to control source output power. This source may be controlled through either fixed, internal parameters or variable external signals. The external inputs that can be control are described as follows:

(a) V : Line-to-Line, RMS Voltage Magnitude [kV]
(b) F : Frequency [Hz]
(c) Ph : Phase angle [°] or [rad]

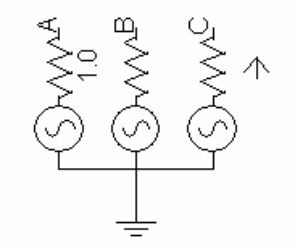

Figure 4.7: Three-phase voltage source model 1

The source impedance may be entered as one of four different types which is purely resistive, purely inductive, parallel RL or parallel RL in series with a resistance. For this type of three-phase voltage source, the zero-sequence (neutral) impedance may be entered only as a parallel RL. The following basic parameters are set for three-phase voltage source model 1:

Base MVA	: 100 MVA
Base Voltage	: 132 kV
Base Frequency	: 50 Hz
Positive Sequence Impedance	: 1 Ω
Voltage Magnitude	: 132 kV
Frequency	: 50 Hz
Phase	: 0°

4.4.2 Synchronous Machine

This component includes an option to model two damper windings in the Q-axis and hence, it can be used as either a round rotor machine or a salient pole machine. The speed of the machine may be controlled directly by inputting a positive value into the *w* input of the machine, or a mechanical torque may be applied to the *Tm* input.

There are many advanced options included in this component for modelling a synchronous machine. For general use, those parameters identified as 'Advanced' can be left to default values, without changing the expected performance of the machine. These features are aimed mainly at initializing the simulation and to reach the desired steady state quickly. The desired steady-state conditions may be known from a load flow. Once the steady-state is reached in the simulation, faults,

disturbances etc. may be applied to see the transient response. Figure 4.8 shown the synchronous machine which used as generator in this study.

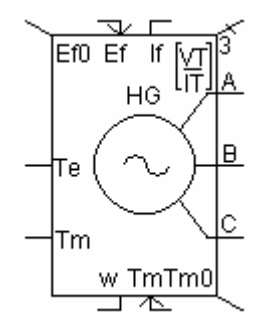

Figure 4.8: Synchronous Machine

The following fundamental parameters are set into the synchronous machine on busbars 1 to 4:

Type of Settings for Initial Condition	: Power
Rated RMS Line-to-Neutral Voltage	: 9.238 kV
Rated RMS Line Current	: 5.413 kA
Initial Constant	: 3.117
Terminal Voltage Magnitude at Time = 0	: 1.0 p.u
Terminal Voltage Phase at Time = 0	: 0 rad
Terminal Real Power at Time = 0	: 90.00 MW
Terminal Reactive Power at Time = 0	: -37.75 MVA

Generator Data: R_a, T_a, X_d, $X_{d'}$, $T_{do'}$, $T_{do''}$, $X_{q'}$ etc. are sets refer to data provided by TNB and can be seen in Appendix D.6.

4.4.3 Type AC Exciter

This component models a standard IEEE type exciter. All input parameters are either entered in seconds (time constants) or per-unit (all other inputs). Type AC

exciter is shown as in Figure 4.9. The various external inputs and outputs described below:

Inputs:

- Ef0: This input defines the output field voltage to the machine during the initialization period. Ef0 can be either defined by the user or can be defined from within the attached synchronous machine (through a Wire).
- [VT/IT]: This input is a 3-element array and receives its data from the attached synchronous machine (provided that the machine is set to output this data). VT is the RMS terminal voltage. IT is the synchronous machine terminal current and is complex (i.e. has a real and imaginary component). The real component of IT is in phase with VT and the imaginary component of IT is in quadrature (lagging is positive) with VT.
- VS: This input is provided only when using the exciter with a power system stabilizer.
- Vref: This input defines the voltage reference for the synchronous machine terminals. The value can be derived from a number of different components, which might include a slider, a real constant component or some other signal.

Outputs:

- Ef: This output is the computed field voltage applied directly to synchronous machine. A Wire may be used to make the connection.
- Vref0: This output is the initialized value of the reference voltage Vref and can be applied at the user discretion.

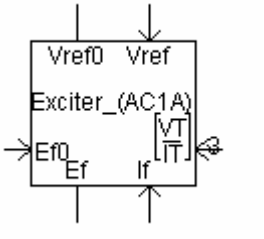

Figure 4.9: Type AC Exciter

The following fundamental parameters are set for type AC exciter at busbars 1 to 4:

AC Exciter Type	: AC1A
Regulator Gain (KA)	: 400.0 p.u.
Regulator Time Constant	: 0.02 sec
Max Reg. Internal Voltage (VAMAX)	: 14.5 p.u.
Min Reg. Internal Voltage (VAMIN)	: 14.5 p.u.
Max Regulator Output (VRMAX)	: 6.03 p.u.
Min Regulator Output (VRMIN)	: -5.43 p.u.

AC1A Exciter Parameters: KF, TF, TE, KE, KC, KD etc. are sets as the data given in Appendix D.6.

4.4.4 Three-Phase UMEC Transformer

This component models a three-phase, 3/5 limb transformer and is based on the UMEC modelling approach. Options are provided so that the user may model the core saturation characteristic directly as an I-V curve. If desired, the magnetizing branch can be eliminated altogether, leaving the transformer in 'ideal' mode, where all that remains is a series leakage reactance. Some elements of core geometry (i.e. core type, yoke and winding limb dimensions, etc.) are required for data input as well. Inter-phase coupling is represented in this model. Figure 4.10 is shown the three-phase UMEC transformer.

Transformers are the main component used in this study to perform a conversion from three-phase double-circuit to six-phase single-circuit transmission. In this case, two three-phase transformers are required. There is one option that can be sets into the three-phase UMEC transformer to configure this transformer whether

to have Wye or Delta connection. Configuration is sets depending on the winding type and vector group of the transformer connection.

In these studies, Wye-Delta three-phase transformer is selected. Configuration should be made whether Delta connection is lagging or leading Wye connection bye 30°. In this case, one of the transformers has Delta lagging Wye connection and another has Delta leading Wye connection. This configuration is applied to form a three-to-six-phase conversion transformer to use in the study.

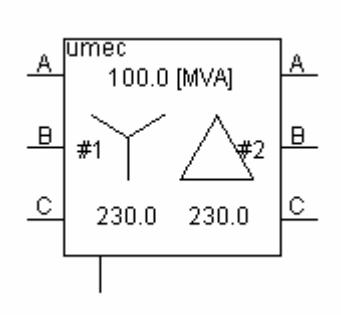

Figure 4.10: Three-phase UMEC transformer

The following basic parameters are set for three-phase UMEC transformer:

Transformer MVA	: 100 MVA
Primary Voltage (Line-Line, RMS)	: 132 kV
Secondary Voltage (Line-Line, RMS)	: 229 kV
Winding #1 Type	: Wye
Winding #2 Type	: Delta
Delta Lag or Leads Wye	: lags (for DY1) and lead (for DY11)
Base Operation Frequency	: 50 Hz
Leakage Reactance	: 0.15 p.u.

4.4.5 Fixed Load

This component models the load characteristics as a function of voltage magnitude and frequency, where the load real and reactive powers are considered separately. The load is sets based on the value of the real and reactive power demands at specified locations. The fixed load is as shown in Figure 4.11

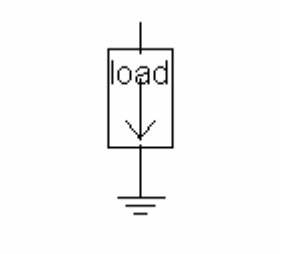

Figure 4.11: Fixed Load

The following basic parameters are set for fixed load:

Rated Real Power per Phase	: 100 MW
Rated Reactive Power per Phase	: 25 MVAR
Rated Load Voltage	: 132 kV

4.4.6 Transmission Line Interface

The Transmission Line Interface component is used to identify and provide the number of electrical connections at each end of the transmission corridor (right of way). This component must be used along with the Transmission Line Configuration component. Electrical connections to the interface are numbered from top to bottom, 1 being at the top.

With the Transmission Line Interface dialog window open, we can edit the existing number of conductors in the "Number of equivalent conductors" input field. In this study, number of conductors is equal to six considering six-phase transmission lines. The Transmission Line Interface for Kuala Krai to Gua Musang is as shown in Figure 4.12.

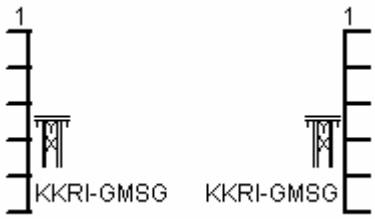

Figure 4.12: Transmission Line Interface

4.4.7 Transmission Line Configuration

The Transmission Line Configuration component is used to define the basic properties of the transmission corridor, as well as to provide access to the Transmission Line Configuration Editor. This component must be used along with the Transmission Line Interface component. Transmission line properties can be edited through the Transmission Line Configuration dialog window. There are three parameters that can be edited which are Steady State Frequency (Hz), Length of Line (km) and Number of Equivalent Conductors (up to a maximum of 20). The Transmission Line Configuration is as shown in Figure 4.13. As an example to change the line length, with the Transmission Line Configuration dialog window open, edit the existing line length in the "Length of Line" input field. This will represent the total length of the transmission corridor from the sending end, to the receiving end interface.

Figure 4.13: Transmission Line Configuration

4.4.8 Transmission Line Tower

PSCAD contains a variety of pre-constructed transmission line towers. The tower components are used to define the geometric configuration of the transmission line system within the Transmission Line Configuration Editor. The Transmission Line Tower in Figure 4.14 has shown the example of the tower configuration used by TNB Malaysia. This tower is also used for the transmission line from Kuala Krai to Gua Musang, Kelantan. Several parameters that can be edited in this tower are height of the lowest conductor, vertical and horizontal spacing between conductor, conductor radius, DC resistance and conductor sag.

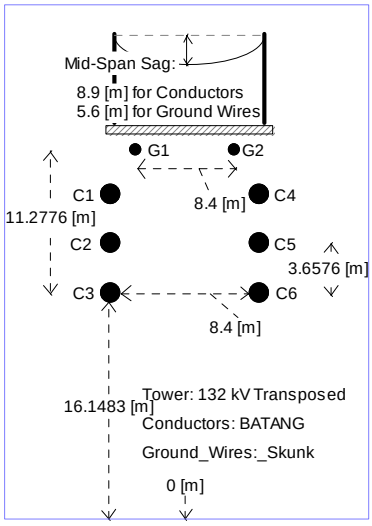

Figure 4.14: Transmission Line Tower

4.4.9 PI Section

PI Sections can be used to model mutually coupled three-phase lines, or for transmission line systems whose length is very short in relation to the simulation time step. The PI Section is formed from RLC components, based on the information entered by a user. Unlike distributed transmission line models (i.e. Bergeron or Frequency Dependent (Phase) or (Mode)), the sending and receiving end of the PI Section must be on the same page. The PI Section is as shown in Figure 4.15.

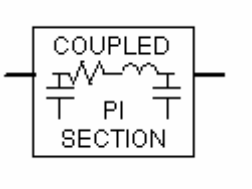

Figure 4.15: PI Section

The following basic parameters can be sets inside the PI Section:

Line Rated Frequency	: 50 Hz
Line Length	: 100 m
Rated Voltage L-L	: 132 kV
MVA for All Phases	: 100 MVA
+Seq. Resistance	: 0.3368E-7 p.u./m
+Seq. Inductive Reactance	: 0.5933E-6 p.u./m
+Seq. Capacitive Susceptance	: 1.934E-6 p.u./m

4.4.10 Other Components

Other basic components such as passive components (RLC), meters (current and voltage), input output devices (switch, plot meter channel), breakers and fault also used but not described in details here. The rest of components can be found in the PSCAD/EMTDC library [22].

4.5 Methodology of Analyses

There are several steps to be performed to run the simulation using PSCAD/EMTDC. First step is to finalize and obtain the data for all the test systems and 19-Bus TNB Kelantan System. All the data will be used as input to the MATPOWER power flow program in MATLAB and the PSCAD/EMTDC software. The complete data for all test systems including IEEE Test Systems and 19-Bus TNB Kelantan System which is used in this research can be found in appendices D.

The second step is solving the power flow analysis for the system by using MATLAB program. Load flow analysis has been conducted by using the Fast Decouple Method provided by MATPOWER [27]. The results of load flow studies can be seen in Appendices E. These result then used in the initialization and start-up process of the generators in PSCAD/EMTDC.

Parameters use by PSCAD/EMTDC software is in the real values while all the given systems data in Appendix D is in the p.u. values. Based on this reason, the p.u. values should be converted to the real values to make sure all the data entered as inputs of components model in PSCAD/EMTDC is accurate. Then, the modelling of the systems by using PSCAD/EMTDC can be conducted.

The general method of initialization and start-up, which is used normally, is based on firstly entering the terminal voltage magnitude and phase. In this study, the voltage magnitude and angle, real and reactive power from load flow results have been used into start-up and initialization process and entered as input into the generator models. The network solution progresses from the start-up with the voltage source firmly fixed so that the network can reach its steady state condition. To ensure that the steady state condition of the network is reached smoothly the source voltage magnitude may ramp to its specified value over a time interval as entered. When the steady state of the network has been reached, the voltage sources

representing each machine switched to a constant speed condition with the machine model in place. The machine equations will hold. Whenever the desired steady-state condition is achieved in the simulation, faults and disturbances may be applied to see the transient response.

Using the systems model developed in PSCAD, one location of a transmission line is converted to the six-phase transmission system. From the simulation, a load flow results are recorded. This step will be repeated for the same systems model considering only one new location of transmission line is converted to the six-phase transmission at one time. All the load flow results are recorded and comparisons are made. Based on the load flow results, a suitable location to apply the six-phase transmission system has been decided. Simulations are applied to the models were developed in PSCAD/EMTDC for both systems with three-phase double-circuit and systems with six-phase single-circuit transmission system for the purpose of comparisons. Load flow analysis, fault analysis and transient stability analysis have been conducted to the systems and all the results will be discussed in the chapter VI.

CHAPTER V

DEVELOPMENT OF A LABORATORY PROTOTYPE

5.1 Introduction

A laboratory prototype of the Kuala Krai to Gua Musang TNB Kelantan Thevenin equivalent system's has been developed to evaluate the real time performance of the six-phase transmission system. One of the main aspects of the design was to keep the cost of the prototype as low as possible. Choosing and designing hardware and software capable of handling the high voltage while keeping the cost low was a difficult task. It was decided to develop the prototype with the hardware resources readily available in the industry, identify their limitations and study the requirements for the final product. Several configurations were attempted and numerous technical difficulties had to be addressed before the final implementation.

Ahead the implementation of the laboratory prototype, a small scale electrical circuit representation of the laboratory prototype that named as small scale prototype was developed. The small scale prototype was developed by using smaller electrical components. The purpose of the small scale prototype was to ensure the implementation feasibilities of the three to six-phase conversion in an electric energy

system by using a conversion transformer. This is an important step was taken ahead the development of the laboratory prototype.

In this chapter, the small scale prototype and the hardware and software aspects of the laboratory prototype implementation are discussed. The biggest challenge faced during the implementation was capturing high voltage and current signals at high sampling rates and hence more emphasis will be made to the details of the data acquisition system.

5.2 Small Scale Prototype

Small scale prototype was developed to ensure the feasibility of the conversion from three-phase double-circuit to six-phase single-circuit transmission by using single-phase transformer. 12 single-phase two windings transformers are used in this study to form as the three-to-six-phase conversion transformer and six-to-three-phase conversion transformer. The component used for this prototype has a smaller rate than used in the laboratory prototype. Figure 5.1 shows the schematic diagram of the small scale prototype.

As we can see from Figure 5.1, voltage source is 41.5 V phase-to-phase. The voltage then stepped up to 415 V using step-up transformer named as 3-to-6 Phase Transformer. The 3-to-6 Phase Transformer was constructed using six single-phase two windings transformers. Primary rating is 41.5 V and secondary is 415 V. As generally practices, impedance contains resistance and inductance used to model the transmission lines. At the sending end, 6-to-3 Phase Transformer used to convert six-phase transmission line back to the three-phase line. This transformer also used six single-phase two windings transformers. Static loads are connected at the end of the circuit.

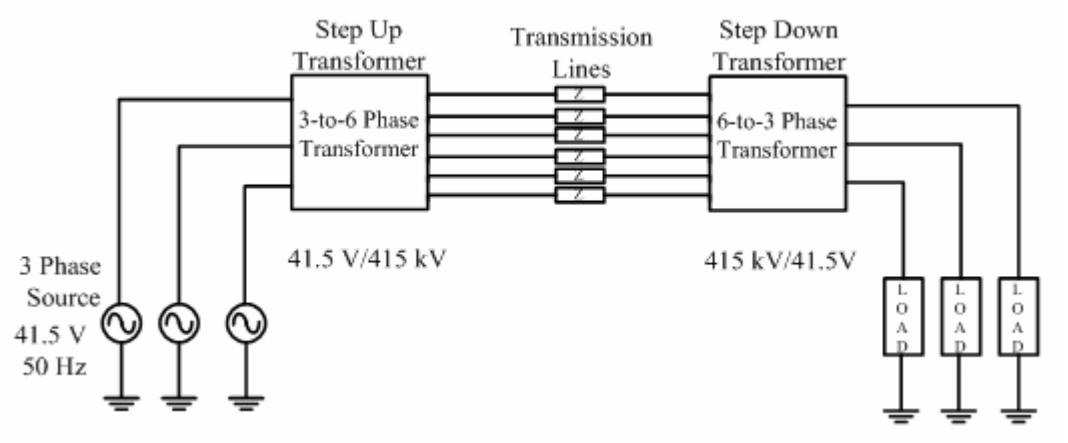

Figure 5.1: Schematic diagram of small scale prototype

Experimental study has been conducted using Lab-Volt ElectroMechanical System (EMS) and facilitated using Lab-Volt simulation software of the ElectroMechanical System (LVSIM-EMS). LVSIM-EMS faithfully simulates the Lab-Volt ElectroMechanical System (EMS), a system designed to teach electrical power technology system which consists of a set of modules (a power supply, resistive, inductive, and capacitive loads, transformers, motors, etc.) that can be installed in a laboratory workstation. These modules can be interconnected with wires to implement various electromechanical circuits. LVSIM-EMS faithfully recreates this laboratory environment on a computer screen, and thereby, allows practical study of electric power technology to begin on a desktop.

Figure 5.2 shows the opening screen with the metering application of LVSIM-EMS. It runs on IBM compatible computer under the Microsoft Windows™ operating environment. The LVSIM-EMS work space on the computer screen is a laboratory workstation which is identical to that used in the actual EMS system. Modules corresponding to those used in the EMS system can be installed in the LVSIM-EMS workstation and interconnected using wires to implement various circuits. As in the actual EMS system, the operation and behaviour of the circuits simulated with LVSIM-EMS can be observed by measuring voltages, currents,

powers, speeds, torques, etc. using the Lab-Volt Data Acquisition and Management (LVDAM-EMS) software. A Lab-Volt set of Windows™ applications consisting of several modern and versatile instruments.

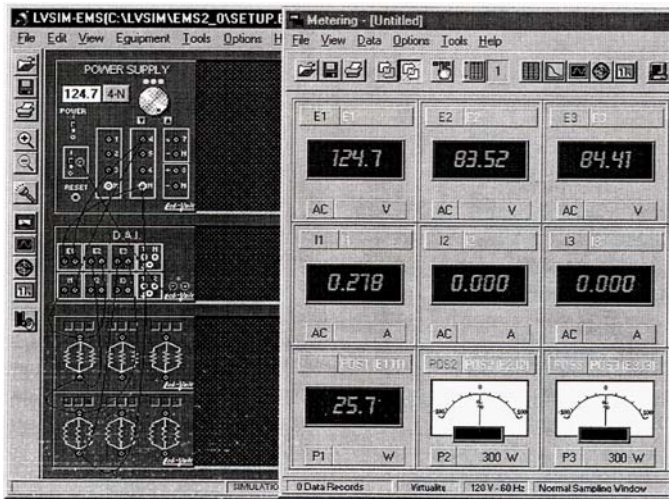

Figure 5.2: Opening screen with the metering application of LVSIM-EMS.

The equipment box is an array of buttons corresponds to modules of the EMS system. These buttons are used when installing modules in the workstation. Several significant buttons of the equipment box and the name of the module corresponding to each button used in the experiment are discussed here. There are the Data Acquisition Interface (D.A.I.), power supply and loads. D.A.I. module is required to perform voltage, current, speed, and torque measurements using LVDAM-EMS. It consists of three voltage inputs (E1, E2, and E3), three current inputs (I1, I2, and I3), a torque input (T), a speed input (N), and two control outputs (analog outputs 1 and 2). Access to the various inputs and the analog outputs is through terminals on the module front panel.

The D.A.I. module is automatically connected to the computer that runs the LVDAM-EMS applications when it is installed in the workstation. The D.A.I. module requires low-voltage ac power (24 V) to operate. Two input jacks located in

the lower right corner of the front panel allow the module to be connected to the 24V ac power source on the power supply. An LED located over these input jacks lights up when correct power is supplied to the module. Figure 5.3 show the Data Acquisition Interface module.

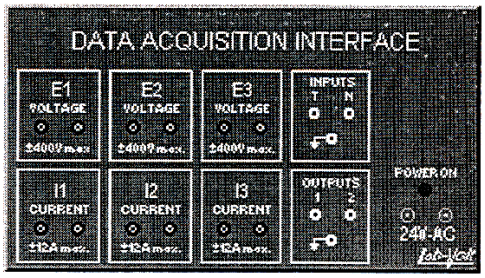

Figure 5.3: Data Acquisition Interface

Another important module button is Power Supply. The Power Supply is the primary power source in the Lab-Volt EMS System. It mainly consists of the following five power sources:

- a fixed-voltage, three-phase, four-wire power source
- a variable-voltage, three-phase, four-wire power source
- a fixed-voltage dc power source
- a variable-voltage dc power source
- a 24 V ac power source

The Power Supply is automatically connected to a three-phase ac power network when it is installed in the workstation. The Power Supply module of LVSIM-EMS is as shown in Figure 5.4.

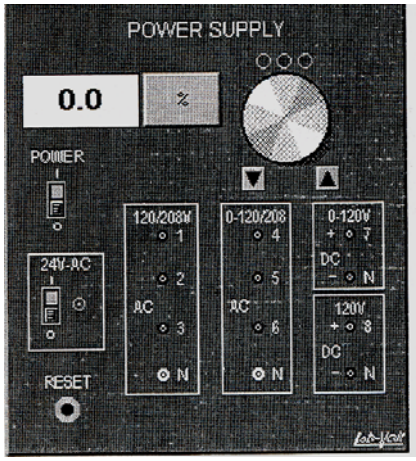

Figure 5.4: Power Supply

Another module buttons used in the experiment is static loads. There are three types of loads namely resistive, inductive and capacitive. Only resistive load is discussed here. The Resistive Load module is divided in three identical sections, each consisting of three resistors which can be connected to a single pair of terminals located on the module front panel. These resistors are schematized on the module front panel. A check box, located over each resistor on the module front panel, controls the connection of the resistor to the terminals. The connection is made or broken by clicking the check box. A check appears in the check box when the resistor is connected to the terminals. Figure 5.5 show the Resistive Load module.

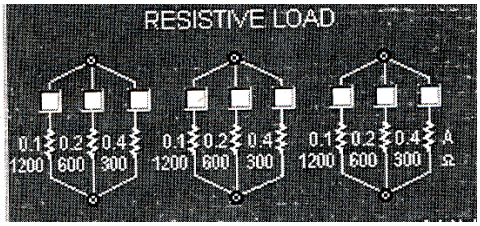

Figure 5.5: Resistive Load

The LVSIM-EMS is used because it came with LVDAM-EMS system. LVDAM-EMS system is a full instrumentation package that runs on IBM compatible

computer under Microsoft Windows™ operating environment. Virtual Instruments like voltmeters, ammeters, power meters, an oscilloscope and a phasor analyzer is available in this software. EMS is directly connected to the LVSIM-EMS software and all the experimental results from EMS are illustrated on the computer monitor.

Oscilloscope and phasor analyzer are the important tools used in this study to identify the phase shift between adjacent phases of the six-phase lines. The circuit of small scale prototype has been test using these tools. Both tools are used to verify the phase angle between phase-to-phase voltages of the six-phase transmission line. Oscilloscope used to see the six-phase voltage and current waveform while phasor analyzer used to measure phase shift between phase-to-phase voltages. This steps are important to validate the simulation results which shown a three-phase transmission line can be converted to a six-phase transmission line using six single-phase two windings transformers. Figure 5.6 show the oscilloscope application to observe the voltage and current waveform in LVSIM-EMS. The application of phasor analyzer is shown in Figure 5.7. From voltage and current waveforms and also phase shift between adjacent phases, it is shown that the six-phase system can be generated using six single phase two windings transformers.

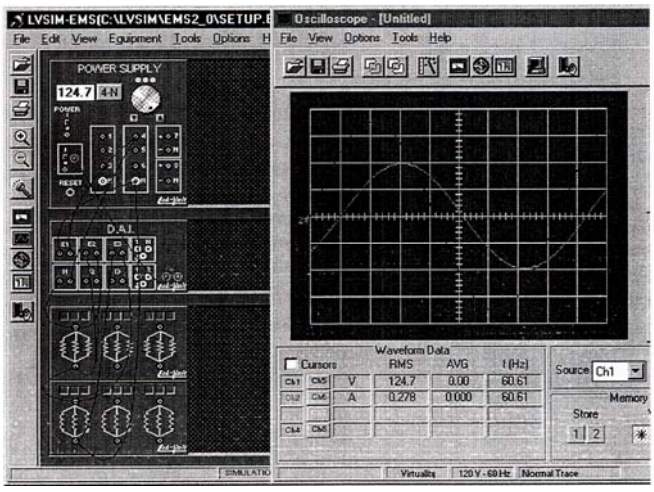

Figure 5.6: Oscilloscope application in LVSIM-EMS

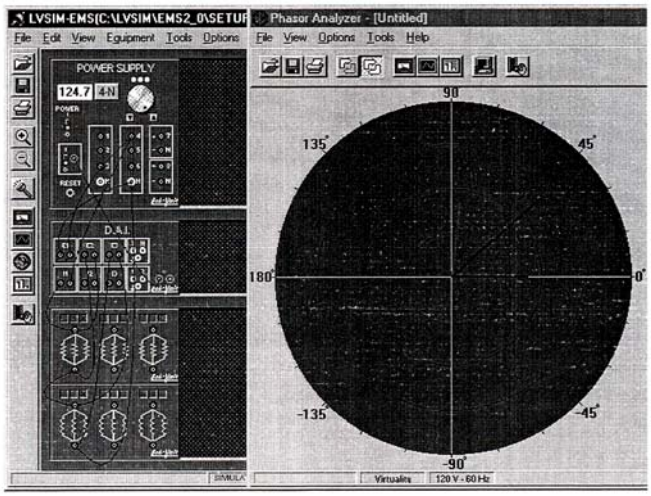

Figure 5.7: Phasor analyzer application in LVSIM-EMS

The analyses results of the small scale prototype lead to the development of the laboratory prototype. The important steps in the design and development of the laboratory prototype comprise design consideration, choice of hardware and software, system configuration and implementation.

5.3 Laboratory Prototype

The experimental results of the small scale prototype have been shown that the single-phase two windings transformers can be used to form a three-to-six-phase conversion transformer. It has been verified the feasibility to model a six-phase transmission system. These experimental results associated with the simulation results using PSCAD/EMTDC described in previous chapter would take into design considerations of laboratory prototype.

5.3.1 Design Considerations

While the individual components of power system can be prototyped, the total system itself (especially when it is as large as the TNB's generation and transmission system) can never be hardware modeled in the lab environment. However, as is the common practice for any experimental investigation related to a power system as a whole, a Theveninized laboratory prototype of the Kuala Krai to Gua Musang TNB Kelantan System has been constructed with respect to the particular line converted into a six-phase one. Figure 5.8 shows the schematic diagram of laboratory prototype which represented the real Kuala Krai to Gua Musang TNB Kelantan Thevenin equivalent system. As can be seen, the prototype has comprised an emf source (generator) in series with a Thevenin's reactance. This then series-connected to the three-to-six-phase conversion transformer and also to the converted six-phase transmission line. The transmission line was represented by using resistance and inductance. The other end of the line was connected to the six-to-three-phase conversion transformer in series with the loads. The Thevenin's emf and reactances are found in per unit from base MVA and fault current data provided by TNB for respective ends between which the converted line exists in the actual system.

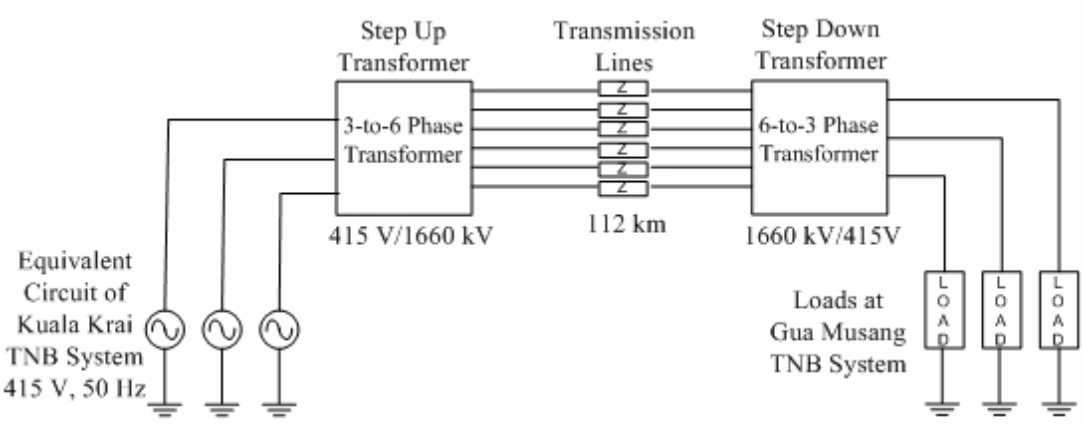

Figure 5.8: Schematic diagram of laboratory prototype

The conversion transformers are constructed using two pairs of identical Delta-Wye three-phase transformers. One of each pair of transformers has reverse polarity to obtain the required 60° phase shift. All the three-phase transformers have the same ratings as 415 V on Delta side and 1660 V on Wye side, 10 kVA and 0.05 p.u impedance. The value for the resistor and inductor are refers to the transmission line length from Kuala Krai to Gua Musang. The line length is about 112 km long. With the 100 MVA and 132 kV base on the transmission side, the transmission line resistance and inductance is equivalent to 8.134 Ω and 110 mH respectively. Because of the difficulties to get the precise resistance value to 8.134 Ω, the 10 Ω resistance value has been used as alternative to model the resistances of transmission line. Loads are not included in the laboratory prototype. For the experimental purposes, the existing three-phase loads bank from Advance Power Laboratory is used.

5.3.2 System Requirements

The simulations in the previous chapter were done in an ideal environment. The voltage and current signals measured at any locations were in their discrete format and hence the error associated with the measuring process was not considered. Some knowledge about signal conditioning and data acquisition system for high voltage measurement are useful for the design process.

The current and voltage at selected points are measured with current transformers (CT's) and voltage transformers (VT's) respectively. The current transformers usually have a bandwidth of several hundred kilohertz [28]. In HV lines, the voltage is usually measured using capacitive voltage transformers (CVT's). CVT's had a limited bandwidth and show a linear frequency range of about 1 kHz [29]. Hence the measured voltage waveforms will lack the information of the high frequency transients. The recently developed voltage transformers (VT's) have high

bandwidth and are capable of reproducing a fairly accurate replica of the high frequency wavefronts. For the transient analysis used in HV lines, VT must be preferred over CVT. The magnitudes of the measured signals on the secondary side of the voltage and current transducers are further reduce using transformers in order to bring the signal levels down to acceptable levels for data acquisition system. All these stages in the measuring process introduce noise to the measured signal. In order to improve the signal to noise ratio, high precision components and high accuracy with ultra-low noise precision Operational Amplifier (Op-Amp) must be used.

No signal is truly deterministic and therefore in practice has infinite bandwidth. However, the energy of higher frequency components becomes increasingly smaller so that at a certain value it can be considered to be irrelevant. Analog magnitudes measured from the circuit need to be converted to digital values. This because of the digital value is capable to communicate with the computer. However, analog to digital conversion will introduce an aliasing affect due to the sampling of the continuous signals. In order to reduce the effect of aliasing, the signals used for the signal conditioning circuit should have an upper limit in the bandwidth.

The amount of aliasing that can be tolerated is eventually dependent upon the resolution of the system. If the system has low resolution, then the noise floor is already relatively high and aliasing does not have a significant effect. However, with a high resolution system, aliasing can increase the noise floor considerably. One way to prevent aliasing is to increase the sampling rate. However, the maximum sampling rate is limited by the type of data converter used and also by the maximum clock rate of the digital processor receiving the data. Therefore, to reduce the effects of aliasing, analog filters must be used to limits the input signal spectrum.

The voltage and current transducer outputs are captured by sample and hold circuit at pre-specified time instances. These samples are then converted to discrete

values by an analog to digital converter (ADC). The ADC chosen must have a linear gain throughout the input voltage range, and should not have any offset or non-linearity errors. When nonlinearity errors are present, the values on the actual transfer function of ADC can deviate from a straight line. The analog input to an ADC is a continuous signal with an infinite number of possible states, whereas the digital output is by its nature a discrete function with a number of different stages determined by the resolution of the ADC. Hence some information can be lost and distortions may be introduced into the signal. This is known as quantization noise. A high resolution ADC minimizes the effects of quantization noise. However, the cost of the ADC increases with the increase in resolution. Analysis of the waveforms showed that an ADC having a 12-16 bit resolution can provided adequate resolution while keeping the cost low.

For the laboratory prototype, the A/D board must have at least 24 analog input channels to measure 12 voltage and 12 current signals. All 24 channels must be sampled simultaneously to facilitate the recognition of the relative position of the wavefronts. The sampled voltage and current signals are then sent to the microprocessor for processing.

Online experimental results from laboratory prototype can be monitored through personal computer. It is used Human Computer Interface (HCI) concept. HCI can be divided into three parts which is the input/data acquisition, the computer recognition and processing, and the output/display. Figure 5.9 shows all these three parts. The input/data acquisition is the way in which information about the experimental results is conveyed to the computer.

Figure 5.9: The Human Computer Interface structure

Figure 5.10 shows the common process of how information from the human is passed to the computer. It separates the process into three parts which is sensors, signal conditioning, and data acquisition. For this project, only signal conditioning and data acquisition will be used and discussed here. This is because no sensors are required since all signal quantities are in the electrical quantities. The choices made in the design of these systems ultimately determine how intuitive, appropriate, and reliable the interaction is between human and computer.

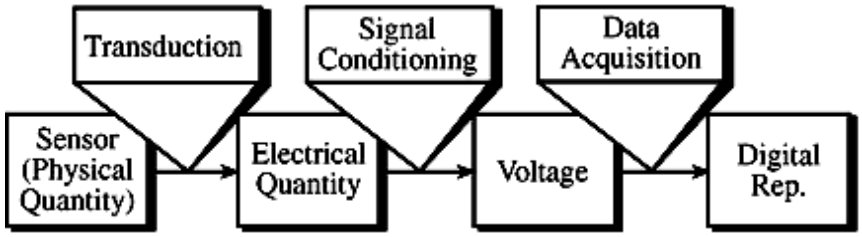

Figure 5.10: The path from human to computer

5.4 Signal Conditioning

The electrical quantities from laboratory prototype are in the form of high voltages and currents. All these quantities must be changed to appropriate values to form as input into the data acquisition system. In most applications this means changing the electrical quantities from high level to low level outputs, modifying the dynamic range to maximize the accuracy of the data acquisition system, removing unwanted signals, and limiting the spectrum. Additionally, analog signal processing for both linear and nonlinear may be desired to alleviate processing load from the data acquisition system and the computer. Figure 5.11 shows the schematic diagram of the main component used to form the signal conditioning circuit. As can be seen,

it contains CT's, VT's, Pre-Amplifier (Pre-Amp), Filter and Operational Amplifier (Op-Amp).

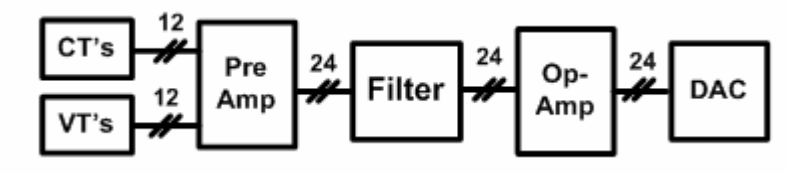

Figure 5.11: Signal conditioning diagram

Many times it is desirable to perform pre-processing on the electrical signal before data acquisition. Depending on the application, this can help lower the required computer processing time, lower the necessary system sampling rate, or even perform functions that will enable the use of a much simpler data acquisition system entirely. Several processes conducted to the electrical signal are as isolation, pre-amplification, filtering and operational amplification. In many applications it is necessary to isolate the data acquisition system from the high voltage circuit. This is done through the uses of the CT's and VT's. The output of these transducers usually still at high levels. To step down the voltage and current to the appropriate value for input of data acquisition, transformer has been used. Pre-amp circuit used to amplify the output of the transducers. This is significant step taken before the filtering process.

Many electrical components are not ideal components. It comes with noise and undesirable signal components. It may be desirable or even necessary to remove such components before the signal is digitized. Additional other signals may corrupt the electrical output. This noise can also be removed using analog circuitry. The signal with noise is amplified to make the original signal is easier to be recognized over the noise and undesirable signals. The filtering process will filtered only undesired noise and signals from the original signals.

Voltage and current transducers chosen here have output as a voltage waveform. Thus no signal conditioning circuitry is needed to perform the conversion to a voltage. However, dynamic range modification, impedance transformation, and bandwidth reduction may all be necessary in the signal conditioning system depending on the amplitude and bandwidth of the signal and the impedance of the transducers. The circuits discussed in this section are treated as building blocks of a human-computer input system used in this project. Their defining equations for their operation are given without proof. More detailed description of how they work can be seen in reference [30]. It is especially important to review the analysis of ideal op-amp circuits.

5.4.1 Amplifiers

The most common circuit used for signal conditioning is the inverting amplifier circuit as shown in Figure 5.12. This amplifier was first used when op-amps only had one input, the inverting (-) input. The voltage gain of this amplifier is $-\frac{R_F}{R_1}$. Thus the level of transducer outputs can be matched to the level necessary for the data acquisition system. The input impedance is approximately and the output impedance is nearly zero. Thus, this circuit provides impedance transformation between the transducers and the data acquisition system.

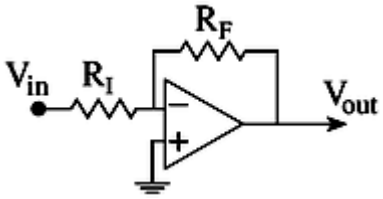

Figure 5.12: Inverting amplifier

It is important to state here that the voltage swing of the output of the amplifier is limited by the amplifier's power supply as shown in Figure 5.13. In this example, the power supply is +/- 13 V. When the amplifier output exceeds this level, the output is clipped. Just as the dynamic range of the amplifier is limited by power supply. Op-amps have a fixed gain-bandwidth product which is specified by the manufacturer. If, for example, the op-amp is specified to have a 3 MHz gain-bandwidth product, and it is connected to have a gain of 100, this means that the bandwidth of the amplifier will be limited to 30 kHz (100*30kHz =3Mhz).

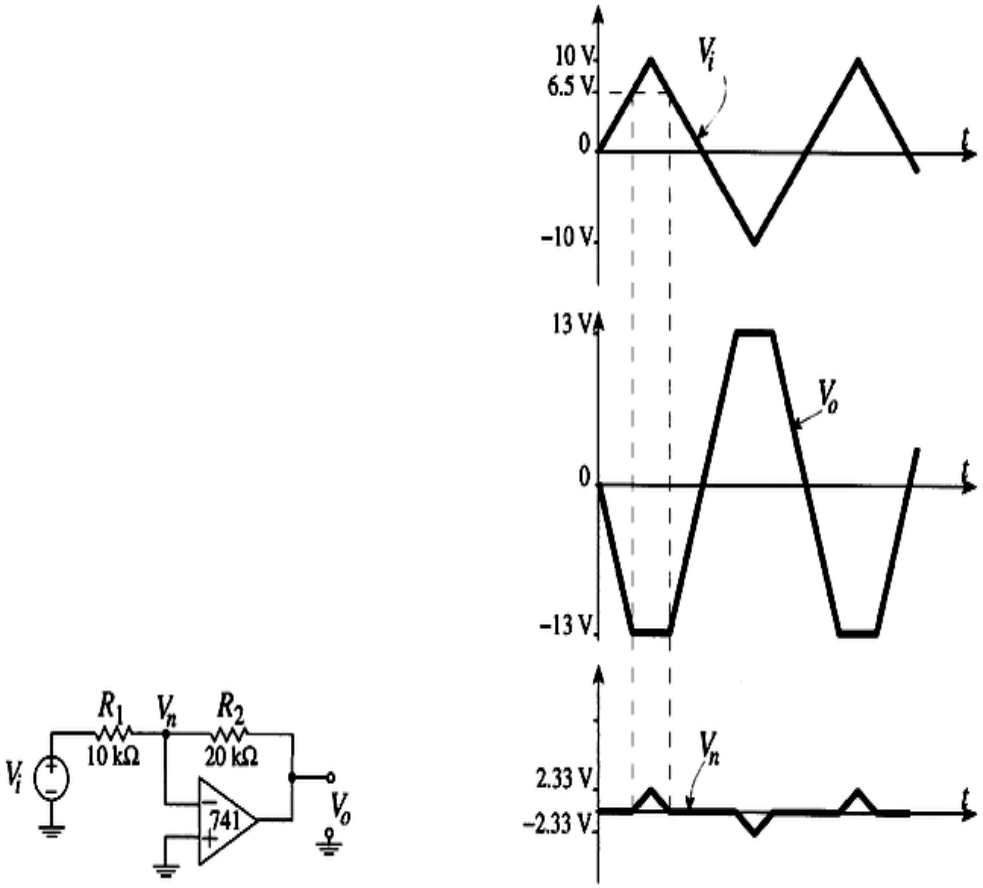

Figure 5.13: Clipping of an amplifier's output

Another important limitation of the amplifier circuit is noise. All op-amps introduce noise to the signal. The amount and characteristics of the noise are specified by the manufacturer of the op-amp. Also, the resistors introduce noise. The equation for this thermal noise is [30]:

$$V_{\text{noise}}{}^2 = 4kTBR \tag{5.1}$$

Where, k is Boltzmann's constant, T is the temperature, B is the bandwidth of the measurement device, and R is the value of the resistance. The main point to remember, is the larger the resistor values used, the larger the amount of noise introduced. One more limitation of the op-amp is offset voltage. All op-amps have a small amount of voltage present between the inverting and non-inverting terminals. This DC potential is then amplified just as if it was part of the signal from the transducer. There are many other limitations of the amplifier circuit that are important for the HCI designer to be aware [30].

Another commonly used amplifier configuration is shown in Figure 5.14. The gain of this circuit is given as $1 + \frac{R_1}{R_2}$. The input impedance is nearly infinite (limited only by the op-amp's input impedance) and the output impedance is nearly zero. The circuit is ideal for transducers that have high source impedance and thus would be affected by the current draw of the data acquisition system.

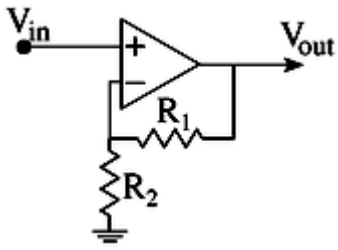

Figure 5.14: Non-inverting amplifier

5.4.2 Lowpass and Highpass Filters

The non-inverting amplifier configuration can be modified to limit the bandwidth of the incoming signal. For example, the feedback resistor can be replaced with a resistor/capacitor combination as shown in Figure 5.15. Thus the gain of the circuit is [30]:

$$A_v = H_0 \frac{1}{1 + j(f_0)} \tag{5.2}$$

where

$$H_0 = -\frac{R_1}{R_2} \text{ and } f_0 = \frac{1}{2\pi R_2 C} \tag{5.3}$$

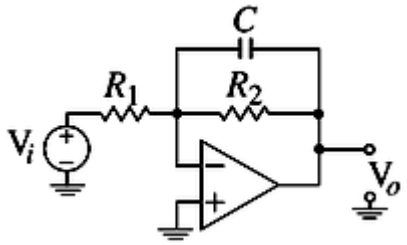

Figure 5.15: Single pole low-pass filter

A filter "rolls off" at 20dB per 10-times increase in frequency (20dB/decade) times the order of the filter, i.e.:

$$\text{Rate of attenuation} = (\text{order of filter})*(20\text{dB/decade}) \tag{5.4}$$

Thus a first order filter "rolls off" at 20dB/decade as shown in Figure 5.16.

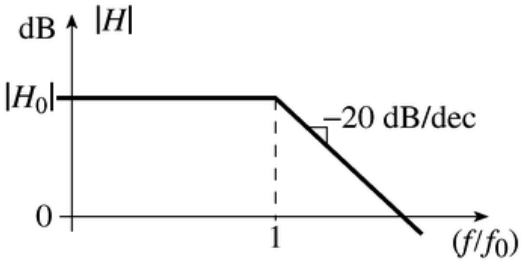

Figure 5.16: Frequency response of single pole lowpass filter

The input resistor of the inverting amplifier can also be replaced by a resistor/capacitor pair to create a highpass filter as shown in Figure 5.17. The gain of this filter is given by [30]:

$$A_v = H_0 \frac{j(\frac{f}{f_0})}{1 + j(\frac{f}{f_0})} \tag{5.5}$$

where

$$H_0 = -\frac{R_2}{R_1} \text{ and } f_0 = \frac{1}{2\pi R_1 C} \tag{5.6}$$

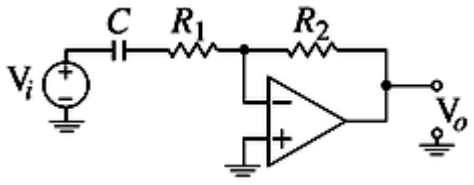

Figure 5.17: Single pole highpass filter

The frequency response of this filter is shown in Figure 5.18.

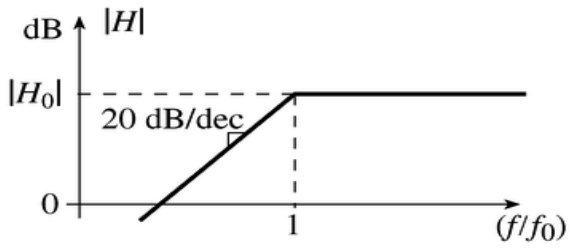

Figure 5.18: Frequency response of a single pole highpass filter

Higher order filters, which consequently have faster attenuation rates, can be created by cascading many first-order filters. Alternatively, the filter circuit can include more resistor/capacitor pairs to increase its order. The technique for doing this can be found in the reference [30]. The correct design of the signal conditioning system is critical in mapping the electrical output to the data acquisition input. Thus, it is important to note the changes in the properties of the electrical signal caused by the conditioning circuitry.

5.5 Data Acquisition

Data acquisition is a process to acquire the data from online measurement. This data will go through the anti-aliasing, sample/hold and quantization process. This is important to recognize the data so that the computer can receive, process and give the output to display. Three step of data acquisition is shown in Figure 5.19.

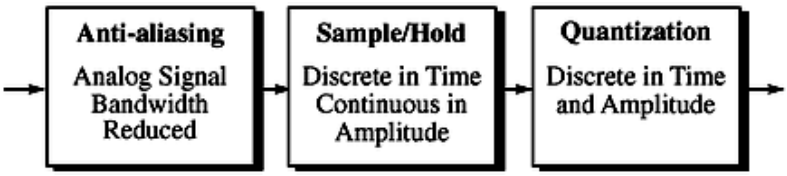

Figure 5.19: Steps of data acquisition

5.5.1 Anti-aliasing

The Nyquist criterion dictates that all signals must be band limited to less than half the sampling rate of the sampling system [30]. Many signals already have a limited spectrum, so this is not a problem. However, for broad spectrum signals, an analog lowpass filter must be placed before the data acquisition system. The minimum attenuation of this filter at the aliasing frequency should be at least: $A_min = 20\log(\sqrt{3} * 2^B)$ where B is the number of bits of the ADC. This formula is derived from the fact that there is a minimum noise level inherent in the sampling process and there is no need to attenuate the transducer signal more than to below this noise level [30]. Some problems face in this project with the anti-aliasing filter is as follows:

1. Time Response: In designing an anti-aliasing filter, there is a temptation to have its attenuation roll-off extremely quickly. The way to achieve this is to increase the order of the filter. A so-called brick-wall filter (one with infinitely high order), however, causes a sinc function time response that decays proportionally to 1/t. What this means is that an extremely high order filter that eliminates all signals above the cutoff frequency will cause signals that change rapidly to ring on for a long time. This is an undesirable effect.

2. Phase Distortion / Time delay: Most analog filters have a non-linear phase response. This problem since non-linear phase causes an unequal time (group) delay as a function of frequency. The higher frequency signals will arrive later than low frequency signals. This can especially be a problem when multiple transducers outputs are compared such as when using a microphone array.

3. Amplitude Distortion: By definition, the filter will modify the frequency structure of the stransducers signal which is usually not desired

The solutions to be considered for all the problem states above is increase the sampling rate of the ADC have a linear phase filters. This allows the antialiasing filter to have a higher cutoff frequency and still eliminate aliasing. This enables the filter rolloff can be more shallow that allowing a better time response.

5.5.2 Sample and Hold

The purpose of the sample and hold circuitry is to take a snapshot of the transducer signal and hold the value. The ADC must have a stable signal in order to accurately perform a conversion. An equivalent circuit for the sample and hold is shown in Figure 5.20. The switch connects the capacitor to the signal conditioning circuit once every sample period. The capacitor then holds the voltage value measured until a new sample is acquired. Many times, the sample and hold circuitry is incorporated into the same integrated circuit package.

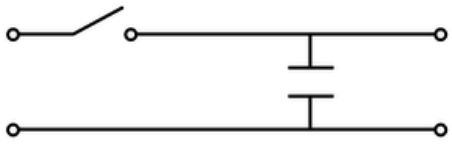

Figure 5.20: Equivalent circuit for a sample and hold

Some problems face in this project with the sample and Hold is as follows:

1. Finite Aperture Time: The sample and hold takes a period of time to capture a sample of the transducers signal. This is called the aperture time.

Since the signal will vary during this time, the sampled signal can be slightly off.

2. Signal Feedthrough: When the sample and hold is not connected to the signal, the value being held should remain constant. Unfortunately, some signal does bleed through the switch to the capacitor, causing the voltage being held to change slightly.

3. Signal Droop: The voltage being held on the capacitor starts to slowly decrease over time if the signal is not sampled often enough.

The main solution to these problems is to have a small aperture time relative to the sampling period. This means that the sample and hold must be quite small.

5.5.3 Analog to Digital Conversion

The purpose of the analog to digital is to quantize the input signal from the sample and hold circuit to $2B$ discrete levels. B is the number of bits of the analog to digital converter (ADC). The input voltage can range from 0 to Vref (or -Vref to +Vref for a bipolar ADC). What this means is that the voltage reference of the ADC is used to set the range of conversion of the ADC. For a monopolar ADC, a 0V input will cause the converter to output all zeros. If the input to the ADC is equal to or larger than V_{ref}, then the converter will output all ones. For inputs between these two voltage levels, the ADC will output binary numbers corresponding to the signal level. For a bipolar ADC, the minimum input is $-V_{ref}$, not 0V.

Some problems face in this project with the ADC is a noise. Because the ADC outputs only 2^B levels there is inherently noise in the quantized output signal.

The ratio of the signal to this quantization noise is called SQNR. The SQNR in dB is approximately equal to 6 times the number of bits of the ADC [30]:

$$20 \log (\text{SQNR}) = 6 * \textit{Bits}$$

So for a 16 bit ADC this means that the SQNR is approximately equal to 96 dB. There are, of course, other sources of noise that corrupts the output of the ADC. These include noise from the transducers, from the signal conditioning circuitry, and from the surrounding digital circuitry.

To overcome this problem, the input signal needs to be maximized. The key to reducing the effects of the noise is to maximize the input signal level. What this means is that the gain of the signal conditioning circuitry needs to be increased until the maximum transducer output is equal to the V_{ref} of the ADC. It is also possible to reduce down V_{ref} to the maximum level of the transducer. The problem with this is that the noise will corrupt the small signals. A good rule of thumb is to keep V_{ref} at least as large as the maximum digital signal, usually 5V.

5.5.4 National Instruments Data Acquisition Card

All the theories described in the previous sections are used in the selection of the data acquisition card. As final results, National Instruments data acquisition card model PCI 6224 is chosen as appropriated to the laboratory prototype. The details of this hardware can be seen in Appendix H. Figure 5.21 depicts a simplified block diagram of the National Instruments data acquisition card that will be used in this study. It has 24 analog channels which can either be configured as 24 single ended inputs, or 12 differential inputs. This is accomplished by the multiplexer, or switching circuit and is software configurable.

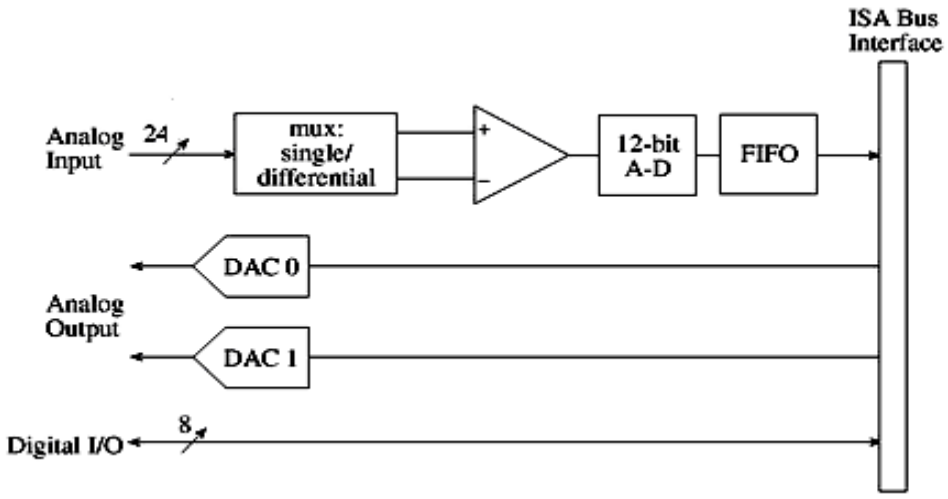

Figure 5.21: Block diagram of the National Instruments data acquisition card

The output of the multiplexer feeds into an amplifier is programmable through software. This circuit allows the programmer to select amplification appropriate to the signal that is to be measured. The board used in the prototype is capable of implementing gains from 0.5 up to 100. As an example of how this programmable gain would be used, consider a bipolar (both positive and negative) input signal. The analog to digital converter has an input voltage range of ±5 V, hence a gain of 0.5 would enable the board to handle voltages ranging between ± 10 V (5/0.5). Similarly, a gain of 100 would result in a maximum range of ± 50 mV (5/100) at the input to the board.

In addition to the analog to digital converters, there are 2 digital to analog converters which allow one to generate analog signals. Eight general purpose digital I/O lines are also provided which allow the board to control external digital circuitry or monitor the state of external devices such as switches or buttons. Low level communication with the data acquisition board is handled through drivers provide by National Instruments. These drivers allow the programmer to perform all the necessary tasks such as initializing, configuring, and sending and receiving data from the board. It is possible to use these drivers from most of the common C compilers

available, but we will primarily use a compiler/development package called LabView. This tool is designed for use specifically with these boards and helps to shield the programmer from many of the potentially unnecessary low level details of the hardware.

The signal conditioning circuit and the data acquisition circuit are connected together with the prototype and placed inside the laboratory prototype control panel. Figure 5.22 show the wiring of the components inside the laboratory prototype of Kuala Krai to Gua Musang Thevenin equivalent system.

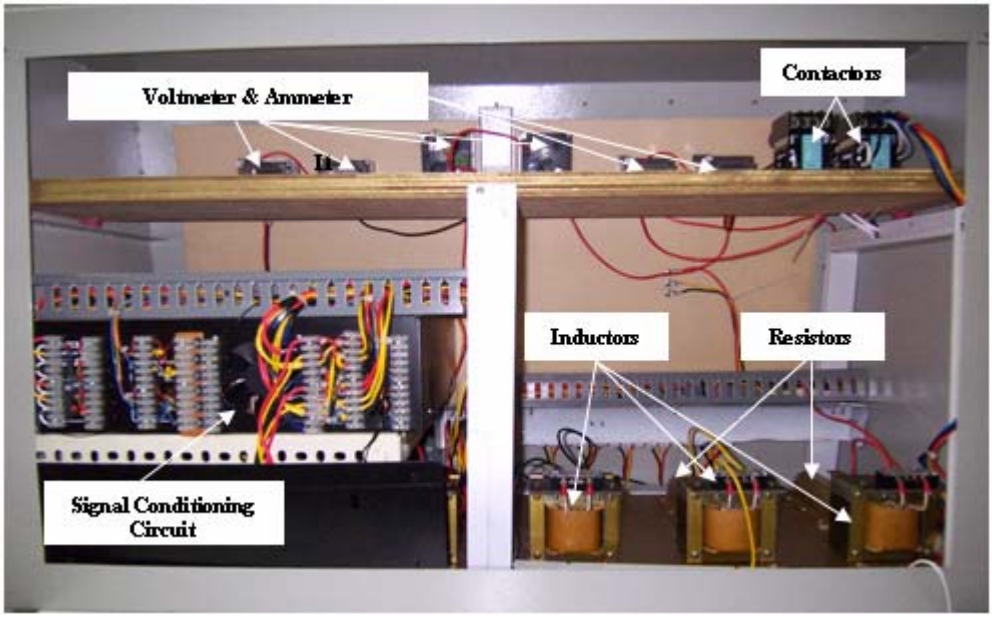

Figure 5.22: Wiring system of the laboratory prototype of Kuala Krai to Gua Musang TNB Kelantan Thevenin equivalent system

The control panel of the Kuala Krai to Gua Musang TNB Kelantan Thevenin equivalent system is as shown in Figure 5.23. This panel have been used in this study and the experimental data have been captured and analyzed on-line using data

acquisition cards and interfacings with PC and plotter. These data is used for comparison with computer simulation results to verify the model that has been developed in PSCAD. All the comparison results from simulations and experimental will be described in Chapter VI.

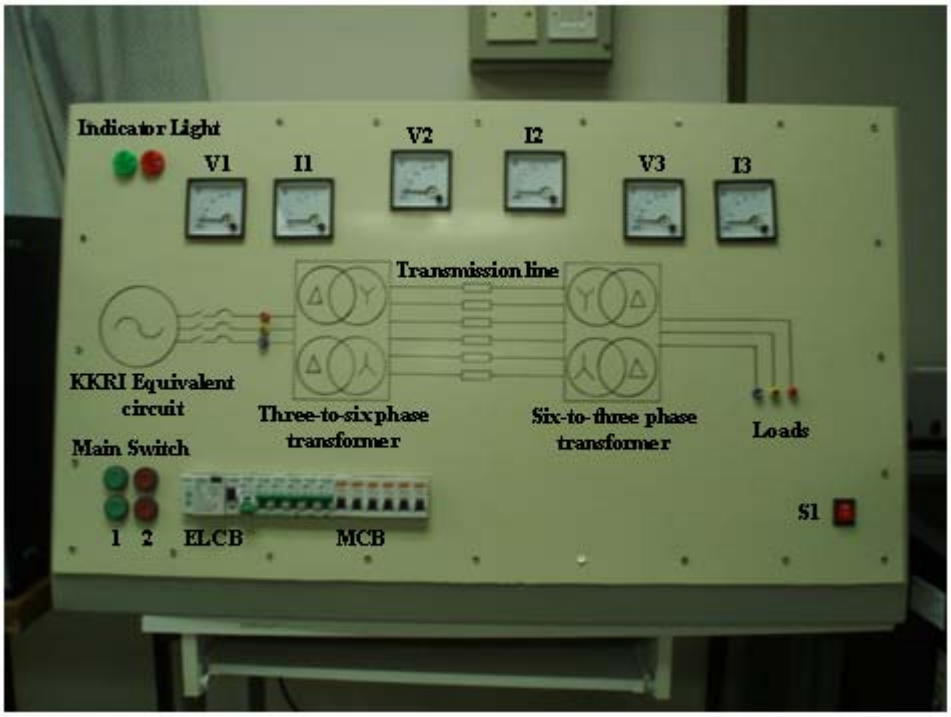

Figure 5.23: Laboratory Prototype of Kuala Krai to Gua Musang TNB Kelantan Thevenin equivalent system

5.6 LabVIEW Software

To monitor the experimental result online, LabVIEW software from National Instruments has been used as the interfacing software. This is due to reason that the

data acquisition card also provided National Instruments. This will make the modelling process and analysis become much easier because LabVIEW have many features and functions that can be used together with data acquisition card from National Instruments. LabVIEW is a graphical programming language that uses icons instead of lines of text to create applications. In contrast to text-based programming languages, where instructions determine program execution, LabVIEW uses dataflow programming, where the flow of data determines execution. In LabVIEW, a user interface can be built with a set of tools and objects. The user interface is known as the front panel. Graphical representations of functions are used to adding codes to control the front panel objects. The block diagram contains this code. In some ways, the block diagram resembles a flowchart. LabVIEW programs are called virtual instruments, or VIs, because their appearance and operation imitate physical instruments, such as oscilloscopes and multimeters. Every VI uses functions that manipulate input from the user interface or other sources and display that information or move it to other files or other computers. A VI contains three components, front panel, block diagram and Icon and connector pane.

5.6.1 Front Panel

The front panel is the user interface of a VI. In this project, the front panel was build with controls and indicators, which are the interactive input and output terminals of the VI, respectively. Controls are knobs, push buttons, dials, and other input devices. Indicators are graphs, LEDs, and other displays. Controls simulate instrument input devices and supply data to the block diagram of the VI. Indicators simulate instrument output devices and display data the block diagram acquires or generates. Property dialog boxes or shortcut menus have been used to configure the controls and indicators appearance on the front panel. Figure 5.24 show the front panel of the LabVIEW software.

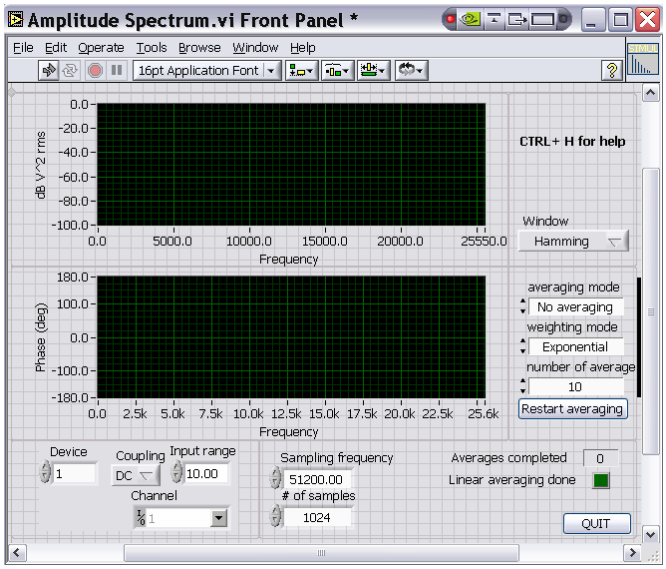

Figure 5.24: LabVIEW front panel

5.6.2 Block Diagram

Block diagram contains the graphical source code that defines the functionality of the VI. After building the front panel, codes are added using graphical representations of functions to control the front panel objects. The block diagram contains this graphical source code. Objects on the block diagram include terminals, nodes, and functions. Figure 5.25 show the block diagram of the LabVIEW software.

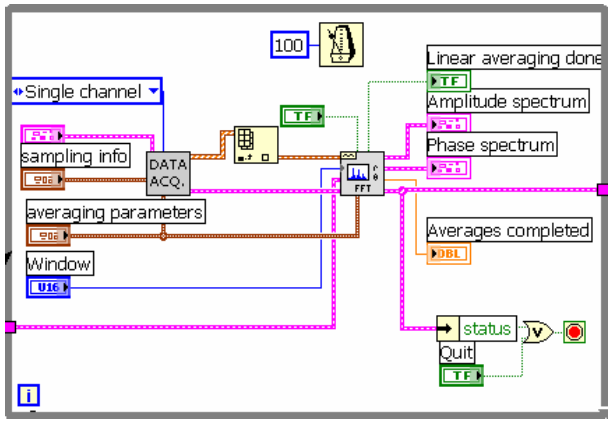

Figure 5.25: LabVIEW block diagram

5.6.3 Icon and Connector Pane

Icon and connector pane identifies the VI so that users can use the VI in another VI. A VI within another VI is called a subVI. A subVI corresponds to a subroutine in text-based programming languages. Every VI displays an icon, such as the one shown at left, in the upper right corner of the front panel and block diagram windows. An icon is a graphical representation of a VI. It can contain text, images, or a combination of both. The connector pane is a set of terminals that correspond to the controls and indicators of that VI, similar to the parameter list of a function call in text-based programming languages. The connector pane defines the inputs and outputs that can be wired to the VI so we can use it as a subVI. A connector pane receives data at its input terminals and passes the data to the block diagram code through the front panel controls and receives the results at its output terminals from the front panel indicators. Figure 5.26 show the side view of the control panel connected to the personal computer while Figure 5.26 show the labVIEW software that used to monitor the experimental results of laboratory prototype.

Figure 5.26: Laboratory prototype connected to the external loads

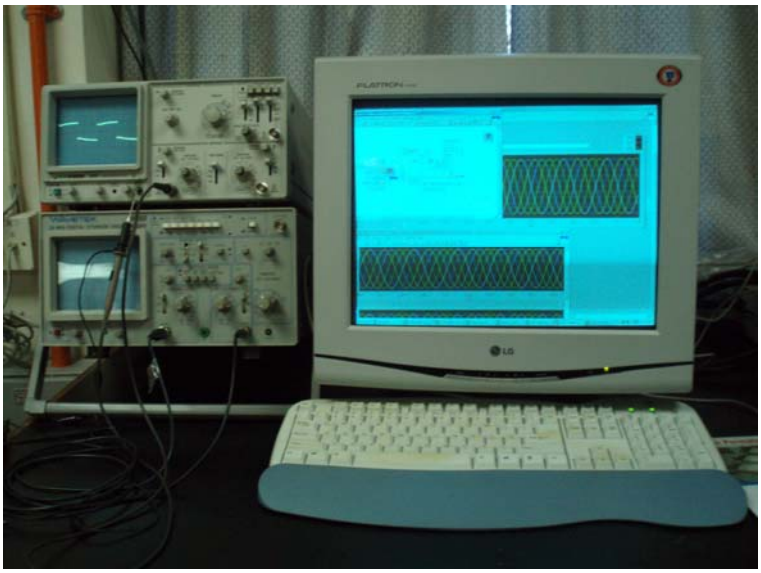

Figure 5.27: LabVIEW used to monitor the experimental results

5.7 Summary

This chapter discussed the design considerations of the laboratory prototype. This included the theoretical of the components used include signal conditioning circuit and data acquisition card. Amplification and filtering circuits also discussed in this chapter. Beside that, hardware and software from National Instruments are also described in brief.

CHAPTER VI

SIMULATION RESULTS AND DISCUSSION

6.1 Introduction

In this chapter the methods and techniques which were describes in the previous chapter will be used into digital load flow analysis, fault analysis and transient stability analysis of test systems including IEEE Test Systems and 19-Bus TNB Kelantan System. The analysis is performed considering both cases the test systems with three-phase and six-phase transmission system. The networks are assumed in a balance situation. Based on this assumption, the digital load flow analysis, fault analysis and transient stability analysis of IEEE Test Systems and 19-Bus TNB Kelantan System considering conversion of its existing three-phase double-circuit lines into six-phase ones have been performed.

The load flow analysis is performed contingencies studies and the results are used to choose an appropriate transmission line to fix into the six-phase transmission. While a suitable line to apply six-phase transmission is decided, fault analysis and transient stability analysis then can be conducted to that test systems considering the converted six-phase transmission line. PSCAD is used to carry out the load flow

analysis, fault analysis and transient stability analysis. The analysis and simulation results will be covered in this chapter.

6.2 Results of Load Flow Analysis

The load flow studies are used to determine the bus voltage, branch current, active and reactive power flow for a specified generation and load conditions in the test systems. The results of the power flow analysis are the starting point for the fault analysis and transient stability analysis. Load flow analysis has been conducted by using the Fast Decouple Method provided by MATPOWER [27]. The results of load flow studies can be seen in Appendix E. These result then used in the initialization and start-up process of the generators in PSCAD/EMTDC.

Parameters used by PSCAD is in the real values while all the given power systems data in Appendix D is in the p.u. values. Therefore, the p.u. values should be converted to the real values to be used as inputs of components model in PSCAD. Subsequently, the modeling of the test systems by using PSCAD can be conducted.

Approach used in the load flow analysis has been described in brief. Initialization or start-up process is needed to start the modeling using PSCAD. This process is set a generator in PSCAD with the magnitude and phase angle of the terminal voltage. Real and reactive power also used while setting the generators. These values are taken from the load flow results using MATLAB. In load flow analysis, the test systems are modeled by using PSCAD. Subsequently, load flow analysis has been conduct to validate the test systems model in PSCAD by making comparisons between PSCAD and MATLAB results. The modeling process will be repeated until the comparison of load flow results from PSCAD and MATLAB are within acceptable value. After the model of test systems in PSCAD is corrected, one

of the three-phase double-circuit transmission lines has been converted to the six-phase transmission. From the simulation, a load flow results are tabulated. This step will be repeated for the same test systems model considering only one new location of transmission line is converted to a six-phase transmission at one time. All the load flow results are tabulated and comparisons are made.

Simulations are applied to the test systems model were developed in PSCAD/EMTDC for both systems with three-phase double-circuit and systems with six-phase single-circuit transmission line for the purpose of comparisons. Based on the load flow results, a suitable location to apply the six-phase transmission system has been determined. The criteria used in the selection of the suitable line are based on the total power losses and the acceptable voltage limits at all busbars. These load flow analysis procedures are repeated to run the load flow analysis for all five test systems cases. The load flow results for all five test systems cases are discussed in details in the following subsections.

6.2.1 Test System I

Test System I is used validate the model of the six-phase transmission by using PSCAD/EMTDC software. This test system consists of 4 busbars and 2 generators system. All the transmission lines are assumed as a short transmission lines which less than 80km. The data of test system is given in appendix D.2. Modeling process for the test system in the PSCAD is used the load flow analysis procedures as described in the previous section.

Four cases are tested by converting one of the three-phase double-circuit to the six-phase line at a time. Load flow analysis for each case is simulated and the results have been shown in Figure 6.1 to Figure 6.11. Figures 6.1 and 6.2 are shown

the comparison of load flow analysis results using MATLAB, Power Education Toolbox (PET) and PSCAD software packages. The color bars are representing the load flow results. Purple is MATLAB, brown is PET and yellow is PSCAD results respectively. Figure 6.1 shows the real power flow while Figure 6.2 shows the reactive power flow. The load flow analyses for the three different software packages given the same results. This validated the model developed in the PSCAD.

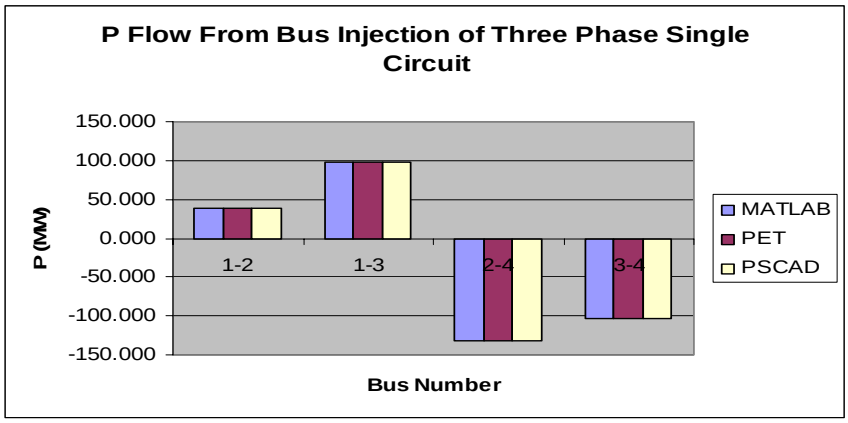

Figure 6.1: Comparison of P flows for three-phase single-circuit cases

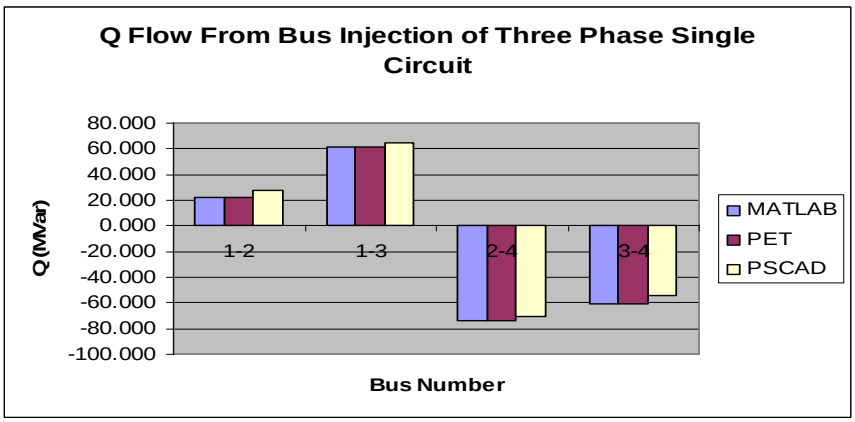

Figure 6.2: Comparison of Q flows for three-phase single-circuit cases

Figure 6.3 shown the comparison of real power (P) while Figure 6.4 shown the comparison of reactive power (Q) between three-phase double-circuit (3PDC) and six-phase single-circuit (6PSC) respectively. As can be seen from Figures 6.3 and 6.4, the real and reactive power flows through every branch is a bit different for both 3PDC and 6PSC transmission cases. The variations percentage of the power flow results between 3PDC and 6PSC cases are ±10%. This is due to the fact that, in 6PSC, the conversion transformers are added on both ends of the transmission line. This will increased the impedance of the line and hence affected the real and reactive power flows.

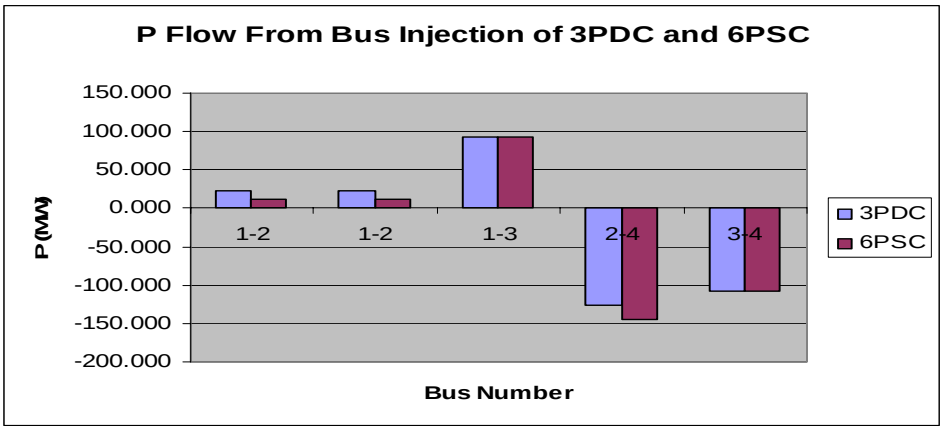

Figure 6.3: Comparison of P flows between 3PDC and 6PSC cases

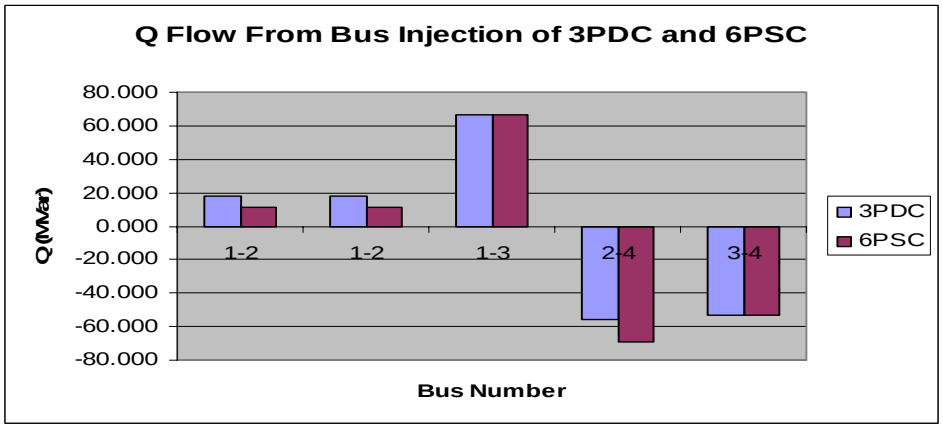

Figure 6.4: Comparison of Q flows between 3PDC and 6PSC cases

Figure 6.5 show the comparison of the terminal voltages between 3PDC and 6PSC transmission. As shown, the voltage level for both cases does not much different. Only on bus 2, the voltage is 1 % less while 3PDC is converted to 6PSC transmission. The overall system voltages are within the acceptable limits.

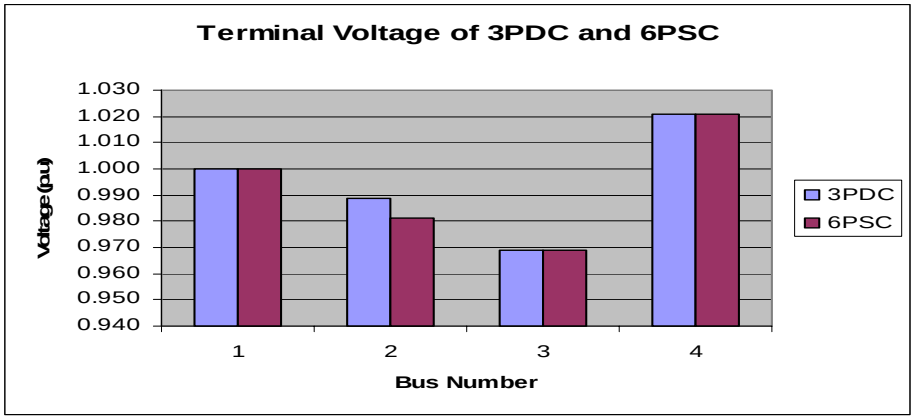

Figure 6.5: Comparison of terminal voltage between 3PDC and 6PSC cases

Figures 6.6 and 6.7 shows the comparison of real power and reactive power generated from generators on bus 1 and bus 4 between 3PDC and 6PSC transmission cases. Both generators will generate different level of real and reactive powers based on the sufficient generator will generate more power to the nearest loads.

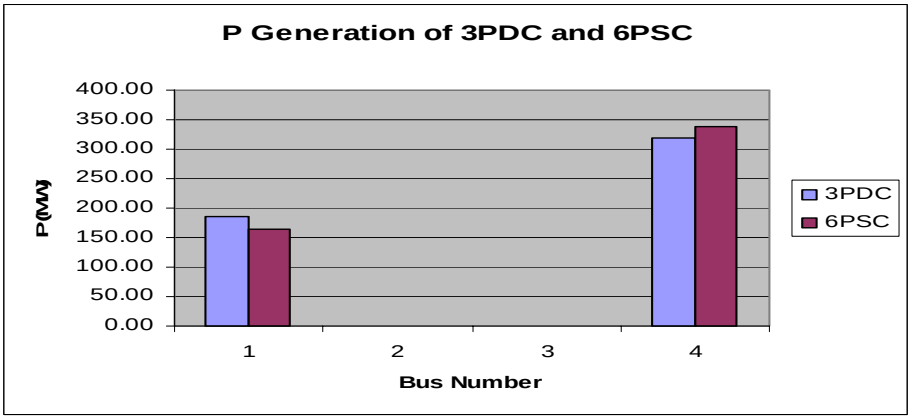

Figure 6.6: Comparison of P generated between 3PDC and 6PSC cases

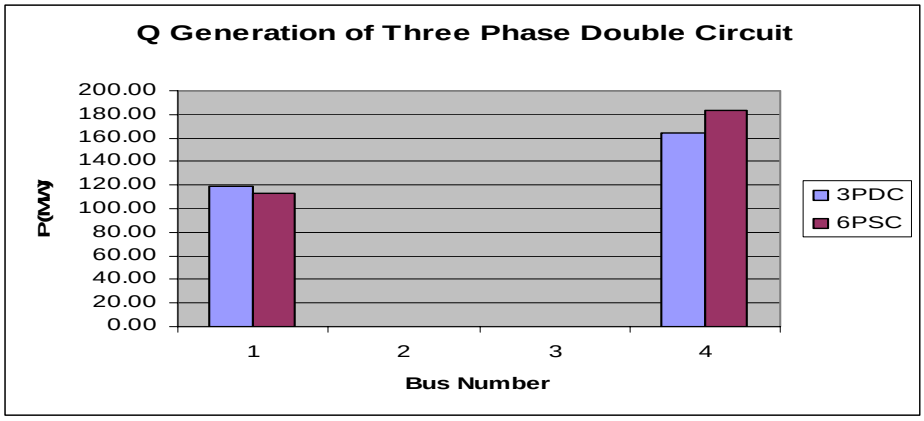

Figure 6.7: Comparison of Q generated between 3PDC and 6PSC cases

The comparison of power loss for the both 3PDC and 6PSC cases are shown in the Figure 6.8 and Graph 6.9. Figure 6.8 shows the comparison of the real power loss while Figure 6.9 shows the comparison of the reactive power loss. From both Figures 6.8 and 6.9, the power losses are minimum when the conversion is applied to the line 3-4. Conversion of other lines from 3PDC to 6PSC has massive losses. As an example, conversion of transmission line 1-3 from 3PDC to 6PSC operation will give highest losses.

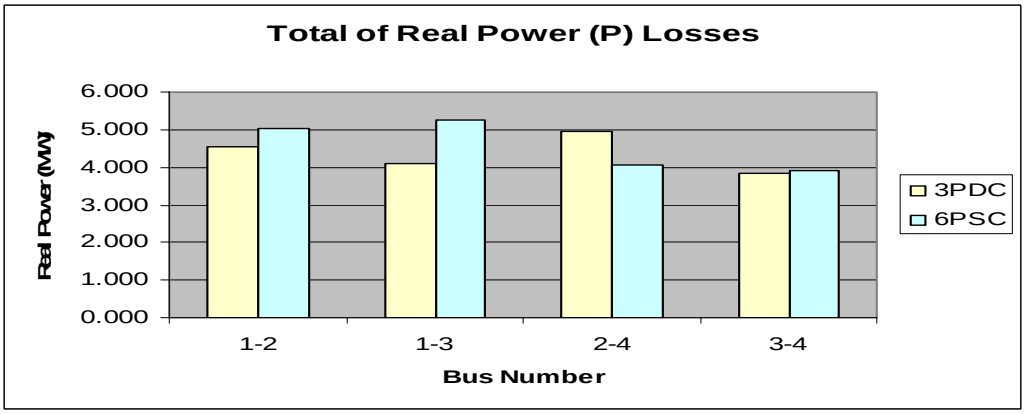

Figure 6.8: Comparison of total P losses between 3PDC and 6PSC cases

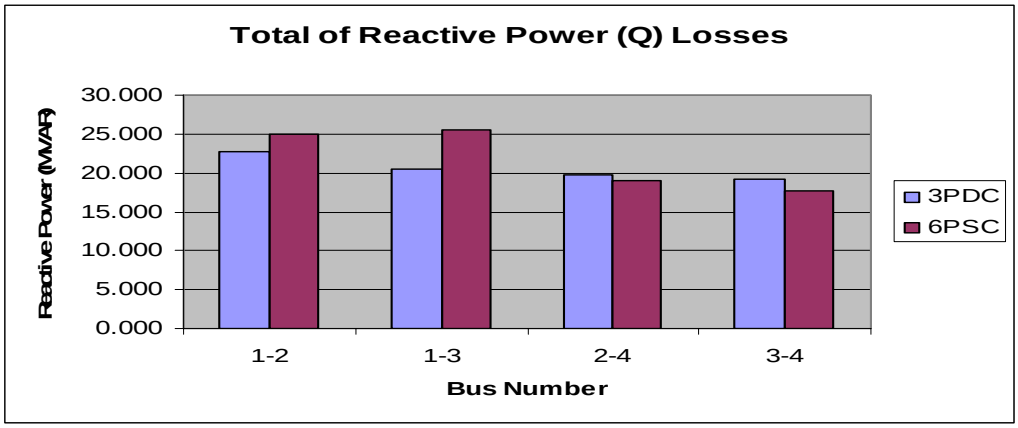

Figure 6.9: Comparison of total Q losses between 3PDC and 6PSC cases

Figure 6.10 shows the total of real power loss while Figure 6.11 shows the reactive power loss whenever one of the 3PDC transmission lines is converted to the 6PSC operation. As can be seen, the conversion of line 3-4 and also line 2-4 will give less power losses compare to other lines of conversion.

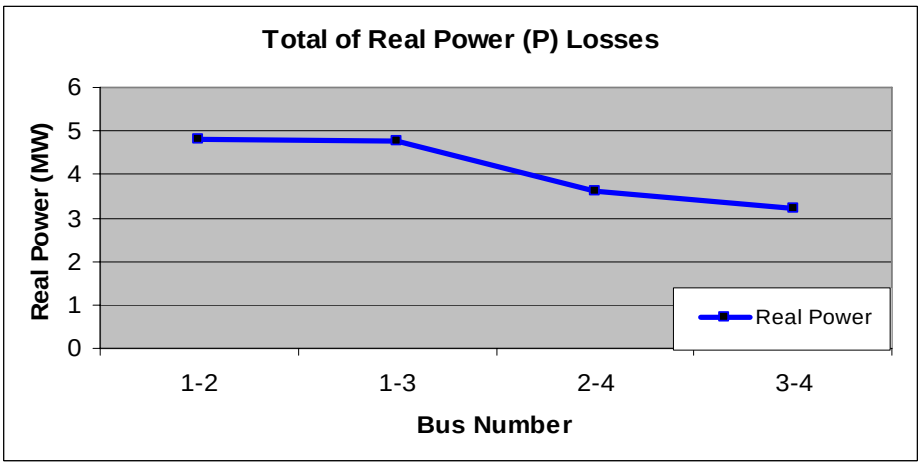

Figure 6.10: The total of P losses for 6PSC cases

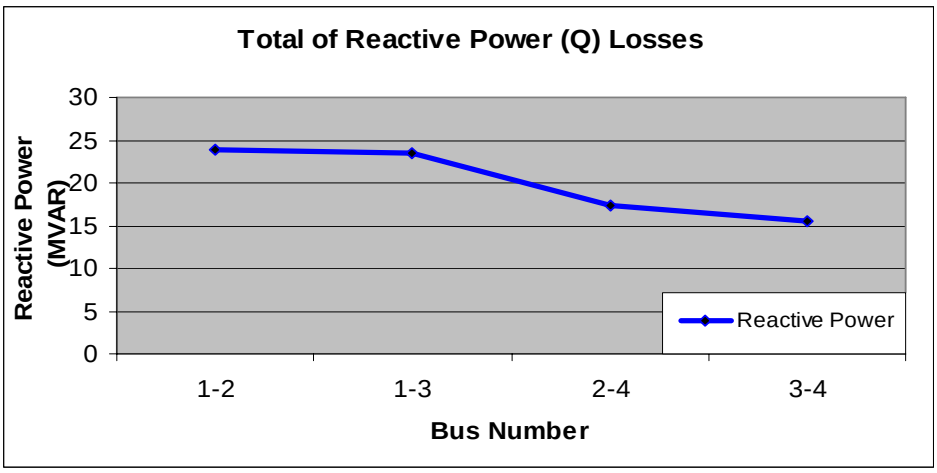

Figure 6.11: The total of Q losses for 6PSC cases

From the simulation and load flow results, there are two possible locations can be chosen to apply the 6PSC transmission which is line 2-4 and line 3-4. But the most suitable location to apply a conversion from 3PDC to a 6PSC is by making a conversion to the line 3-4. This is due to the minimum real and reactive power losses when this line is converted to the six-phase operation. Moreover, the magnitude of terminal voltage remains in the acceptable limit. For the Test System I, the most suitable location to fix the six-phase transmission is at line 3-4. More results can be seen in Appendix G.1.

6.2.2 Test System II

Test System II consists of 9 busbars and 3 generators system. All the transmission lines were assumed as a short transmission lines which less than 80km. The data of test system is given in appendix D.3. Modeling process of Test System II in the PSCAD is used the same procedures as described in the previous section.

Nine cases are tested by converting one of the three-phase double-circuits to the six-phase line at a time. Load flow analysis for every case is shown in the Figure 6.12 to Figure 6.15. Figure 6.12 shows the comparisons of real power while Figure 6.13 shows the comparisons of reactive powers between 3PDC and 6PSC respectively. As can be seen from Figures 6.12 and 6.13, the real and reactive power flows through every branch is different for both 3PDC and 6PSC transmission cases. The variations percentage of the power flow results between 3PDC and 6PSC cases are ±20%.

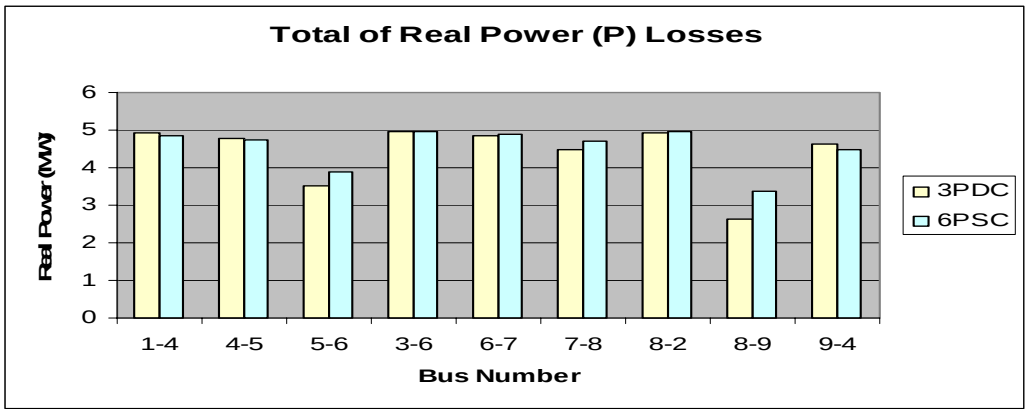

Figure 6.12: Comparisons of P losses between 3PDC and 6PSC cases

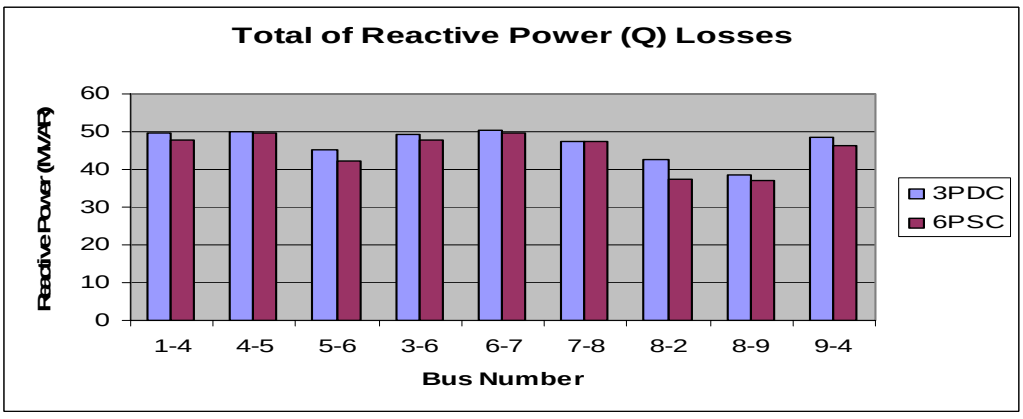

Graph 6.13: Comparisons of Q losses between 3PDC and 6PSC cases

Figure 6.14 shows the total of real power losses while Figure 6.15 shows the reactive power losses whenever one of the 3PDC transmission lines is converted to the 6PSC operation. As can be seen, the conversion of line 5-6 and line 8-9 will give the smallest power losses compare to other lines of conversion.

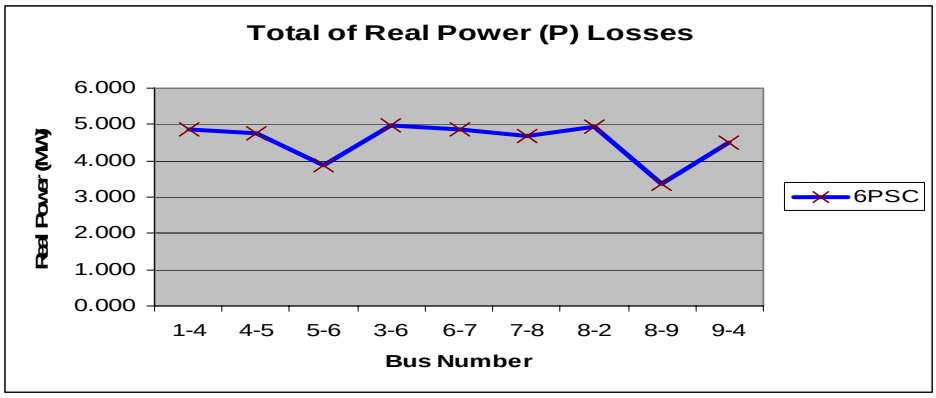

Figure 6.14: The total of P losses for 6PSC cases

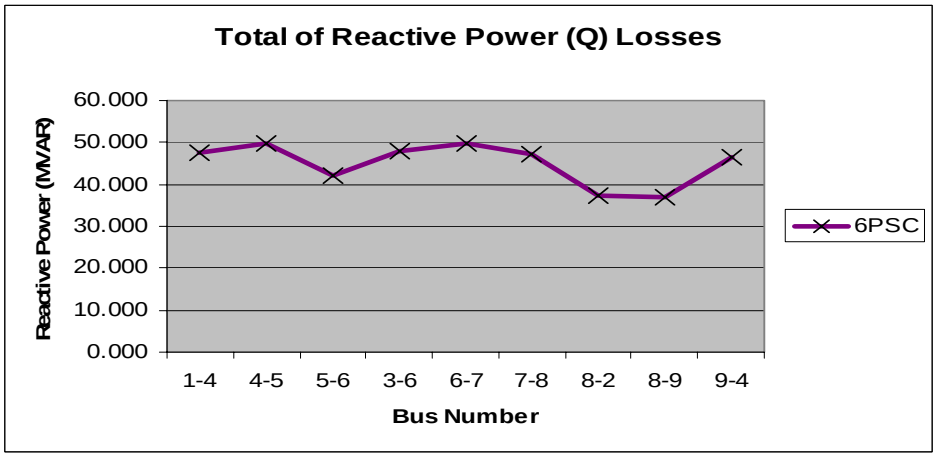

Figure 6.15: The total of Q losses for 6PSC cases

From the load flow results, there are two possible locations to apply the six-phase transmission which is line 5-6 and line 8-9. The most suitable location to apply a conversion from 3PDC to 6PSC transmission is by making a conversion to the line 8-9. This is due to the minimum real and reactive power losses when this line is converted to the six-phase transmission. Furthermore, the magnitude of terminal voltage remains in the acceptable. For the Test System II, the most suitable location to fix the six-phase transmission is at line 8-9. More results can be seen in Appendix G.2.

6.2.3 Test System III

Test System III consists of 14 busbars and 5 generators system. The transmission lines are assumed a short transmission lines which is less than 80km. The data of test system is given in Appendix D.4. Modeling process of Test System III in the PSCAD is using the load flow analysis procedures as described in the previous section.

15 cases are tested by converting one of the three-phase double-circuits to the six-phase line at a time. Load flow analysis for every case was simulated and the results are shown in Figure 6.16 to Figure 6.19. Figure 6.16 shows the comparisons of real power while Figure 6.17 shows the comparisons of reactive powers between 3PDC and 6PSC respectively. As can be seen from Figures 6.16 and 6.17, the real and reactive power flows through every branch is different for both 3PDC and 6PSC transmission cases. The variations percentage of the power flow results between 3PDC and 6PSC cases are ±20%.

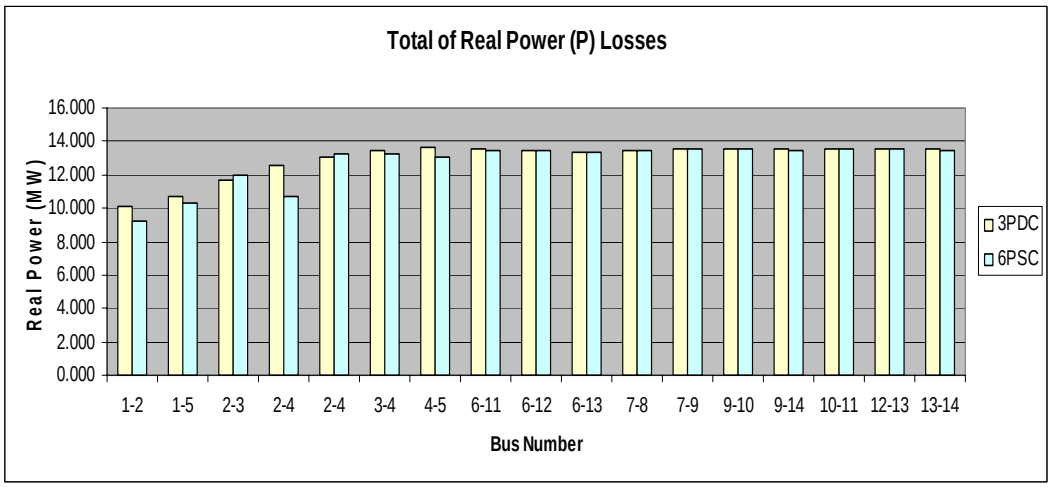

Figure 6.16: Comparison of P losses between 3PDC and 6PSC cases

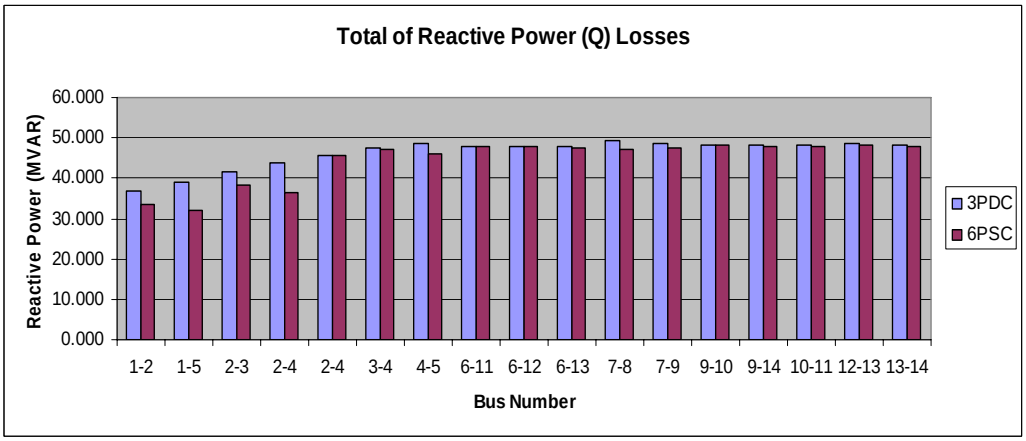

Figure 6.17: Comparison of Q losses between 3PDC and 6PSC cases

Figure 6.18 shows the total of real power losses while Figure 6.19 shows the reactive power losses whenever one of the 3PDC transmission lines is converted to the 6PSC operation. As can be seen, the conversion of the line 1-2 and line 1-5 will give the smallest power losses compare to other lines of conversion.

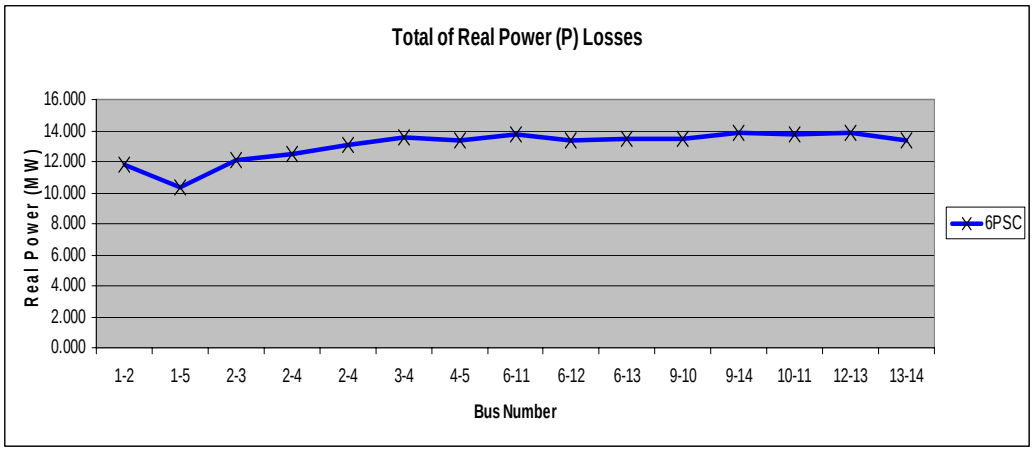

Figure 6.18: The total of P losses for 6PSC cases

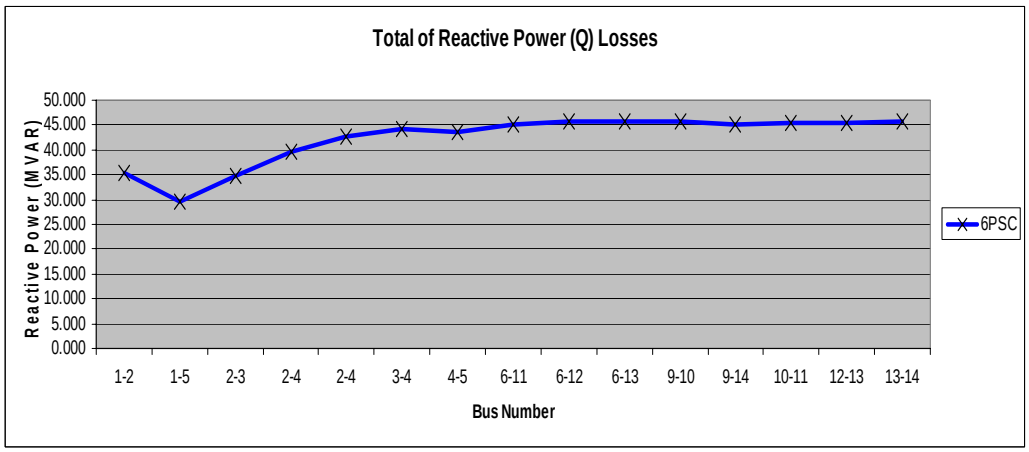

Figure 6.19: The total of Q losses for 6PSC cases

From the load flow results, there are four possible locations to apply the six-phase transmission which is line-1-2, line1-5, line 2-3 and line 2-4. The most suitable location to apply a conversion from 3PDC to 6PSC is by making a conversion to the line 1-5. This is due to the minimum real and reactive power losses occurred when this line is converted to the six-phase operations. The magnitude of terminal voltage also remains within the acceptable limit. For the Test System III, the most suitable location to apply the six-phase transmission is at the line 1-5. More results can be seen in Appendix G.3.

6.2.4 Test System IV

Test System IV consists of 30 busbars and 6 generators system. The data of test system is given in appendix D.5. Modeling process for the test system in the PSCAD is using the load flow analysis procedures as described in the previous section.

34 cases are tested by converting one of the three-phase double-circuits to the six-phase line at a time. Load flow analysis for every case has been simulated and the results are shown in Figure 6.20 to 6.26. Figure 6.20 shows the comparisons of real power while Figure 6.21 shows the comparisons of reactive power between 3PDC and 6PSC respectively. As can be seen from Figures 6.20 and 6.21, the real and reactive powers flows through every branch is a bit different for both 3PDC and 6PSC transmission cases. The variations percentage of the power flow results between 3PDC and 6PSC cases are ±15%.

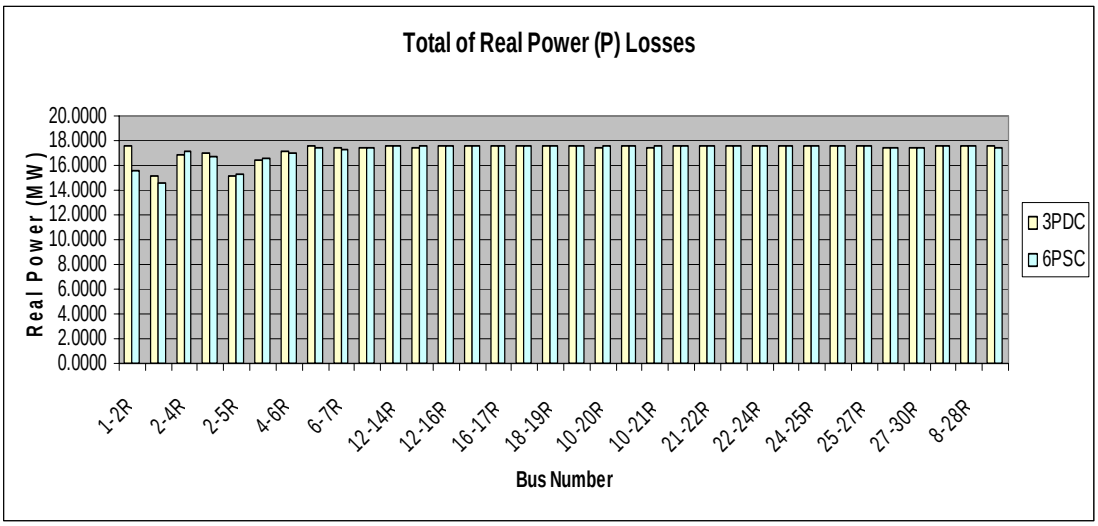

Figure 6.20: Comparison of P losses between 3PDC and 6PSC cases

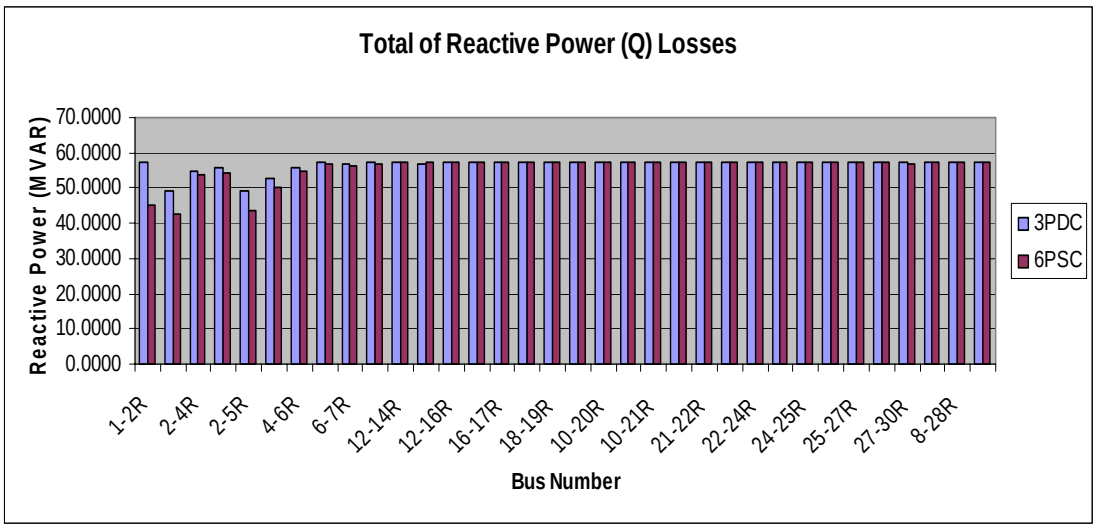

Figure 6.21: Comparison of Q losses between 3PDC and 6PSC cases

Figures 6.22 and 6.23 are same as Figures 6.20 and 6.21 respectively. Instead of showing the results using the bars chart, the line graph used to make sure the results is accessible.

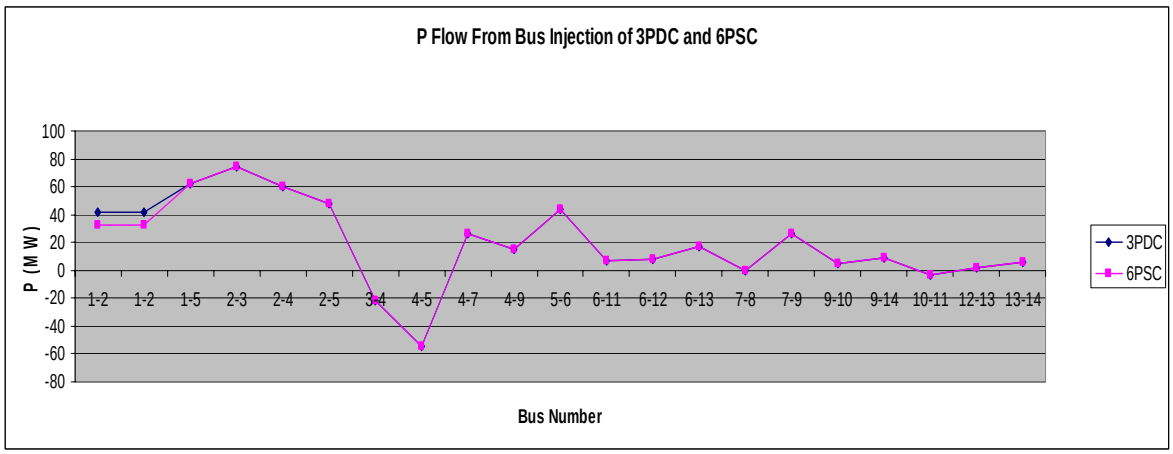

Figure 6.22: Comparison of P losses results for 3PDC and 6PSC cases

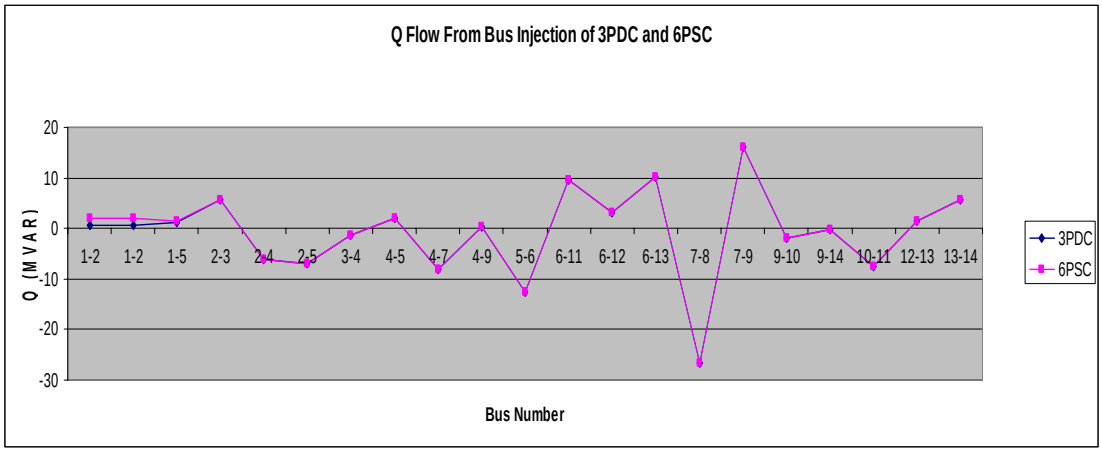

Figure 6.23: Comparison of Q losses between 3PDC and 6PSC cases

Figure 6.24 shows the total of real power losses while Figure 6.25 shows the reactive power losses whenever one of the 3PDC transmission lines is converted to the 6PSC operation. As can be seen, the conversion of the transmission line 1-2, line 1-3 and line 2-5 will give less power losses compare to other lines of conversion.

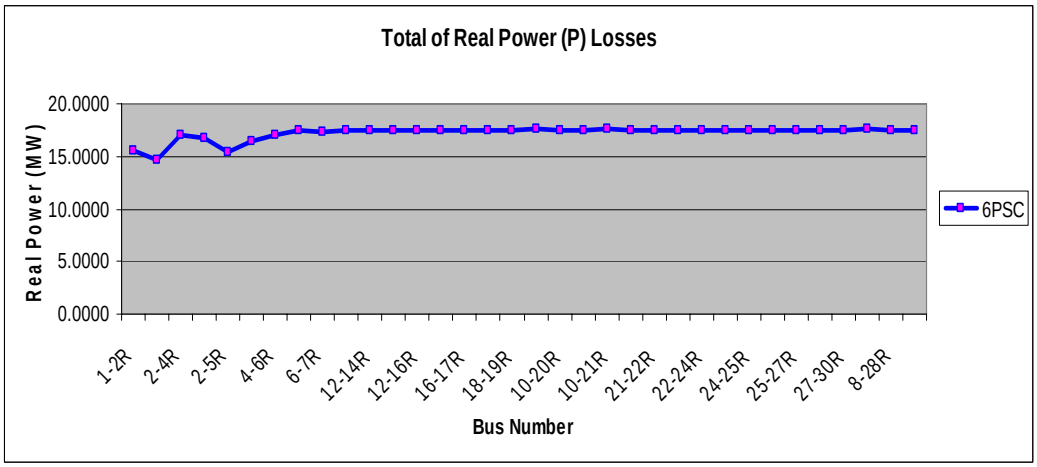

Figure 6.24: The total of P losses for 6PSC cases

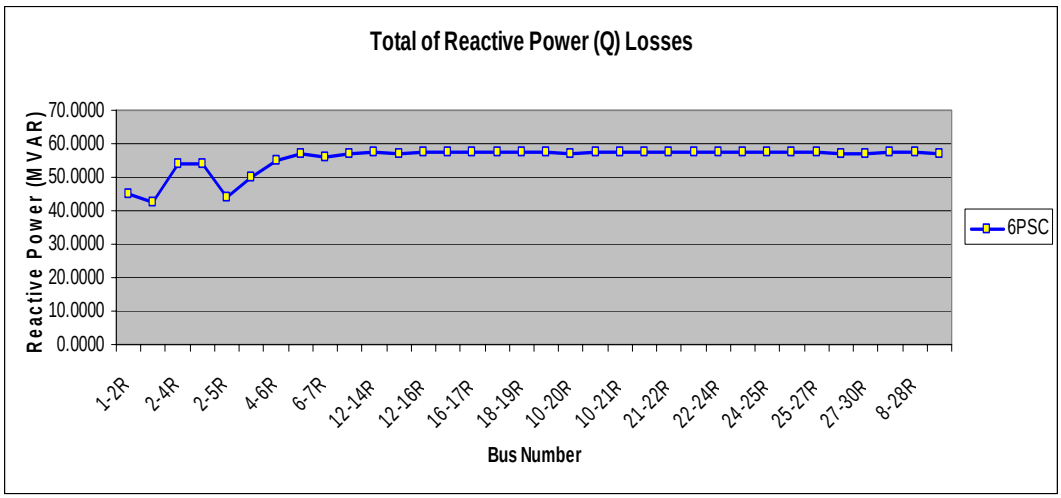

Figure 6.25: The total of Q losses for 6PSC cases

From the comparisons of load flow results, there are three possible locations to apply the six-phase transmission which are line bus 1-2, line 1-3 and line 2-5. The most suitable location to apply a conversion from 3PDC to 6PSC is line 1-3. This is due to the minimum real and reactive power losses when this line is converted to the six-phase operation. The magnitude of terminal voltage also remains within the acceptable limit. For the Test System IV, the most suitable location to apply the six-phase transmission is on the line 1-3.

6.2.5 19-Bus TNB Kelantan System

19-Bus TNB Kelantan System consists of 19 busbars and 8 generators system. The system data is given in appendix D.6. Modeling process for the system in the PSCAD is using the load flow analysis procedures as described in the previous section. Based on the previous test systems results, a suitable location to fix 6PSC transmission is at the longest transmission line which carries huge amount of power. For 19-Bus TNB Kelantan System, line 3-7 has been chosen as appropriated location

to fix the 6PSC transmission. This is based on the fact that, line 3-7 is the longest transmission line of the 19-Bus TNB Kelantan System. The length of the line is 113km long. Besides that, this line is expected to become a main corridor which carries a huge amount of power to the Gua Musang area in the future. Figure 6.26 shows the comparison of *P* while Figure 6.27 shows the comparison of *Q* between 3PDC and 6PSC respectively. As can be seen from Figures 6.26 and 6.27, the real and reactive power flows through every branch is similar for both 3PDC and 6PSC transmission cases. The variations percentage of the power flow results between 3PDC and 6PSC cases are less than ±1%.

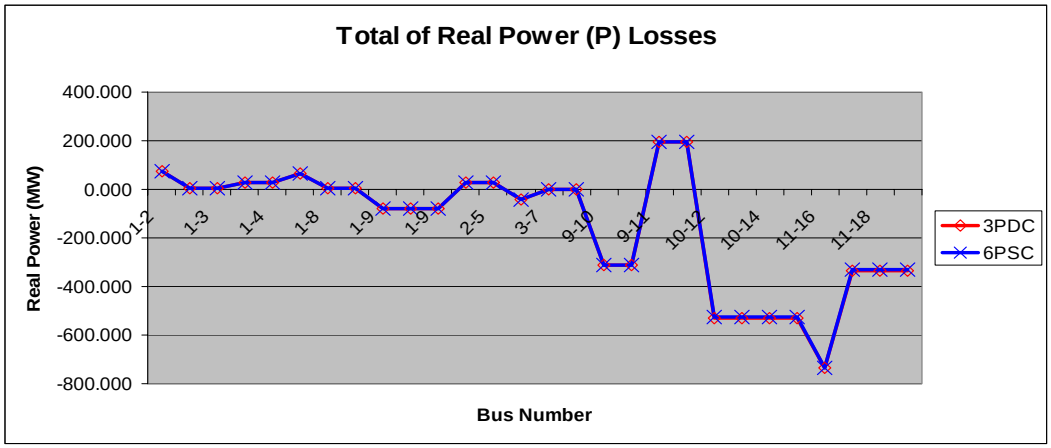

Figure 6.26: Comparison of P losses between 3PDC and 6PSC cases

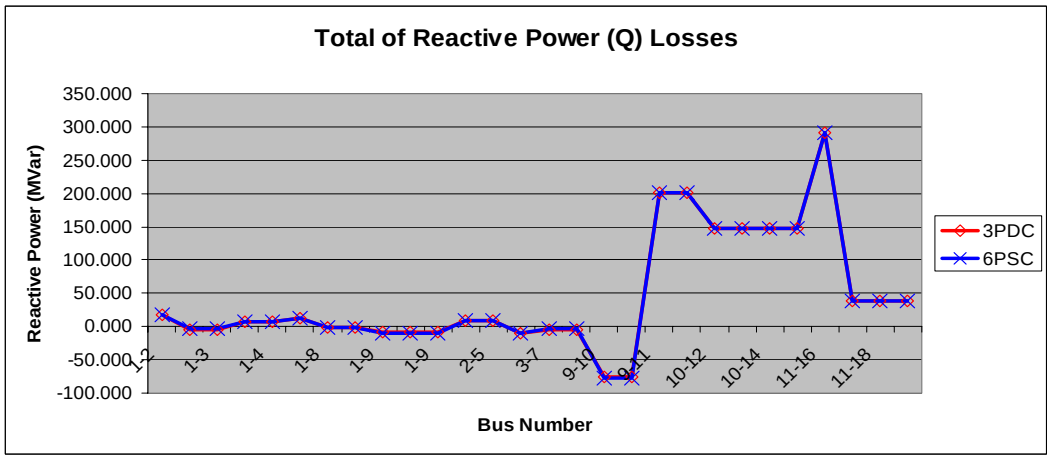

Figure 6.27: Comparison of Q losses between 3PDC and 6PSC cases

Figure 6.28 show the comparison of the terminal voltages between 3PDC and 6PSC transmission. As shown, the voltage level for both cases does not much different. Only on bus-1 to bus-8, the voltage is ±3 % differ while 3PDC is converted to 6PSC transmission. The overall system voltages are within the acceptable limits.

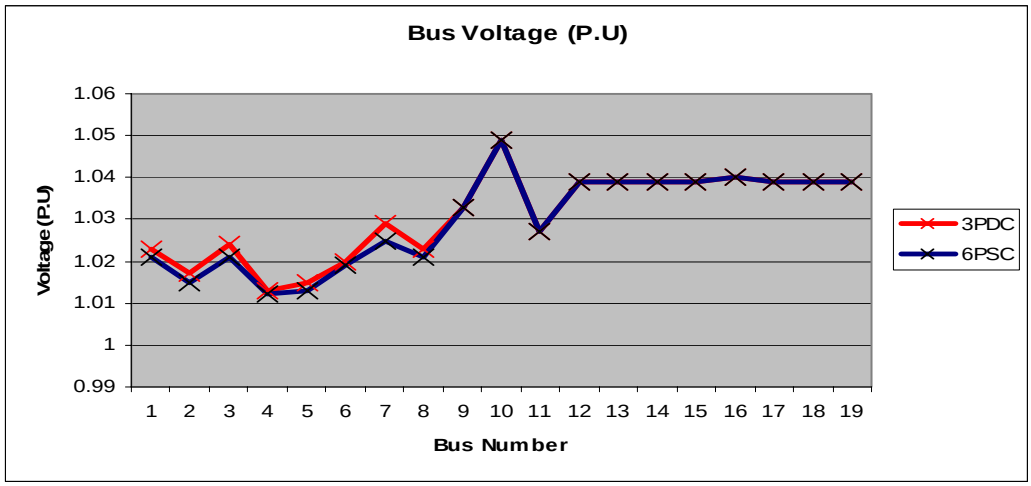

Figure 6.28: Comparison of terminal voltage between 3PDC and 6PSC cases

6.3 Results of Fault Analysis

The purpose of the fault study is to determine the magnitude of fault current and fault level for various types of fault on the converted transmission line. The fault analysis is performed by assuming the phase conversion transformers are connected in Delta (three-phase)–Wye (six-phase). Faults are imposed at the converted line and near to the converted line.

6.3.1 Test System I

Line 3-4 of Test System I has been chosen for the conversion. The fault analysis results for Test System I are shown in Figure 6.29. Details data from fault analysis results for 3PDC and 6PSC transmission cases are tabulated in Table 6.1 and Table 6.2 respectively. Figure 6.29 shows the fault currents flowing in phase *F* for various types of fault on the line 3-4. From the graph, we can observe that the fault current flowing in phase *F* is much smaller when 6PSC transmission is used compare to the 3PDC transmission. This is due to existing of two pairs of phase conversion transformers at each ends of the transmission line for six-phase operation.

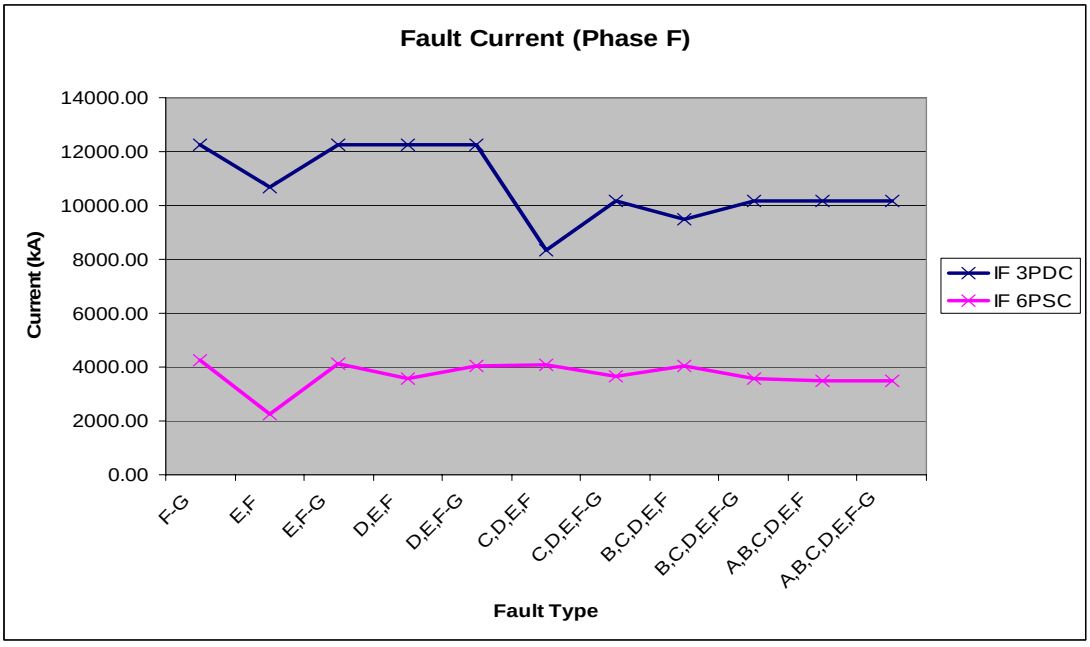

Figure 6.29: Comparison of fault current flowing in phase *F* for 3PDC and 6PSC cases at line 3-4

Table 6.1: List of 3PDC fault currents for various types of fault at mid-point of the transmission line 3-4

Fault Type	Fault Currents (Amps)					
	Ia	*Ib*	*Ic*	*Id*	*Ie*	*If*
1-phase-to-ground *f*	0.00	0.00	0.00	0.00	0.00	12263.80
2-phase *e,f*	0.00	0.00	0.00	0.00	10662.70	10662.70
2-phase-to-ground *e,f-g*	0.00	0.00	0.00	0.00	12315.80	12263.70
3-phase *d,e,f*	0.00	0.00	0.00	12224.30	12315.80	12263.50
3-phase-to-ground *d,e,f-g*	0.00	0.00	0.00	12224.30	12315.80	12263.50
4-phase *c,d,e,f*	0.00	0.00	8331.87	13463.60	13545.90	8331.87
4-phase-to-ground *c,d,e,f-g*	0.00	0.00	10153.60	12224.30	12315.60	10153.60
5-phase *b,c,d,e,f*	0.00	9509.48	9498.76	14084.00	9509.48	9498.76
5-phase-to-ground *b,c,d,e,f-g*	0.00	10197.30	10153.50	12224.20	10197.30	10153.50
6-phase *a,b,c,d,e,f*	10121.60	10197.20	10153.40	10121.60	10197.20	10153.40
6-phase-to-ground *a,b,c,d,e,f-g*	10121.60	10197.20	10153.40	10121.60	10197.20	10153.40

Table 6.2: List of 6PSC fault currents for various types of fault at mid-point of the transmission line 3-4

Fault Type	Fault Currents (Amps)					
	Ia	*Ib*	*Ic*	*Id*	*Ie*	*If*
1-phase-to-ground *f*	0.00	0.00	0.00	0.00	0.00	4267.36
2-phase *e,f*	0.00	0.00	0.00	0.00	2247.19	2247.19
2-phase-to-ground *e,f-g*	0.00	0.00	0.00	0.00	4161.94	4139.65
3-phase *d,e,f*	0.00	0.00	0.00	3602.77	1556.01	3563.19
3-phase-to-ground *d,e,f-g*	0.00	0.00	0.00	4022.05	4012.94	4042.74
4-phase *c,d,e,f*	0.00	0.00	4146.97	2600.08	2651.52	4081.08
4-phase-to-ground *c,d,e,f-g*	0.00	0.00	3657.18	3909.55	3938.52	3657.18
5-phase *b,c,d,e,f*	0.00	4074.20	3227.35	3119.18	3236.78	4056.33
5-phase-to-ground *b,c,d,e,f-g*	0.00	3570.82	3564.39	3820.99	3570.82	3564.39
6-phase *a,b,c,d,e,f*	3473.34	3464.65	3490.57	3473.34	3464.65	3490.57
6-phase-to-ground *a,b,c,d,e,f-g*	3473.34	3464.65	3490.57	3473.34	3464.65	3490.57

From the simulation results, we can conclude that the conversion of 3PDC transmission to 6PSC transmission reducing the magnitude of the fault current. From Table 6.1 and Table 6.2, it is found that for single-line-to-ground fault, the magnitude of the fault current is reducing by 65.2% while for the three-phase fault reduced up to 70.9%.

6.3.2 Test System II

From the load flow analysis, the most suitable line to apply a six-phase transmission is line 8-9. Various types of fault have been conducted to measure the maximum fault current flowing in every line. From the simulation results, the fault current flowing in the 6PSC transmission line is smaller as compare to the similar fault when imposed to 3PDC transmission. Figure 6.30 shows the comparison of fault current for 3PDC and 6PSC transmission system. The details data for three-phase and six-phase fault current are tabulated in Table 6.3 and Table 6.4 respectively.

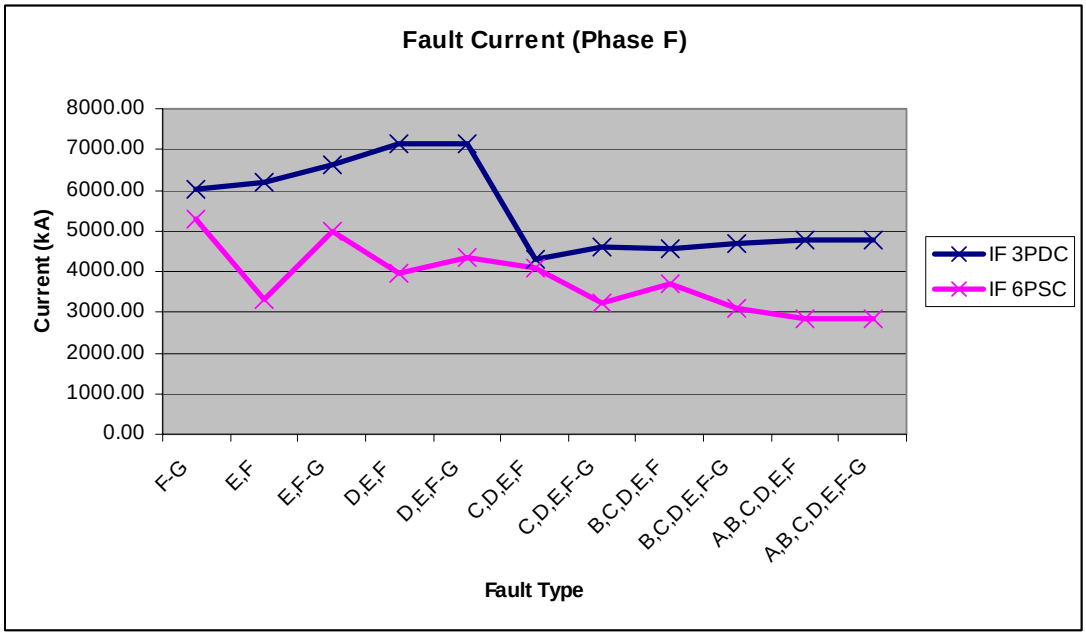

Figure 6.30: Comparison of fault current flowing in phase *F* for 3PDC and 6PSC cases at line 8-9

Table 6.3: List of 3PDC fault currents for various types of fault at mid-point of the transmission line 8-9

Fault Type	Fault Currents (Amps)					
	Ia	*Ib*	*Ic*	*Id*	*Ie*	*If*
1-phase-to-ground *f*	0.00	0.00	0.00	0.00	0.00	6009.36
2-phase *e,f*	0.00	0.00	0.00	0.00	6191.37	6191.37
2-phase-to-ground *e,f-g*	0.00	0.00	0.00	0.00	6774.74	6641.66
3-phase *d,e,f*	0.00	0.00	0.00	7087.35	7138.33	7126.66
3-phase-to-ground *d,e,f-g*	0.00	0.00	0.00	7087.35	7138.33	7126.66
4-phase *c,d,e,f*	0.00	0.00	4293.26	7454.86	7555.22	4293.26
4-phase-to-ground *c,d,e,f-g*	0.00	0.00	4595.04	7207.66	7306.85	4595.04
5-phase *b,c,d,e,f*	0.00	4599.17	4567.52	7746.02	4599.17	4567.52
5-phase-to-ground *b,c,d,e,f-g*	0.00	4717.93	4681.96	7355.62	4717.93	4681.96
6-phase *a,b,c,d,e,f*	4756.23	4790.14	4783.33	4756.23	4790.14	4783.33
6-phase-to-ground *a,b,c,d,e,f-g*	4756.23	4790.14	4783.33	4756.23	4790.14	4783.33

Table 6.4: List of 6PSC fault currents for various types of fault at mid-point of the transmission line 8-9

Fault Type	Fault Currents (Amps)					
	Ia	*Ib*	*Ic*	*Id*	*Ie*	*If*
1-phase-to-ground *f*	0.00	0.00	0.00	0.00	0.00	5273.12
2-phase *e,f*	0.00	0.00	0.00	0.00	3327.25	3327.25
2-phase-to-ground *e,f-g*	0.00	0.00	0.00	0.00	5047.13	5002.21
3-phase *d,e,f*	0.00	0.00	0.00	4042.13	2706.10	3953.57
3-phase-to-ground *d,e,f-g*	0.00	0.00	0.00	4332.14	4325.20	4356.48
4-phase *c,d,e,f*	0.00	0.00	4138.53	2982.31	3030.72	4067.25
4-phase-to-ground *c,d,e,f-g*	0.00	0.00	3225.40	4065.11	4083.66	3225.40
5-phase *b,c,d,e,f*	0.00	3688.50	2731.85	3137.07	2730.82	3689.94
5-phase-to-ground *b,c,d,e,f-g*	0.00	3075.04	3081.48	3687.40	3075.04	3081.48
6-phase *a,b,c,d,e,f*	2840.01	2834.71	2855.44	2840.01	2834.71	2855.44
6-phase-to-ground *a,b,c,d,e,f-g*	2840.01	2834.71	2855.44	2840.01	2834.71	2855.44

From the simulation results, we can conclude that the conversion of 3PDC transmission to 6PSC transmission will reduce the magnitude of the fault current. From Table 6.3 and Table 6.4, it is found that for single-line-to-ground fault, the magnitude of the fault current is reducing by 12.3% while for the three-phase fault reduced up to 44.5%.

6.3.3 Test System III

Line 1-5 of Test System III has been chosen for the conversion. The fault analysis results of Test System III are shown in Figure 6.31. Details data from fault analysis results for 3PDC and 6PSC transmission cases are tabulated in Table 6.5 and Table 6.6 respectively. Figure 6.31 shows the fault currents flowing in phase *F* for various types of fault on the line 1-5. From the graph, we can observe that the fault current flowing in phase *F* is much smaller when six-phase transmission is used compare to the 3PDC transmission. This is due to existing of two pairs of phase conversion transformers at each ends of the transmission line for six-phase operation.

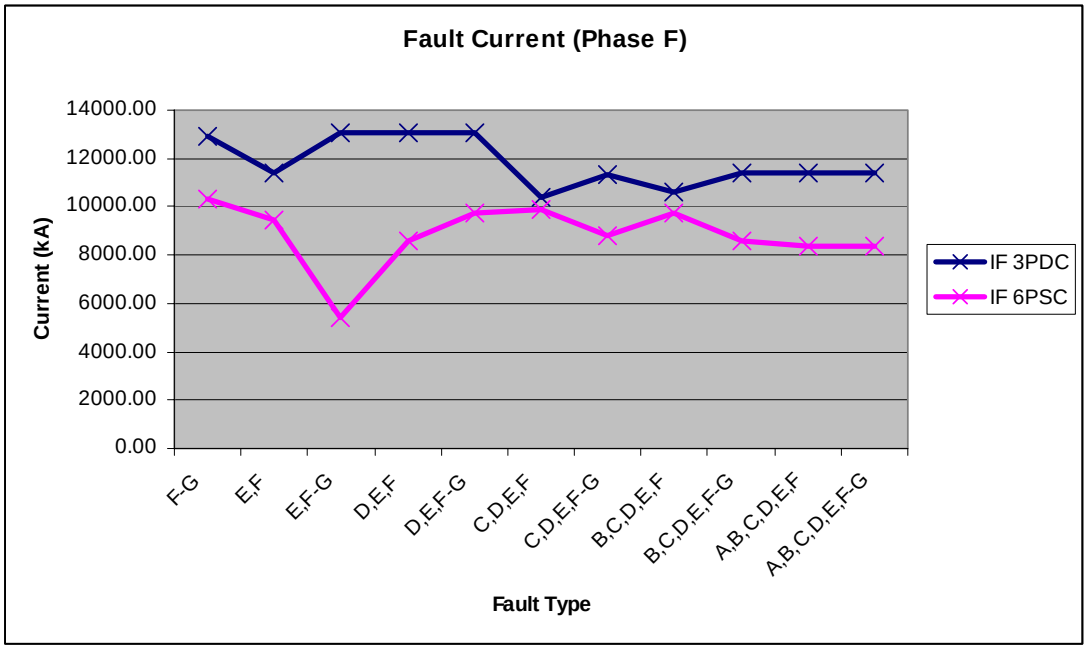

Figure 6.31: Comparison of fault current flowing in phase *F* for 3PDC and 6PSC cases at line 1-5

Table 6.5: List of 3PSC fault currents for various types of fault at mid-point of the transmission line 1-5

Fault Type	Fault Currents (Amps)					
	Ia	*Ib*	*Ic*	*Id*	*Ie*	*If*
1-phase-to-ground *f*	0.00	0.00	0.00	0.00	0.00	12940.90
2-phase *e,f*	0.00	0.00	0.00	0.00	11373.70	11373.70
2-phase-to-ground *e,f-g*	0.00	0.00	0.00	0.00	13022.20	13031.70
3-phase *d,e,f*	0.00	0.00	0.00	13003.40	13101.00	13049.00
3-phase-to-ground *d,e,f-g*	0.00	0.00	0.00	13003.50	13100.90	13049.10
4-phase *c,d,e,f*	0.00	0.00	9145.64	14466.20	14588.20	10415.64
4-phase-to-ground *c,d,e,f-g*	0.00	0.00	11358.40	13054.60	13109.70	11358.40
5-phase *b,c,d,e,f*	0.00	10647.10	10616.70	15125.30	10647.10	10616.70
5-phase-to-ground *b,c,d,e,f-g*	0.00	11402.40	11397.90	13052.20	11402.40	11397.90
6-phase *a,b,c,d,e,f*	11340.60	11425.70	11383.20	11340.60	11425.70	11383.20
6-phase-to-ground *a,b,c,d,e,f-g*	11340.60	11425.70	11383.20	11340.60	11425.70	11383.20

Table 6.6: List of 6PSC fault currents for various types of fault at mid-point of the transmission line 1-5

Fault Type	Fault Currents (Amps)					
	Ia	*Ib*	*Ic*	*Id*	*Ie*	*If*
1-phase-to-ground *f*	0.00	0.00	0.00	0.00	0.00	10296.80
2-phase *e,f*	0.00	0.00	0.00	0.00	9482.06	9482.06
2-phase-to-ground *e,f-g*	0.00	0.00	0.00	0.00	5429.99	5429.99
3-phase *d,e,f*	0.00	0.00	0.00	8671.16	3758.08	8606.29
3-phase-to-ground *d,e,f-g*	0.00	0.00	0.00	9685.13	9660.57	9733.01
4-phase *c,d,e,f*	0.00	0.00	9938.89	6288.61	6353.95	9854.88
4-phase-to-ground *c,d,e,f-g*	0.00	0.00	8784.41	9418.44	9449.84	8784.41
5-phase *b,c,d,e,f*	0.00	9749.07	7753.42	7488.82	7748.47	9757.39
5-phase-to-ground *b,c,d,e,f-g*	0.00	8544.29	8562.24	9167.61	8544.29	8562.24
6-phase *a,b,c,d,e,f*	8303.81	8283.53	8345.47	8303.81	8283.53	8345.47
6-phase-to-ground *a,b,c,d,e,f-g*	8303.81	8283.53	8345.47	8303.81	8283.53	8345.47

From the simulation results, we can conclude that the conversion of 3PDC transmission to 6PDC transmission reducing the magnitude of the fault current. From Table 6.5 and Table 6.6, it is found that for single-line-to-ground fault, the magnitude of the fault current is reducing by 20.4% while for the three-phase fault reduced up to 30%.

6.3.4 Test System IV

Line 1-3 of Test System IV has been chosen for the conversion. The fault analysis results of Test System IV are shown in Figure 6.32. Details data from fault analysis results for 3PDC and 6PSC transmission cases are tabulated in Table 6.7 and Table 6.8 respectively. Figure 6.32 shows the fault currents flowing in phase *F* for various types of fault on the line 1-3. From the graph, we can observe that the fault current flowing in phase *F* is much smaller when 6PSC transmission is used compare to the 3PDC transmission. This is due to existing of two pairs of phase conversion transformers at each ends of the transmission line for six-phase operation.

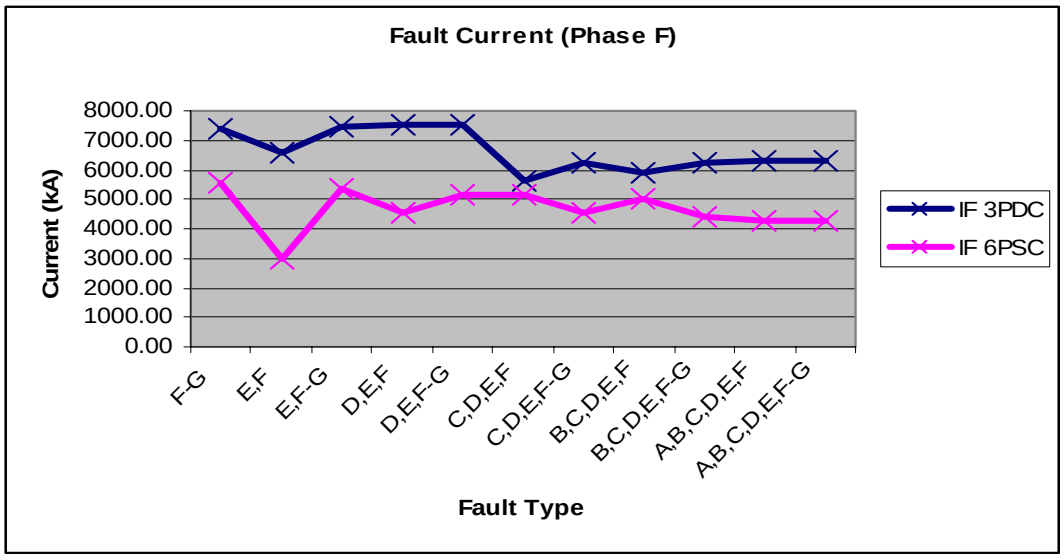

Figure 6.32: Comparison of fault current flowing in phase *F* for 3PDC and 6PSC cases at line 1-3

Table 6.7: List of 3PSC fault currents for various types of fault at mid-point of the transmission line 1-3

Fault Type	Fault Currents (Amps)					
	Ia	*Ib*	*Ic*	*Id*	*Ie*	*If*
1-phase-to-ground *f*	0.00	0.00	0.00	0.00	0.00	7361.09
2-phase *e,f*	0.00	0.00	0.00	0.00	6545.63	6545.63
2-phase-to-ground *e,f-g*	0.00	0.00	0.00	0.00	7454.19	7461.72
3-phase *d,e,f*	0.00	0.00	0.00	7485.72	7541.68	7509.35
3-phase-to-ground *d,e,f-g*	0.00	0.00	0.00	7485.72	7541.68	7509.35
4-phase *c,d,e,f*	0.00	0.00	5143.18	8259.15	8316.84	5143.18
4-phase-to-ground *c,d,e,f-g*	0.00	0.00	6222.23	7540.70	7572.15	6222.23
5-phase *b,c,d,e,f*	0.00	5894.79	5883.96	8627.24	5894.79	5883.96
5-phase-to-ground *b,c,d,e,f-g*	0.00	6271.78	6267.43	7563.95	6271.78	6267.43
6-phase *a,b,c,d,e,f*	6261.44	6308.37	6282.74	6261.44	6308.37	6282.74
6-phase-to-ground *a,b,c,d,e,f-g*	6261.44	6308.37	6282.74	6261.44	6308.37	6282.74

Table 6.8: List of 6PSC fault currents for various types of fault at mid-point of the transmission line 1-3

Fault Type	Fault Currents (Amps)					
	Ia	*Ib*	*Ic*	*Id*	*Ie*	*If*
1-phase-to-ground *f*	0.00	0.00	0.00	0.00	0.00	5536.36
2-phase *e,f*	0.00	0.00	0.00	0.00	2969.92	2969.92
2-phase-to-ground *e,f-g*	0.00	0.00	0.00	0.00	5360.12	5343.14
3-phase *d,e,f*	0.00	0.00	0.00	4609.06	2081.78	4563.21
3-phase-to-ground *d,e,f-g*	0.00	0.00	0.00	5130.38	5117.04	5155.43
4-phase *c,d,e,f*	0.00	0.00	5199.13	3324.93	3374.85	5134.11
4-phase-to-ground *c,d,e,f-g*	0.00	0.00	4537.71	4958.64	4983.70	4537.71
5-phase *b,c,d,e,f*	0.00	5053.01	3974.99	3935.86	3978.69	5045.77
5-phase-to-ground *b,c,d,e,f-g*	0.00	4400.44	4402.39	4793.83	4400.44	4402.39
6-phase *a,b,c,d,e,f*	4247.88	4237.18	4268.89	4247.88	4237.18	4268.89
6-phase-to-ground *a,b,c,d,e,f-g*	4247.88	4237.18	4268.89	4247.88	4237.18	4268.89

From the simulation results, we can conclude that the conversion of 3PDC transmission to 6PSC transmission will reduce the magnitude of the fault current. From Table 6.7 and Table 6.8, it is found that for single-line-to-ground fault, the magnitude of the fault current is reducing by 24.8% while for the three-phase fault reduced up to 39.2%.

6.3.5 19-Bus TNB Kelantan System

Line 3-7 of 19-Bus TNB Kelantan System has been chosen for the conversion. The fault analysis results for19-Bus TNB Kelantan System are shown in Figure 6.33. Details data from fault analysis results for 3PDC and 6PSC transmission cases are tabulated in Table 6.9 and Table 6.10 respectively. Figure 6.33 shows the fault currents flowing in phase *F* for various types of fault on the line 3-7. From the graph, we can observe that the fault current flowing in phase *F* is smaller when 6PSC transmission is used compare to the 3PDC transmission. This is due to existing of two pairs of phase conversion transformers at each ends of the transmission line for six-phase operation.

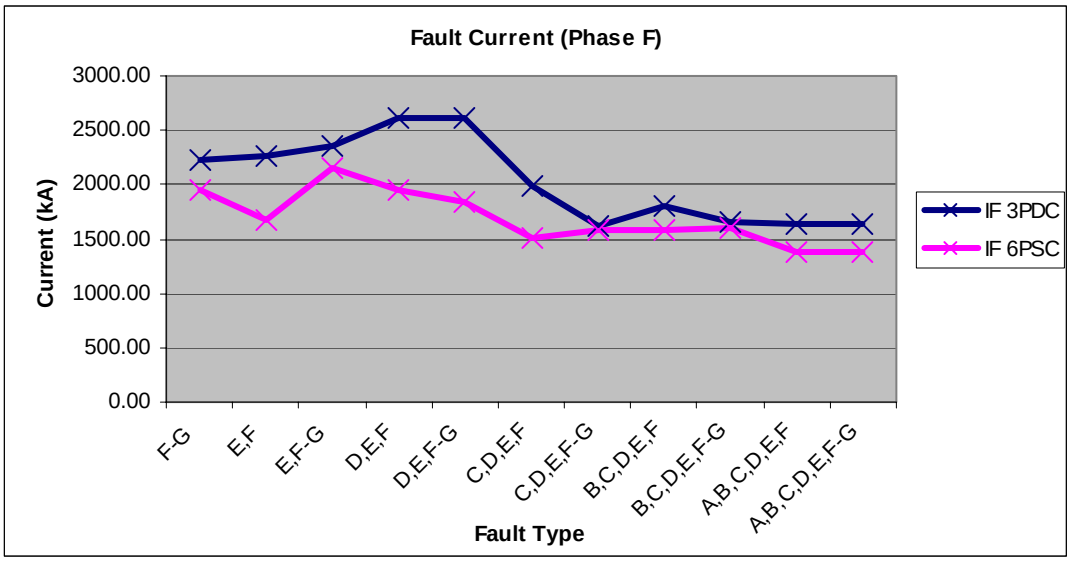

Figure 6.33: Comparison of fault current flowing in phase *F* for 3PDC and 6PSC cases at line 3-7

Table 6.9: List of 3PSC fault currents for various types of fault at mid-point of the transmission line 3-7

Fault Type	Fault Currents (Amps)					
	Ia	*Ib*	*Ic*	*Id*	*Ie*	*If*
1-phase-to-ground *f*	0.00	0.00	0.00	0.00	0.00	2227.37
2-phase *e,f*	0.00	0.00	0.00	0.00	2259.95	2259.95
2-phase-to-ground *e,f-g*	0.00	0.00	0.00	0.00	2417.56	2356.27
3-phase *d,e,f*	0.00	0.00	0.00	2592.21	2593.60	2617.25
3-phase-to-ground *d,e,f-g*	0.00	0.00	0.00	2592.21	2593.60	2617.25
4-phase *c,d,e,f*	0.00	0.00	1514.90	2704.82	2700.93	1995.11
4-phase-to-ground *c,d,e,f-g*	0.00	0.00	1575.89	2644.98	2654.41	1613.90
5-phase *b,c,d,e,f*	0.00	1573.15	1589.39	2781.56	1573.15	1797.97
5-phase-to-ground *b,c,d,e,f-g*	0.00	1601.15	1610.13	2696.10	1601.15	1656.35
6-phase *a,b,c,d,e,f*	1628.71	1629.71	1644.51	1628.71	1629.71	1644.51
6-phase-to-ground *a,b,c,d,e,f-g*	1628.71	1629.71	1644.51	1628.71	1629.71	1644.51

Table 6.10: List of 6PSC fault currents for various types of fault at mid-point of the transmission line 3-7

Fault Type	Fault Currents (Amps)					
	Ia	*Ib*	*Ic*	*Id*	*Ie*	*If*
1-phase-to-ground *f*	0.00	0.00	0.00	0.00	0.00	1949.50
2-phase *e,f*	0.00	0.00	0.00	0.00	1669.56	1669.56
2-phase-to-ground *e,f-g*	0.00	0.00	0.00	0.00	2266.79	2146.58
3-phase *d,e,f*	0.00	0.00	0.00	1993.72	1388.25	1950.47
3-phase-to-ground *d,e,f-g*	0.00	0.00	0.00	1980.11	1892.69	1838.51
4-phase *c,d,e,f*	0.00	0.00	2047.88	1475.58	1511.41	1514.90
4-phase-to-ground *c,d,e,f-g*	0.00	0.00	1764.08	1750.97	1754.56	1575.89
5-phase *b,c,d,e,f*	0.00	1809.69	1332.52	1533.07	1339.49	1589.39
5-phase-to-ground *b,c,d,e,f-g*	0.00	1698.92	1406.71	1638.12	1385.57	1610.13
6-phase *a,b,c,d,e,f*	1375.28	1388.49	1388.02	1375.28	1388.49	1388.02
6-phase-to-ground *a,b,c,d,e,f-g*	1375.28	1388.49	1388.02	1375.28	1388.49	1388.02

From the simulation results, we can conclude that the conversion of 3PDC transmission to 6PSC transmission will reduce the magnitude of the fault current. From Table 6.9 and Table 6.10, it is found that for single-line-to-ground fault, the magnitude of the fault current is reducing by 12.5% while for the three-phase fault reduced up to 29.8%.

6.4 Results of Transient Stability Analysis

The transient stability analysis has been conducted to the test systems for both cases of 3PDC and 6PSC transmission line. In all the studies cases, the power systems were assumed to be balanced. Transient stability analysis has been performed to all test system recommended. Figure 6.34 illustrates the rotor angle swing for the stable condition. The rotor angle will swing when a fault is applied to the test system and after fault is cleared, it will decrease to the original stable region. It can be seen that the rotor angle decreased to the stable point because the duration of fault which applied to the circuit is less than the critical clearing time for that system. Figure 6.35 illustrates the rotor angle swing for unstable condition. As can be seen from Figure 6.35, the rotor angle swing curve start to oscillate just after fault is cleared because the duration of fault which applied to the circuit exceeded the critical clearing time for that system. If fault is clear after the critical clearing time, the system still becomes unstable. If the critical clearing time is exceeded, the system will become unstable although fault or disturbance is isolated from the circuit.

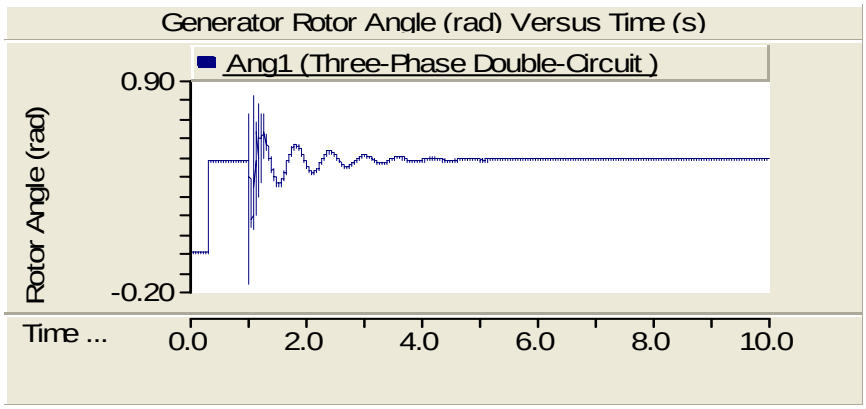

Figure 6.34: Rotor angle swing curve for stable condition

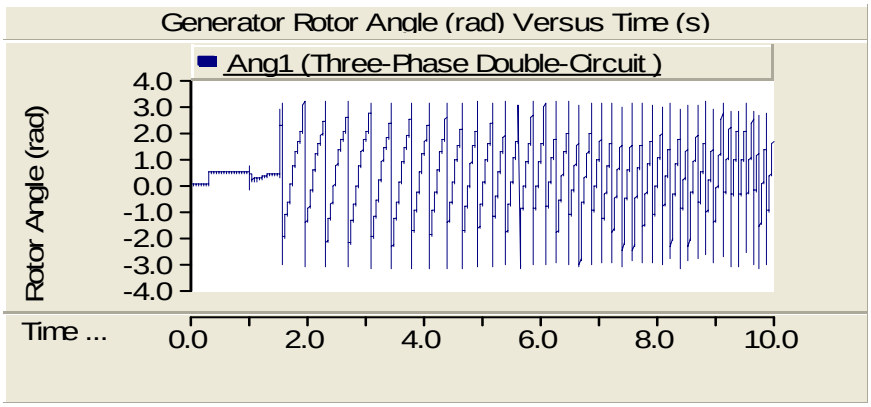

Figure 6.35: Rotor angle swing curve for unstable condition

6.4.1 Test System I

Transient stability analysis has been performed to Test System I in sufficient detail. The purpose of this analysis is to analyse the system stability with the present of the six-phase transmission line. This is done by investigate the critical clearing times for both case of test system with 3PDC and 6PSC respecting to all types of fault.

Figure 6.36 and Figure 6.37 shows the comparisons between swing curve and real power generation from generator unit on bus 4. Both figures are referred to three-phase and six-phase operation of Test System I. As may be seen, the six-phase configurations limited the first swing and damped oscillations for faults on the converted line. Meanwhile, the real power generated also swing following the swing shape of the rotor angle. This is due to additional impedance of the phase conversion transformers on the terminal ends of the six-phase line. Hence, system stability limits is increased with the present of six-phase transmission at line 3-4.

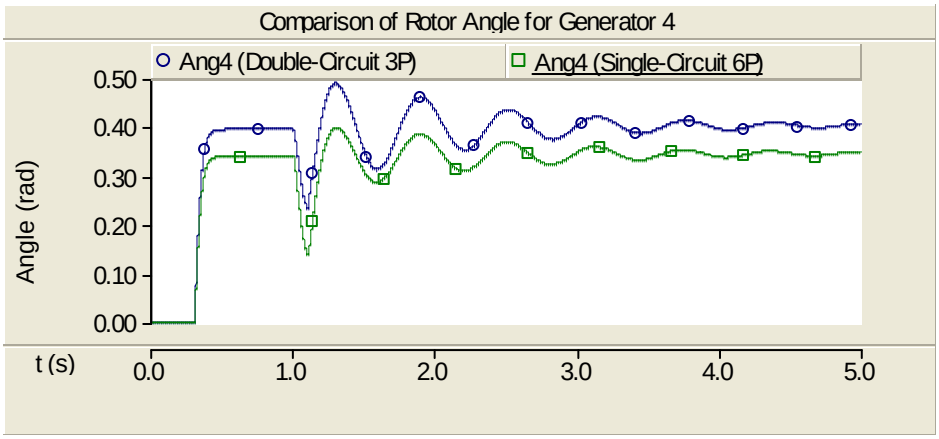

Figure 6.36: Rotor angle swing curve of generator at bus-4

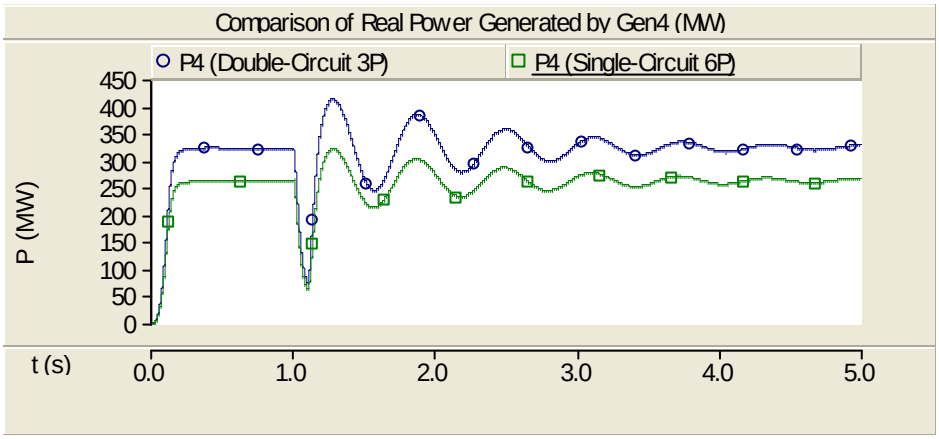

Figure 6.37: Real power generation from generator at bus-4

Table 6.11 and Table 6.12 are the illustrations of all cases considered in this studies and set into tables for comparisons. Critical clearing times for the test system with 3PDC line are tabulated in Table 6.11 while Table 6.12 is critical clearing times for the test system with 6PSC line. As can seen from both of the Tables, the critical clearing times for fault involved six-lines is less compare to the value of critical clearing times for other types of fault. This shows that the six-line-to-ground or six-

line fault is the most severe than other types of fault and this is true for both 3PDC and 6PSC cases. Less value of critical clearing time means that the test system should isolate the fault more quickly compare to the case with higher value of critical clearing times.

Based on Table 6.11 and Table 6.12, the overall critical clearing times for the test system with six-phase converted transmission line is longer compare to the test system with 3PDC transmission lines. For the most severe fault (i.e. six-line-to-ground fault) at the mid point of transmission line, the critical clearing time is increased about 1.4% from 0.4523s to 0.4663s when 3PDC is converted to 6PSC operation. The percentage increase of the critical clearing times is around 1.4% to 49.3% for the test system with six-phase converted transmission line. The most increased in critical clearing time is for four-line fault type. The overall stability performances of Test System I with 6PSC are much better than the 3PDC as it takes a longer time before instability occurs. This means that with 6PSC transmission cause increase in system stability.

Table 6.11: The critical clearing times for the Test System I with 3PDC line

Types of faults	Faulted phases	Critical Clearing Time (s)
1-phase-to-ground (L-G)	a-G	Inherently stable
2-phase (L-L)	a-b	Inherently stable
2-phase-to-ground (L-L-G)	a-b-G	Inherently stable
3-phase (L-L-L)	a-b-c	1.1600
3-phase-to-ground (L-L-L-G)	a-b-c-G	1.1600
4-phase (L-L-L-L)	a-b-c-a'	0.9665
4-phase-to-ground (L-L-L-L-G)	a-b-c-a'-G	0.9665
5-phase (L-L-L-L-L)	a-b-c-a'-b'	0.8685
5-phase-to-ground (L-L-L-L-L-G)	a-b-c-a'-b'-G	0.8660
6-phase (L-L-L-L-L-L)	a-b-c-a'-b'-c'	0.4523
6-phase-to-ground (L-L-L-L-L-L-G)	a-b-c-a'-b'-c'-G	0.4523

Table 6.12: The critical clearing times for the Test System I with 6PSC line

Types of faults	Faulted phases	Critical Clearing Time (s)
1-phase-to-ground (L-G)	a-G	Inherently stable
2-phase (L-L)	a-b	Inherently stable
	a-c	Inherently stable
	a-d	Inherently stable
2-phase-to-ground (L-L-G)	a-b-G	Inherently stable
	a-c-G	Inherently stable
	a-d-G	Inherently stable
3-phase (L-L-L)	a-b-c	Inherently stable
	a-b-d	Inherently stable
	a-c-e	1.3503
3-phase-to-ground (L-L-L-G)	a-b-c-G	1.3478
	a-b-d-G	Inherently stable
	a-c-e-G	1.3478
4-phase (L-L-L-L)	a-b-c-d	1.4595
	a-b-c-e	0.9743
	a-b-d-e	1.0490
4-phase-to-ground (L-L-L-L-G)	a-b-c-d-G	0.9560
	a-b-c-e-G	0.9558
	a-b-d-e-G	1.0490
5-phase (L-L-L-L-L)	a-b-c-d-e	0.8985
5-phase-to-ground (L-L-L-L-L-G)	a-b-c-d-e-G	0.8830
6-phase (L-L-L-L-L-L)	a-b-c-d-e-f	0.4663
6-phase-to-ground (L-L-L-L-L-L-G)	a-b-c-d-e-f-G	0.4663

6.4.2 Test System II

Transient stability analysis has been performed to Test System II in sufficient detail. The purpose of this analysis is to analyse the system stability with the present of the six-phase transmission line. This is done by investigate the critical clearing times for both case of test system with 3PDC and 6PSC respecting to all types of fault.

Table 6.13 and Table 6.14 are the illustration of all cases considered for the Test System II and set into tables for comparisons. Critical clearing times for the test system with

3PDC line are tabulated in Table 6.13 while Table 6.14 is critical clearing times for the test system with 6PSC line. As can seen from both of the Tables, the critical clearing times for fault involved six-lines is less compare to the value of critical clearing times for other types of fault. This shows that the six-line-to-ground or six-line fault is the most severe than other types of fault and this is true for both 3PDC and 6PSC cases.

Refers to Table 6.13 and Table 6.14, the overall critical clearing times for the test system with six-phase converted transmission line is longer compare to the test system with 3PDC transmission lines. For the most severe fault (i.e. six-line-to-ground fault) on the middle of transmission line, the critical clearing time is increased 48.5% when 3PDC is converted to 6PSC operation. The percentage increase of the critical clearing times is around 48.5% to 73.4% for the test system with six-phase converted transmission line. The most increased in critical clearing time is for four-line fault type. The overall stability performances of Test System II with 6PSC are much better than the 3PDC as it takes a longer time before instability occur. This means that with 6PSC transmission cause increase in the system stability

Table 6.13: The critical clearing times for the Test System II with 3PDC line

Types of faults	Faulted phases	Critical Clearing Time (s)
1-phase-to-ground (L-G)	a-G	Inherently stable
2-phase (L-L)	a-b	Inherently stable
2-phase-to-ground (L-L-G)	a-b-G	Inherently stable
3-phase (L-L-L)	a-b-c	0.8919
3-phase-to-ground (L-L-L-G)	a-b-c-G	0.8919
4-phase (L-L-L-L)	a-b-c-a'	0.6480
4-phase-to-ground (L-L-L-L-G)	a-b-c-a'-G	0.6480
5-phase (L-L-L-L-L)	a-b-c-a'-b'	0.5885
5-phase-to-ground (L-L-L-L-L-G)	a-b-c-a'-b'-G	0.5881
6-phase (L-L-L-L-L-L)	a-b-c-a'-b'-c'	0.5360
6-phase-to-ground (L-L-L-L-L-L-G)	a-b-c-a'-b'-c'-G	0.5360

Table 6.14: The critical clearing times for the Test System II with 6PSC line

Types of faults	Faulted phases	Critical Clearing Time (s)
1-phase-to-ground (L-G)	a-G	Inherently stable
2-phase (L-L)	a-b	Inherently stable
	a-c	Inherently stable
	a-d	Inherently stable
2-phase-to-ground (L-L-G)	a-b-G	Inherently stable
	a-c-G	Inherently stable
	a-d-G	Inherently stable
3-phase (L-L-L)	a-b-c	Inherently stable
	a-b-d	Inherently stable
	a-c-e	1.3912
3-phase-to-ground (L-L-L-G)	a-b-c-G	1.3906
	a-b-d-G	1.3809
	a-c-e-G	1.3906
4-phase (L-L-L-L)	a-b-c-d	1.3823
	a-b-c-e	1.1753
	a-b-d-e	1.2136
4-phase-to-ground (L-L-L-L-G)	a-b-c-d-G	1.1329
	a-b-c-e-G	1.1325
	a-b-d-e-G	1.2136
5-phase (L-L-L-L-L)	a-b-c-d-e	1.0996
5-phase-to-ground (L-L-L-L-L-G)	a-b-c-d-e-G	1.0992
6-phase (L-L-L-L-L-L)	a-b-c-d-e-f	1.0788
6-phase-to-ground (L-L-L-L-L-L-G)	a-b-c-d-e-f-G	1.0788

6.4.3 Test System III

Transient stability analysis has been performed to Test System III in sufficient detail. The purpose of this analysis is to analyse the system stability with the present of the six-phase transmission line. This is done by investigate the critical clearing times for both case of test system with 3PDC and 6PSC respecting to all types of fault.

Table 6.15 and Table 6.16 are illustrations of all cases considered for the Test System III and set into tables for comparisons. Critical clearing times for the test system with 3PDC line are tabulated in Table 6.15 while Table 6.16 is critical clearing times for the test system with 6PSC line. As can seen from both of the Tables, the critical clearing times for fault involved six-lines is less compare to the value of critical clearing times for other types of fault. This shows that the six-line-to-ground or six-line fault is the most severe than other types of fault and this is true for both 3PDC and 6PSC cases.

Refers to Table 6.15 and Table 6.16, the overall critical clearing times for the test system with six-phase converted transmission line is longer compare to the test system with 3PDC transmission lines. For the most severe fault (i.e. six-line-to-ground fault) on the middle of transmission line, the critical clearing time is increased 44% when 3PDC is converted to 6PSC operation. The percentage increase of the critical clearing times is around 30.9% to 61.2% for the test system with six-phase converted transmission line. The most increased in critical clearing time is for four-line fault type. The overall stability performances of Test System III with 6PSC are mush better than the 3PDC as it takes a longer time before instability occurs. This means that with 6PSC transmission cause increase in the system stability

Table 6.15: The critical clearing times for the Test System III with 3PDC line

Types of faults	Faulted phases	Critical Clearing Time (s)
1-phase-to-ground (L-G)	a-G	Inherently stable
2-phase (L-L)	a-b	Inherently stable
2-phase-to-ground (L-L-G)	a-b-G	Inherently stable
3-phase (L-L-L)	a-b-c	1.1074
3-phase-to-ground (L-L-L-G)	a-b-c-G	1.1074
4-phase (L-L-L-L)	a-b-c-a'	0.8046
4-phase-to-ground (L-L-L-L-G)	a-b-c-a'-G	0.8046
5-phase (L-L-L-L-L)	a-b-c-a'-b'	0.7306
5-phase-to-ground (L-L-L-L-L-G)	a-b-c-a'-b'-G	0.7302
6-phase (L-L-L-L-L-L)	a-b-c-a'-b'-c'	0.6655
6-phase-to-ground (L-L-L-L-L-L-G)	a-b-c-a'-b'-c'-G	0.6655

Table 6.16: The critical clearing times for the Test System III with 6PSC line

Types of faults	Faulted phases	Critical Clearing Time (s)
1-phase-to-ground (L-G)	a-G	Inherently stable
2-phase (L-L)	a-b	Inherently stable
	a-c	Inherently stable
	a-d	Inherently stable
2-phase-to-ground (L-L-G)	a-b-G	Inherently stable
	a-c-G	Inherently stable
	a-d-G	Inherently stable
3-phase (L-L-L)	a-b-c	Inherently stable
	a-b-d	Inherently stable
	a-c-e	1.4258
3-phase-to-ground (L-L-L-G)	a-b-c-G	1.4252
	a-b-d-G	1.4152
	a-c-e-G	1.4252
4-phase (L-L-L-L)	a-b-c-d	1.4166
	a-b-c-e	1.2045
	a-b-d-e	1.2438
4-phase-to-ground (L-L-L-L-G)	a-b-c-d-G	1.1611
	a-b-c-e-G	1.1606
	a-b-d-e-G	1.2438
5-phase (L-L-L-L-L)	a-b-c-d-e	1.1269
5-phase-to-ground (L-L-L-L-L-G)	a-b-c-d-e-G	1.1265
6-phase (L-L-L-L-L-L)	1	1.1056
6-phase-to-ground (L-L-L-L-L-L-G)	a-b-c-d-e-f-G	1.1056

6.4.4 Test System IV

Transient stability analysis has been performed to Test System IV in sufficient detail. The purpose of this analysis is to analyse the system stability with the present of the six-phase transmission line. This is done by investigate the critical clearing times for both case of test system with 3PDC and 6PSC respecting to all types of fault.

Table 6.17 and Table 6.18 are illustrations of all cases considered for the Test System IV and set into tables for comparisons. Critical clearing times for the test system

with 3PDC line are tabulated in Table 6.17 while Table 6.18 is critical clearing times for the test system with 6PSC line. As can seen from both of the Tables, the critical clearing times for fault involved six-lines is less compare to the value of critical clearing times for other types of fault. This shows that the six-line-to-ground or six-line fault is the most severe than other types of fault and this is true for both 3PDC and 6PSC cases.

Based on Table 6.17 and Table 6.18, the overall critical clearing times for the test system with six-phase converted transmission line is longer compare to the test system with 3PDC transmission lines. For the most severe fault (i.e. six-line-to-ground fault) on the middle of transmission line, the critical clearing time is increased 56.8% when 3PDC is converted to 6PSC operation. The percentage increase of the critical clearing times is around 49.8% to 77.2% for the test system with six-phase converted transmission line. The most increased in critical clearing time is for four-line fault type. The overall stability performances of Test System IV with 6PSC are much better than the 3PDC as it takes a longer time before instability occurs. This means that with 6PSC transmission cause increase in the system stability.

Table 6.17: The critical clearing times for the Test System IV with 3PDC line

Types of faults	Faulted phases	Critical Clearing Time (s)
1-phase-to-ground (L-G)	a-G	Inherently stable
2-phase (L-L)	a-b	Inherently stable
2-phase-to-ground (L-L-G)	a-b-G	Inherently stable
3-phase (L-L-L)	a-b-c	1.0310
3-phase-to-ground (L-L-L-G)	a-b-c-G	1.0310
4-phase (L-L-L-L)	a-b-c-a'	0.7491
4-phase-to-ground (L-L-L-L-G)	a-b-c-a'-G	0.7491
5-phase (L-L-L-L-L)	a-b-c-a'-b'	0.6802
5-phase-to-ground (L-L-L-L-L-G)	a-b-c-a'-b'-G	0.6799
6-phase (L-L-L-L-L-L)	a-b-c-a'-b'-c'	0.6224
6-phase-to-ground (L-L-L-L-L-L-G)	a-b-c-a'-b'-c'-G	0.6196

Table 6.18: The critical clearing times for the Test System IV with 6PSC line

Types of faults	Faulted phases	Critical Clearing Time (s)
1-phase-to-ground (L-G)	a-G	Inherently stable
2-phase (L-L)	a-b	Inherently stable
	a-c	Inherently stable
	a-d	Inherently stable
2-phase-to-ground (L-L-G)	a-b-G	Inherently stable
	a-c-G	Inherently stable
	a-d-G	Inherently stable
3-phase (L-L-L)	a-b-c	Inherently stable
	a-b-d	Inherently stable
	a-c-e	1.5310
3-phase-to-ground (L-L-L-G)	a-b-c-G	1.5303
	a-b-d-G	1.5196
	a-c-e-G	1.5303
4-phase (L-L-L-L)	a-b-c-d	1.5212
	a-b-c-e	1.2934
	a-b-d-e	1.3356
4-phase-to-ground (L-L-L-L-G)	a-b-c-d-G	1.2468
	a-b-c-e-G	1.2463
	a-b-d-e-G	1.3356
5-phase (L-L-L-L-L)	a-b-c-d-e	1.2101
5-phase-to-ground (L-L-L-L-L-G)	a-b-c-d-e-G	1.2097
6-phase (L-L-L-L-L-L)	a-b-c-d-e-f	1.1875
6-phase-to-ground (L-L-L-L-L-L-G)	a-b-c-d-e-f-G	1.1872

6.4.5 19-Bus TNB Kelantan System

Transient stability analysis has been performed to 19-Bus TNB Kelantan System in sufficient detail. The purpose of this analysis is to analyse the system stability with the present of the six-phase transmission line. This is done by investigate the critical clearing times for both cases of test system with 3PDC and 6PSC respecting to all types of fault.

Table 6.19 and Table 6.20 are illustrations of all cases considered for the 19-Bus TNB Kelantan System and set into tables for comparisons. Critical clearing times for the

test system with 3PDC line are tabulated in Table 6.19 while Table 6.20 is critical clearing times for the test system with 6PSC line. As can seen from both of the Tables, the critical clearing times for fault involved six-lines is less compare to the value of critical clearing times for other types of fault. This shows that the six-line-to-ground or six-line fault is the most severe than other types of fault and this is true for both 3PDC and 6PSC cases.

Based on Table 6.19 and Table 6.20, the overall critical clearing times for the test system with six-phase converted transmission line is longer compare to the test system with 3PDC transmission lines. For the most severe fault (i.e. six-line-to-ground fault) on the middle of transmission line, the critical clearing time is increased 49.2% when 3PDC is converted to 6PSC operation. The percentage increase of the critical clearing times is around 37.5% to 68.1% for the test system with six-phase converted transmission line. The most increased in critical clearing time is for four-line fault type. The overall stability performances of 19-Bus TNB Kelantan System with 6PSC are much better than the 3PDC as it takes a longer time before instability occurs. This means that with 6PSC transmission cause increase in the system stability.

Table 6.19: The critical clearing times for the 19-Bus TNB Kelantan System with 3PDC line

Types of faults	Faulted phases	Critical Clearing Time (s)
1-phase-to-ground (L-G)	a-G	Inherently stable
2-phase (L-L)	a-b	Inherently stable
2-phase-to-ground (L-L-G)	a-b-G	Inherently stable
3-phase (L-L-L)	a-b-c	1.1520
3-phase-to-ground (L-L-L-G)	a-b-c-G	1.1520
4-phase (L-L-L-L)	a-b-c-a'	0.8370
4-phase-to-ground (L-L-L-L-G)	a-b-c-a'-G	0.8370
5-phase (L-L-L-L-L)	a-b-c-a'-b'	0.7600
5-phase-to-ground (L-L-L-L-L-G)	a-b-c-a'-b'-G	0.7596
6-phase (L-L-L-L-L-L)	a-b-c-a'-b'-c'	0.6925
6-phase-to-ground (L-L-L-L-L-L-G)	a-b-c-a'-b'-c'-G	0.6923

Table 6.20: The critical clearing times for the 19-Bus TNB Kelantan System with 6PSC line

Types of faults	Faulted phases	Critical Clearing Time (s)
1-phase-to-ground (L-G)	a-G	Inherently stable
2-phase (L-L)	a-b	Inherently stable
	a-c	Inherently stable
	a-d	Inherently stable
2-phase-to-ground (L-L-G)	a-b-G	Inherently stable
	a-c-G	Inherently stable
	a-d-G	Inherently stable
3-phase (L-L-L)	a-b-c	Inherently stable
	a-b-d	Inherently stable
	a-c-e	1.5278
3-phase-to-ground (L-L-L-G)	a-b-c-G	1.5271
	a-b-d-G	1.5164
	a-c-e-G	1.5271
4-phase (L-L-L-L)	a-b-c-d	1.5180
	a-b-c-e	1.2906
	a-b-d-e	1.3327
4-phase-to-ground (L-L-L-L-G)	a-b-c-d-G	1.2442
	a-b-c-e-G	1.2436
	a-b-d-e-G	1.3327
5-phase (L-L-L-L-L)	a-b-c-d-e	1.2075
5-phase-to-ground (L-L-L-L-L-G)	a-b-c-d-e-G	1.2071
6-phase (L-L-L-L-L-L)	a-b-c-d-e-f	1.1849
6-phase-to-ground (L-L-L-L-L-L-G)	a-b-c-d-e-f-G	1.1847

6.5 Summary

This chapter investigates the steady state and transient stability of three-to six-phase conversion of selected transmission line for all test systems including IEEE Test Systems and 19-Bus TNB Kelantan System. The investigation is conducted by analyse the load flow and the voltage level considering three to six-phase conversions of selected transmission lines. From power flow solutions, the most suitable location to fix a six-phase transmission system is determined. By applying six-phase transmission on the selected transmission line, fault analysis and transient stability analysis have been conducted. From the analyses of the simulation results,

we can see that the fault currents flowing in faulted phases for test systems with six-phase transmission is less than the fault current flowing for same type of fault while 3PDC is used. From transient stability analysis, we can conclude that the system stability of the test systems with 6PSC transmission is more stable comparing to the test systems with 3PDC transmission.

CHAPTER VII

CONCLUSIONS AND SUGGESTIONS

7.1 Conclusions

This research is conducted to investigate the feasibility to implement the six-phase single-circuit transmission into the three-phase double-circuit transmission system. From the literature reviews, it is shows that the six-phase single-circuit transmission system is a viable alternative to be implemented in a three-phase power system since they can be tapped to the three-phase connections. For the purpose of comparisons, the advantages and disadvantages of six-phase transmission over three-phase double-circuit transmission will be discussed here. The six-phase transmission has the following advantages over existing three-phase double-circuit transmission system:

i. There is smaller voltage between adjacent phases, which means that for six-phase systems, say 132 kV phase-to-neutral voltage corresponds to 132 kV between adjacent phases, compared to (132 kV x $\sqrt{3}$) between phases for three-phase systems.

ii. Due to (1) above, it becomes much easier to insulate one phase from another, spacing between phases are reduced, and conductor surface gradients are less, resulting in lower noise levels.

iii. Since in six-phase systems phase-to-neutral voltages are equal to phase-to-phase voltages on adjacent phases, there is a possible of at least up to 173% in the power transmission capability when a three phase double-circuit line is converted to six-phase with existing conductor thermal limits.

iv. Consequently, the rights-of-way are better utilized if existing three-phase double-circuit line are converted into six-phase since the phase-to-phase voltages between adjacent phases remain the same as those of three-phase, and hence the same transmission towers can be used for six-phase lines. Thus, the electrical rights-of-way are utilized more effectively and efficiently, giving potentially better public acceptance.

v. The noise levels and radio interference levels are lower in a six-phase transmission system.

vi. The static stability characteristics of the lines are improved in a six-phase system.

The six-phase transmission system has the following disadvantages over the existing three-phase system.

i. It may be noted that multiphase transmission system, if ever realize, will always be integrated in an otherwise three-phase system. Substation and tap-point equipment changes should be made by using three-phase/multiphase transformer to connect a six-phase system to the existing three-phase network at all levels, which will create problems regarding coordination with existing three-phase lines and systems.

ii. Lack of experience in operating and maintaining a six-phase system. Since the six-phase transmission is a new idea and no other countries in this world use it as a commercial transmission system, it seems to have difficulties in implementation such new idea.

iii. Higher ground gradients and some possible reliability penalties. It is known that the maximum surface electric field decreases with phase order, whereas the maximum ground electric field increases with phase order. Also, the addition of shield wires increases the surface field on the conductors and reduces the ground-level field. Thus, the electric field for one conductor opens and unfaulted (single-pole switching) shows small variation as compared with the same conductor open and grounded.

iv. The protection scheme for a six-phase transmission system is much more complicated than for a three-phase system. The complexity of the protection system of a six-phase line compared to the protection system of a conventional three-phase system results from the increase in the number of possible fault combination. Considering short circuit faults with all six phases in service and no open circuit faults, the total number of fault combinations for the six-phase line is 120. The total number of possible faults in three-phase system is 11.

A thorough analysis of the digital load flow, short circuit, and transient stability cases of the test systems including IEEE Test Systems and the 19-Bus TNB Kelantan System is investigated in time domain considering conversion of three-phase double-circuit to six-phase single circuit transmission system by using PSCAD/EMTDC. The test systems are successfully modeled into PSCAD/EMTDC simulation package for the load flow, short circuit and transient stability analysis studies. The modeling procedure has employed some useful functional block models that are available in the PSCAD/EMTDC program such as the generator, exciter, three-phase two windings transformer, etc.

The studies was performed in sufficient detail to determine how the six-phase conversion will affect steady state operation, fault current duties, and system stability. From the power flow analysis that have been conducted to all test systems including IEEE Test Systems and 19-Bus TNB Kelantan System, it is shows that the conversion of selected three-phase double-circuit transmission line into six-phase single-circuit one has not much affected to the real and reactive power flows and voltage levels of that test systems. Considering the test systems have the same loads level as three-phase double-circuit transmission, the flows of real and reactive powers will varies around ± 10% when the line is converted to the six-phase operation. The real and reactive powers will flows to other path depends on the transmission line impedance and also voltage levels. This is due to the additional three-to-six-phase conversion transformer at both transmission line ends. The voltage levels at every busbars only has a very small changes less than ± 1% and can be said that does not affected by this conversion and it is kept in the acceptable limits.

Fault analysis then conducted to the test systems to measure maximum currents flow in the faulted phases. All possible types of fault on the mid point of transmission lines have been applied to all test systems considering both cases of three-phase double-circuit and also six-phase single-circuit transmission system. From the results, it is shows that the fault currents flowing in the faulted phase are reduced to the smaller values when the conversion is applied to the test systems. This is due to the additional impedance of two conversion transformers that has been added to the test systems. A minor decrease about 6.12% is noticed for single line-to-ground fault, while a significant decrease around 50% is experienced for three-phase fault on six-phase transmission lines.

Final stage of analysis is the transient stability analysis has been conducted to test systems. The investigation is done by monitoring system stability of all the test systems. All possible types of grounded and ungrounded faults on the mid point of transmission lines have been applied to all test systems and critical clearing times is estimated for comparison. From the simulation results and the comparisons made, it

is shown that the power system with six-phase single-circuit transmission have a better stability limits compare to the three-phase double-circuit transmission. The overall critical clearing times for six-phase converted transmission line is more longer compare to the transmission system with three-phase double-circuit. For the most severe fault (i.e. six-line-to-ground fault) on the mid point of transmission line, the critical clearing time is increased around 3.1% to 4.8% when three-phase double-circuit is converted to six-phase operation. The percentage increase of the critical clearing times is around 3.1% to 16.16% for the systems with six-phase converted transmission line. The most severe increased in critical clearing time is for three-line-to-ground fault. The least and most reduction is occurred when single-line-to-ground fault and six-line-to-ground fault respectively.

The overall stability performances with six-phase transmission are better than the systems with three-phase double-circuit transmission because it takes a longer time before instability results, which means six-phase single-circuit transmission will increase the stability of power system.

7.2 Suggestions

Designing a power system is indeed a thorough and tedious process. Just understanding a few parts of the power system does not guaranteed a successful design of a power system. To implement a six-phase transmission as an alternative to the three-phase double-circuit transmission still needs further works and research. Though there is much to be studied, the process is expected to be challenging. The future works is recommended as an extension of this research in the following areas:

i. Modeling and development of a three-to-six-phase conversion transformer instead of using the combinations of two identical Delta-Wye three-phase transformers. The disadvantage of using a pair of three-phase transformer is

the space occupied by these two transformers is much bigger comparing if only one three-to-six-phase conversion transformer is used. Due to this fact, studies must be conducted to investigate the feasibility to model a three-to-six-phase conversion transformer.

ii. The research are not studied the impacts of shunt and series compensation for the converted transmission line. A detailed study has to be done how the compensation schemes can be effectively combined with the six-phase transmission system.

iii. The analysis was only simulated and tested on a simple power networks. Further tests have to be carried out to study the impacts of the six-phase converted transmission line in a complex power system.

iv. The six-phase protection system is needed before the implementation of six-phase transmission line. Research works and analysis has to be conducted to build such protection system.

v. The laboratory prototype requires further improvements with completed set of the protection system. Thus, the contingencies analyses can be carried out to the laboratory prototype.

REFERENCES

[1] Barthold, L. D., and Barnes, H. C. (1972). High-Phase Order Transmission. *CIGRE Study Committee*. No. 31 Report. London.

[2] Fostescue, C. L. (1918). Method of Symmetrical Coordinates Applied to the Solution of Polyphase Networks. *AIEE Transactions*. Vol. 37. 1027-1140.

[3] Glover, J. D., and Sarma, M. S. (2002). *Power System Analysis and Design*. 3rd ed. USA: Brooks/Cole Thomson Learning Companies. 5-11.

[4] Clark, E. (1943). *Circuit Analysis of AC Power System*. Vol. I. John Wiley & Sons, Inc. New York. 286.

[5] Bhatt, N. B., Venkata, S. S., Guyker, W. C., and Booth, W. H. (1977). Six-Phase (Multi-Phase) Power Transmission Systems: Fault Analysis. *IEEE Transmissions on PA&S*, Vol. PAS-96, No. 3.

[6] Guyker, W. C., Booth, W. H., and Janson, M. A. (1978). Transmission System Feasibility. *American Power Conference Paper*. Chicago, Illionis.

[7] Guyker, W. C., Booth, W. H., Kontragunta, J. R., Stanek, E. K., and Venkata, S. S. (1979). Protection of 138 kV Six Phase Transmission Systems. *Proceedings of the Pennsylvania Electrical Association's (PEA) Electric Relay Committee Meeting in Tamiment, Pennsylvania*.

[8] (1984). Fault Protection for High Phase Order Transmission Lines. Volume 1: Basic Concept, Models and Computations. *EPRI Project 1764-5, EL-3316*. Volume 1.

[9] Dorazio, T. F. (1990). High Phase Order Transmission. *IEEE No. 90TH0313-7*. NYSEG. Binghamton, New York.

[10] Stewart, J. R., and Wilson, D. D. (1978). High Phase Order Transmission – A Feasibility Analysis: Part I – Steady State Considerations. *IEEE Transaction on Power Apparatus and System.* Vol. PAS-97, No. 6. 2300-2307.

[11] Stewart, J. R., and Wilson, D. D. (1978). High Phase Order Transmission – A Feasibility Analysis: Part II – Overvoltages and Insulation Requirements. *IEEE Transaction on Power Apparatus and System.* Vol. PAS-97, No. 6. 2308-2317.

[12] Brown, M. T., Rebbapragada, R. V., Dorazio, T. F., and Stewart, J. R. (1991). Utility System Demonstration of Six Phase Power Transmission. *Proceedings - IEEE Power Engineering Society, Transmission and Distribution Conference*. 983-989.

[13] Stewart, J. R., Oppel, L.J., Thomann, G. C., Dorazio, T. F., and Brown, M. T. (1992). Insulation Coordination, Environmental and System Analysis of Existing Double Circuit Line Reconfigured to Six-Phase Operation. *IEEE Transaction on Power Delivery.* Vol. 7, No. 3. 1628-1633.

[14] Stewart, J. R., Dale, S. J., and Klein, K. W. (1993). Magnetic Field Reduction Using High Phase Order Lines. *IEEE Transaction on Power Delivery.* Vol. 8, No. 2. 628-636.

[15] Apostolov, A. P., and Raffensperger, R. G. (1996). Relay Protection Operation for Fault on NYSEG's Six-Phase Transmission Line. *IEEE Transaction on Power Delivery.* Vol. 11, No. 1. 191-196.

[16] Stewart, J. R., Oppel, L.J., and Richeda, R. J. (1998). Corona and Field Effects Experience on an Operating Utility Six-Phase Transmission line. *IEEE Transaction on Power Delivery.* Vol. 13, No. 4. 1363-1369.

[17] Gole, A.M., Nayak, O.B., Sidhu, T.S., and Sachdev, M.S. (1996). A Graphical Electromagnetic Simulation Laboratory for Power Systems Engineering Programs. *IEEE Transactions on Power Systems.* Vol. 11, No. 2. 599-606.

[18] Venkata, S. S. (1977). Reliability and Economics Analysis of Higher Phase Order Electric Transmission System. *Final Report on Grant No. 74 ENGR 10400*.

[19] Nanda, S. P., Tiwari, S. N., and Singh, L. P. (1981). Fault Analysis of Six-Phase Systems. *Electrical Power Systems Research Journal*. No. 3, Vol. 4. 201.

[20] Venkata, S. S., Guyker, W. C., Kondragunta, J., Saini, N. K., and Stanek, E. K. (1982). 138 kV, Six-Phase Transmission System: Fault Analysis. *IEEE Transactions on Power Apparatus and Systems*. Vol. PAS-101, No. 5. 1203-1218.

[21] Badawy, E. H., El-Sherbiny, M. K., and Ibrahim, A. A. (1991). A Method of Analyzing Unsymmetrical Faults on Six-Phase Power Systems. *IEEE Transaction on Power Delivery*. Vol. 6, No.3. 1139-1145.

[22] Woodford, D. (2004). *Introduction to PSCAD V4.1*. Manitoba: Manitoba HVDC Research Centre Inc.

[23] Dorazio, T. F. and Stewart, J. R. (1992). System Parameters Are Analyzed for Six-Phase Configuration and Operation. *Transmission & Distribution*. *ABI/ANFORM Global*. Vol. 44, No.5. 24.

[24] Kundur, P. (2001). *Power System Stability and Control*. McGraw-Hill, Inc. New York

[25] Tahir, N. and Jais, O. (2000). *Mesin Elektrik*. Universiti teknologi Malaysia. 2-3.

[26] Morched, A.S. and Brandwajn, V. (1983). "Transmission Network Equivalents for Electromagnetic Transients Studies." *IEEE Transactions on Power Apparatus and Systems*. Vol. PAS-102, No. 9. 2984-2993.

[27] Zimmerman, R. D., Carlos, E. M., and Gan, D. (2004). *MATPOWER- A MATLAB™ Power System Simulation Package*. Power Systems Engineering Reseach Center (PSERC), School of Electrical Engineering, Cornell University, Ithaca, NY. User's Manual, Version 3.0b1.

[28] Douglass. D. A. (1981). Current Transformer accuracy with symmetric and high frequency fault currents. *IEEE Transactions on Power Apparatus and Systems*. Vol. 100, No. 3, 1006-1012.

[29] Douglass. D. A. (1981). Potential Transformer Accuracy at 60 Hz Voltage and Below Rating and Frequencies Above 60 Hz. *IEEE Transactions on Power Apparatus and Systems*. Vol. 100, No. 3, 1370-1375.

[30] Franco (1988). Design with Operational Amplifiers and Analog Integrated Circuits.

[31] Stewart, J. R., Oppel, L.J., Thomann, G. C., Dorazio, T. F., and Rebbapragada, R. V. (1991). Transformer Winding Selection Associated with Reconfiguration of Existing Double Circuit Line to Six-Phase Operation. *IEEE Transaction on Power Delivery*. Vol. 7, No. 3. 991-997.

APPENDIX A

EMTDC Program Algorithm Flow Chart

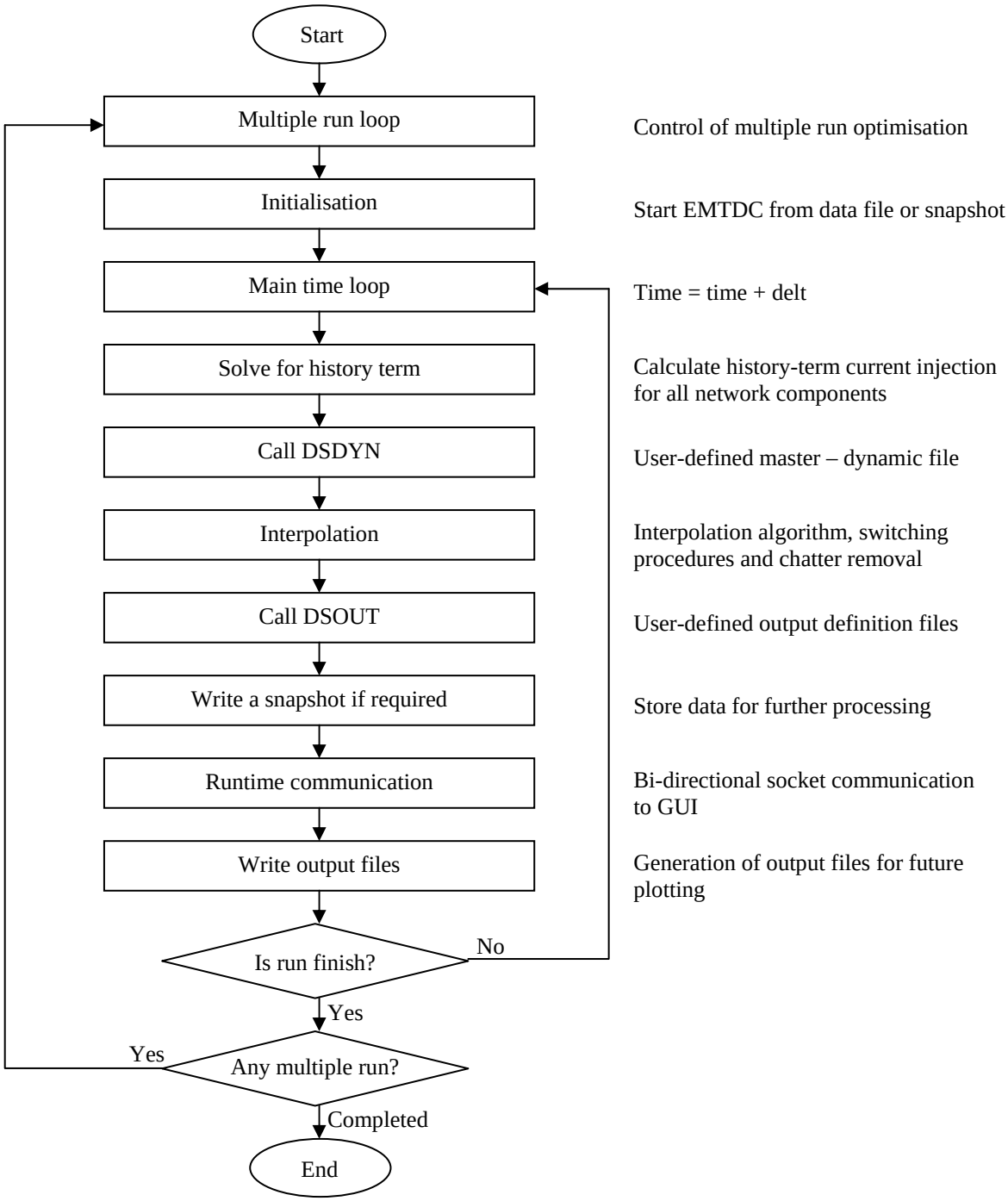

APPENDIX B

PSCAD/EMTDC Software

PSCAD/EMTDC consists of a set of program, which enables the efficient simulation of a wide variety of power system networks. EMTDC (Electromagnetic transient and DC) is an implementation of the EMTP-type method of solving the transient response of circuits. PSCAD (Power system computer aided design) is a graphical Unix-based user interface for EMTDC which can also run on PCs. PSCAD consists of software enabling the user to enter a circuit graphically, create new custom components, solve transmission-line and cable parameters, interact with an EMTDC simulation while in progress and to process the results of a simulation. The strength of EMTDC lies on its ability to model virtually any conceivable power system. The user is provided with an extensive library of power system component models. Users may also choose to develop their own unique models for use with EMTDC.

The following are some common models found in systems studied using PSCAD:

- Resistors, inductors, capacitors
- Mutually coupled windings, such as transformers
- Frequency dependent transmission lines and cables (including the most accurate time domain line model in the world!)
- Current and voltage sources
- Switches and breakers
- Protection and relaying
- Diodes, thyristors and GTOs
- Analog and digital control functions
- AC and DC machines, exciters, governors, stabilizers and inertial models
- Meters and measuring functions
- Generic DC and AC controls
- HVDC, SVC, and other FACTS controllers
- Wind source, turbines and governors

EMTP Method

The EMTP method is an integrated approach to the problems of [22]

(i) Forming the network differential equations;

(ii) Collecting the equations into a coherent system to be solved;

(iii) Numerical solution of the equations.

The method is based upon the discretisation of components, given a predetermined time step, which are then combined in a solution for the nodal voltage. The simplest element is a resistor connected between nodes k and m, as shown in Figure B.1.

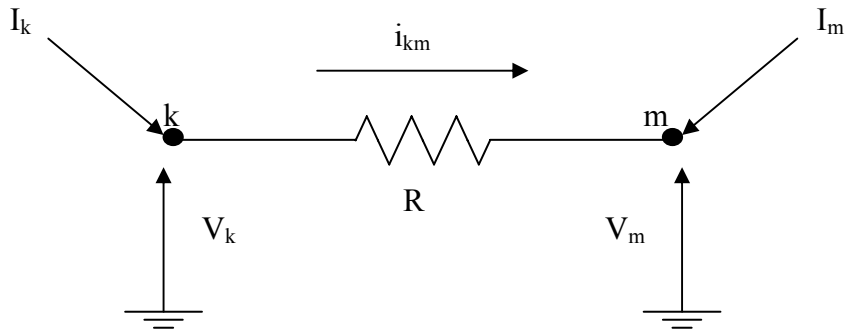

Figure B.1: Resistive branch

$$i_{km}(t) = \frac{1}{R}\left[V_k(t) - V_m(t)\right] \tag{B.1}$$

In a nodal form, it can be expressed as,

$$\begin{bmatrix} I_k \\ I_m \end{bmatrix} = \begin{bmatrix} \frac{1}{R} & -\frac{1}{R} \\ -\frac{1}{R} & \frac{1}{R} \end{bmatrix} \begin{bmatrix} V_k \\ V_m \end{bmatrix} \tag{B.2}$$

where I_k, I_m are the current injections at nodes k and m while V_k and V_m are the voltage at nodes k and m. For an inductor,

$$V_k(t) - V_m(t) = L\frac{di_{km}(t)}{dt} \tag{B.3}$$

Integrating from the previous time step,

$$i_{km}(t) - i_{km}(t - \Delta t) = \frac{1}{L} \int_{t-\Delta t}^{t} \left[V_k(\tau) - V_m(\tau) \right] d\tau \tag{B.4}$$

as illustrated in Figure B.2.

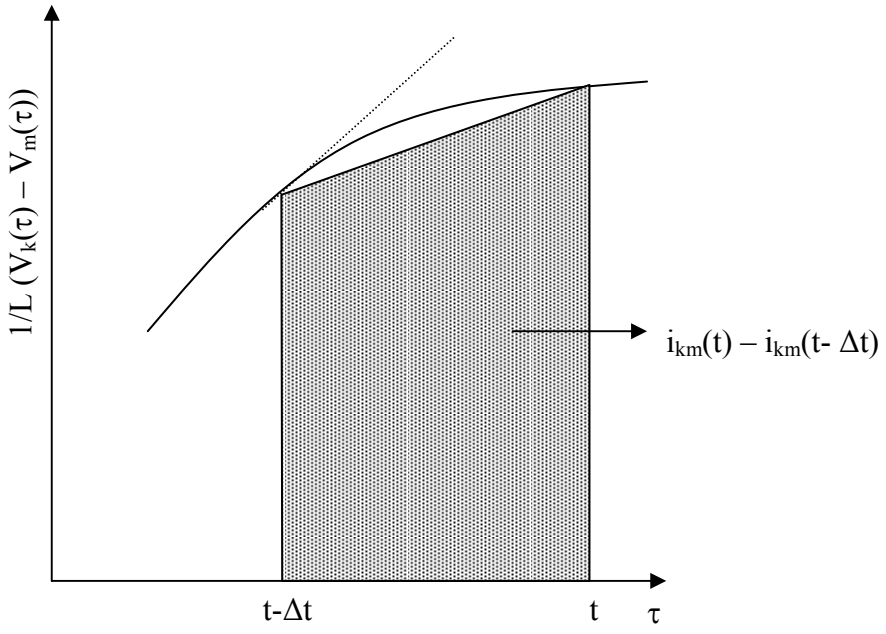

Figure B.2: Trapezoidal integration of inductor current

The right hand side of equation (B.4) is approximated by the shaded trapezoidal, yielding [22],

$$i_{km}(t) - i_{km}(t - \Delta t) \cong \frac{1}{2}.\Delta t.\left[\frac{1}{L}(V_k(t) - V_m(t)) + \frac{1}{L}(V_k(t - \Delta t) - V_m(t - \Delta t)) \right] \tag{B.5}$$

or,

$$i_{km}(t) \cong i_{km}(t - \Delta t) + \frac{\Delta t}{2L}\left[V_k(t - \Delta t) - V_m(t - \Delta t) \right] + \frac{\Delta t}{2L}\left[V_k(t) - V_m(t) \right] \tag{B.6}$$

The branch current, therefore, consists of two components, one related to the nodal voltages at the current time steps which are to be solved, and the other independent of the current-time step voltages. The independent component can be represented as a current

source, and the dependent component as a branch resistance, yielding the Norton equivalent, shown in Figure B.3. For inductor,

$$i_{km} = I_{km}(t-\Delta t) + \frac{\Delta t}{2L}\left[V_k(t) - V_m(t)\right] \tag{B.7}$$

where

$$I_{km}(t-\Delta t) = i_{km}(t-\Delta t) + \frac{\Delta t}{2L}\left[V_k(t-\Delta t) - V_m(t-\Delta t)\right] \tag{B.8}$$

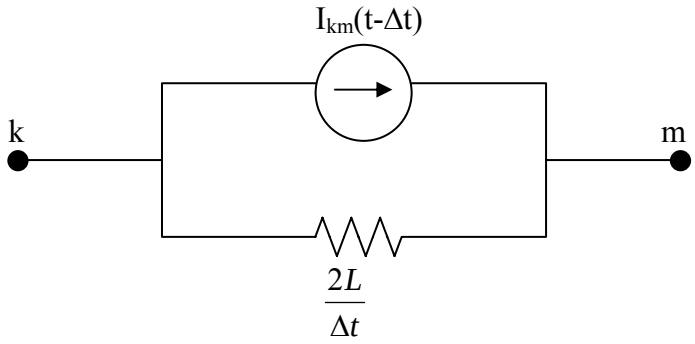

Figure B.3: Inductive branch

Equation (B.8) can be rewritten as,

$$\begin{bmatrix} I_k \\ I_m \end{bmatrix} = \begin{bmatrix} \frac{2L}{\Delta t} & -\frac{2L}{\Delta t} \\ -\frac{2L}{\Delta t} & \frac{2L}{\Delta t} \end{bmatrix} \begin{bmatrix} V_k \\ V_m \end{bmatrix} + \begin{bmatrix} -I_{km} \\ I_{km} \end{bmatrix} \tag{B.9}$$

The analysis for a capacitor is similar in nodal form, yielding,

$$\begin{bmatrix} I_k \\ I_m \end{bmatrix} = \begin{bmatrix} \frac{\Delta t}{2C} & -\frac{\Delta t}{2C} \\ -\frac{\Delta t}{2C} & \frac{\Delta t}{2C} \end{bmatrix} \begin{bmatrix} V_k \\ V_m \end{bmatrix} + \begin{bmatrix} -I_{km} \\ I_{km} \end{bmatrix} \tag{B.10}$$

and the Norton equivalent is as shown in Figure B.4.

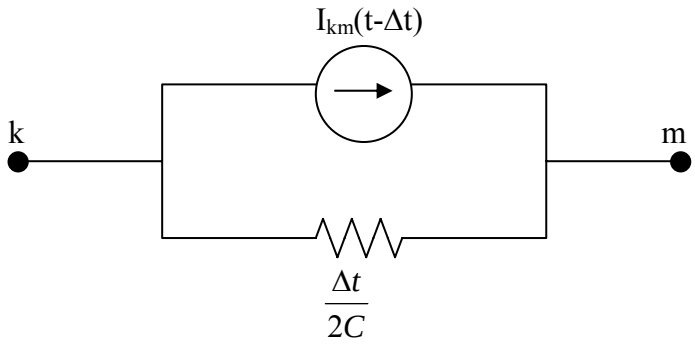

Figure B.4: Capacitive branch

EMTDC Structure

The purpose of the main program is to [22]

(i) Read data defining electric circuit parameters.

(ii) Assemble networks of resistor, inductor and capacitor components together with Thevenin and Norton sources, mutually coupled windings and distributed transmission line and cable models.

(iii) Interface a user's model assembled in subroutine DSDYN (Digital Simulator DYNamic subroutine) with the electric network. In DSDYN, node voltages and branch current in the network can be read at each time step, processed by the user's model, and returned to the network to control values of Thevenin or Norton sources, or switch branch components to new values.

(iv) At the user's definition, any computed output quantity is formulated or processed by modelling statements into an array each time step and printed into output files at the specified print interval along with the time of that print step. The output subroutine DSOUT (Digital Simulator OUTput subroutine) also written by the user can be used for this purpose.

(v) During or at the end of the run, the complete electric network and/or its associated dynamic model defined in DSDYN can be frozen in time for future use in a "SNAPSHOT" file. Multiple reruns can also be automatically initiated to search for an optimum value of a parameter.

APPENDIX C

Frequency Dependent (Mode) Transmission Line Model

Generally in electromagnetic transients simulations, there are two main ways to represent transmission lines. The most familiar method is using PI line sections. Single or multi-phase lines can be modelled. The second method is to use a distributed transmission line, which is most suited for transient line response modelling using a digital computer. A distributed model operates on the principle of travelling waves. A voltage disturbance will travel along a conductor at its propagation velocity (near the speed of light), until it is reflected at the line's end. In a sense, a transmission line or cable is a delay function. Whatever is fed into one end will appear at the other end, perhaps slightly distorted, after some delay. However, there are some other considerations which must be dealt with which include mutual coupling with other conductors, and wave-shape attenuation as it travels along the line.

Model Selection

There are three basic transmission line or cable modelling techniques in EMTDC: PI sections, the Bergeron Model, and Frequency-Dependent Line Models. The requirements of your study will determine which of the three models is suitable.

A simple PI section model will give the correct fundamental impedance, but cannot accurately represent other frequencies unless many sections are used (which is inefficient). It also cannot accurately represent the frequency dependent parameters of a line (such as skin effect). It is suitable for very short lines where the travelling wave models cannot be used. For EMTDC, PI sections are not considered a very elegant means of transmission line modelling for the following reasons:

- Greater computational time and increased matrix sizes

- Not practical with a large number of mutually coupled conductors
- Frequency dependent attenuation of the travelling waves is not easily or accurately incorporated

The Bergeron model represents the L and C elements of a PI section in a distributed manner (not using lumped parameters like PI sections). It is roughly equivalent to using an infinite number of PI sections except that the resistance is lumped (1/2 in the middle of the line, ¼ at each end). Like PI sections, it also accurately represents the fundamental frequency. It also represents impedances at other frequencies, except that the losses do not change. This model is suitable for studies where the fundamental frequency load-flow is most important (i.e. relay studies). The Bergeron model is discussed in detail later in this document.

The Frequency-Dependent Line Model represents the frequency dependence of all parameters. This model takes longer to run than the Bergeron model, but is necessary for studies requiring a very detailed representation of the line over a wide frequency range. Frequency dependent models can be solved using modal techniques (as in PSCAD V2 models) or using the more advanced phase domain techniques (the best model). These models are discussed in detail a little later on.

The T-LINE and CABLE constant processors are used to generate the data required by the EMTDC line models. Only the conductor properties (resistance, radius ...) and geometry (Horizontal & Vertical tower dimensions) are required to model the line. The T-LINE and CABLE constant processors then store the solved line constants data in output files.

The Frequency-Dependent Line Models are basically distributed R-L-C travelling wave models which incorporate the frequency dependence of all parameters. Because the Bergeron model is adequate for studies which essentially only require the correct fundamental frequency impedance, the Frequency-Dependent Line Model should be used for all studies which require frequencies other than the fundamental to be represented accurately (such as transient overvoltages, harmonic analysis...).

Two frequency dependent models are available. The Phase Domain Model is the most accurate as it represents the frequency dependence of internal transformation matrices, whereas the Modal Model assumes a constant transformation. For systems of ideally transposed conductors (or 2 conductor horizontal configurations), the 2 models will give identical results (as the transformation is constant anyway).

The phase domain model is numerically robust and more accurate than any other commercially available line/cable model, and should thus be preferred.

Phase Domain General Theory

The phase domain line model is best described in:

"Transmission Line Models for the Simulation of Interaction Phenomena Between Parallel AC and DC Overhead Lines", Gustavsen, Irwin et al, IPST 99 Proceedings, P. 61-67.

The model represents all frequency dependent effects for both lines and cables. This model is superior to modal methods as it does not use the approximation of a constant transformation.

Mode Domain General Theory

In order to arrive at the time domain formation of the line equations, it is convenient to first work in the frequency domain, where an exact solution for a given frequency is possible. Consider the following circuit of a transmission line as seen from the terminations:

Frequency Domain Line Circuit

For a given frequency, the voltages and currents at one end of the line may be represented in terms of the voltage and current at the other end by:

$$V_k(\omega) = \cosh\left[\gamma(\omega) \cdot L\right] V_m(\omega) - Z_c(\omega) \cdot \sinh\left[\gamma(\omega) \cdot L\right] i_m(\omega) \tag{C.1}$$

$$i_k(\omega) = \frac{\sinh\left[\gamma(\omega) \cdot L\right]}{Z_c(\omega)} V_m(\omega) - \cosh\left[\gamma(\omega) \cdot L\right] i_m(\omega) \tag{C.2}$$

where:

$\gamma(\omega) = \sqrt{Y(\omega) Z(\omega)}$ is the propagation constant

$Z_c(\omega) = \sqrt{\frac{Z(\omega)}{Y(\omega)}}$ is the surge impedance

$Y(\omega) = G + jC\omega$ is the shunt admittance of the line

$Z(\omega) = R + jL\omega$ is the series impedance of the line.

By introducing the forward and backward travelling wave functions F_k and B_k.

$$F_k(\omega) = V_k(\omega) + Z_c(\omega) \cdot i_k(\omega) \tag{C.3}$$

$$B_k(\omega) = V_k(\omega) - Z_c(\omega) \cdot i_k(\omega) \tag{C.4}$$

and similarly at node m:

$$F_m(\omega) = V_m(\omega) + Z_c(\omega) \cdot i_m(\omega) \tag{C.5}$$

$$B_m(\omega) = V_m(\omega) - Z_c(\omega) \cdot i_m(\omega) \tag{C.6}$$

Removing $i_k(\omega)$ from equation (C.3) using equation (C.4) yields:

$$F_k(\omega) = 2V_k(\omega) - B_k(\omega) \tag{C.7}$$

and similarly:

$$F_m(\omega) = 2V_m(\omega) - B_m(\omega) \tag{C.8}$$

Expressions (C.1) and (C.2) (and their equivalents at node m) can now be expressed in terms of the forward and backward travelling functions:

$$B_k(\omega) = A(\omega) \cdot F_m(\omega) \tag{C.9}$$

$$B_m(\omega) = A(\omega) \cdot F_k(\omega) \tag{C.10}$$

where,

$$A(\omega) = \frac{1}{\cosh\left[\gamma(\omega) \cdot L\right] \sinh\left[\gamma(\omega) \cdot L\right]} = e^{-\gamma(\omega)L} \tag{C.11}$$

$A(\omega)$ is known as the propagation constant and is a complex number. The real part (α) is the attenuation constant, and the imaginary part ($j\beta$) is the phase constant. Equation (C.4) and (C.6) can be represented with the equivalent circuit as shown below.

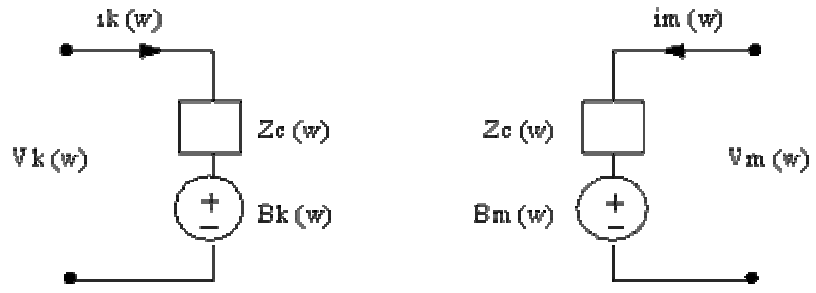

Frequency Domain Equivalent Circuit

Equations (C.8) and (C.9) relate the source $B_k(\omega)$ with the m side quantities $V_m(\omega)$ and $B_m(\omega)$:

$$B_k(\omega) = A(\omega)\cdot\left[2V_m(\omega) - B_m(\omega)\right] \tag{C.12}$$

and similarly

$$B_m(\omega) = A(\omega)\cdot\left[2V_k(\omega) - B_k(\omega)\right] \tag{C.13}$$

The goal is to represent the circuit of the above figure and equations (C.11) and (C.13) in the time domain. The problem however, is the multiplication of $A(\omega)\cdot F_m(u)$ in Equation (C.13). A multiplication of the frequency domain becomes a convolution in the time domain:

$$A(\omega)\cdot F_m(\omega) \leftrightarrow \int_{\tau}^{t} A(u)\cdot F_m(t-u)du \tag{C.14}$$

Note the lower limit of the integral of equation (C.14) is τ (the travel time), because an impulse on one end of the line will not reach the other end until τ seconds. The travel time is calculated using the imaginary term β of the propagation constant.

Equation (C.14) is still in a very inconvenient form for a time domain solution, because with each time step more and more terms of the convolution integral must be evaluated. Fortunately, the convolution can be computed in a recursive form suitable for time domain solution. The recursive convolution algorithm requires $A(\omega)$ to be in the form of a sum of exponentials. This is achieved in the T-LINE/CABLE constant processors. T-LINE and CABLE constant processors first generate $A(\omega)$ for 100 frequencies equally spaced on a log scale over a wide frequency range. This curve is then approximated with Nth order rational function $A(s)$ using curve fitting techniques. The number of pole zeroes required depends on the maximum allowed error between the curves. The function $A(s)$ can then be broken down (using partial fraction expansion) into a sum of exponential terms. The more terms there are in $A(s)$, the more terms there are in the recursive convolution, which means the line model takes longer to run.

One point not yet discussed is the representation of the surge impedance $Z_c(\omega)$ in the time domain. The line constants program (T-LINE/CABLE constant processors) generates a curve for $Z_c(\omega)$. The same curve fitting routine used to generate $A(s)$ is used to generate an approximate $Z_c(s)$. This function is now realized by replacing $Z_c(\omega)$ in the last figure with an R-C circuit which has the same impedance as $Z_c(s)$. The R-C circuit is then solved using the same trapezoidal integration technique as is used in the main program. Finally, the extension of this theory to multi-conductor lines is achieved using the same modal transformations discussed earlier. Early attempts at curve fitting the modal transformation option were available in PSCAD V2, but were found to be non-reliable and were therefore dropped in PSCAD V3 (only a constant transformation is calculated).

It is only necessary to approximate the current transformation matrix (this transforms modal currents to phase currents). It is also necessary to transform the phase voltages to modal quantities, (which requires the inverse of the voltage transformation matrix.

The last section of this manual discusses the equations used in the TLINE/CABLE line constants programs. This section also describes the mathematical techniques required to determine the transformation matrices, attenuation constant and surge impedance for each frequency.

Data File Format for the Frequency-Dependent Line Model

The Frequency Dependent line model data is contained in a linename.tlo file located in the casename.emt subdirectory. This file is automatically created by the Line Constants program when it solves. Sending end nodes can be in a different subsystem to its receiving end nodes.

The data file format for the Frequency-Dependent Line Model consists mainly of poles and zeroes for the rational function approximation of Z_c (the surge impedance), A (the attenuation constant), and T (the current transformation matrix) for each mode. This data is generated automatically by the T-LINE/CABLE constant processors.

The complexity and amount of data required by the Frequency-Dependent Line Model makes manual calculation nearly impossible.

Frequency Dependent Line Model Options

The frequency dependent line model has a number of parameters which can be selected or adjusted from the line/cable constants options menu. The effect of interpolating the travel time has already been discussed earlier.

The maximum number of poles/zeroes is usually entered as 20. This is usually the default dimension internal to EMTDC. If the curve fitting uses all 20 poles, then the approximated curve for the parameter being curve fitted will be constant for all higher frequencies.

The maximum error will affect the number of poles/zeroes used in the approximation. In general, a smaller error will result in less error in the curve fitting but will result in a less efficient model due to a larger number of poles. The error is calculated as a percentage of the maximum of the curve. For the attenuation constant and the transform, this is consistent as 1.0. For the surge impedance however, the maximum value will depend on the starting frequency.

The user must select a starting and an end frequency. The upper frequency may be beyond the highest frequency which can be represented with the chosen time step, but the program will truncate the curve fitting data to preserver efficiency. A good choice for the end frequency is 1.0E6 Hz.

The lower frequency must be selected cautiously however. Internally in the line constants equations, the shunt conductance (G) of the line is 0.0. This means that the surge impedance ($\sqrt{[(R+jWL)/(G+jWC)]}$) will tend to become larger as the frequency decreases. The selection of the starting frequency will introduce an effective shunt conductance G' ($Zdc = \sqrt{(R/G')}$). This means that if the curve fitting is started at 10 Hz, a significant shunt conductance will be introduced. If the starting frequency is reduced, then the shunt conductance is smaller (less shunt losses).

Care must also be taken as the choice of the starting frequency will affect the accuracy of the curve fitting of the surge impedance. This is because the maximum error is specified as a percentage of the maximum, and the surge impedance will get larger as the starting frequency is lowered. Finally, choosing too low of a starting frequency means that there may be poles/zeroes at these low frequencies. This can introduce very long time constants in the line models which means you must run for a long time to reach steady state. A good starting frequency is about 0.5 Hz.

APPENDIX D

Power System Data

D.1 General

This appendix lists the one line diagram including the system data of IEEE test systems that used throughout the study. The distributions of bus voltages are determined using the fast-decoupled loadflow method. The test systems are, namely:

Test System I	- 4 busbars, 2 generators, 4 lines
Test System II	- 9 busbars, 3 generators, 9 lines
Test System III	- 14 busbars, 5 generators, 20 lines
Test System IV	- 30 busbars, 6 generators, 41 lines
19-Bus TNB Kelantan System	- 19 busbars, 8 generators, 29 lines

D.2 Test System I

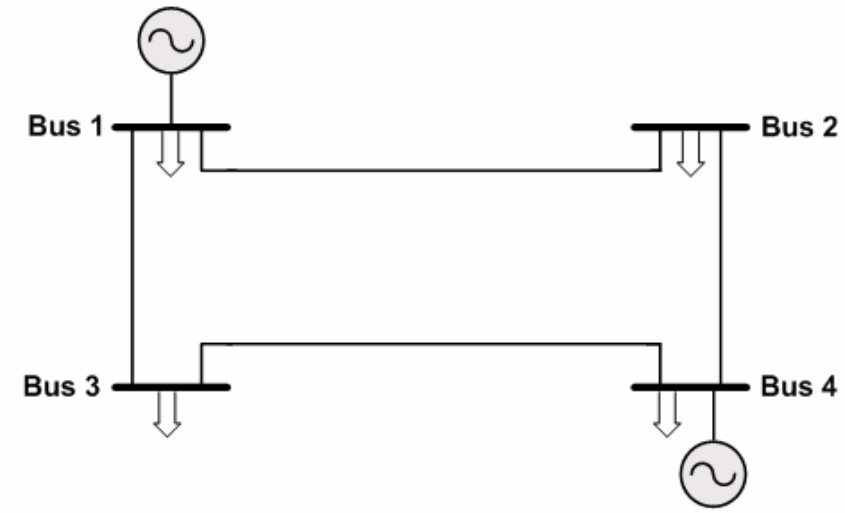

Figure D.1: Single line diagram of Test System I

Table D2.1: Exciter Data

Exciter Bus No.	1	4
K_A	400	400
T_A	0.02	0.02
T_B	0.00	0.00
T_C	0.00	0.00
V_{Rmax}	6.03	6.03
V_{Rmin}	-5.43	-5.43
K_E	1.00	1.00
T_E	0.8	0.8
K_F	0.03	0.03
T_F	1.00	1.00

Table D2.2: Generator Parameters

Generator	G_1	G_4
S (MVA)	232	418
V (kV)	230	230
I (kA)	0.5824	1.0493
ω_s (rad/s)	376.99	376.99
H (s)	2.6	6.0
T_a (s)	0.278	0.278
X_d (p.u)	1.014	1.014
X_d' (p.u)	0.314	0.314
X_d" (p.u)	0.280	0.280
T_{do}' (s)	6.55	6.55
T_{do}" (s)	0.039	0.039
X_q (p.u)	0.77	0.77
X_q" (p.u)	0.375	0.375
T_{qo}" (s)	0.071	0.071

Table D2.3: Transformer Parameters

Transformer	T1	T2	T3	T4
S (MVA)	100	100	100	100
f (hz)	60	60	60	60
X (p.u)	0.015	0.015	0.015	0.015
Winding 1 (V_{L-L}) kV	230	230	398	398
Winding 2 (V_{L-L}) kV	398	398	230	230
Winding #1 Type	Delta	Delta	Y	Y-Inverted
Winding #2 Type	Y	Y-Inverted	Delta	Delta

Table D2.4: Line Data

Line	Busbar	R (p.u)	X (p.u)	B (p.u)
1	1-2	0.01008	0.05040	0.10250
2	1-3	0.00744	0.03720	0.07750
3	2-4	0.00744	0.03720	0.07750
4	3-4	0.01272	0.06360	0.12750

Table D2.5: Bus Data

Busbar	Voltage		Load		Power Generated	
	Magnitude (p.u)	Angle (°)	Active (MW)	Reactive (MVAr)	Active (MW)	Reactive (MVAr)
1	1.000	0.000	50.00	30.99	186.81	114.50
2	0.982	-0.976	170.00	105.35	0.00	0.00
3	0.969	-1.872	200.00	123.94	0.00	0.00
4	1.020	1.523	80.00	49.58	318.00	181.43

D.3 Test System II

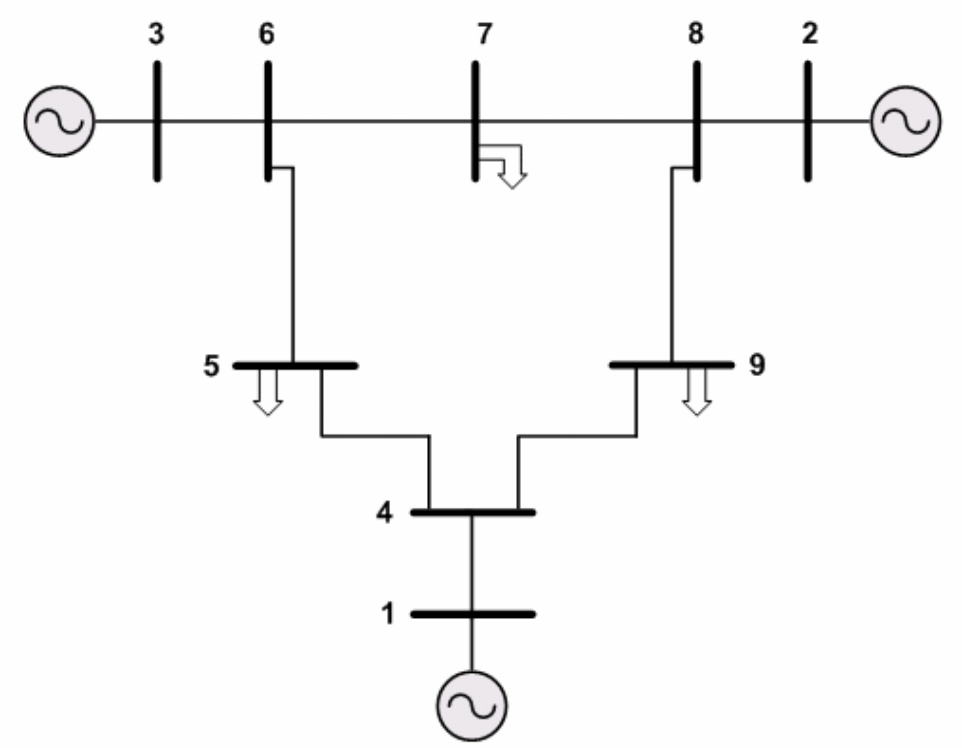

Figure D.2: Single line diagram of Test System II

Table D3.1: Exciter Data

Exciter Bus No.	1	2	3
K_A	400	400	400
T_A	0.02	0.02	0.02
T_B	0.00	0.00	0.00
T_C	0.00	0.00	0.00
V_{Rmax}	6.03	6.03	6.03
V_{Rmin}	-5.43	-5.43	-5.43
K_E	1.00	1.00	1.00
T_E	0.8	0.8	0.8
K_F	0.03	0.03	0.03
T_F	1.00	1.00	1.00

Table D3.2: Generator Parameters

Generator	G_1	G_2	G_3
S (MVA)	250	300	270
V (kV)	100	100	100
I (kA)	1.4434	1.7321	1.5589
ω_s (rad/s)	376.99	376.99	376.99
H (s)	2.0	2.25	2.1
T_a (s)	0.278	0.278	0.278
X_d (p.u)	1.014	1.014	1.014
X_d' (p.u)	0.314	0.314	0.314
X_d" (p.u)	0.280	0.280	0.280
T_{do}' (s)	6.55	6.55	6.55
T_{do}" (s)	0.039	0.039	0.039
X_q (p.u)	0.77	0.77	0.77
X_q" (p.u)	0.375	0.375	0.375
T_{qo}" (s)	0.071	0.071	0.071

Table D3.3: Transformer Parameters

Transformer	T1	T2	T3	T4
S (MVA)	100	100	100	100
f (hz)	60	60	60	60
X (p.u)	0.015	0.015	0.015	0.015
Winding 1 (V_{L-L}) kV	100	100	173	173
Winding 2 (V_{L-L}) kV	173	173	100	100
Winding #1 Type	Delta	Delta	Y	Y-Inverted
Winding #2 Type	Y	Y-Inverted	Delta	Delta

Table D3.4: Line Data

\ Line	Busbar	R (p.u)	X (p.u)	B (p.u)
1	1-4	0.0000	0.0576	0.0000
2	4-5	0.0170	0.0920	0.1580
3	5-6	0.0390	0.1700	0.3580
4	3-6	0.0000	0.0586	0.0000
5	6-7	0.0119	0.1008	0.2090
6	7-8	0.0085	0.0720	0.1490
7	8-2	0.0000	0.0625	0.0000
8	8-9	0.0320	0.1610	0.3060
9	9-4	0.0100	0.0850	0.1760

Table D3.5: Bus Data

Busbar	Voltage		Load		Power Generated	
	Magnitude (p.u)	Angle (°)	Active (MW)	Reactive (MVAr)	Active (MW)	Reactive (MVAr)
1	1.000	0.000	0.00	0.00	71.95	24.07
2	1.000	9.669	0.00	0.00	163.00	14.46
3	1.000	4.771	0.00	0.00	85.00	-3.65
4	0.987	-2.407	0.00	0.00	0.00	0.00
5	0.975	-4.017	90.00	30.00	0.00	0.00
6	1.003	1.926	0.00	0.00	0.00	12.2
7	0.986	0.622	100.00	35.00	0.00	0.00
8	0.996	3.799	0.00	0.00	0.00	17.4
9	0.958	-4.350	125.00	50.00	0.00	0.00

D.4 Test System III

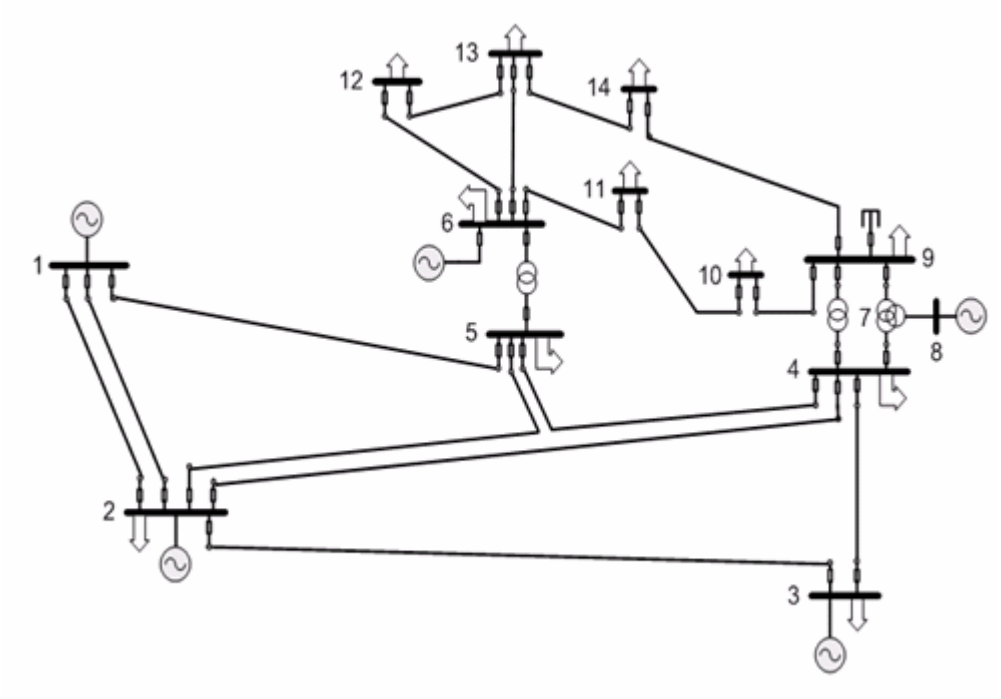

Figure D.3: Single line diagram of Test System III

Table D4.1: Exciter Data

Exciter Bus No.	1	2	3	6	8
K_A	400	400	400	400	400
T_A	0.02	0.02	0.02	0.02	0.02
T_B	0.00	0.00	0.00	0.00	0.00
T_C	0.00	0.00	0.00	0.00	0.00
V_{Rmax}	6.03	6.03	6.03	6.03	6.03
V_{Rmin}	-5.43	-5.43	-5.43	-5.43	-5.43
K_E	1.00	1.00	1.00	1.00	1.00
T_E	0.8	0.8	0.8	0.8	0.8
K_F	0.03	0.03	0.03	0.03	0.03
T_F	1.00	1.00	1.00	1.00	1.00

Table D4.2: Generator Data

Generator	G_1	G_2	G_3	G_6	G_8
S (MVA)	332.39	140	100	100	100
V (kV)	69	69	69	13.8	18
I (kA)	2.7812	1.1714	0.8367	4.1837	3.2075
ω_s (rad/s)	376.99	376.99	376.99	376.99	376.99
H (s)	2.5	2.3	2.0	2.0	2.0

T_a (s)	0.278	0.278	0.278	0.278	0.278
X_d (p.u)	1.014	1.014	1.014	1.014	1.014
X_d' (p.u)	0.314	0.314	0.314	0.314	0.314
X_d" (p.u)	0.280	0.280	0.280	0.280	0.280
T_{do}' (s)	6.55	6.55	6.55	6.55	6.55
T_{do}" (s)	0.039	0.039	0.039	0.039	0.039
X_q (p.u)	0.77	0.77	0.77	0.77	0.77
X_q" (p.u)	0.375	0.375	0.375	0.375	0.375
T_{qo}" (s)	0.071	0.071	0.071	0.071	0.071

Table D4.3: Transformer Data

Transformer	T1	T2	T3	T4
S (MVA)	100	100	100	100
f (hz)	60	60	60	60
X (p.u)	0.01	0.01	0.01	0.01
Winding 1 (V_{L-L}) kV	69	69	120	120
Winding 2 (V_{L-L}) kV	120	120	69	69
Winding #1 Type	Delta	Delta	Y	Y-Inverted
Winding #2 Type	Y	Y-Inverted	Delta	Delta

Table D4.4: Line Data

Line	Busbar	R (p.u)	X (p.u)	B (p.u)
1	1-2	0.01938	0.05917	0.05280
2	1-5	0.05403	0.22304	0.04920
3	2-3	0.04699	0.19797	0.04380
4	2-4	0.05811	0.17632	0.03740
5	2-5	0.05695	0.17388	0.03400
6	3-4	0.06701	0.17103	0.03460
7	4-5	0.01335	0.04211	0.01280
8	4-7	0.00000	0.20912	0.00000
9	4-9	0.00000	0.55618	0.00000
10	5-6	0.00000	0.25202	0.00000
11	6-11	0.09498	0.19890	0.00000
12	6-12	0.12291	0.25581	0.00000
13	6-13	0.06615	0.13027	0.00000
14	7-8	0.00000	0.17615	0.00000
15	7-9	0.00000	0.11001	0.00000
16	9-10	0.03181	0.08450	0.00000
17	9-14	0.12711	0.27038	0.00000
18	10-11	0.08205	0.19207	0.00000
19	12-13	0.22092	0.19988	0.00000
20	13-14	0.17093	0.34802	0.00000

Table D4.5: Bus Data

Busbar	Voltage		Load		Power Generated	
	Magnitude (p.u)	Angle (°)	Active (MW)	Reactive (MVAr)	Active (MW)	Reactive (MVAr)
1	1.060	0.000	0.000	0.000	232.39	-16.89
2	1.045	-4.981	21.70	12.70	40.00	42.40
3	1.010	-12.718	94.20	19.00	0.00	23.39
4	1.019	-10.324	47.80	-3.90	0.00	0.00
5	1.020	-8.783	7.60	1.60	0.00	0.00
6	1.070	-14.223	11.20	7.50	0.00	12.24
7	1.062	-13.368	0.000	0.000	0.00	0.00
8	1.090	-13.368	0.000	0.000	0.00	17.36
9	1.056	-14.947	29.50	16.60	0.00	0.00
10	1.051	-15.104	9.00	5.80	0.00	0.00
11	1.057	-14.795	3.50	1.80	0.00	0.00
12	1.055	-15.077	6.10	1.60	0.00	0.00
13	1.050	-15.159	13.50	5.80	0.00	0.00
14	1.036	-16.039	14.90	5.00	0.00	0.00

D.5 Test System IV

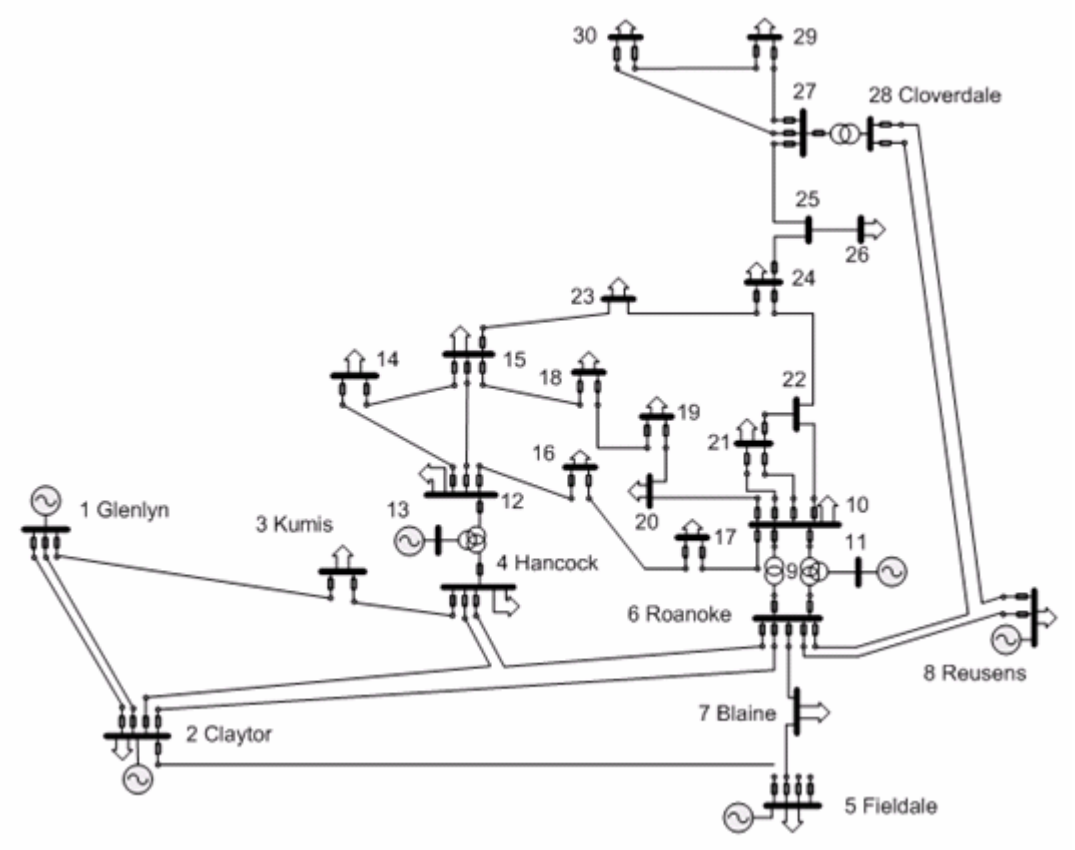

Figure D.4: Single line diagram of Test System IV

Table D5.1: Exciter Data

Exciter Bus No.	1	2	5	8	11	13
K_A	400	400	400	400	400	400
T_A	0.02	0.02	0.02	0.02	0.02	0.02
T_B	0.00	0.00	0.00	0.00	0.00	0.00
T_C	0.00	0.00	0.00	0.00	0.00	0.00
V_{Rmax}	6.03	6.03	6.03	6.03	6.03	6.03
V_{Rmin}	-5.43	-5.43	-5.43	-5.43	-5.43	-5.43
K_E	1.00	1.00	1.00	1.00	1.00	1.00
T_E	0.8	0.8	0.8	0.8	0.8	0.8
K_F	0.03	0.03	0.03	0.03	0.03	0.03
T_F	1.00	1.00	1.00	1.00	1.00	1.00

Table D5.2: Generator Data

Generator	G_1	G_2	G_5	G_8	G_{11}	G_{13}
S (MVA)	360.2	140	100	100	100	100
V (kV)	132	132	132	132	11	11
I (kA)	1.5755	0.6123	0.4374	0.4374	5.2486	5.2486
ω_s (rad/s)	376.99	376.99	376.99	376.99	376.99	376.99
H (s)	2.5	2.3	2.0	2.0	2.0	2.0
T_a (s)	0.278	0.278	0.278	0.278	0.278	0.278
X_d (p.u)	1.014	1.014	1.014	1.014	1.014	1.014
X_d' (p.u)	0.314	0.314	0.314	0.314	0.314	0.314
X_d" (p.u)	0.280	0.280	0.280	0.280	0.280	0.280
T_{do}' (s)	6.55	6.55	6.55	6.55	6.55	6.55
T_{do}" (s)	0.039	0.039	0.039	0.039	0.039	0.039
X_q (p.u)	0.77	0.77	0.77	0.77	0.77	0.77
X_q" (p.u)	0.375	0.375	0.375	0.375	0.375	0.375
T_{qo}" (s)	0.071	0.071	0.071	0.071	0.071	0.071

Table D5.3: Transformer Data

Transformer	T1	T2	T3	T4
S (MVA)	100	100	100	100
f (hz)	60	60	60	60
X (p.u)	0.01	0.01	0.01	0.01
Winding 1 (V_{L-L}) kV	132	132	230	230
Winding 2 (V_{L-L}) kV	230	230	132	132
Winding #1 Type	Delta	Delta	Y	Y-Inverted
Winding #2 Type	Y	Y-Inverted	Delta	Delta

Table D5.4: Line Data

Line	Busbar	R (p.u)	X (p.u)	B (p.u)
1	1-2	0.01920	0.05750	0.05280
2	1-3	0.04520	0.16520	0.04080
3	2-4	0.05700	0.17370	0.03680
4	3-4	0.01320	0.03790	0.00840
5	2-5	0.04720	0.19830	0.04180
6	2-6	0.05810	0.17630	0.03740
7	4-6	0.01190	0.04140	0.00900
8	5-7	0.04600	0.11600	0.02040
9	6- 7	0.02670	0.08200	0.01700
10	6-8	0.01200	0.04200	0.00900
11	6-9	0.00000	0.20800	0.00000
12	6-10	0.00000	0.55600	0.00000
13	9-11	0.00000	0.20800	0.00000
14	9-10	0.00000	0.11000	0.00000
15	4-12	0.00000	0.25600	0.00000
16	12-13	0.00000	0.14000	0.00000
17	12-14	0.12310	0.25590	0.00000
18	12-15	0.06620	0.13040	0.00000
19	12-16	0.09450	0.19870	0.00000
20	14-15	0.22100	0.19970	0.00000
21	16-17	0.05240	0.19230	0.00000
22	15-18	0.10730	0.21850	0.00000
23	18-19	0.06390	0.12920	0.00000
24	19-20	0.03400	0.06800	0.00000
25	10-20	0.09360	0.20900	0.00000
26	10-17	0.03240	0.08450	0.00000
27	10-21	0.03480	0.07490	0.00000
28	10-22	0.07270	0.14990	0.00000
29	21-22	0.01160	0.02360	0.00000
30	15-23	0.10000	0.20200	0.00000
31	22-24	0.11500	0.17900	0.00000
32	23 -24	0.13200	0.27000	0.00000
33	24-25	0.18850	0.32920	0.00000
34	25-26	0.25440	0.38000	0.00000
35	25-27	0.10930	0.20870	0.00000
36	28-27	0.00000	0.39600	0.00000
37	27-29	0.21980	0.41530	0.00000
38	27-30	0.32020	0.60270	0.00000
39	29-30	0.23990	0.45330	0.00000
40	8 -28	0.06360	0.20000	0.04280
41	6-28	0.01690	0.05990	0.01300

Table D5.5: Bus Data

Busbar	Voltage		Load		Power Generated	
	Magnitude (p.u)	Angle (°)	Active (MW)	Reactive (MVAr)	Active (MW)	Reactive (MVAr)
1	1.060	0.000	0.00	0.00	260.96	-20.42
2	1.045	-5.378	21.70	12.70	40.00	56.07
3	1.021	-7.529	2.40	1.20	0.00	0.00
4	1.012	-9.279	7.60	1.60	0.00	0.00
5	1.010	-14.149	94.20	19.00	0.00	35.66
6	1.011	-11.055	0.00	0.00	0.00	0.00
7	1.003	-12.852	22.80	10.90	0.00	0.00
8	1.010	-11.797	30.00	30.00	0.00	36.11
9	1.051	-14.098	0.00	0.00	0.00	0.00
10	1.045	-15.688	5.80	2.00	0.00	0.00
11	1.082	-14.098	0.00	0.00	0.00	16.06
12	1.057	-14.933	11.20	7.50	0.00	0.00
13	1.071	-14.933	0.00	0.00	0.00	0.00
14	1.043	-15.825	6.20	1.60	0.00	0.00
15	1.038	-15.916	8.20	2.50	232.39	-16.89
16	1.045	-15.515	3.50	1.80	40.00	42.40
17	1.040	-15.850	9.00	5.80	0.00	23.39
18	1.028	-16.530	3.20	0.90	0.00	0.00
19	1.026	-16.704	9.50	3.40	0.00	0.00
20	1.030	-16.507	2.20	0.70	0.00	12.24
21	1.033	-16.131	17.50	11.20	0.00	0.00
22	1.034	-16.116	0.00	0.00	0.00	17.36
23	1.027	-16.307	3.20	1.60	0.00	0.00
24	1.022	-16.483	8.70	6.70	0.00	0.00
25	1.018	-16.055	0.00	0.00	0.00	0.00
26	1.000	-16.474	3.50	2.30	0.00	0.00
27	1.024	-15.530	0.00	0.00	0.00	0.00
28	1.007	-11.677	0.00	0.00	0.00	0.00
29	1.004	-16.759	2.40	0.90	0.00	0.00
30	0.992	-17.642	10.60	1.90	0.00	0.00

D.6 19-Bus TNB Kelantan System

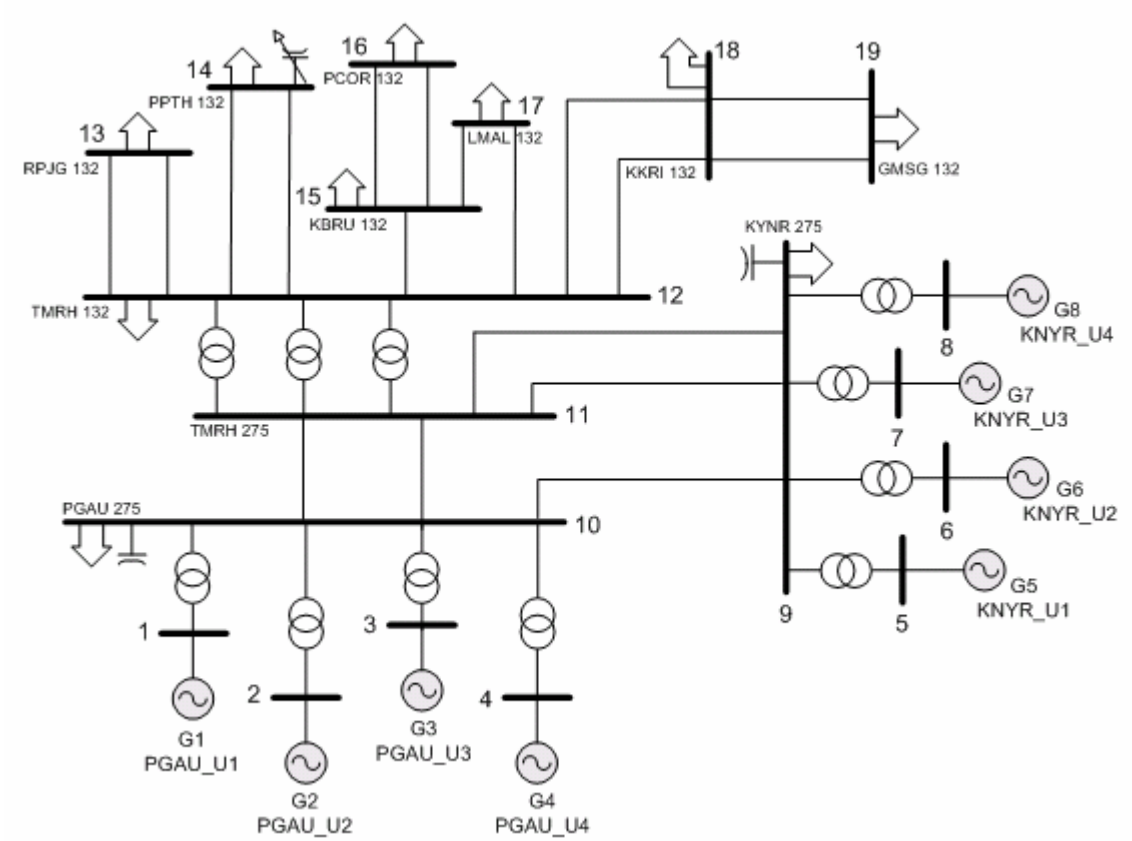

Figure D.5: Single line diagram of TNB 19-Bus Test System

Table D6.1: Exciter Data

Exciter Bus No.	12	13	14	15	16	17	18	19
K_A	185	185	185	185	595	595	595	595
T_A	0.01	0.01	0.01	0.01	0.05	0.05	0.05	0.05
T_B	0.00	0.00	0.00	0.00	0.00	0.00	0.00	0.00
T_C	0.00	0.00	0.00	0.00	0.00	0.00	0.00	0.00
V_{Rmax}	7.52	7.52	7.52	7.52	2.72	2.72	2.72	2.72
V_{Rmin}	-7.06	-7.06	-7.06	-7.06	-2.18	-2.18	-2.18	-2.18
K_E	1.00	1.00	1.00	1.00	1.00	1.00	1.00	1.00
T_E	0.8	0.8	0.8	0.8	0.8	0.8	0.8	0.8
K_F	0.00054	0.00054	0.00054	0.00054	0.055	0.055	0.055	0.055
T_F	0.22	0.22	0.22	0.22	1.5	1.5	1.5	1.5

Table D6.2: Generator Data

Generator	G_{12}	G_{13}	G_{14}	G_{15}	G_{16}	G_{17}	G_{18}	G_{19}
S (MVA)	100	100	100	100	150	150	150	150
V (kV)	13.8	13.8	13.8	13.8	16	16	16	16
I (kA)	4.1837	4.1837	4.1837	4.1837	5.4127	5.4127	5.4127	5.4127
ω_s (rad/s)	314.16	314.16	314.16	314.16	376.99	376.99	376.99	376.99
H (s)	3.74	3.74	3.74	3.74	3.46	3.46	3.46	3.46
T_a (s)	0.278	0.278	0.278	0.278	0.278	0.278	0.278	0.278
X_d (p.u)	1.18	1.18	1.18	1.18	1.04	1.04	1.04	1.04
X_d' (p.u)	0.316	0.316	0.316	0.316	0.22	0.22	0.22	0.22
X_d" (p.u)	0.216	0.216	0.216	0.216	0.165	0.165	0.165	0.165
T_{do}' (s)	9.48	9.48	9.48	9.48	11.3	11.3	11.3	11.3
T_{do}" (s)	0.097	0.097	0.097	0.097	0.062	0.062	0.062	0.062
X_q (p.u)	0.72	0.72	0.72	0.72	0.62	0.62	0.62	0.62
X_q" (p.u)	0.375	0.375	0.375	0.375	0.375	0.375	0.375	0.375
T_{qo}" (s)	0.019	0.019	0.019	0.019	0.062	0.062	0.062	0.062

Table D6.3: Transformer Data

Transformer	T1	T2	T3	T4
S (MVA)	100	100	100	100
f (hz)	60	60	60	60
X (p.u)	0.01	0.01	0.01	0.01
Winding 1 (V_{L-L}) kV	132	132	230	230
Winding 2 (V_{L-L}) kV	230	230	132	132
Winding #1 Type	Delta	Delta	Y	Y-Inverted
Winding #2 Type	Y	Y-Inverted	Delta	Delta

Table D6.4: Line Data

Line	Busbar	R (p.u)	X (p.u)	B (p.u)
1	1-2	0.00972	0.05758	0.02768
2	1-3	0.01436	0.06124	0.01433
3	1-3	0.01436	0.06124	0.01433
4	1-4	0.02276	0.09710	0.02272
5	1-4	0.02276	0.09710	0.02272
6	1-6	0.00487	0.02887	0.01388
7	1-8	0.00760	0.04501	0.02163
8	1-8	0.00760	0.04501	0.02163
9	1-9	0.00000	0.09267	0.00000
10	1-9	0.00000	0.09267	0.00000
11	1-9	0.00000	0.09267	0.00000
12	2-5	0.00524	0.03104	0.01492
13	2-5	0.00524	0.03104	0.01492
14	2-6	0.00969	0.05738	0.02758

15	3-7	0.05904	0.25187	0.05892
16	3-7	0.05904	0.25187	0.05892
17	9-10	0.00936	0.06022	0.46769
18	9-10	0.00936	0.06022	0.46769
19	9-11	0.00217	0.01394	0.10826
20	9-11	0.00217	0.01394	0.10826
21	10-11	0.00874	0.03536	0.00000
22	10-12	0.00000	0.10268	0.00000
23	10-13	0.00000	0.10268	0.00000
24	10-14	0.00000	0.10268	0.00000
25	10-15	0.00000	0.10268	0.00000
26	11-16	0.00000	0.10269	0.00000
27	11-17	0.00000	0.10269	0.00000
28	11-18	0.00000	0.10269	0.00000
29	11-19	0.00000	0.10269	0.00000

Table D6.5: Bus Data

Busbar	Voltage		Load		Power Generated	
	Magnitude (p.u)	Angle (°)	Active (MW)	Reactive (MVAr)	Active (MW)	Reactive (MVAr)
1	1.021	-21.291	23.89	8.67	0.00	0.00
2	0.999	-23.574	62.12	22.55	0.00	0.00
3	1.023	-21.510	7.96	2.89	0.00	0.00
4	1.007	-22.644	53.62	19.62	0.00	0.00
5	0.995	-24.042	55.58	20.17	0.00	0.00
6	1.012	-22.245	19.62	7.12	0.00	0.00
7	1.029	-21.784	2.77	1.00	0.00	0.00
8	1.020	-21.428	11.44	4.15	0.00	0.00
9	1.041	-17.316	0.00	0.00	0.00	0.00
10	1.081	-11.802	-1932.33	2884.29	0.00	0.00
11	1.036	-17.770	1365.33	5048.27	0.00	0.00
12	1.040	-7.087	0.00	0.00	90.00	-37.75
13	1.040	-7.087	0.00	0.00	90.00	-37.75
14	1.040	-7.087	0.00	0.00	90.00	-37.75
15	1.040	-7.087	0.00	0.00	90.00	-37.75
16	1.040	0.000	0.00	0.00	320.29	53.89
17	1.040	-17.770	0.00	0.00	0.00	3.82
18	1.040	-17.770	0.00	0.00	0.00	3.82
19	1.040	-17.770	0.00	0.00	0.00	3.82

APPENDIX E

MATLAB 6.5.1 Load Flow Analysis Results / Solutions

E.1 Test System I

```
Newton's method power flow converged in 3 iterations.

Converged in 0.25 seconds
==========================================================================
|     System Summary                                                     |
==========================================================================

How many?                How much?              P (MW)       Q (MVAr)
---------------------    --------------------  --------  -----------------
Buses               4    Total Gen Capacity      650.0      0.0 to +20.0
Generators          2    On-line Capacity        650.0      0.0 to +20.0
Commited Gens       2    Generation (current)    504.8        295.9
Loads               4    Load                    500.0        309.9
Branches            4    Losses (I^2 * Z)          4.81        24.05
Transformers        0    Branch Charging (inj)      -          38.0
Areas               1    Shunt (inj)               0.0          0.0
Inter-ties          0    Total Inter-tie Flow      0.0          0.0

                        Minimum                      Maximum
                    -------------------------  --------------------------------
Voltage Magnitude    0.969 p.u. @ bus 3          1.020 p.u. @ bus 4
Voltage Angle       -1.87 deg   @ bus 3          1.52 deg   @ bus 4
P Losses (I^2*R)             -                 1.84 MW    @ line 3-4
Q Losses (I^2*X)             -                 9.18 MVAr  @ line 3-4

==========================================================================
|     Bus Data                                                           |
==========================================================================
Bus      Voltage          Generation             Load
 #   Mag(pu)  Ang(deg)   P (MW)   Q (MVAr)   P (MW)   Q (MVAr)
---  -------  --------  --------  --------  --------  --------
  1   1.000     0.000    186.81    114.50     50.00     30.99
  2   0.982    -0.976       -         -      170.00    105.35
  3   0.969    -1.872       -         -      200.00    123.94
  4   1.020     1.523    318.00    181.43     80.00     49.58
                        --------  --------  --------  --------
               Total:    504.81    295.93    500.00    309.86

==========================================================================
|     Branch Data                                                        |
==========================================================================
Brnch   From   To    From Bus Injection   To Bus Injection     Loss (I^2 * Z)
  #     Bus    Bus    P (MW)   Q (MVAr)   P (MW)   Q (MVAr)   P (MW)   Q (MVAr)
-----  -----  -----  --------  --------  --------  --------  --------  --------
   1      1      2     38.69     22.30    -38.46    -31.24     0.227     1.13
   2      1      3     98.12     61.21    -97.09    -63.57     1.031     5.16
   3      2      4   -131.54    -74.11    133.25     74.92     1.715     8.58
   4      3      4   -102.91    -60.37    104.75     56.93     1.835     9.18
                                                             --------  --------
                                                  Total:     4.809     24.05
```

E.2 Test System II

```
Newton's method power flow converged in 4 iterations.

Converged in 0.69 seconds
==========================================================================
|     System Summary                                                     |
==========================================================================

How many?                How much?              P (MW)       Q (MVAr)
---------------------    --------------------  ---------  -----------------
Buses               9    Total Gen Capacity      820.0   -900.0 to +900.0
Generators          3    On-line Capacity        820.0   -900.0 to +900.0
Commited Gens       3    Generation (current)    320.0         34.9
Loads               3    Load                    315.0        115.0
Branches            9    Losses (I^2 * Z)          4.95        51.31
Transformers        0    Branch Charging (inj)      -          131.4
Areas               1    Shunt (inj)              0.0            0.0
Inter-ties          0    Total Inter-tie Flow     0.0            0.0

                          Minimum                     Maximum
                    ------------------------  --------------------------------
Voltage Magnitude    0.958 p.u. @ bus 9          1.003 p.u. @ bus 6
Voltage Angle       -4.35 deg   @ bus 9          9.67 deg   @ bus 2
P Losses (I^2*R)             -                 2.46 MW    @ line 8-9
Q Losses (I^2*X)             -                16.74 MVAr  @ line 8-2

==========================================================================
|     Bus Data                                                           |
==========================================================================
Bus      Voltage          Generation             Load
 #   Mag(pu)  Ang(deg)   P (MW)   Q (MVAr)   P (MW)   Q (MVAr)
---  -------  --------  --------  --------  --------  --------
  1   1.000     0.000     71.95     24.07       -         -
  2   1.000     9.669    163.00     14.46       -         -
  3   1.000     4.771     85.00     -3.65       -         -
  4   0.987    -2.407       -         -         -         -
  5   0.975    -4.017       -         -       90.00     30.00
  6   1.003     1.926       -         -         -         -
  7   0.986     0.622       -         -      100.00     35.00
  8   0.996     3.799       -         -         -         -
  9   0.958    -4.350       -         -      125.00     50.00
                        --------  --------  --------  --------
              Total:    319.95     34.88    315.00    115.00

==========================================================================
|     Branch Data                                                        |
==========================================================================
Brnch   From   To    From Bus Injection   To Bus Injection     Loss (I^2 * Z)
  #     Bus    Bus    P (MW)   Q (MVAr)   P (MW)   Q (MVAr)   P (MW)   Q (MVAr)
-----  -----  -----  --------  --------  --------  --------  --------  --------
   1      1      4     71.95     24.07    -71.95    -20.75     0.000      3.32
   2      4      5     30.73     -0.59    -30.55    -13.69     0.174      0.94
   3      5      6    -59.45    -16.31     60.89    -12.43     1.449      6.31
   4      3      6     85.00     -3.65    -85.00      7.89     0.000      4.24
   5      6      7     24.11      4.54    -24.01    -24.40     0.095      0.81
   6      7      8    -75.99    -10.60     76.50      0.26     0.506      4.29
   7      8      2   -163.00      2.28    163.00     14.46     0.000     16.74
   8      8      9     86.50     -2.53    -84.04    -14.28     2.465     12.40
   9      9      4    -40.96    -35.72     41.23     21.34     0.266      2.26
                                                             --------  --------
                                                   Total:     4.955     51.31
```

E.3 Test System III

Newton's method power flow converged in 2 iterations.

Converged in 0.95 seconds

System Summary

How many?		How much?	P (MW)	Q (MVAr)
Buses	14	Total Gen Capacity	772.4	-52.0 to +148.0
Generators	5	On-line Capacity	772.4	-52.0 to +148.0
Commited Gens	5	Generation (current)	272.4	78.5
Loads	11	Load	259.0	73.5
Branches	20	Losses (I^2 * Z)	13.39	54.50
Transformers	3	Branch Charging (inj)	-	28.3
Areas	1	Shunt (inj)	0.0	21.2
Inter-ties	0	Total Inter-tie Flow	0.0	0.0

	Minimum	Maximum
Voltage Magnitude	1.010 p.u. @ bus 3	1.090 p.u. @ bus 8
Voltage Angle	-16.04 deg @ bus 14	0.00 deg @ bus 1
P Losses (I^2*R)	-	4.29 MW @ line 1-2
Q Losses (I^2*X)	-	13.11 MVAr @ line 1-2

Bus Data

Bus #	Voltage Mag(pu)	Voltage Ang(deg)	Generation P (MW)	Generation Q (MVAr)	Load P (MW)	Load Q (MVAr)
1	1.060	0.000	232.39	-16.89	-	-
2	1.045	-4.981	40.00	42.40	21.70	12.70
3	1.010	-12.718	0.00	23.39	94.20	19.00
4	1.019	-10.324	-	-	47.80	-3.90
5	1.020	-8.783	-	-	7.60	1.60
6	1.070	-14.223	0.00	12.24	11.20	7.50
7	1.062	-13.368	-	-	-	-
8	1.090	-13.368	0.00	17.36	-	-
9	1.056	-14.947	-	-	29.50	16.60
10	1.051	-15.104	-	-	9.00	5.80
11	1.057	-14.795	-	-	3.50	1.80
12	1.055	-15.077	-	-	6.10	1.60
13	1.050	-15.159	-	-	13.50	5.80
		Total:	272.39	78.50	259.00	73.50

Branch Data

Brnch #	From Bus	To Bus	From Bus Injection P (MW)	From Bus Injection Q (MVAr)	To Bus Injection P (MW)	To Bus Injection Q (MVAr)	Loss (I^2 * Z) P (MW)	Loss (I^2 * Z) Q (MVAr)
1	1	2	156.83	-20.39	-152.54	27.66	4.295	13.11
2	1	5	75.55	3.50	-72.79	2.58	2.764	11.41
3	2	3	73.19	3.57	-70.87	1.58	2.320	9.77
4	2	4	56.14	-2.29	-54.46	3.39	1.677	5.09
5	2	5	41.51	0.76	-40.61	-1.63	0.902	2.75
6	3	4	-23.33	2.81	23.70	-5.42	0.371	0.95
7	4	5	-61.22	15.67	61.74	-15.37	0.517	1.63
8	4	7	28.09	-9.42	-28.09	11.11	0.000	1.69
9	4	9	16.09	-0.32	-16.09	1.62	0.000	1.30
10	5	6	44.06	12.82	-44.06	-8.39	0.000	4.43
11	6	11	7.34	3.47	-7.29	-3.36	0.055	0.11
12	6	12	7.78	2.49	-7.71	-2.34	0.072	0.15
13	6	13	17.74	7.17	-17.53	-6.75	0.212	0.42
14	7	8	-0.00	-16.91	0.00	17.36	0.000	0.45
15	7	9	28.09	5.80	-28.09	-4.99	0.000	0.80
16	9	10	5.24	4.31	-5.23	-4.27	0.013	0.03
17	9	14	9.44	3.67	-9.32	-3.42	0.117	0.25
18	10	11	-3.77	-1.53	3.79	1.56	0.012	0.03
19	12	13	1.61	0.74	-1.60	-0.74	0.006	0.01
20	13	14	5.63	1.69	-5.58	-1.58	0.054	0.11
					Total:		13.386	54.50

E.4 Test System IV

```
Newton's method power flow converged in 2 iterations.

Converged in 0.22 seconds
==========================================================================================
|     System Summary                                                                     |
==========================================================================================

How many?                How much?              P (MW)       Q (MVAr)
---------------------    --------------------  --------  -----------------
Buses              30    Total Gen Capacity      900.2   -102.0 to +188.0
Generators          6    On-line Capacity        900.2   -102.0 to +188.0
Commited Gens       6    Generation (current)    301.0        133.9
Loads              21    Load                    283.4        126.2
Branches           41    Losses (I^2 * Z)         17.56        67.69
Transformers        4    Branch Charging (inj)      -          34.7
Areas               1    Shunt (inj)              0.0          25.3
Inter-ties          0    Total Inter-tie Flow     0.0           0.0

                          Minimum                      Maximum
                    -------------------------  ---------------------------------
Voltage Magnitude    0.992 p.u. @ bus 30        1.082 p.u. @ bus 11
Voltage Angle      -17.64 deg   @ bus 30         0.00 deg   @ bus 1
P Losses (I^2*R)             -                  5.21 MW    @ line 1-2
Q Losses (I^2*X)             -                 15.61 MVAr  @ line 1-2

==========================================================================================
|     Bus Data                                                                           |
==========================================================================================
Bus      Voltage          Generation             Load
 #   Mag(pu)  Ang(deg)   P (MW)   Q (MVAr)   P (MW)   Q (MVAr)
---  -------  --------  --------  --------  --------  --------
  1   1.060     0.000    260.96    -20.42       -         -
  2   1.045    -5.378     40.00     56.07     21.70     12.70
  3   1.021    -7.529       -         -       2.40      1.20
  4   1.012    -9.279       -         -       7.60      1.60
  5   1.010   -14.149      0.00     35.66     94.20     19.00
  6   1.011   -11.055       -         -         -         -
  7   1.003   -12.852       -         -       22.80     10.90
  8   1.010   -11.797      0.00     36.11     30.00     30.00
  9   1.051   -14.098       -         -         -         -
 10   1.045   -15.688       -         -       5.80      2.00
 11   1.082   -14.098      0.00     16.06       -         -
 12   1.057   -14.933       -         -       11.20     7.50
 13   1.071   -14.933      0.00     10.45       -         -
 14   1.043   -15.825       -         -       6.20      1.60
 15   1.038   -15.916       -         -       8.20      2.50
 16   1.045   -15.515       -         -       3.50      1.80
 17   1.040   -15.850       -         -       9.00      5.80
 18   1.028   -16.530       -         -       3.20      0.90
 19   1.026   -16.704       -         -       9.50      3.40
 20   1.030   -16.507       -         -       2.20      0.70
 21   1.033   -16.131       -         -      17.50     11.20
 22   1.034   -16.116       -         -         -         -
 23   1.027   -16.307       -         -       3.20      1.60
 24   1.022   -16.483       -         -       8.70      6.70
 25   1.018   -16.055       -         -         -         -
 26   1.000   -16.474       -         -       3.50      2.30
 27   1.024   -15.530       -         -         -         -
 28   1.007   -11.677       -         -         -         -
 29   1.004   -16.759       -         -       2.40      0.90
 30   0.992   -17.642       -         -      10.60      1.90
                        --------  --------  --------  --------
               Total:    300.96    133.93    283.40    126.20
```

Branch Data								
Brnch #	From Bus	To Bus	From Bus Injection P (MW)	From Bus Injection Q (MVAr)	To Bus Injection P (MW)	To Bus Injection Q (MVAr)	Loss (I^2 * Z) P (MW)	Loss (I^2 * Z) Q (MVAr)
1	1	2	173.31	-24.70	-168.09	34.47	5.213	15.61
2	1	3	87.65	4.28	-84.54	2.65	3.108	11.36
3	2	4	43.65	4.75	-42.63	-5.54	1.018	3.10
4	3	4	82.14	-3.85	-81.29	5.44	0.856	2.46
5	2	5	82.36	2.78	-79.42	5.17	2.943	12.36
6	2	6	60.38	1.37	-58.43	0.58	1.946	5.90
7	4	6	72.13	-15.91	-71.50	17.19	0.632	2.20
8	5	7	-14.78	11.49	14.95	-13.13	0.169	0.43
9	6	7	38.13	-2.78	-37.75	2.23	0.381	1.17
10	6	8	29.56	-7.20	-29.46	6.66	0.108	0.38
11	6	9	27.72	-8.09	-27.72	9.72	0.000	1.62
12	6	10	15.84	0.19	-15.84	1.10	0.000	1.28
13	9	11	-0.00	-15.60	0.00	16.06	0.000	0.46
14	9	10	27.72	5.88	-27.72	-5.08	0.000	0.80
15	4	12	44.19	14.41	-44.19	-9.72	0.000	4.69
16	12	13	0.00	-10.32	-0.00	10.45	0.000	0.13
17	12	14	7.86	2.40	-7.78	-2.25	0.074	0.15
18	12	15	17.89	6.79	-17.67	-6.36	0.217	0.43
19	12	16	7.24	3.35	-7.19	-3.24	0.054	0.11
20	14	15	1.58	0.65	-1.58	-0.64	0.006	0.01
21	16	17	3.69	1.44	-3.68	-1.41	0.008	0.03
22	15	18	6.02	1.60	-5.98	-1.52	0.039	0.08
23	18	19	2.78	0.62	-2.77	-0.61	0.005	0.01
24	19	20	-6.73	-2.79	6.74	2.83	0.017	0.03
25	10	20	9.03	3.71	-8.94	-3.53	0.082	0.18
26	10	17	5.33	4.43	-5.32	-4.39	0.014	0.04
27	10	21	15.79	10.01	-15.67	-9.77	0.111	0.24
28	10	22	7.62	4.60	-7.57	-4.49	0.053	0.11
29	21	22	-1.83	-1.43	1.83	1.43	0.001	0.00
30	15	23	5.04	2.91	-5.00	-2.84	0.031	0.06
31	22	24	5.74	3.06	-5.69	-2.99	0.046	0.07
32	23	24	1.80	1.24	-1.80	-1.23	0.006	0.01
33	24	25	-1.21	2.01	1.22	-2.00	0.010	0.02
34	25	26	3.54	2.37	-3.50	-2.30	0.045	0.07
35	25	27	-4.76	-0.37	4.79	0.42	0.024	0.05
36	28	27	18.07	5.04	-18.07	-3.75	0.000	1.29
37	27	29	6.19	1.67	-6.10	-1.51	0.086	0.16
38	27	30	7.09	1.66	-6.93	-1.36	0.162	0.31
39	29	30	3.70	0.61	-3.67	-0.54	0.034	0.06
40	8	28	-0.54	-0.54	0.55	-3.80	0.002	0.01
41	6	28	18.67	0.11	-18.62	-1.23	0.058	0.20
						Total:	17.557	67.69

E.5 19-Bus TNB Kelantan System

```
%   POWER FLOW RESULTS FOR 19-BUS TENAGA NATIONAL BERHAD SYSTEM.
% ------------------------------------------------------------
%   Data given by:                                  Aras 1, Banggunan NLDC,
%   Ahmad Khairulnizam Bin Khairuddin               129, Jalan Bangsar, 59200,
%   Planning Eng. (Grid System Planning)            Wilayah Persekutuan K.L.
%   System Planning and Development Unit            Office  : 03-22966805
%   System Planning and Operation Department        Mobile  : 019-3382806
%   Transmission Division                           Fax     : 03-22822906
%   TENAGA NATIONAL BERHAD

Newton's method power flow converged in 4 iterations.

Converged in 1.36 seconds
================================================================================
|     System Summary                                                           |
================================================================================

How many?                How much?              P (MW)       Q (MVAr)
---------------------    --------------------  --------  -----------------
Buses              19    Total Gen Capacity     1000.0   -279.2 to +619.2
Generators          8    On-line Capacity       1000.0   -279.2 to +619.2
Commited Gens       8    Generation (current)    680.3        -85.7
Loads              10    Load                  -3060.7       8018.7
Branches           29    Losses (I^2 * Z)        17.04        240.20
Transformers       11    Branch Charging (inj)     -          163.3
Areas               1    Shunt (inj)           -3723.9       8181.3
Inter-ties          0    Total Inter-tie Flow      0.0          0.0

                         Minimum                      Maximum
                    -------------------------  --------------------------------
Voltage Magnitude    0.995 p.u. @ bus 5          1.081 p.u. @ bus 10
Voltage Angle      -24.04 deg   @ bus 5          0.00 deg   @ bus 16
P Losses (I^2*R)             -                  9.31 MW    @ line 10-11
Q Losses (I^2*X)             -                100.15 MVAr  @ line 11-16

================================================================================
|     Bus Data                                                                 |
================================================================================
Bus      Voltage          Generation             Load
 #   Mag(pu)  Ang(deg)   P (MW)   Q (MVAr)   P (MW)   Q (MVAr)
---  -------  --------  --------  --------  --------  --------
  1   1.021   -21.291       -         -       23.89      8.67
  2   0.999   -23.574       -         -       62.12     22.55
  3   1.023   -21.510       -         -        7.96      2.89
  4   1.007   -22.644       -         -       53.62     19.62
  5   0.995   -24.042       -         -       55.58     20.17
  6   1.012   -22.245       -         -       19.62      7.12
  7   1.029   -21.784       -         -        2.77      1.00
  8   1.020   -21.428       -         -       11.44      4.15
  9   1.041   -17.316       -         -          -         -
 10   1.081   -11.802       -         -    -1932.33   2884.29
 11   1.036   -17.770       -         -    -1365.33   5048.27
 12   1.040    -7.087     90.00    -37.75       -         -
 13   1.040    -7.087     90.00    -37.75       -         -
 14   1.040    -7.087     90.00    -37.75       -         -
 15   1.040    -7.087     90.00    -37.75       -         -
 16   1.040     0.000    320.29     53.89       -         -
 17   1.040   -17.770      0.00      3.82       -         -
 18   1.040   -17.770      0.00      3.82       -         -
 19   1.040   -17.770      0.00      3.82       -         -
                        --------  --------  --------  --------
               Total:    680.29    -85.66  -3060.66   8018.75
```

Branch Data								
Brnch #	From Bus	To Bus	From Bus Injection P (MW)	From Bus Injection Q (MVAr)	To Bus Injection P (MW)	To Bus Injection Q (MVAr)	Loss (I^2 * Z) P (MW)	Loss (I^2 * Z) Q (MVAr)
1	1	2	75.14	25.48	-74.55	-24.79	0.594	3.52
2	1	3	5.38	-5.70	-5.37	4.23	0.007	0.03
3	1	3	5.38	-5.70	-5.37	4.23	0.007	0.03
4	1	4	26.98	7.24	-26.81	-8.83	0.174	0.74
5	1	4	26.98	7.24	-26.81	-8.83	0.174	0.74
6	1	6	63.27	20.83	-63.07	-21.02	0.209	1.24
7	1	8	5.72	-0.16	-5.72	-2.08	0.002	0.01
8	1	8	5.72	-0.16	-5.72	-2.08	0.002	0.01
9	1	9	-79.49	-19.24	79.49	25.19	0.000	5.95
10	1	9	-79.49	-19.24	79.49	25.19	0.000	5.95
11	1	9	-79.49	-19.24	79.49	25.19	0.000	5.95
12	2	5	27.84	8.87	-27.79	-10.09	0.045	0.27
13	2	5	27.84	8.87	-27.79	-10.09	0.045	0.27
14	2	6	-43.24	-15.50	43.45	13.90	0.201	1.19
15	3	7	1.39	-5.68	-1.38	-0.50	0.005	0.02
16	3	7	1.39	-5.68	-1.38	-0.50	0.005	0.02
17	9	10	-184.47	-57.16	187.50	23.97	3.027	19.48
18	9	10	-184.47	-57.16	187.50	23.97	3.027	19.48
19	9	11	65.23	19.37	-65.14	-30.42	0.098	0.63
20	9	11	65.23	19.37	-65.14	-30.42	0.098	0.63
21	10	11	346.20	68.25	-336.88	-30.57	9.314	37.68
22	10	12	-90.00	46.79	90.00	-37.75	0.000	9.04
23	10	13	-90.00	46.79	90.00	-37.75	0.000	9.04
24	10	14	-90.00	46.79	90.00	-37.75	0.000	9.04
25	10	15	-90.00	46.79	90.00	-37.75	0.000	9.04
26	11	16	-320.29	46.26	320.29	53.89	0.000	100.15
27	11	17	-0.00	-3.81	0.00	3.82	0.000	0.01
28	11	18	-0.00	-3.81	0.00	3.82	0.000	0.01
29	11	19	-0.00	-3.81	0.00	3.82	0.000	0.01
					Total:		17.037	240.20

```
% TNB Load Flow Results
% Date: 14-07-2006
% Prepared by: Mohd Redzuan bin Ahmad
```

APPENDIX F

PSCAD/EMTDC V4 Schematic Diagram

E.1 Test System I

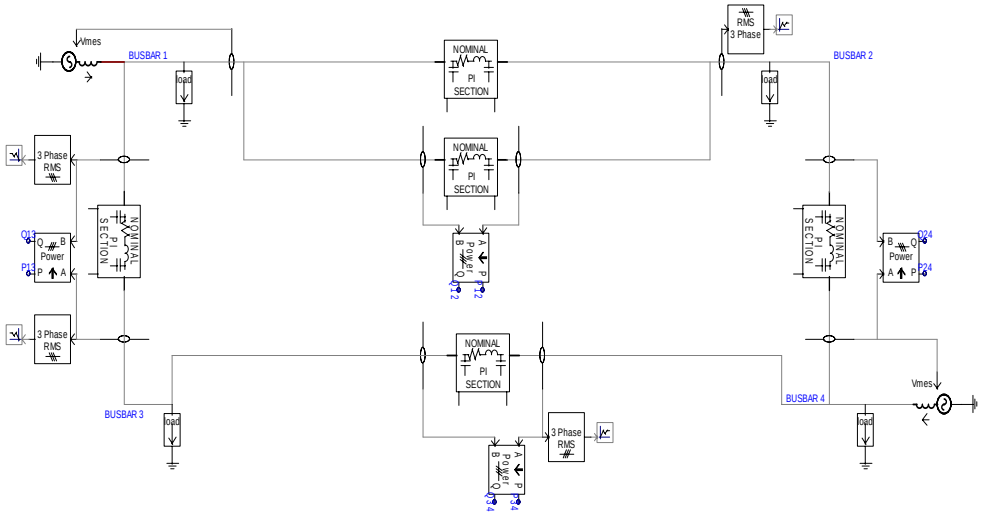

(a) Test System I with three-phase double-circuit transmission line

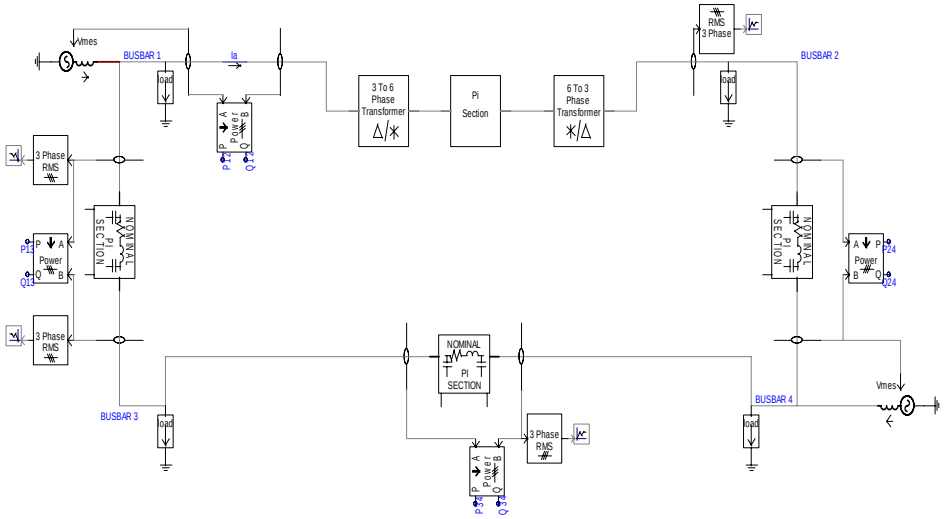

(b) Test system I with six-phase single-circuit transmission line

E.2 Test System II

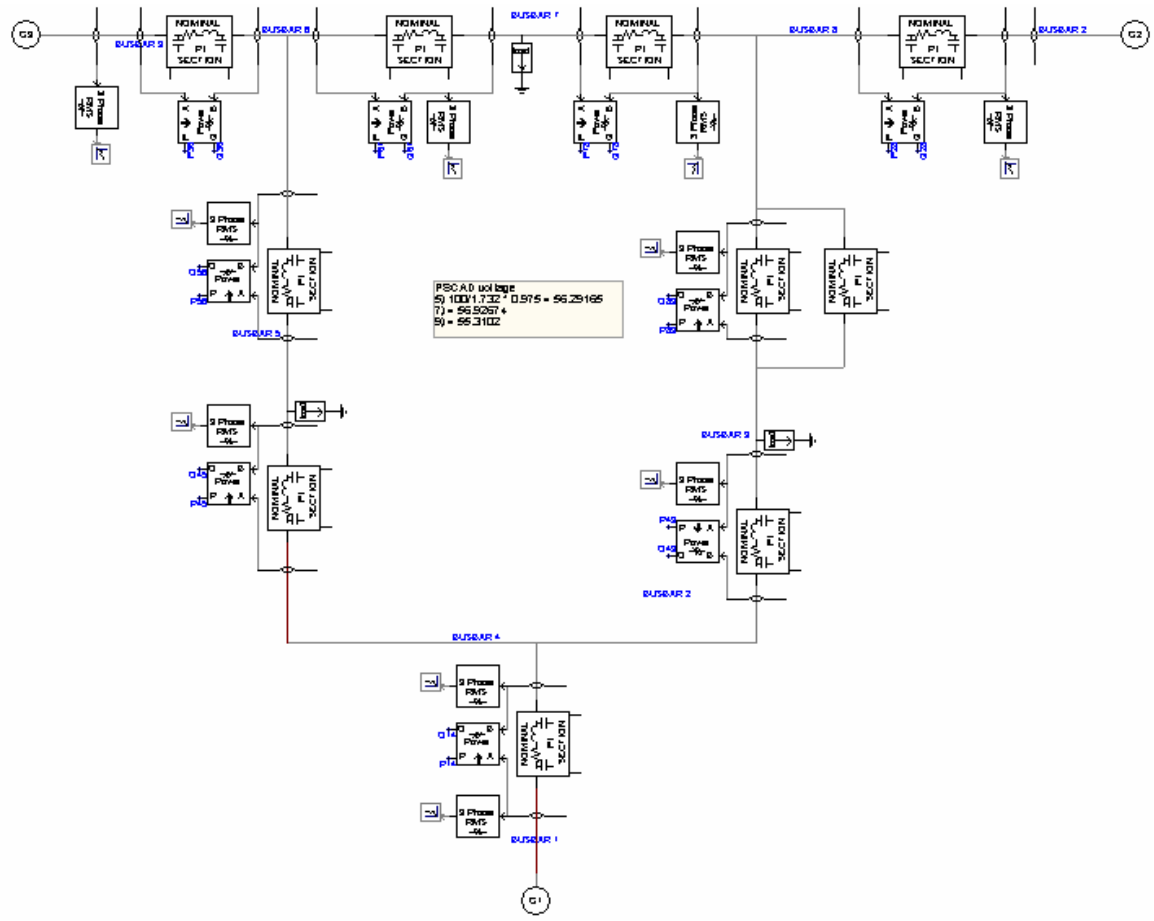

(a) Test System II with three-phase double-circuit transmission line

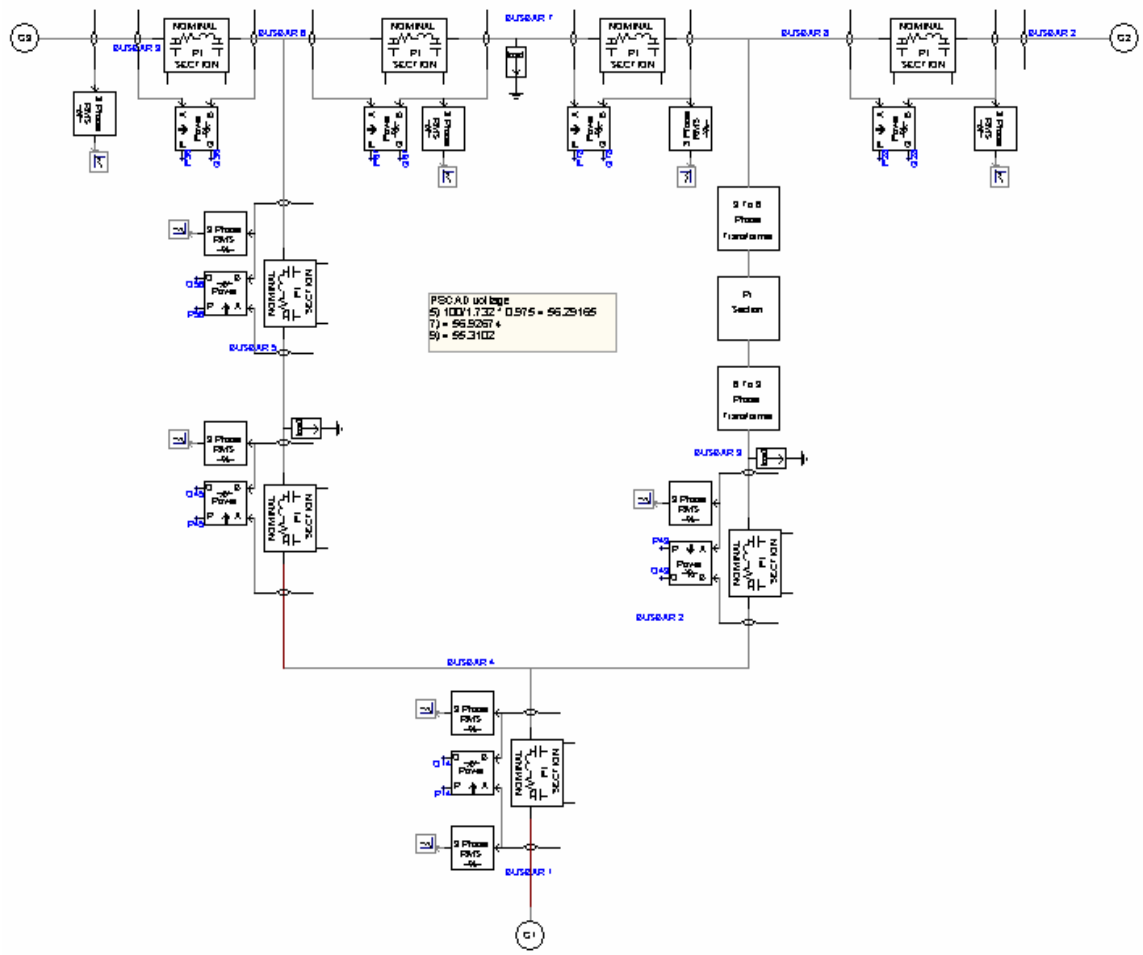

(b) Test System II with six-phase single-circuit transmission line

E.3 Test System III

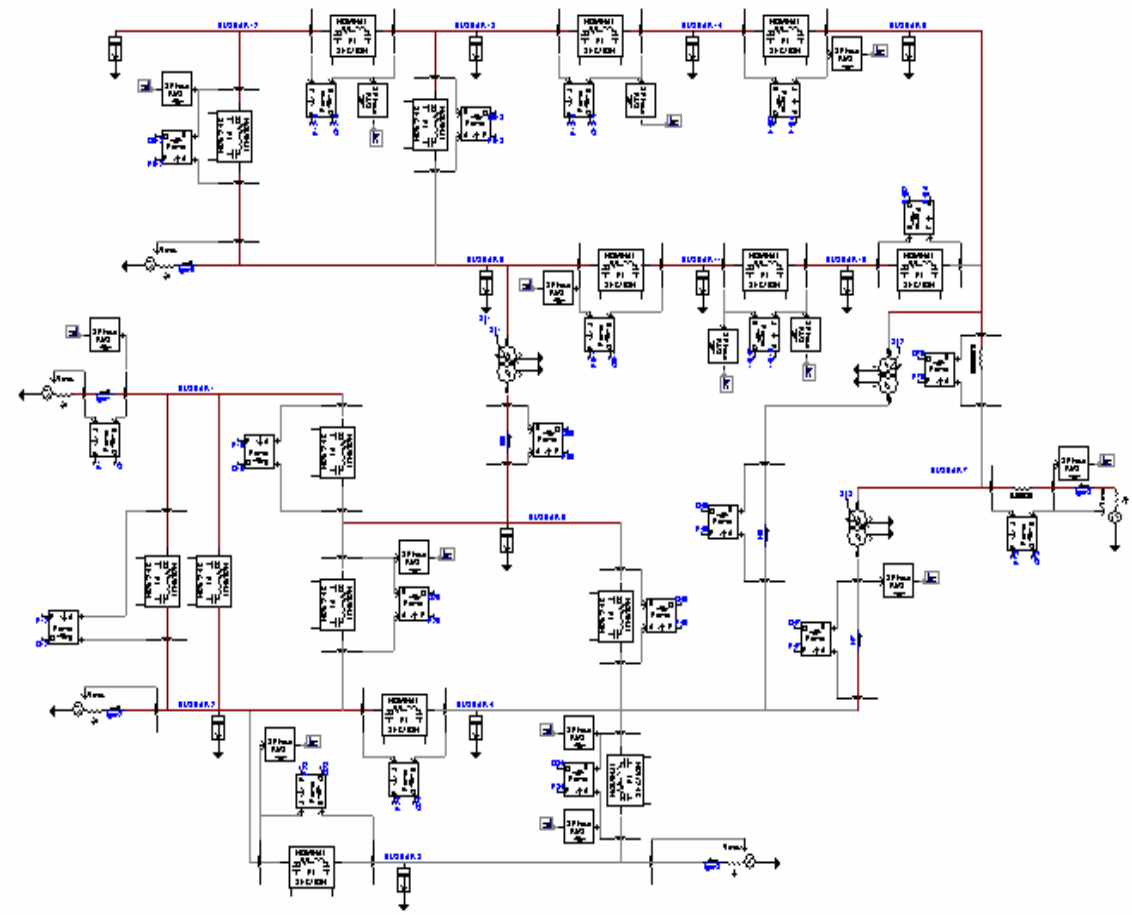

(a) Test System III with three-phase double-circuit transmission line

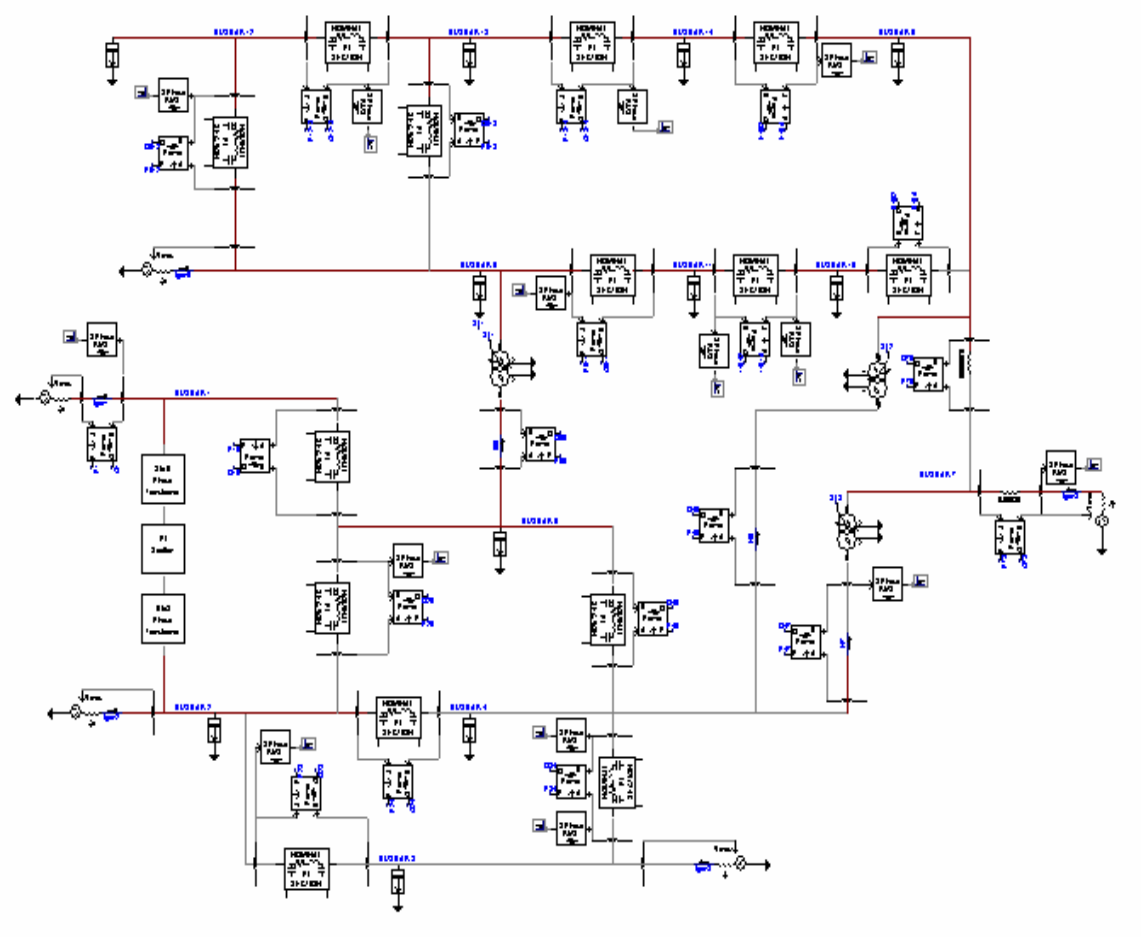

(b) Test System III with six-phase single-circuit transmission line

E.4 Test System IV

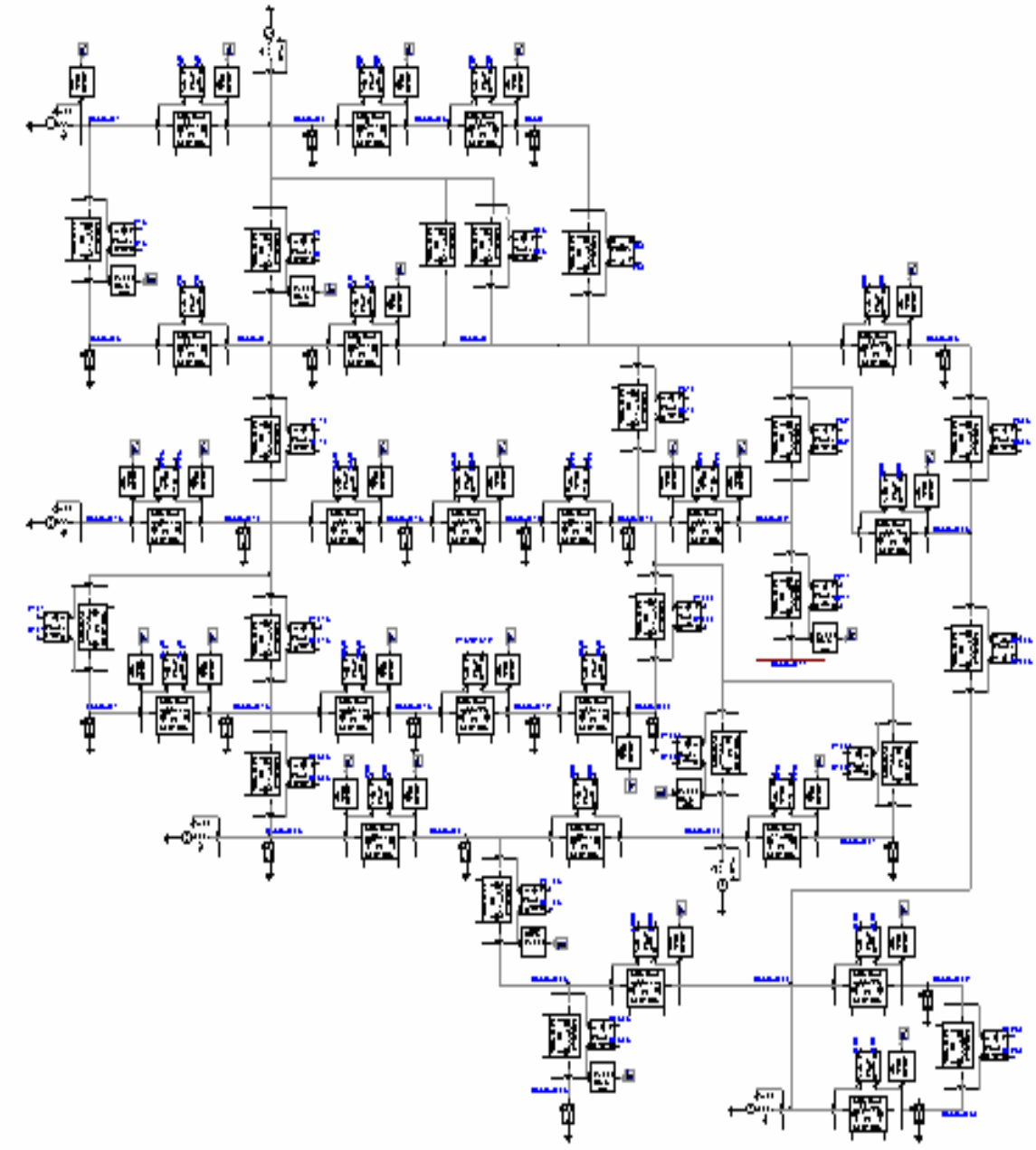

(a) Test System IV with three-phase double-circuit transmission line

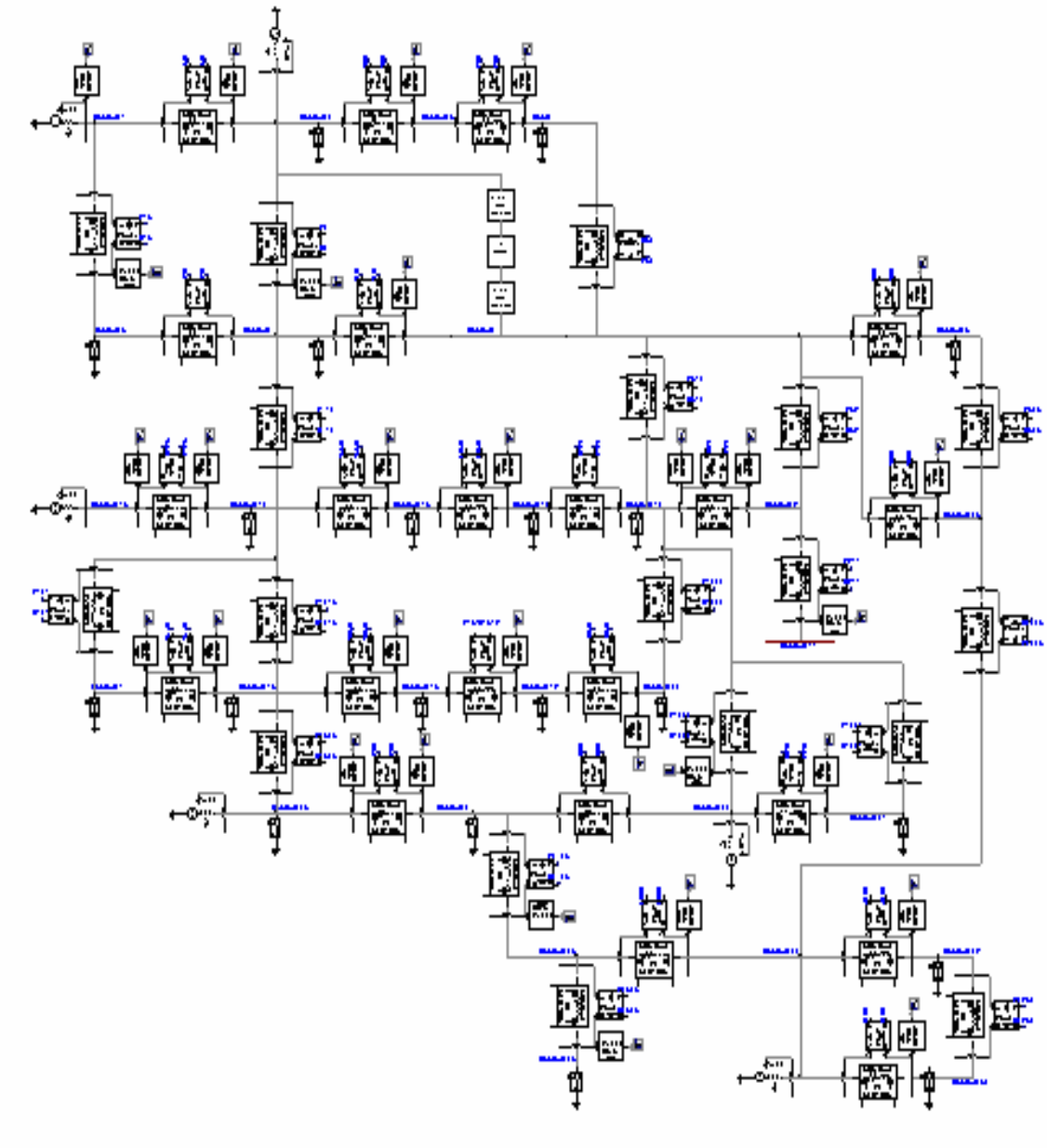

(a) Test System IV with six-phase single-circuit transmission line

E.6 19-Bus TNB Kelantan System

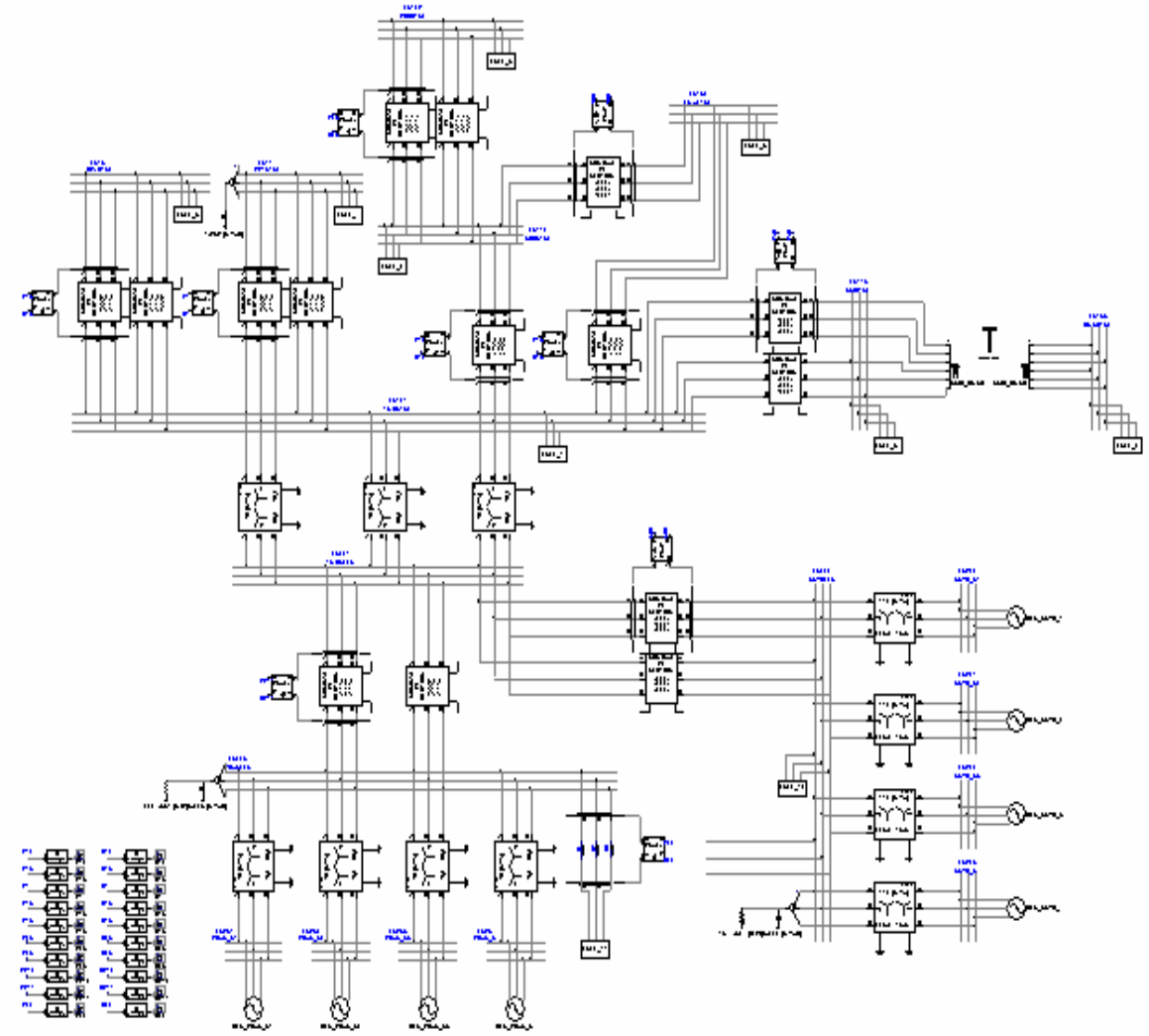

(a) 19-Bus TNB Kelantan System with three-phase double-circuit transmission line

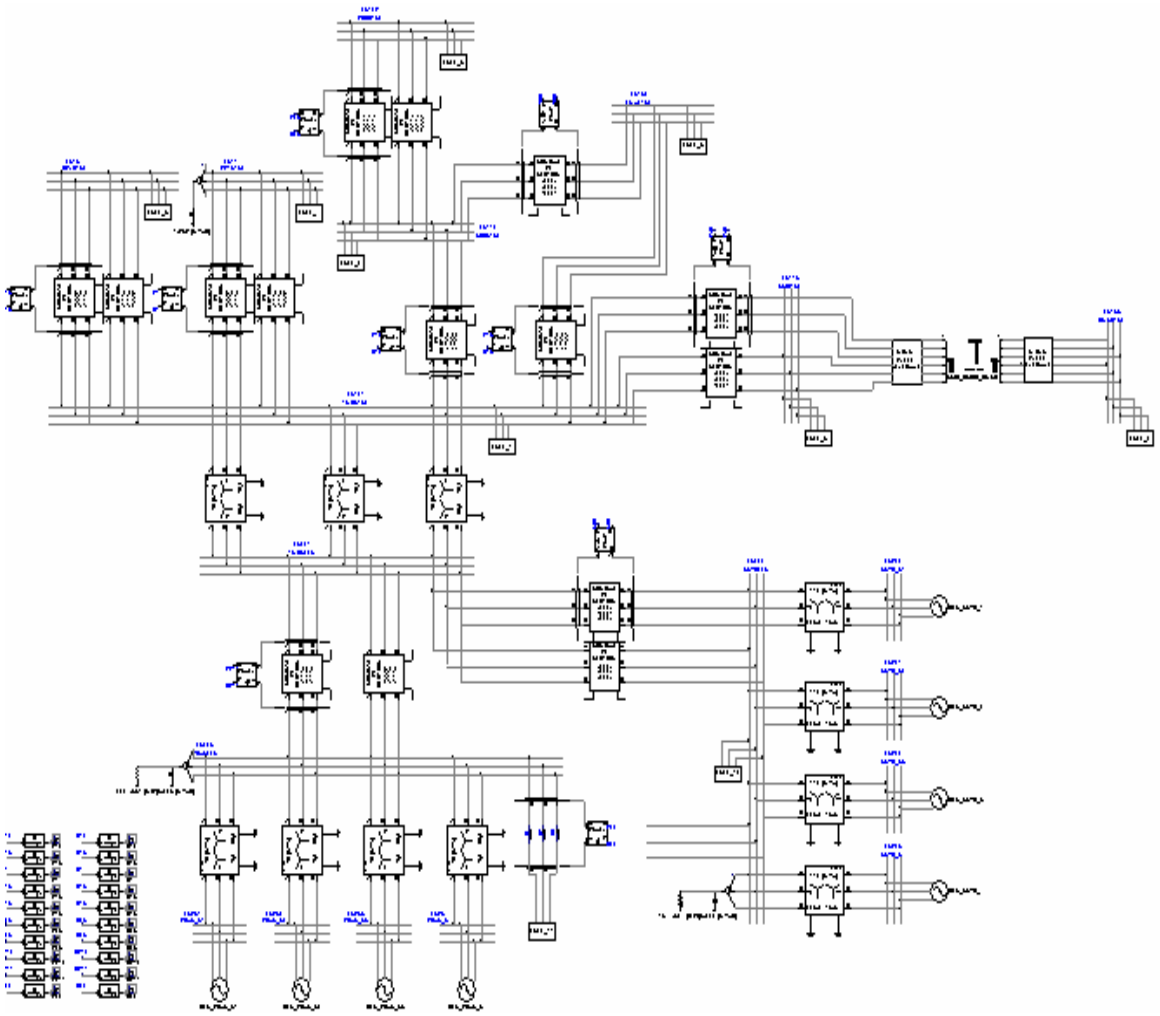

(b) 19-Bus TNB Kelantan System with six-phase single-circuit transmission line

APPENDIX G

PSCAD/EMTDC V4 Load Flow Analysis, Fault Analysis and Transient Stability Analysis Results

G.1 Test System I

Comparison of power flow for three-phase single-circuit (3PSC) and three-phase double-circuit (3PDC) by using MATLAB, PET and PSCAD/EMTDC

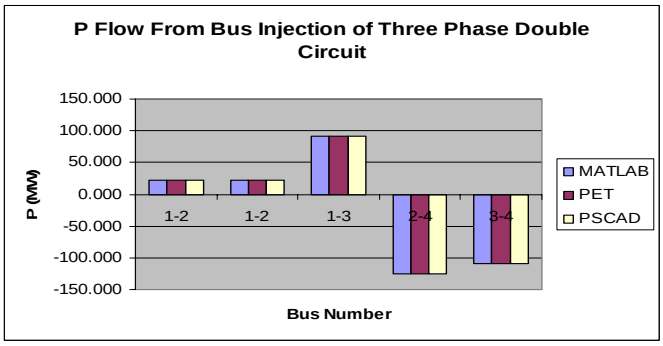

Graph G.1: The flow of real power P(MW) from bus injection of 3PDC at bus 1-2

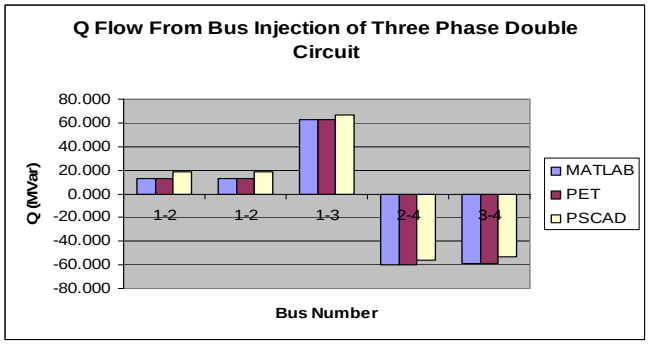

Graph G.2: The flow of reactive power Q(MVAR) from bus injection of 3PDC at bus 1-2

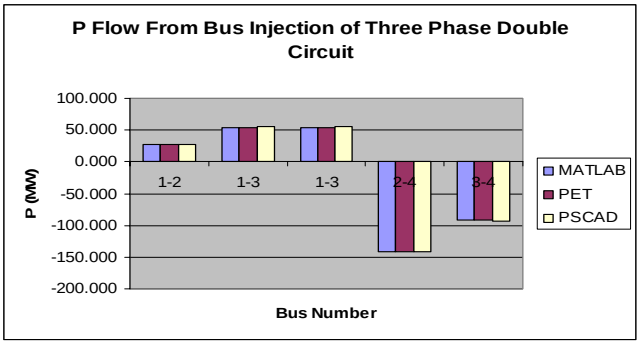

Graph G.3: The flow of P from bus injection of 3PDC at bus 1-3

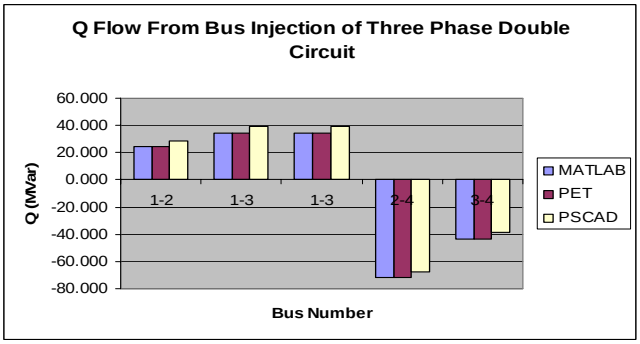

Graph G.4: The flow of Q from bus injection of 3PDC at bus 1-3

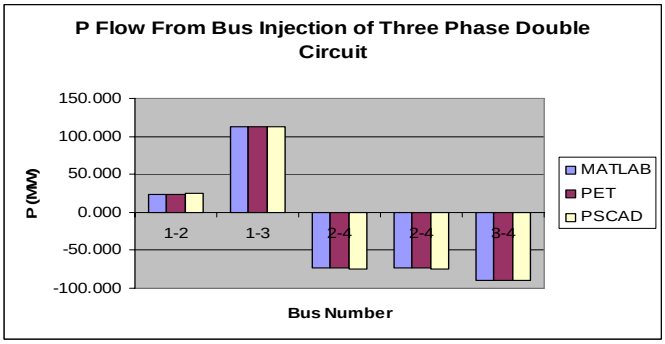

Graph G.5: The flow of P from bus injection of 3PDC at bus 2-4

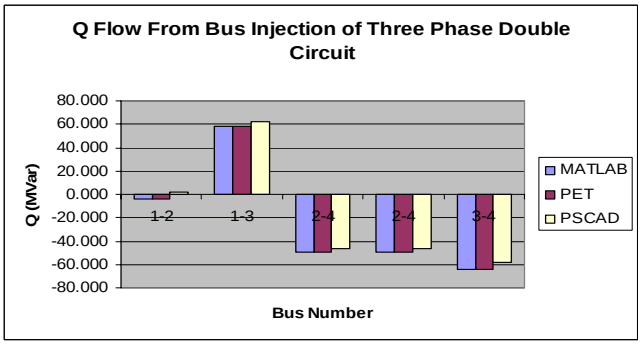

Graph G.6: The flow of Q from bus injection of 3PDC at bus 2-4

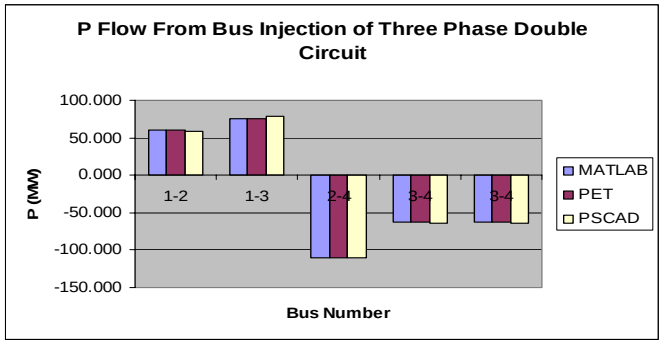

Graph G.7: The flow of P from bus injection of 3PDC at bus 3-4

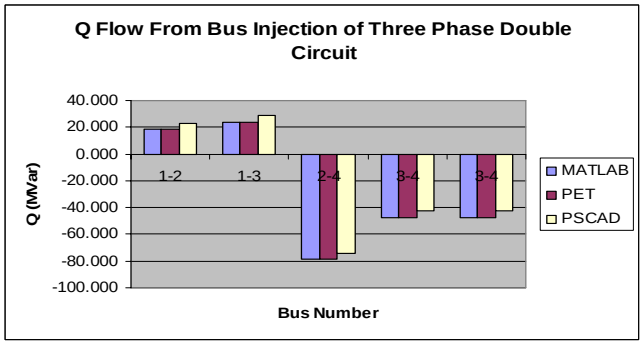

Graph G.8: The flow of Q from bus injection of 3PDC at bus 3-4

Comparison of voltage and generated power for 3PSC and 3PDC by using MATLAB, PET and PSCAD

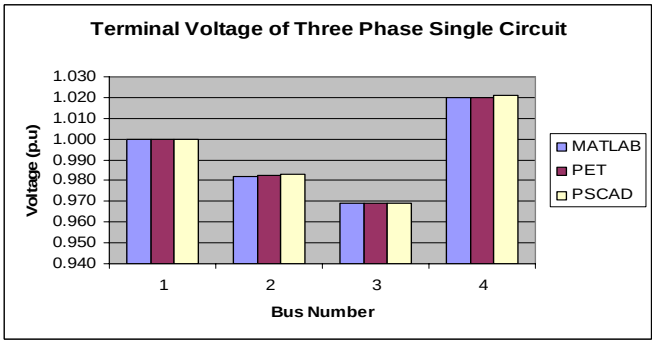

Graph G.9: Voltage of 3PSC

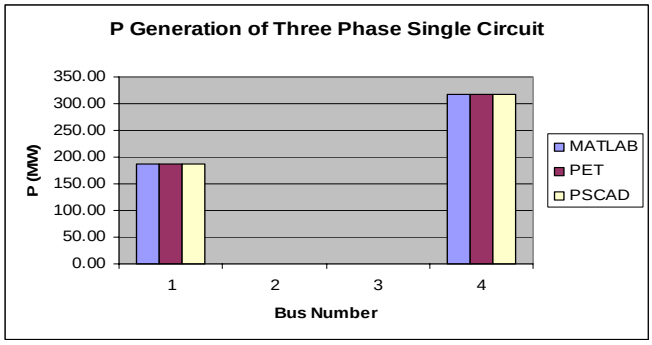

Graph G.10: P generated of 3PSC

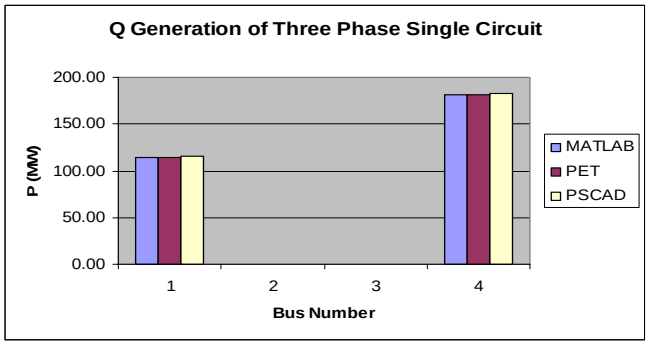

Graph G.11: Q generated of 3PSC

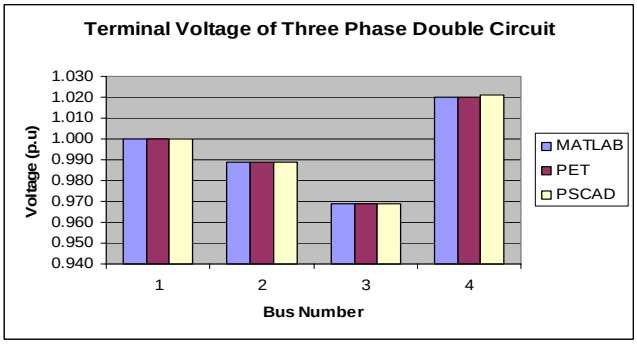

Graph G.12: Voltage for 3PDC transmission at bus 1-2

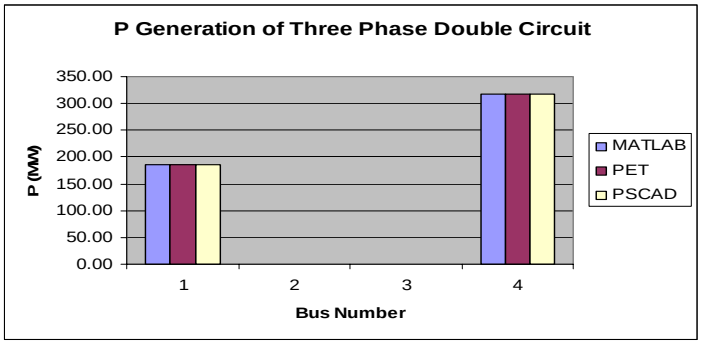

Graph G.13: P generated of 3PDC transmission at bus 1-2

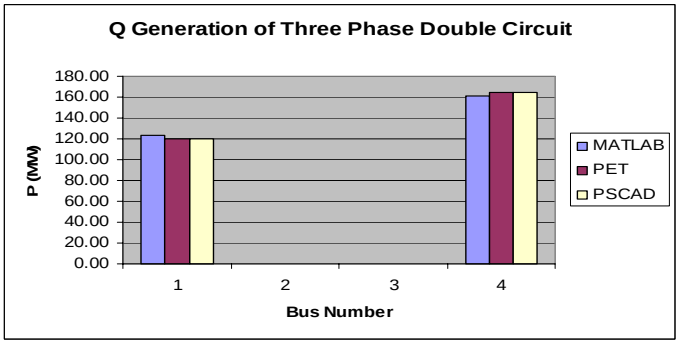

Graph G.14: Q generated of 3PDC transmission at bus 1-2

Comparison of power flow results for 3PDC and 6PSC transmission system by using PSCAD/EMTDC

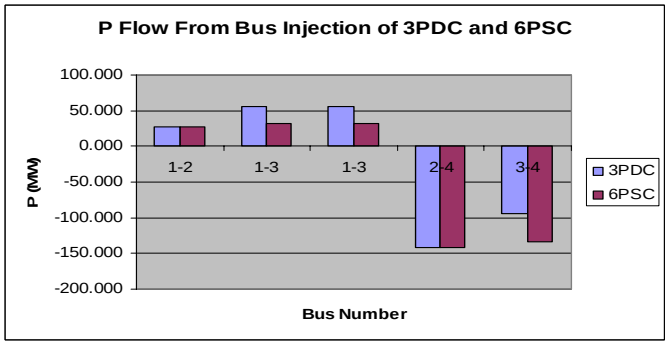

Graph G.15: The flow of P for 3PDC and 6PSC transmission at bus 1-2

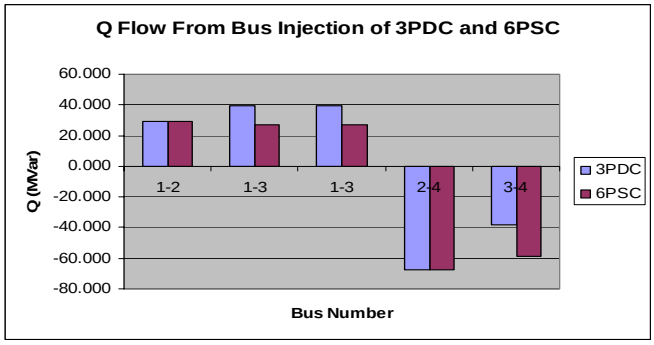

Graph G.16: The flow of Q for 3PDC and 6PSC transmission at bus 1-2

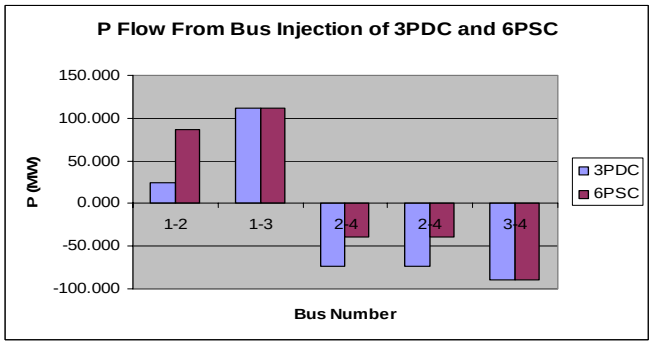

GraphG.17: The flow of P for 3PDC and 6PSC transmission at bus 2-4

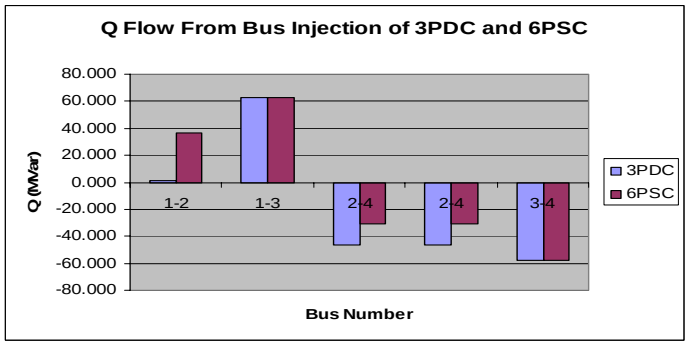

Graph G.18: The flow of Q for 3PDC and 6PSC transmission at bus 2-4

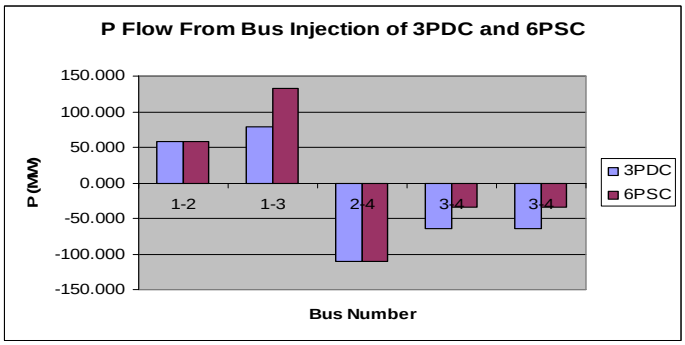

Graph G.19: The flow of P for 3PDC and 6PSC transmission at bus 3-4

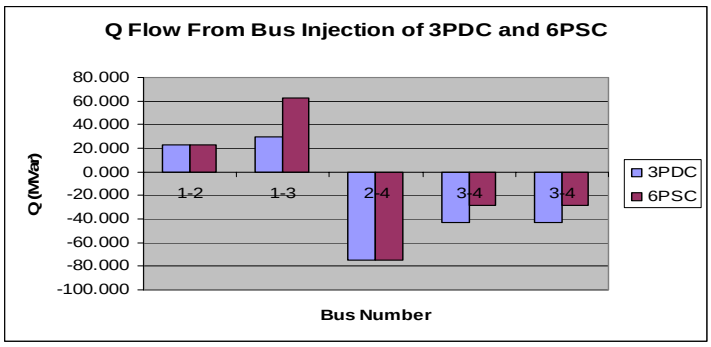

Graph G.20: The flow of Q for 3PDC and 6PSC transmission at bus 3-4

Comparison of terminal voltage, real power and reactive power results for 3PDC and 6PSC transmission system by using PSCAD/EMTDC

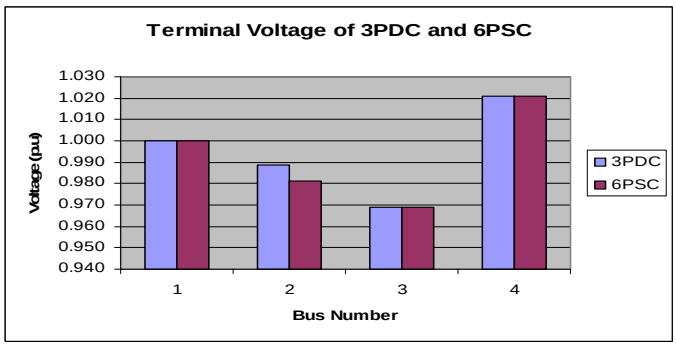

Graph G.21: Terminal voltage of 3PDC and 6PSC transmission at bus 1-2

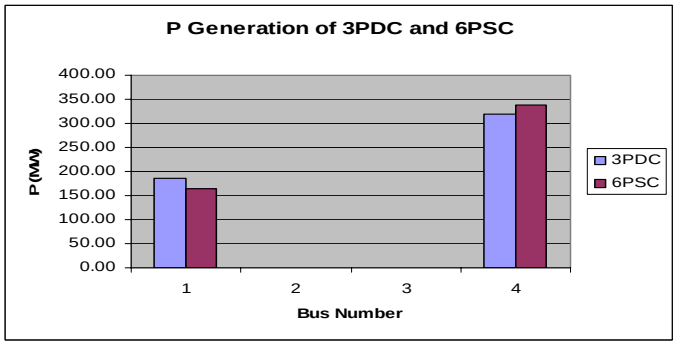

Graph G.22: P generated of 3PDC and 6PSC transmission at bus 1-2

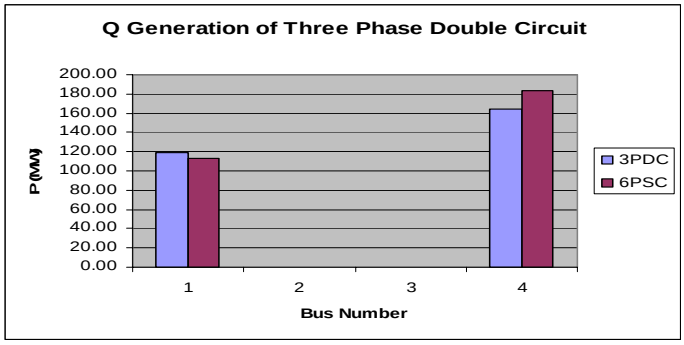

Graph G.23: Q generated of 3PDC and 6PSC transmission at bus 1-2

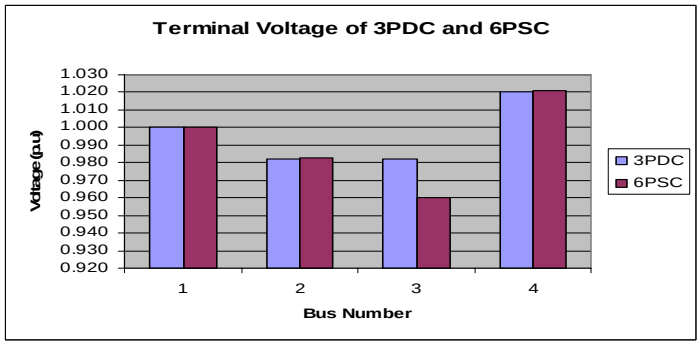

Graph G.24: Terminal voltage of 3PDC and 6PSC transmission at bus 1-3

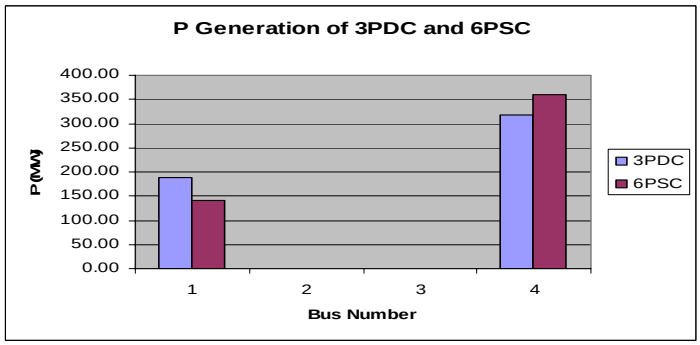

Graph G.25: P generated of 3PDC and 6PSC transmission at bus 1-3

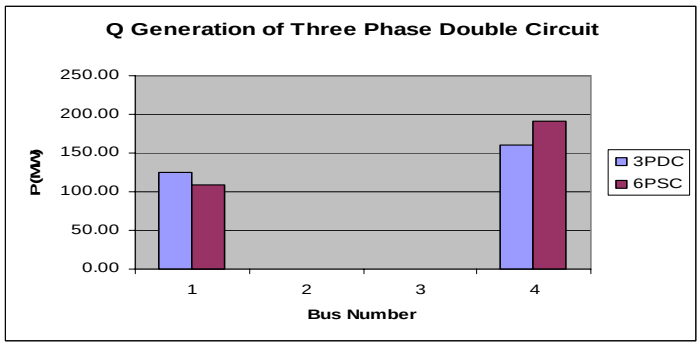

Graph G.26: Q generated of 3PDC and 6PSC transmission at bus 1-3

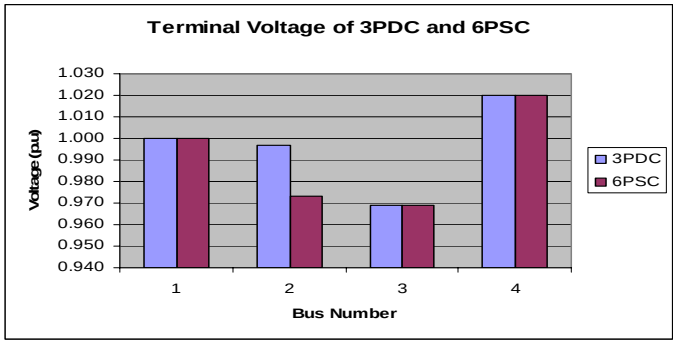

Graph G.27: Terminal voltage of 3PDC and 6PSC transmission at bus 2-4

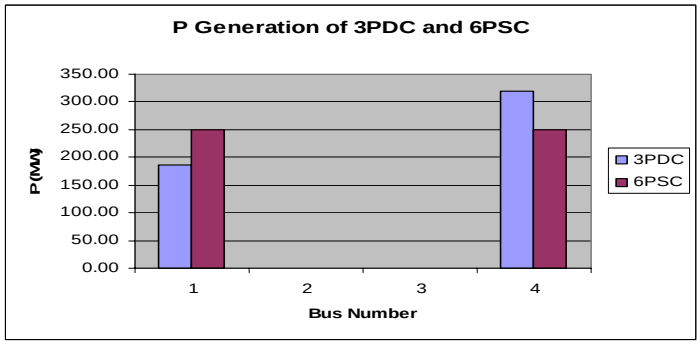

Graph G.28: P generated of 3PDC and 6PSC transmission at bus 2-4

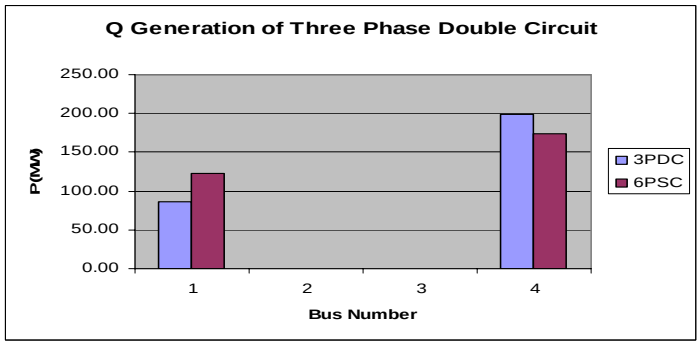

Graph G.29: Q generated of 3PDC and 6PSC transmission at bus 2-4

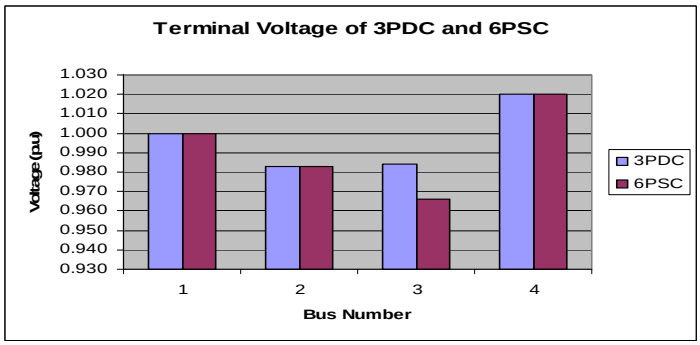

Graph G.30: Terminal voltage of 3PDC and 6PSC transmission at bus 3-4

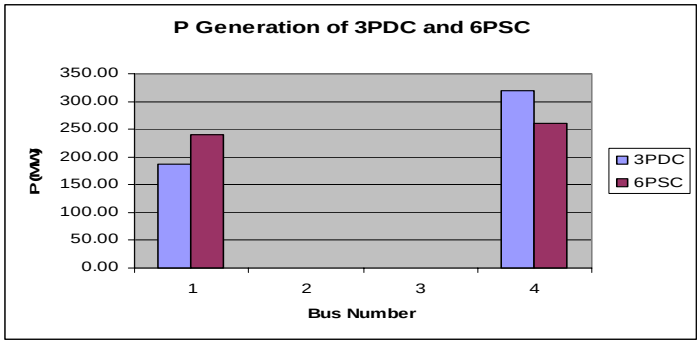

Graph G.31: P generated of 3PDC and 6PSC transmission at bus 3-4

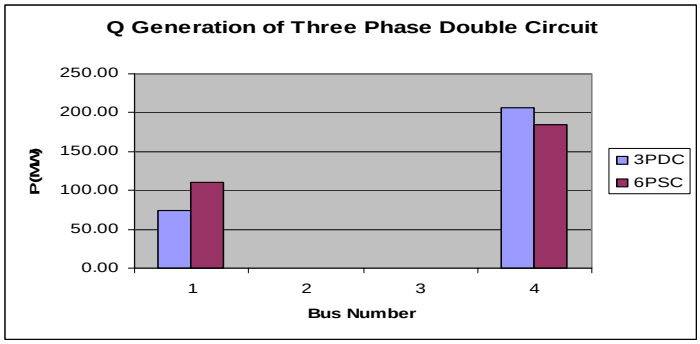

Graph G.32: Q generated of 3PDC and 6PSC transmission at bus 3-4

G.2 Test System II

Comparison of power flow results for 3PDC and 6PSC transmission system by using PSCAD/EMTDC

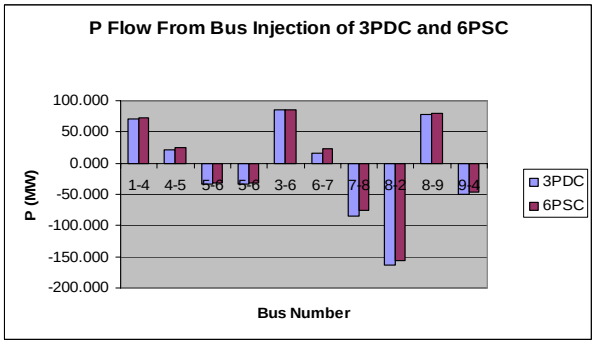

Graph G.33: The flow of P for 3PDC and 6PSC transmission at bus 5-6

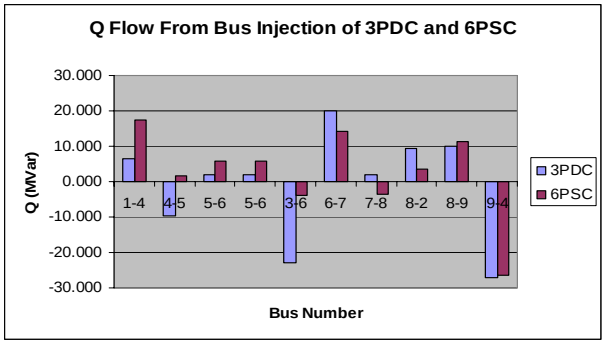

Graph G.34: The flow of Q for 3PDC and 6PSC transmission at bus 5-6

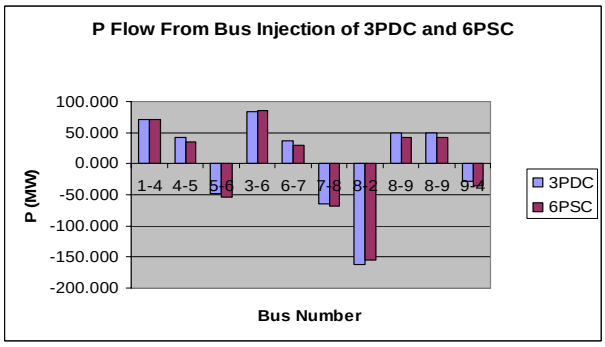

Graph G.35: The flow of P for 3PDC and 6PSC transmission at bus 8-9

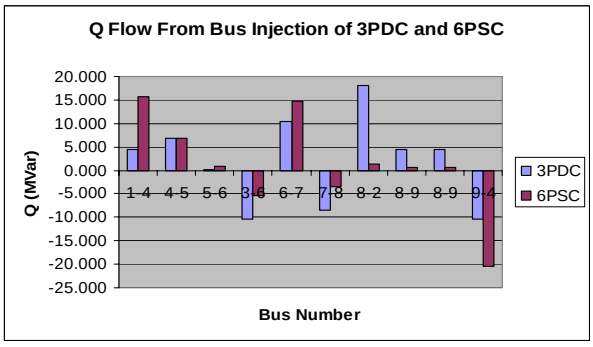

Graph G.36: The flow of Q for 3PDC and 6PSC transmission at bus 8-9

Comparison of terminal voltage, real power and reactive power results for 3PDC and 6PSC transmission system by using PSCAD/EMTDC

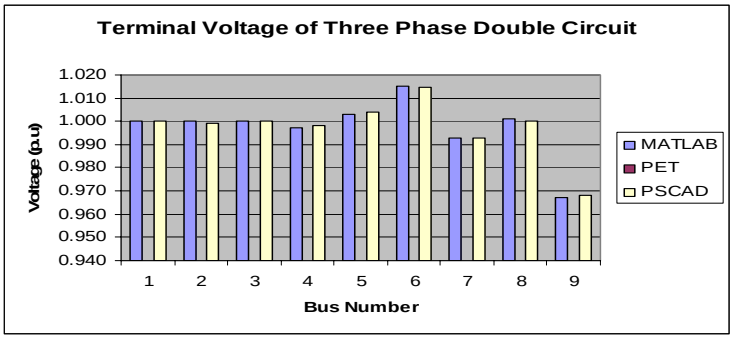

Graph G.37: Terminal voltage of 3PDC and 6PSC transmission at bus 5-6

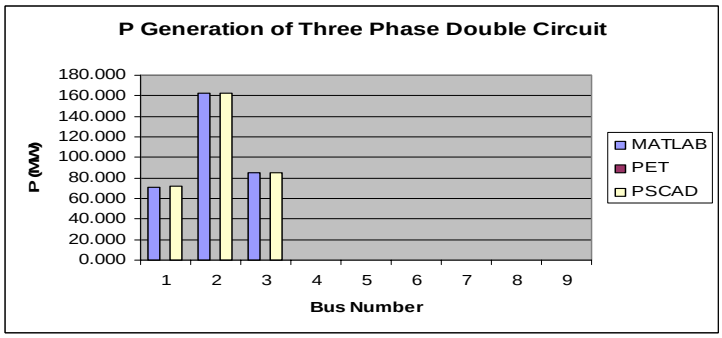

Graph G.38: P generated of 3PDC and 6PSC transmission at bus 5-6

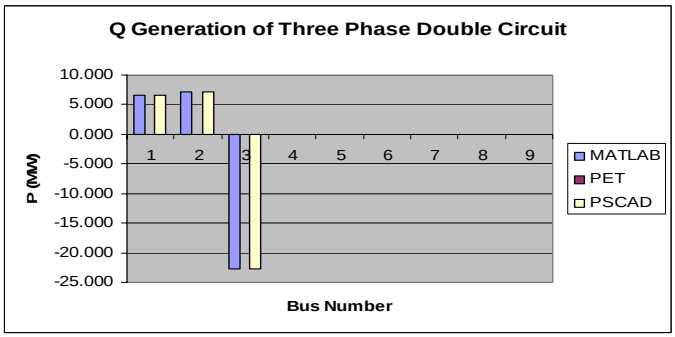

Graph G.39: Q generated of 3PDC and 6PSC transmission at bus 5-6

G.3 Test System III

Comparison of power flow results for 3PDC and 6PSC transmission system by using PSCAD/EMTDC

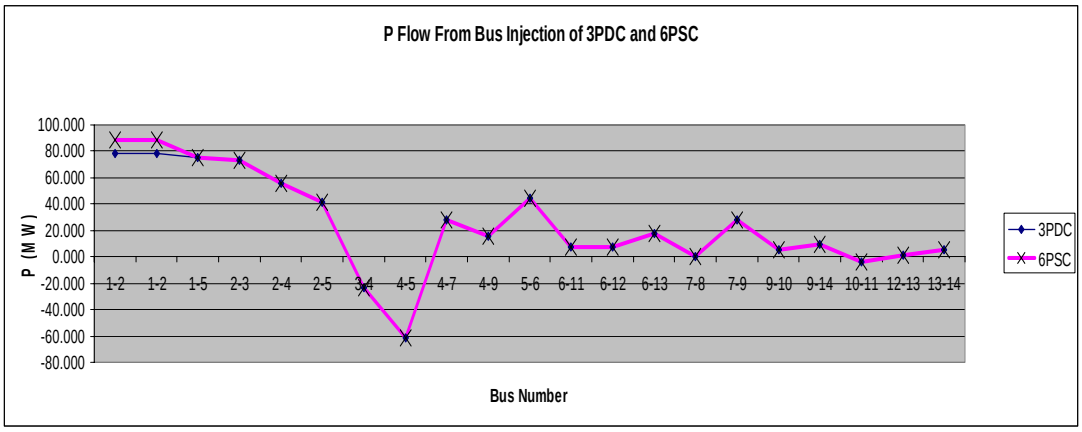

Graph G.40: The flow of P for 3PDC and 6PSC transmission at bus 1-2

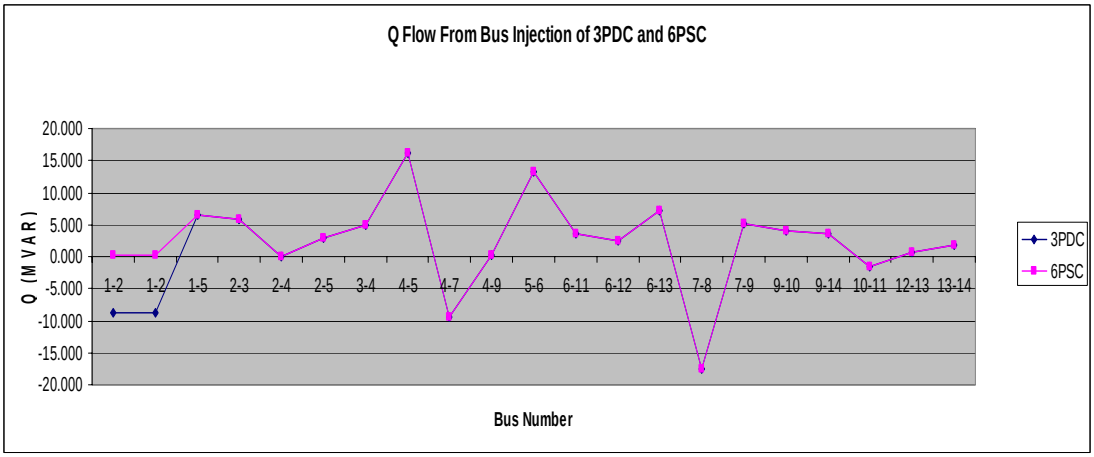

Graph G.41: The flow of Q for 3PDC and 6PSC transmission at bus 1-2

Comparison of terminal voltage results for 3PDC and 6PSC transmission system by using PSCAD/EMTDC

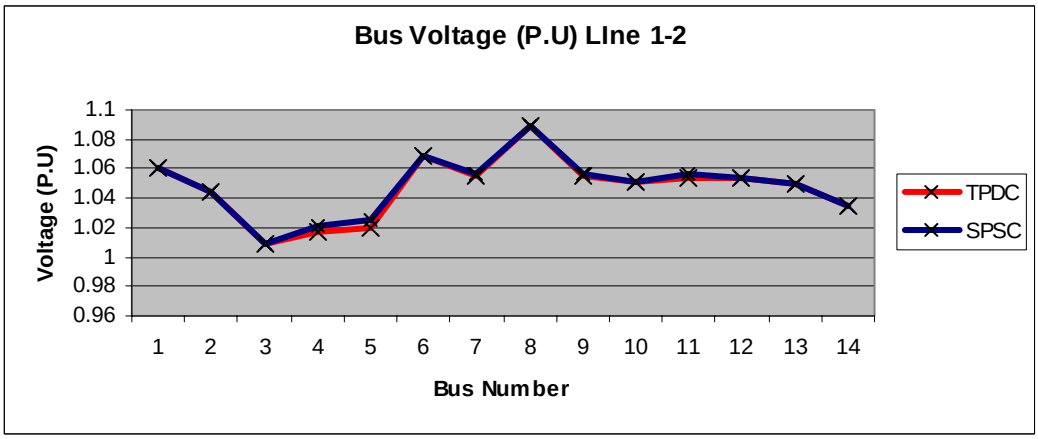

Graph G.42: Terminal voltage of 3PDC and 6PSC transmission at bus 1-2